平成 29 年度
放射線安全規制研究戦略的推進事業費
短寿命α核種等の RI 利用における
合理的な放射線安全管理のあり方に関する研究

事業報告書

平成３０年３月

主任研究者　細野　眞

目　　次

研究の概要

本研究は，医療において放射性同位元素を用いた診断・治療が発展し続けている現在において，短寿命α核種等を用いた内用療法を含む放射線医療の更なる発展を目指した国内における研究開発が，科学的知見に基づく合理的な安全管理の下に促進されるために，放射線防護を関連法令や指針の上でどのように確保し，将来の国民医療の向上につなげるかについて，放射線業務に従事する者及び公衆の防護の最適化の観点から検討を進めた。これまで，厚生労働科学研究費補助金研究（地域医療基盤開発推進研究事業）「医療における放射線防護と関連法令の整備に関する研究（H26-医療-一般-019）」など長年に渡り高度な放射線診療に対応した放射線防護を推進するための研究を進められ，既にその成果の一部が医療法等の関係法令に取り入れられ，放射線診療の発展と放射線防護の整備に寄与している。例えば，α核種である Ra-223 は治療薬として承認されて広く利用され，臨床上の適用拡大に向けた取り組みも進められている。更に At-211, Ac-225 などの他の短寿命α核種，α核種以外にも Lu-177, Cu-67 などの短寿命核種について，放射線治療に関する基礎研究及び臨床研究が進められ，国内外で急速に利用が高まりつつある。一方で，前臨床・臨床研究等の研究開発におけるこのような核種の利用は，我が国においては，放射性同位元素等による放射線障害の防止に関する法律（昭和 32 年法律第 167 号。以下，「障害防止法」という。）の規制下で取り扱われることとなるが，同法及び関係法令におけるこのような将来の医療利用が期待される短寿命α核種に対する規制は，長寿命α核種を想定したものであり，短寿命α核種に適用すると過剰な管理となり，使用及び管理に伴う作業の非効率化につながりかねない。安全の確保を前提とする一方で，科学的知見に基づく合理的な規制が導入されなければ，国の目指す放射線療法の更なる充実に支障を来し，世界の医薬品開発競争にも後れをとることが懸念される。このような課題を解決することは極めて重要であり，本研究では平成 29 年度から 2 年間の計画で国内外における医療用又は医療用として期待される短寿命α核種等の研究開発と安全管理，短寿命α核種等の利用の将来ニーズについて調査し，実態に則した規制のあり方について検討を進めることとした。

１． 研究目的及び研究方法

近年，RI 内用療法の有効性を高める研究が近年精力的に行われ，短寿命α核種が治療薬の研究・開発に必須となっており，世界各地の先進的な研究施設において，短寿命α核種の臨床応用に向けた研究が進められている[1][2]。しかしながら，このような将来の医療利用が期待される短寿命α核種の利用はこれまでは，利用実態がほとんどなかった。その証拠にアイソトープ等流通統計によると，主な非密封 RI 供給量に示された 36 核種に α 核種は含まれず，全体の流通量の 10,036,880MBq に対して，リスト外のその他核種全体量 194 MBq の一部に過ぎない（2016 年度）[3]。このようにこれまで利用の想定がなかったこともあり，障害防止法及び関係法令における，実態を踏まえた規制については十分に検討されているとは言い難く，従来α核種に対する規制はその核種毒性[1)]（Radionuclide toxicity），半減期による，内部被ばくした際のα線の人体への影響を考慮した極めて厳しいものであり，この規制がそのまま短寿命核種に適用されることは，実態にそぐわない過剰な管理となり，使用及び管理に伴う作業の非効率化につながりかねない。安全の確保を前提とする一方で，科学的知見に基づく合理的な規制が導入されなければ，国の目指す放射線療法の更なる充実が，実態にそぐわない規制により支障が来され，世界の医薬品開発競争にも後れをとることも懸念される。このような背景の下，平成 29 年度は医療用又は医療用として期待される短寿命α核種等の利用における規制，安全管理に関して，我が国の現在の規制における課題の解決に向けた，以下の研究を行った。

[1)] IAEA Technical Report Series No.15-A Basic Toxicity Classification of Radionuclides (1963) [4]による分類

1.1 国内外の実態調査及び国内規制における課題の検討

(1) 国内主要施設における実態調査及び国内規制における課題の検討

国内における実態調査は，当該核種の利用状況や利用における放射線防護措置に関して調査するため，短寿命α核種等を実際に利用して研究に取り組んでいる先進的な施設である量子科学技術研究開発機構放射線医学総合研究所（以下，「放射線医学総合研究所」という。），

福島県立医科大学，国立医薬品食品衛生研究所において，利用実態を踏まえた規制の妥当性の観点からそれぞれの施設において以下の調査を実施するとともに短寿命α核種等の RI 利用に際して許可申請時に必要となる空気中濃度などの，我が国の規制下で求められる評価について検討し，実態との乖離などのような点について改善が図られるべきか，そのために科学的視点で明らかにすべきことは何か等を 1.2 の研究連絡会議において議論した。

○放射線医学総合研究所では,At-211 にて標識したカテコールアミン類似物質である At-211 MABG の合成を開発するなど放射性薬剤の基礎的検討がなされているので，α核種の新規薬剤開発における規制を中心に検討した。

○福島県立医科大学では，α核種 RI 内用療法の臨床応用を計画しているので，α 核種の臨床研究における規制を中心に検討した。

○国立医薬品食品衛生研究所では，放射性医薬品等の規制科学の立場で，短寿命α核種を含む RI を利用している。使用者の立場で規制のあり方について検討する他，医薬品研究開発から承認への全プロセスに精通した立場で，規制のあり方について検討を進めた。

(2) 諸外国における実態調査

諸外国においても実際にα核種を利用して医療における研究開発に取り組んでいる高度な施設は限られている。そこで本研究では，α核種の利用状況や利用における放射線防護措置及び規制の実態を調査するため，α核種の臨床応用の研究開発に世界的な業績を持つ以下の２施設を訪問し，施設責任者を含めた研究者との対面での質疑応答，施設・設備の詳細な確認によって，利用実態を踏まえた規制の妥当性の観点からそれぞれの施設において調査を実施した。また，本研究に関連する施設として空気中濃度モニタリング手法やその品質保証に関連した知見をもつ IRSN エアロゾル計量物理学研究所におけるα核種の利用状況や利用における放射線防護措置及びモニタリングの実態の調査を実施した。

○ヨーテボリ大学は，α核種の製造及びα核種の新規薬剤の開発を実施しており，また研究者が本主任研究者とともに ICRP[2] の RI 内用療法の Publication において α 核種を中心に関わっていることから国際的なα核種の使用，廃棄，技術基準，規制等について調査検討を行った。

[2] 国際放射線防護委員会（International Commission on Radiological Protection の略）

○ARRONAX 研究所は，これまで α 核種及び β 核種を含めた RI 内用療法の臨床応用に長年

に渡って先駆的研究を実施しており，本主任研究者が留学した研究施設（フランス保健医学研究所 U211）の後継的研究施設でもあるところから，α 核種の臨床研究における規制を中心にして，欧州諸国における RI 内用療法の規制を含めて，調査研究を行った。

○IRSN エアロゾル計量物理学研究所は，放射性エアロゾルモニタリングの計量に係わる専門機関であり，内部被ばく評価において特に重要なα核種を利用するほか，フランスにおける取扱い施設におけるモニタリング及びその品質保証に関する知見を有する。本機関では，取扱い実態及びフランスにおけるモニタリング手法とその品質保証に関する調査を主に実施した。

1.2　研究連絡会議の設置及び開催等

本研究を的確かつ円滑に推進することを目的として，本研究に携わる研究者等による研究連絡会議を 2 回（9 月及び 1 月）開催した。会議には主任研究者，研究協力者，研究参加者，プログラムオフィサー及びプログラムオフィサー補佐が参加した。本会議においては，1.1 の具体的内容を議論し，研究成果を本報告書にとりまとめた。

2.　研究結果

2.1　国内主要施設における実態調査及び国内規制における課題の検討

国内における実態調査は，短寿命α核種等を実際に利用して研究に取り組んでいる先進的な施設である放射線医学総合研究所，福島県立医科大学，国立医薬品食品衛生研究所において実施し，次のことが明らかとなった。

・国内外において，表１に示すような短寿命α核種の臨床応用に向けた研究が進められていることがわかった[5][6]。
・At-211 の臨床応用に向けた前臨床研究において必要とされる量について検討し，およそ 222 MBq（6 mCi）程度を想定すべきであることがわかった。
・臨床応用の場合，米国デューク大学にて行われた At-211 標識抗体（At-211-81C6）による神経細胞芽腫治療に関する治験（Phase I, II）によると 71 - 347 MBq （1.9 - 9.4 mCi）／ヒトの投与量[7]の想定が必要であることがわかった。

表 1　臨床利用可能なアルファ線放出核種の例 *

α核種	系列	半減期	Eα	親核種 **	子孫核種	最終安定核	放出粒子数	族分類
At-211	4n+3	7.2 h	5.98, 7.59 MeV	[Bi-209] Rn-211 (14.6 h)	Po-211, Bi-207	Pb-207	1α	ハロゲン
Bi-212	4n	61 min	6.21 MeV	Pb-212 (10.6 h)	Po-212+	Pb-208	1α1β	窒素族
Bi-213	4n+1	46 min	8.54 MeV (Po-213)	Ac-225 (10.0 d)	Po-213+	Bi-209	1α2β	窒素族
Ra-223	4n+3	11.4 d	5.98 MeV	Th-227 (18.7 d)	Rn-219+	Pb-207	4α2β	アルカリ土類金属
Ac-225	4n+1	10.0 d	5.94 MeV	[Ra-226 (1600y)] Th-229 (7880y)	Fr-221+	Bi-209	4α2β	アクチノイド
Th-227	4n+3	18.7 d	6.14 MeV	Ac-227	Ra-223+	Pb-207	5α2β	アクチノイド
Tb-149	――	4.2 h	4.08 MeV	[Gd-152, Eu-151]	Eu-145+	Nd-145	0.2α2β	ランタノイド

*細野眞, Isotope News (2013)[1]を一部改変

** [ ] 内は加速器で製造する場合に利用するターゲット元素を示す

・このような臨床応用が期待される短寿命α核種の利用に際しては，種々の係数（排気／空気中濃度限度等）が，表2の例に示すとおり，他の短寿命核種と比較して 1 ～ 2 桁厳しい評価となっているため，その他 RI の使用量を相当圧迫する要因となっている他，これまでのように一律に過剰に安全側な値を採用すると，全てのファクタについて安全係数が大きいため，規制基準値の厳しいα核種では，短寿命であるにもかかわらず全体として実態にそぐわない相当保守的な評価となりうることが見込まれた。このような課題ついて改善が図られるべきか，そのために必要な科学的知見については，海外における事例も参考に，今後典型的なモデルの例を用いた事例研究を行うことで明らかにすべきであると考えられた。また，表3に示す通り，上記の種々の係数の下となっている実効線量率定数について ^{226}Ra（半減期：1600 年）と ^{223}Ra（半減期：11.43 日）とを比較すると，両核種の半減期は大きく異なるにも関わらす，定数は同じオーダであり，根拠となっている実効線量率定数そのものの正当性についても確認することが望ましいと考えられた。

・放射性医薬品の開発承認申請の前臨床においては，動物実験が必須になるが，特に空気中濃度の評価に際しては，動物へ投与された RI は，投与以降，その飛散率を 1 として扱われるため，一般的な施設では小規模の代謝実験程度しか現実的に扱えず，より実態を踏まえた科学的知見に基づく評価が必要であることが示唆された。

表２　医療応用に関連する核種等の空気中濃度限度の例

核種	空気中濃度限度(Bq/cm^3)	空気中又は排気中濃度限度(Bq/cm^3)
^{211}At	8×10^{-4}	7×10^{-6}
^{223}Ra	4×10^{-6}	2×10^{-8}
^{99m}Tc	1×10^{0}	9×10^{-3}
^{131}I	2×10^{-3}	1×10^{-5}

表 3　実効線量率定数の例

COMMITTED EFFECTIVE DOSE PER UNIT INTAKE e(g) VIA INHALATION AND INGESTION (IAEA BSS)
^{223}Ra　5.7×10^{-3}（inhalation）1.0×10^{-4}（ingestion） ^{226}Ra　2.2×10^{-3}（inhalation）2.8×10^{-4}（ingestion）
Limits of radioactivity concentration for the air in controlled areas
^{223}Ra　4×10^{-6} ^{226}Ra　9×10^{-6}
Limits of radioactivity concentration for discharged air from controlled areas
^{223}Ra　2×10^{-8} ^{226}Ra　4×10^{-8}
Limits of radioactivity concentration for discharged water from controlled areas
^{223}Ra　5×10^{-3} ^{226}Ra　2×10^{-3}

以上のことから，国内における規制に関連して検討すべき項目は以下のとおりと考えられる。

・空気中濃度限度，空気中／排気濃度限度が，実際の線量評価に及ぼす影響とその妥当性

・実効線量率定数の妥当性

・飛散率の妥当性（(例) 動物実験における飛散率：1，等）

2.2　諸外国における実態調査

本研究では，スウェーデン１施設及びフランス２施設を訪問調査した。

ヨーテボリ大学は，短寿命α核種の製造及びα核種の新規薬剤の開発を実施している。本調査においては，国際的な臨床応用に向けた短寿命α核種の利用の現状，今後の利用が期待される核種等の研究開発ニーズの現状について調査した。また，関連する施設を訪問し，利用の実態について調査を進めた。更に，訪問先研究者が本主任研究者とともにICRPのRI内用療法のPublicationにおいてα核種を中心に関わっていることから国際的な短寿命α核種の使用，廃棄，技術基準，規制等について意見交換を行った。訪問先において，我が国おける標的 α 線治療（TAT[3]）の現状を紹介し，今後の TAT 発展のための課題などについて議論した。

ARRONAX研究所は，短寿命α核種であるAt-211などの製造及びα核種の新規薬剤の開発のための前臨床研究を実施している。同施設の施設見学を行うとともに，短寿命α核種等の使用，廃棄，技術基準，規制等について調査した。更に，我が国おける標的TATの現状を紹介し，今後のTAT発展のための課題などについて議論した。

空気モニタリング装置の試験のための放射性エアロゾル暴露場を保有しているIRSN-Aerosol Physics and Metrology Laboratoryでは，RI使用施設における空気モニタリングとその品質保証に関して調査した。

以上の海外調査によって，次のことが明らかとなった。

・スウェーデンでは，90年代半ばから短寿命α核種の研究が進められ，当初は長半減期核種と同様に核種毒性について規制当局は懸念していたが，短寿命であり放射線防護の観点から影響は無視できるレベルであることを説明し，物理的半減期などの科学的知見に基づいて，合理的に安全管理が行われていることが分かった。

・フランスにおいても，施設の運用にあたっては，施設と行政の間で合理的な管理について議論し，短寿命α核種の利用によって得られる医学的利益に対して，その利用によるリスクのレベルが許容範囲内であれば，合理的な規制の下で安全を確保しつつ利用されていることが確認できた。

・各国においてDIS[4]は国際的に共通認識である年10μSvの基準に基づいて運用されていた。ただし，本手法の運用が合理的かは，保管設備の規模や核種の分別の容易性など各施設によって異なり，全ての施設が本基準に基づく措置をとっているわけではないことも分かっ

た。

・非密封 RI 施設における RI 利用では，リスク評価に基づく規制の運用と，安全確保のためのモニタリングを基本とした考え方に基づき実運用されていることが確認できた。

・運用にあたっては，IAEA BSS No. GSR Part 3[5]に基づき欧州各国に先駆けて使用核種の特性に応じた合理的な規制（Graded approach など）が導入されていた。以下に，その具体例を示す。

(1) 各国施設では高度な専門知識を有する放射線防護を専門とする物理士の下に安全管理体制が構築され，このような専門家が規制当局への対応も行っている。

(2) ARRONAX 研究所では，入退室は IC カードにより，各室への入室許可はこのカードで管理され，放射線業務従事者が全ての室に入室できるわけではなく，個別に制限し，入室許可は，放射線業務従事者の各作業に関する教育訓練に基づき与えられている。

(3) 近年，我が国においても水晶体等価線量評価に関して ICRP Pub103 の取り入れが検討されているが，ARRONAX 研究所では，規制要求されていないものの作業者の防護メガネ及び線量計の装着を独自に実施している。

これらは IAEA BSS No. GSR Part 3 の以下の要求事項などに基づくものと考えられる。

①Requirement 6: Graded approach

The application of the requirements of these Standards in planned exposure situations shall be commensurate with the characteristics of the practice or the source within a practice, and with the likelihood and magnitude of exposures.

研究の内容や核種の性質に応じた合理的な Graded approach で施設を運用し研究を実施

②Requirement 11: Optimization of protection and safety

The government or the regulatory body shall establish and enforce requirements for the optimization of protection and safety, and registrants and licensees shall ensure that protection and safety is optimized.

高度な専門家が構築した管理体制による防護の最適化

③Requirement 15: Prevention and mitigation of accidents

Registrants and licensees shall apply good engineering practice and shall take all practicable measures to prevent accidents and to mitigate the consequences of those

accidents that do occur.

モニター，安全装置，安全設備，（鍵）などによる事故防止，万が一の場合の汚染や被ばくの抑止

④Requirement 26: Information, instruction and training

Employers, registrants and licensees shall provide workers with adequate information, instruction and training for protection and safety.

教育訓練の実施，およびその受講に応じた利用許可の付与など

[3] α線内用療法（Targeted Alpha Therapy の略）

[4] DIS　Decay in Storage の略。許可を受けた RI が比較的半減期の短い核種で汚染された廃棄物を，減衰させることを目的に一定期間適切に保管すること。

[5] Radiation Protection and Safety of Radiation Sources: International Basic SafetyStandards General Safety Requirements Part 3 （放射線防護と放射線源の安全：国際基本安全基準）

３．まとめ

本研究では，実際にα核種を利用して研究開発を実施している高度な施設（国内：放射線医学総合研究所，福島県立医科大学，国立医薬品食品衛生研究所，海外：ヨーテボリ大学，ARRONAX 研究所，IRSN-Aerosol Physics and Metrology Laboratory）を対象に施設責任者を含めた研究者との質疑応答，施設設備の確認によって調査を実施し，短寿命α核種等の利用に対する合理的規制，安全管理等について研究を進めた。本研究によって臨床応用に向けた短寿命α核種を用いた研究が国内外で行われ，我が国においても将来に渡って利用ニーズがあることが分かった。一方で，本研究における国内調査は，短寿命α核種の製造能力を有する 2 施設及び研究利用施設 1 施設の調査にとどまっており，本研究で抽出された課題が国内における利用ニーズを完全に網羅したものとは言い難く，更に広範囲の調査を実施し，具体的な規制見直しのニーズについて取りまとめるとともに，その効果について検討する必要があることが認識された。海外調査においては，短寿命α核種等を用いた新しい手法の開発促進おいては，IAEA BSS No. GSR Part 3 の考え方に基づく合理的な規制の運用がなさることが重要であり，それが実際に可能であることが確認できた。また，短寿命核種の利用に際し

て，各国においてDISが実運用されていることが確認できた。例えば，フランスにおいては，Code de l'environnement 環境法（Art.L 542.1-1）において，code de la santé publique （公衆衛生法）に規定される活動（医療など）に係る，非常に半減期の短い核種の放射性廃棄物は，放射性廃棄物としての特別な認可ない部門で扱えるよう，十分に減衰させる，という趣旨の規定があり，very short lived-waste として 100days 未満が適用可能となっていることがわかった[8]。

なお，各施設が短寿命α核種の利用にあたって合理的な安全管理を行う上で，実際にどのような評価を行っているか，具体的に規制当局が要求している事項は何かなどのより詳細事項については，具体的に規制に生かす視点から，調査の成果を具体的に示すために，今後調査研究の必要があることが認識された。

謝辞

本研究は，原子力規制庁平成 29 年度放射線対策委託費（放射線安全規制研究戦略的推進事業費）の支援のもと実施した。ここに謝意を表する。

平成29年度放射線安全規制研究戦略的推進事業費（短寿命 α 核種等のRI利用における合理的な放射線安全管理のあり方に関する研究）事業

委員名簿

平成３０年３月現在（敬称略）

	氏名	所属
主任研究者	細野　眞	近畿大学　医学部　教授
研究協力者	織内　昇	福島県立医科大学先端臨床研究センター　ふくしま国際医療科学センター　先端臨床研究センター教授／副センター長
〃	右近　直之	福島県立医科大学先端臨床研究センター　ふくしま国際医療科学センター　先端臨床研究センター助教
〃	永津　弘太郎	国立研究開発法人量子科学技術研究開発機構　標識薬剤開発部　放射性核種製造チーム　主任研究員
研究参加者	伊藤　哲夫	近畿大学　原子力研究所　所長
〃	山西　弘城	近畿大学　原子力研究所　教授
〃	松田　外志朗	近畿大学　原子力研究所　准教授
〃	山田　崇裕	近畿大学　原子力研究所　准教授
外部有識者	蜂須賀　暁子	国立医薬品食品衛生研究所　生化学部　第一室長
プログラムオフィサー	中村　吉秀	公益社団法人日本アイソトープ協会　シニアアドバイザー

参考文献

[1] 細野眞 （2013） α線内用療法の現状と展望，Isotope News, No.711, 2-7

[2] Dekempeneer, et al.（2016）Targeted alpha therapy using short-lived alpha-particles and the promise of nanobodies as targeting vehicle

[3] 日本アイソトープ協会 （2017） アイソトープ等流通統計 2017

[4] IAEA Technical Report Series No.15-A Basic Toxicity Classification of Radionuclides (1963)

[5] Sophie Poty, et al. Alpha Emitters for Radiotherapy: Basic Radiochemistry to Clinical Studies – Part 2. Journal of Nuclear Medicine, published on March 1, 2018 as doi:10.2967/jnumed.117.204651 (2018)

[6] George Sgouros et al. Radiobiology and Dosimetry of a-Particle Emitters for Targeted Radionuclide Therapy*. THE JOURNAL OF NUCLEAR MEDICINE・Vol. 51・No. 2・February 2010

[7] Guérard F, Gestin JF, Brechbiel MW. Production of [^{211}At]-astatinated radiophamaceuticals and applications in targeted a-particle therapy. Cancer Biotherapy and Radiopharmaceuticals （2013） DOI: 10.1089/cbr.2012.1292

[8] Radioactive waste management. IRSN Thematic series

主な研究成果

- Hosono M. Radiation protection in therapy with radiopharmaceuticals. BER2018 International Workshop on Biological Effects of Radiation, March 21, 2018, Osaka, Japan.（invited lecture）
- Hosono M. Individualized treatment planning in radionuclide therapy, Symposium:Radiological protection in nuclear medicine for personalized care. World Federation of Nuclear Medicine and Biology 2018, April 22, 2018, Melbourne, Australia.（invited lecture）

参考資料

・1.　第一回研究連絡会議　議事

・2.　第二回研究連絡会議　議事

・3.　Targeted Alpha Therapy Group, University of Gothenburg, Sweden

・4.　ARRONAX 研究所

・5.　Aerosol Physics and Metrology Laboratory　(LPMA)

・6.　量子科学技術研究開発機構　放射線医学総合研究所　施設設備・研究紹介

　　福島県立医科大学　施設設備・研究紹介

・7.　欧州及び我が国における主な短寿命α核種製造・利用研究拠点

参考資料 1

平成 29 年度放射線対策委託費（放射線安全規制研究戦略的推進事業費）
規制等整備・ 運用領域
短寿命α核種等の RI 利用における合理的な放射線安全管理のあり方に関する研究
（細野班）
第 1 回研究連絡会議概要

日　時：平成 29年 9月5 日（火）13時30分 - 16時
場　所：新大阪丸ビル本館 503 号室
　　大阪市東淀川区東中島 1-18-5
出席者：
（主任研究者）細野　眞
（研究協力者）右近直之（織内 昇　代理）、永津弘太郎、伊藤哲夫、山西弘城、松田外志朗、
　　山田崇裕
（外部有識者）蜂須賀暁子
（プログラムオフィサ）中村吉秀
（オブザーバ）原子力規制庁 長官官房　放射線規制部門　制度係長　吉岡正勝

（出席 10 名　順不同、敬称略）

議　事：
1.　細野班研究計画について
2.　我が国における短寿命α核種等の RI 利用の規制における課題について
3. 平成 29 年度研究実施について
（1）海外調査
（2）国内調査
4. 今後の予定

配布資料：
資料 1：平成２９年度放射線安全規制研究戦略的推進事業費（短寿命α核種等の RI 利用における合理的な放射線安全管理のあり方に関する研究）事業 計画書
資料 2：我が国における短寿命α核種等の RI に係る規制の現状と課題について
資料 3：ARRONAX 研究所概要
資料 4：TAT グループ概要
資料 5：Aerosols physics & metrology laboratory, IRSN 概要

以上

参考資料 2

平成 29 年度放射線対策委託費（放射線安全規制研究戦略的推進事業費）
規制等整備・ 運用領域
短寿命α核種等の RI 利用における合理的な放射線安全管理のあり方に関する研究
（細野班）
第２回研究連絡会議概要

日　時：平成 30 年 1 月 31 日（火）13 時 00-15 時 30 分
場　所：近畿大学　東京センター大会議室
〒103-0028　東京都中央区八重洲1 丁目8 番 16号 新槇町ビル13 階
出席者：
（主任研究者）細野 眞
（研究協力者）織内 昇、永津弘太郎、右近直之、伊藤哲夫、松田外志朗、山田崇裕
（外部有識者）蜂須賀暁子
（プログラムオフィサ）中村吉秀
（オブザーバ）原子力規制庁 長官官房　放射線規制部門　制度係長　吉岡正勝

（出席 10 名　順不同、敬称略）

議　事：
1.　海外調査報告
2.　今後の短半減期 α 核種の利用ニーズと規制緩和が望まれる点について
（1）基礎研究、前臨床関連
（2）臨床研究関連
（3）臨床応用に向けた RI 研究利用全般
3.　短半減期 α 核種の利用に際しての規制のあり方についての総合討論
4. 次年度研究計画について
5.　その他

（会議資料）
資料 1　海外調査報告（案）スウェーデン
資料 2　海外調査報告（案）フランス
資料 3　短寿命α核種等の RI 利用における放射線安全管理のあり方に関する研究（細野班）報告書（QST 永津氏）
資料 4　短半減期α核種の利用に際して、規制緩和してもらいたい・今後の短半減期α核種の利用ニーズについて（福島県立医大右近氏）
資料 5　非密封 RI 利用について（国立衛研蜂須賀氏）
（参考資料）
参考資料 1-astatinated radiopharm and cancer therapy
参考資料 2-Ohshima Sudo KY MABG EJNMMI2018
参考資料 3-各国における放射性廃棄物規制除外（クリアランス）の動向（11-03-04-05）- ATOMICA -
参考資料 4-軽水炉の使用済燃料（04-07-01-02）- ATOMICA -

UNIVERSITY OF GOTHENBURG

Targeted Alpha Therapy Group

Targeted Alpha Therapy Group

The Targeted Alpha Therapy Group is the result of collaborations among departments at the University of Gothenburg, Sahlgrenska University Hospital, and Chalmers University of Technology as well as different foreign centers such as the PET & Cyclotron Unit at Rigshospitalet in Copenhagen, the Memorial Sloan-Kettering Cancer Center in New York, and the Institute for Transuranium Elements in Karlsruhe, Germany.

The coordination of all research activities in the group is though perfomed by people working at different departments at the Sahlgrenska Academy, University of Gothenburg.

The main goal is to develop strategies for the treatment of disseminated cancer using alpha-particle emitters as the leading actor. The research areas covered by the Targeted Alpha Therapy Group include studies of the chemistry related to the labeling of radionuclides to different ligands, studies of pharmacokinetics and different aspects of radiation physics such as dosimetry, and clinical studies in which the developed treatment strategies are evaluated, such as in our recently published phase I study.

Targeted Alpha Therapy Group

Research

The goal with the research is to develop strategies for the treatment of disseminated cancer using alpha-particle emitters as the leading actor.

The Targeted Alpha Therapy Group (TAT Group) started its research activities along with the publication of 2 articles in 1998. Since then, 60 articles have been published/accepted in peer-reviewed scientific journals and 8 PhD thesis have been presented, all relating to the work within the group.

Staff working in or in close collaboration with the TAT Group has different backgrounds varying from nuclear or radiation physics, chemistry, medicine and molecular or microbiology.

The cooperation within the group is characterized by a frequent and continuous exchange of ideas and planning of experiments, among the whole or parts of the group.

Targeted Alpha Therapy Group

Main Group Research

The main research areas in the TAT Group range from studies of the labeling chemistry of radionuclides to different ligands, studies of pharmacokinetics and different aspects of radiation physics such as dosimetry, to clinical studies in which treatment strategies are evaluated, such as in our recently completed phase I study.

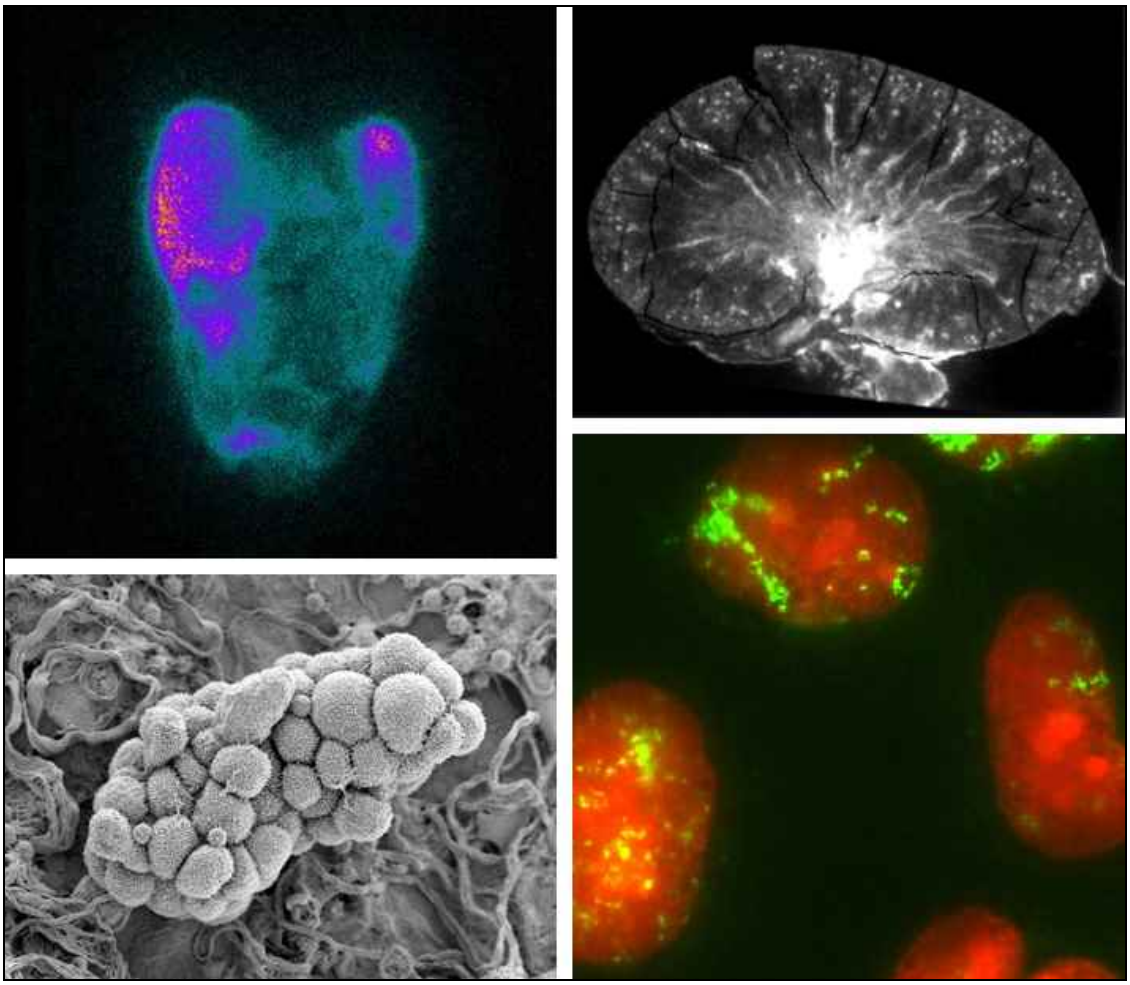

Fig. 1. ***Upper left***: Anteroposterior gamma-camera scan of the abdominal and thoracic area after infusion of 211At-MX35 F(ab´)2 in a patient in the phase I study. ***Upper right***: Distribution of 211At-IgG in mouse kidney 2 h after i.v. injection visualized in a 20 µm cryosection using the Alpha Camera. ***Lower left***: Scanning electron microscopy image showing a small tumor loosely adhered to the peritoneum in a mice. ***Lower right***: Double-strand breaks, visualized as H2AX-foci, in cells irradiated with 1 Gy by alpha particles. Particle passages across the whole nucleus are seen in some cells.

Targeted Alpha Therapy Group

Radiobiology

Cellular Radiobiology of Alpha Particles

DNA-damage and cellular consequences

Initial investigations on in vitro radiobiology effects of alpha particles from ^{211}At were conducted by Stig Palm and collaborators, revealing a severe inhibition of growth in two tumour cell lines, and a RBE of 5 and 12, respectively (Palm et al, 2000a and Palm et al, 2000b). The team now working on cellular effects of irradiation with alpha particles is headed by Associated Professor Kecke Elmroth together with Karin Magnander, Kristina Claesson and other colleagues.

Background

The main focus in our current cellular investigations of high-LET effects is determination of the Relative Biological Effectiveness (RBE) for alpha particles under different conditions. The purpose of studying radiobiology of alpha particles is to increase our knowledge of how damage is inflicted and how cells deal with it in order to improve targeted radiotherapy. It has been generally accepted that double-strand breaks are critical lesions, involved in chromosomal aberrations and decreased survival.

Recently, another type of complex damage, the clustered lesion, has been considered important as well. Clustered lesions are defined as 2 or more lesions induced within 10-20 base pairs and may, if repaired at all, challenge the different repair systems despite the fact that the lesions per se are quite simple (single-strand breaks, base damages or abasic sites). It has been suggested that high-LET radiation induces more clustered lesions compared with low-LET but this has not yet been proved experimentally. Although the induction yield seems to decrease with LET the repair may still be severely compromised.

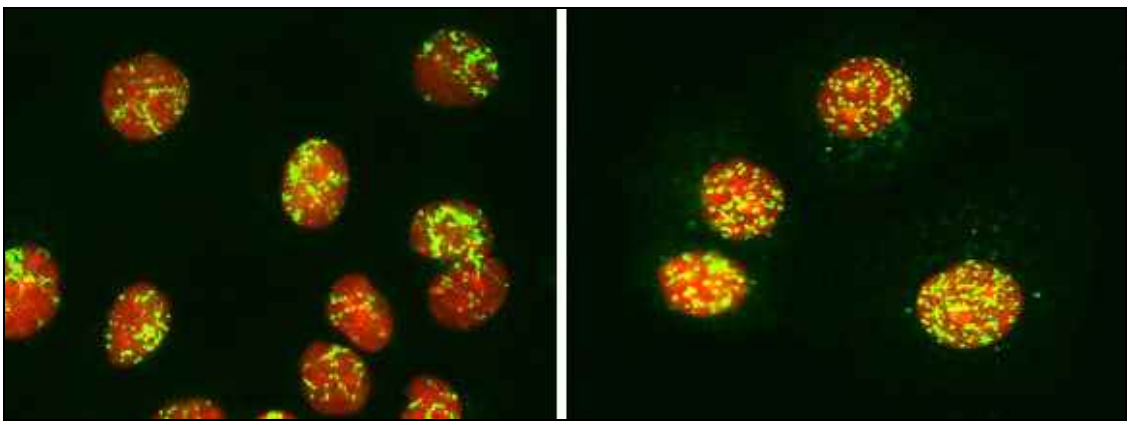

Fig. 1. *Double-strand breaks (green) in irradiated cell nuclei (red). Breaks are visualized by labeling of gamma-H2AX foci, emerging within minutes at the site of DNA breaks. Left: cells*

irradiated with alpha particles from ^{211}At. Right: cells irradiated with X-rays. ***Click image for higher resolution****.*

Alpha particles result in high RBE for induction of double-strand breaks

Recent in vitro investigations focus on induction and repair of complex DNA lesions, i.e. double-strand breaks and clustered lesions induced by alpha particles. Using pulsed field electrophoresis and fragment analysis, which more correctly quantifies non-randomly induced double-strand breaks, we have shown that the induction yield is almost three times higher for alpha particles from ^{211}At than for low-LET radiations at the same absorbed dose (Claesson et al, 2007).

Breaks do not appear randomly in the cell nucleus. When analyzing the DNA fragment distribution resulting from the breaks, an excess of small DNA fragments and a depletion of larger fragments is evident. This is expected due to the inhomogeneous deposit of energy along the radiation track across chromatin fibres (Fig. 1, left). From this work it is also evident that protection against alpha particles by soluble intrinsic scavengers is not as important as for low-LET radiation.

RBE in different cell cycle phases

In studies completed during the spring of 2009, we have further investigated the role of cell cycle position for induction of complex DNA damage. In synchronized fibroblast cells, RBE for both double-strand breaks and clustered DNA lesions in different cell cycle phases was determined. While clustered DNA lesions do not increase with LET or dose, double-strand breaks certainly do, resulting in a RBE close to 3 for all phases. When analyzing the resulting clonogenic survival, the RBE increases dramatically to 8-9 for all phases. The exception is cells in mitosis, showing a more pronounced effect but a lower RBE for both induction and survival.

Ongoing projects

Future experiments include studies on the importance of chromatin structure, survival of cells with different intrinsic radiosensitivity and cell cycle arrest responses in cells irradiated with alpha particles. Another important project just initiated is evaluation of cellular toxicity and biodosimetry after in vivo exposure to alpha particles using visualization of double-strand breaks in individual cells by immunohistochemistry directed against gamma-H2AX foci (Fig. 1). One advantage using this method for quantification of double-strand breaks is that effects after clinically relevant doses can be investigated.

References

1. Claesson K., Stenerlöw B., Jacobsson L. and Elmroth K. Relative Biological Effectiveness of the α-particle emitter ^{211}At for double-strand break induction in human fibroblasts. Radiation Research 167, 312-318, 2007.
2. Palm S., Andersson H., Bäck T., Claesson I., Delle U., Hultborn R., Jacobsson L., Köpf I. and Lindegren S. In vitro effects of free ^{211}At, ^{211}At-albumin and ^{211}At-monoclonal antibody compared to external photon irradiation on two human cancer cell lines. Anticancer Research 20, 1005-1012, 2000a.
3. Palm S., Andersson H., Bäck T., Claesson I., Delle U., Hultborn R., Jacobsson L., Köpf I. and Lindegren S. Cell growth kinetics of the human cell line Colo-205 irradiated with photons and astatine-211 alpha-particles. Anticancer Research 20, 1807-1812, 2000b.

Targeted Alpha Therapy Group

Staff

The persons associated with the Targeted Alpha Therapy Group has different background varying from nuclear or radiation physics, chemistry and medicine to molecular or microbiology.

Some of the people also work within other projects but the co-operation within the group is always characterized by a frequent and continuous exchange of ideas and planning of experiments. In the lists to the left you will find the regular staff, the close collaborators and persons just occasionally appearing as co-workers or co-authors to the group.

Targeted Alpha Therapy Group

Collaborators

Already from the beginning of the research activities performed by the Targeted Alpha Therapy Group there have been a number of different collaborations.

The most important ones are shown in the list to the left. Some of the collaborations have been continuously ongoing for a long period of years, *e.g.* the PET & Cyclotron Unit at Rigshospitalet in Copenhagen and the Department of Nuclear Chemistry at Chalmers University of Technology in Gothenburg, while others are just recently established, *e.g.* The Institute for Transuranium Elements (ITU) in Karlsruhe, Germany.

Targeted Alpha Therapy Group

Publications

Since the Targeted Alpha Therapy Group started its research activities with the publication of 2 papers 1998 there have been 60 papers published/accepted in peer-reviewed scientific journals and books, 7 PhD theses has been presented and 16 MSc theses has been completed.

A number of conferences have also been attended at which both oral and poster presentations have been made. Also, some articles in daily papers and other popular science newspapers have been published.

Please make a choice in the list to the left to view all the articles, PhD theses, MSc theses, or popular science articles related to the Targeted Alpha Therapy Group.

Chemistry

The standard production of ^{211}At is by irradiating stable bismuth with helium ions (alpha-particles) using cyclotron irradiation, and date back to the discovery of the nuclide in 1940 by Corson et al (1).

Although no cyclotron is available in Gothenburg collaborations with the Department of Physics Oslo University, Norway, Forschungszentrum Dresden-Rossendorf, Germany and Cyclotron and PET Unit, Rigshospitalet, Copenhagen, Denmark has provided us with ^{211}At on a regular basis since 1994. Early on much of the work was focused on the procedures, distillation and chemistry to obtain ^{211}At and ^{211}At-labeled antibodies.

In 2001 a novel procedure on distillation and work up of ^{211}At from irradiated Bi-targets was developed (2). With this method the nuclide is rapidly converted into a chemical useful form for subsequent labeling chemistry. The labeling chemistry has been based on the method first developed by Zalutsky and co-workers (3), see Figure 1 below.

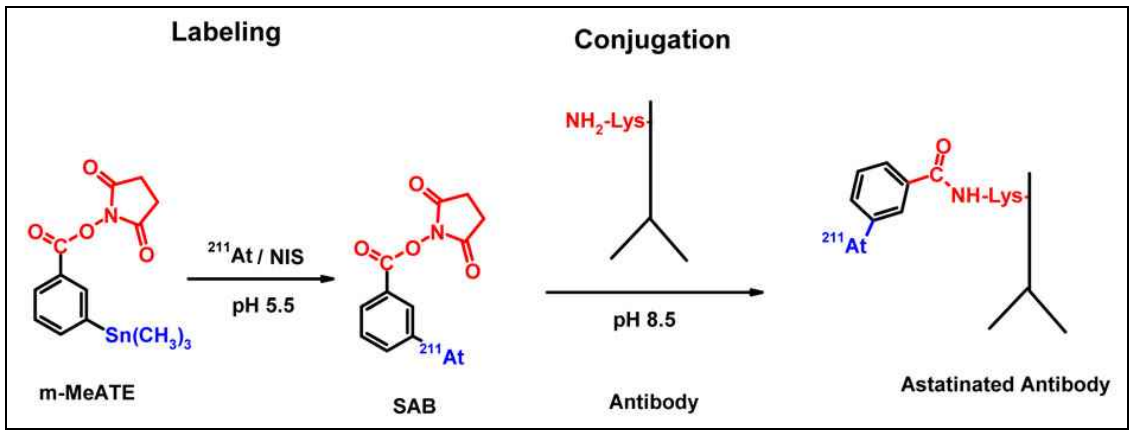

Fig. 1. *Labeling of N-succinimidyl 3-(trimethylstannyl)benzoate followed by conjugation of labeled reagent to antibody.* ***Click image for higher resolution****.*

With this method labeled antibodies which have been sufficient for preclinical evaluations have been produced. However, we encountered problems when taken the research into a clinical phase I study on patients with recurrent ovarian carcinoma. The levels of activity planned for the study were difficult to reach by the conventional procedure for labeling the antibody. Therefore an extensive effort was put on developing the chemistry, and in 2008 a new chemical route that substantially improves the labeling efficacy in astatination of antibodies was developed (4), see Figure 2. In this way the levels of activity required to continue into a phase II clinical study now is possible to reach.

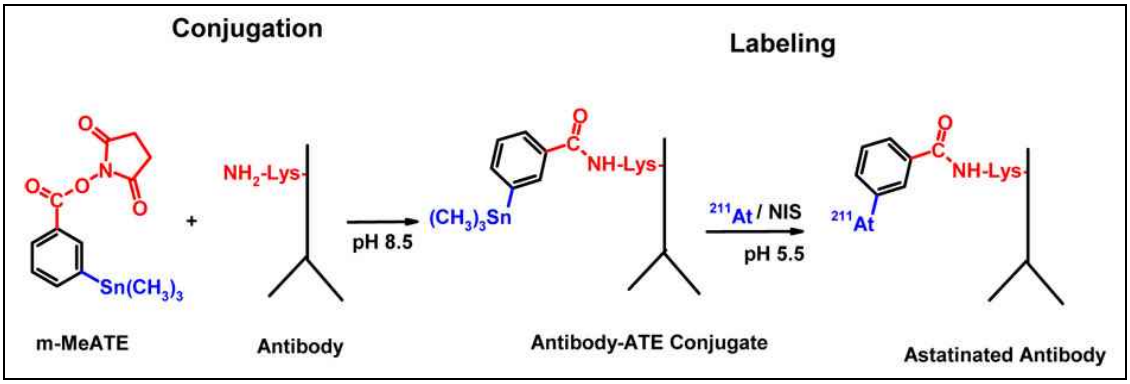

Fig. 2. *Conjugation of antibody with the labeling reagent N-succinimidyl 3-(trimethylstannyl)benzoate (m-MeATE) followed by labeling of immunoconjugate with ^{211}At.* ***Click image for higher resolution****.*

In addition to astatine we have access to another interesting alpha -particle emitting radionuclide, Bismuth-213. It is available through a close collaboration with the Institute of Transuran Elements (ITU) Karlsruhe, Germany. They provide us with ^{225}Ac/^{213}Bi generators from which we can elute ^{213}Bi in a pure chemical form for subsequent labeling to antibodies. The labeling is performed via bifunctional chelates. Several different chelates for antibody are commercially available. Generator protocols and protocols for labeling that result in very good radiochemical yields have been developed at ITU.

The half-life of ^{211}At (7.2 h) and ^{213}Bi (46 min) is generally too short for conventional radioimmunotherapy except for a few special applications such as blood-born or intracavitary cancer treatments, e.g. intraperitoneal (i.p.) and intrathecal (i.t.) treatments (5-7). This is due to the relatively slow in vivo distribution and slow clearance rates of radiolabelled antibodies. Most of the injected radioactivity will therefore decay before reaching its target.

In order to circumvent the unfavourable pharmacokinetics of radiolabeled antibodies, different ways of improving the distribution of the radioactivity have been suggested, employing various pretargeting techniques (8-10). With this type of technique modified antibodies are administered for pre-binding to the tumor antigens. A sufficient time is introduced, to allow non-bound antibodies to be cleared from the circulating system, or a clearing agent is administered to enhance the clearance rate before injecting the labeled effector molecule. The effector molecule recognizes a tag on the antibody and due to the small size of the effector molecule as compared to labeled antibodies, it will localize the target more rapidly and the non-bound fraction will be cleared more efficiently, thus increasing tumor uptake and lowering the dose to normal tissue.

A successful pretargeting protocol will improve the tumor-to-normal tissue absorbed dose ratio for all types of applications involving antibodies for tumor targeting together with radionuclides with short half-lives, e.g. ^{213}Bi and ^{211}At. In this project a pretargeting strategy including the pretargeting molecule avidin/strepavidin conjugated antibody and an effector-molecule based on biotinylated, labeled and charge modified polylysine is investigated, see Figure 3 below.

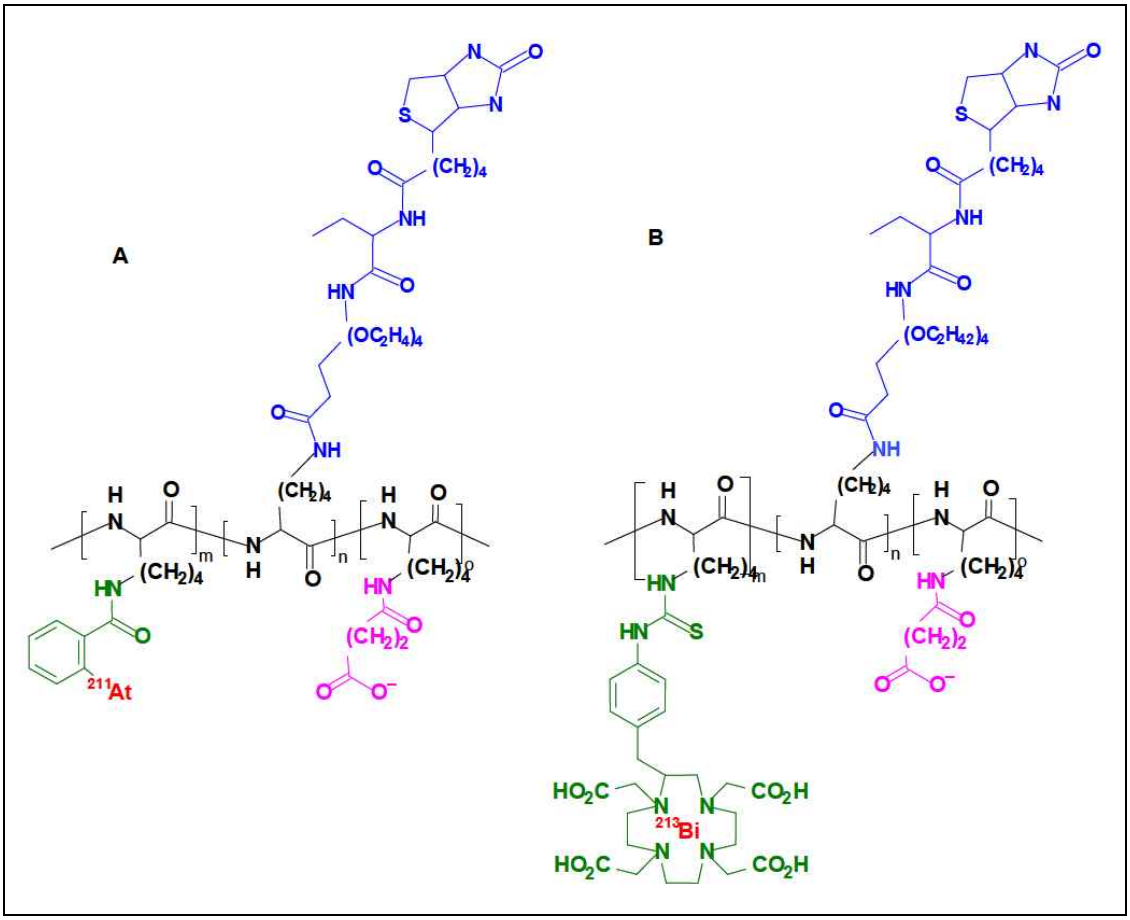

Fig. 3. *Schematic structures of effector molecules.* ***A:*** *Labeled with ^{211}At via N-succinimidyl 3-(trimethylstannyl)benzoate.* ***B:*** *labeled with ^{213}Bi via the kelate DOTA. Different parts of the molecule are presented as, BLUE: biotin residue; GREEN/RED: radiometal-kelate- or radiohalogen-reagent residue; PURPLE: succinic acid residue following charge modification.* ***Click image for higher resolution****.*

References:

1. D.R. Corson, K.R. MacKenzie, Phys. Rev. 58. 672-678 (1940).
2. S. Lindegren, T. Back, H. Jensen, Appl. Radiat. Isot. 55. 157-160 (2001).
3. M.R. Zalutsky, A.S. Narula, Appl. Radiat. Isot. 55. 157-160 (2001).
4. S. Lindegren, S. Frost, T. Bäck, E. Haglund, J. Elgqvist, H. Jensen, J. Nucl. Med.49. 1537-1545 (2008).
5. H. Nakamae, D.S. Wilbur, D.K. Hamlin, M.S. et al. Cancer Res. 6, 2408-2415, (2009)
6. H. Andersson, E. Cederkrantz, T. Bäck, et al. J. Nucl. Med.50, 1153-1160, (2009)
7. E.Y. Song, C.F. Qu, S.M. et al. Cancer Biol Ther. 7, 76-80. (2008)
8. J.M. Pagel, N. Hedin, L. Drouet, et al. Blood, 111, 2261-2268, (2009)
9. D. M. Goldenberg, R. M. Sharkey, G. Paganelli, et al., J. Clin. Oncol., 5, 823-834, (2006).
10. R. M. Sharkey and D. M. Goldenberg, Cancer Invest. 1. 82-97, (2006).

Targeted Alpha Therapy Group

Clinical Studies

All research performed by the Targeted Alpha Therapy Group, irrespective of weather it concerns basic radiobiological, physical or chemical issues, has the final goal of becoming beneficial for the patient. The last 10 years of research by the group has resulted in a phase I study being completed (Journal of Nuclear Medicine 2009;50:1153–1160).

Below follows a short presentation of the methods, results, and conclusion from that study. Questions regardning this study should be addressed to Professor Ragnar Hultborn.

The phase I study:

The alpha-particle emitter ^{211}At labeled to a monoclonal antibody (mAb) has proven safe and effective in treating microscopic ovarian cancer in the abdominal cavity of mice. Beginning in 2005, women in complete clinical remission following second-line chemotherapy for recurrent ovarian carcinoma were enrolled in the study. The aim was to determine the relevant pharmacokinetics for assessing absorbed dose to normal tissues and investigating the toxicity.

Methods: Nine patients underwent laparoscopy 2–5 d before the therapy; a peritoneal catheter was inserted and the abdominal cavity was inspected to exclude the presence of macroscopic tumor growth or major adhesions. Peritoneal scintigraphy was done using 99mTc-LyoMAA to study the fluid distribution in the abdominal cavity. Approximately 500 MBq of ^{211}At was labeled to 0.7 mg of MX35 F(ab')2 using the reagent N-succinimidyl 3 (trimethylstannyl) benzoate. Fifty MBq (3 patients) or 100–200 MBq (6 patients) in 1–2 L of Extraneal was infused via the peritoneal catheter. Gamma camera whole-body scans were acquired at 1, 6, 12, and 20 h (occasionally up to 48 h) after infusion and a single-photon emission computed tomography (SPECT) scan was acquired at 3–6 h. Samples of blood, urine, and peritoneal fluid were collected at 1–48 h. Haematology as well as renal and thyroid function were followed for a median of 23 months.

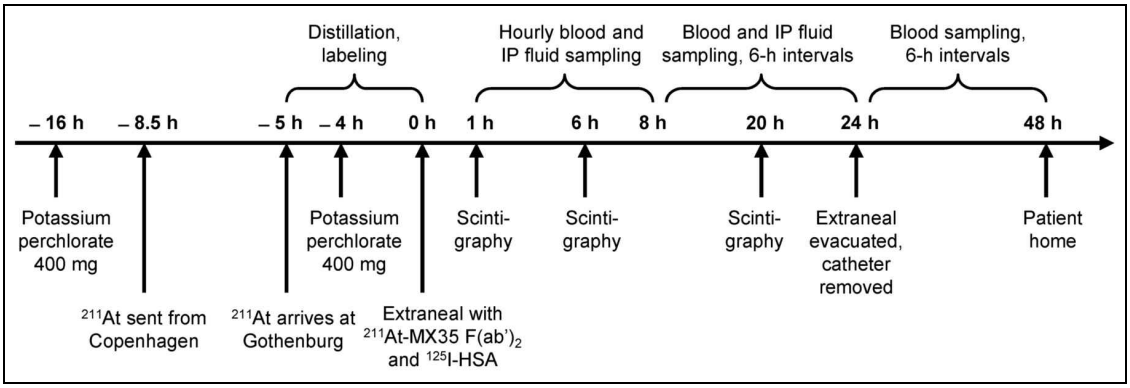

Fig 1. *Schematic overview of logistics of therapeutic procedures. IP = intraperitoneal.* ***Click image for higher resolution****.*

Results: Pharmacokinetics and dosimetric results were related to the initial activity concentration (IC) of the infused solution. The decay-corrected activity concentration decreased with time in the peritoneal fluid to 50% IC at 24 h, increased in serum to 6% IC after 30 h, and increased in the thyroid to 127 ± 63% IC at 20 h without blocking and less than 20% IC with blocking. No other organ uptakes could be detected. The cumulative urinary excretion was 40 kBq/(MBq/L) at 24h. The estimated absorbed dose to the peritoneum was 15.6 ± 1.0 mGy/(MBq/L), to red bone marrow was 0.14 ± 0.04 mGy/(MBq/L), to the urinary bladder wall was 0.77 ± 0.19 mGy/(MBq/L), to the unblocked thyroid was 24.7 ± 11.1 mGy/(MBq/L), and to the blocked thyroid was 1.4 ± 1.6 mGy/(MBq/L) (mean ± 1 SD). No adverse effects were observed either subjectively or in laboratory parameters.

Conclusion: This study indicates that by intraperitoneal administration of ^{211}At-MX35 F(ab')2 it is possible to achieve therapeutic absorbed doses in microscopic tumor clusters without significant toxicity.

Radiation Physics

In preclinical studies, as well as in the clinical phase I study recently published, there are always different aspects of radiation physics that has to be regarded.

These aspects range from the radiation safety during handling of various radioactive sources, calculation of microdosimetric properties regarding irradiation of single cells, dosimetry and the determination of the absorbed dose to tumors, bone marrow or other normal tissues, estimate of the relative biological effectiveness (RBE) for various end-points, estimation of the maximum tolerated absorbed dose or activity for various treatment situations, and considerations regarding tumor cure probability for different treatments and therefore irradiation situations.

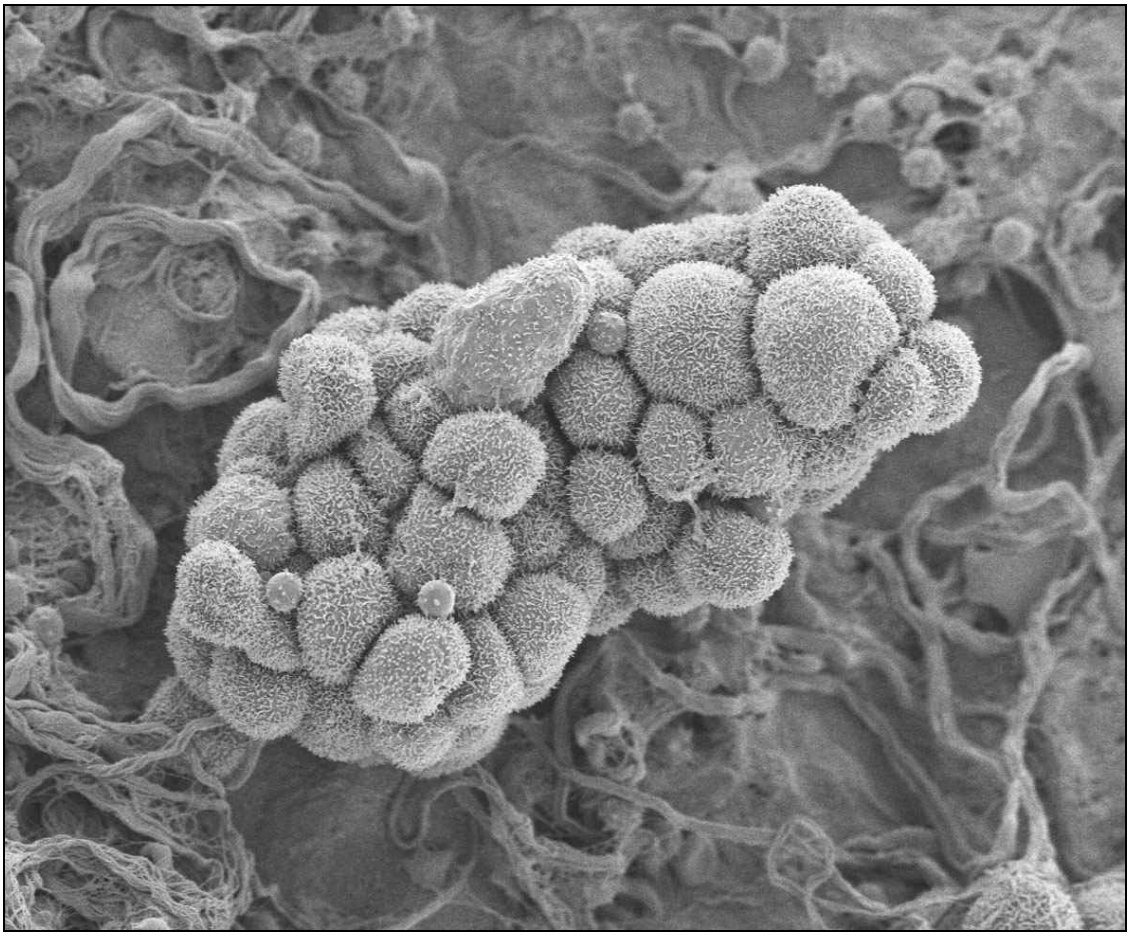

Fig. 1. *The scanning electron microscopy image illustrates microvilli-covered ovarian cancer cells forming a small tumor on thr peritoneum. A network of fibrin, forming individual filaments and more coarse bundles, partly covers the tumor and the peritoneal surface. In the work in J Nucl Med 2006;47:1342–1350 calculations were done in order to estimate the*

absorbed dose to differently sized tumors. ***Click image for higher resolution****.*

Some examples of studies in which different aspects of radiation physics have been considered are presented below.

In the work in Med Phys 2004;31:218-225 a microdosimetric analysis of ^{211}At irradiation of cancer cells was done. A custom-built computer program based on the Monte Carlo method was used to simulate the irradiation. The results show that ^{211}Po atoms, created on a cell surface by the decay of ^{211}At atoms, will diffuse from the cell during its life-span. The increasing distance to the cell nucleus will drastically decrease the probability of the emitted alpha particle to hit the cell nucleus. The conclusion was that for dispersed cells, the diffusion of ^{211}Po atoms will reduce the total absorbed dose from cell-bound ^{211}At by a factor of 2.

In the work in J Nucl Med 2005;46:464–471 the myelotoxicity and the RBE for alpha-particles emitted from ^{211}At was investigated in a pre-clinical study. An RBE of 3.4 ± 0.6 and 5.0 ± 0.9 was found when comparison was made with electrons emitted from ^{99m}Tc or generated by gamma rays emitted from an external ^{60}Co source. The end-point parameter was degree of myelosuppression.

J Nucl Med 2005;46:464–471

Finally, in the work in J Nucl Med 2005;46:2061–2067 the aim was to evaluate the RBE of ^{211}At compared with that of ^{60}Co gamma-irradiation. The endpoint was growth inhibition (GI) of subcutaneous xenografts. The Balb/c received an intravenous injection of ^{211}At-labeled monoclonal antibody MX35 F(ab')2 at different levels of radioactivity (0.33, 0.65, and 0.90 MBq). To calculate the mean absorbed dose to tumor, a separate biodistribution study established the uptake of ^{211}At in tumors and organs at different times after injection. External irradiation of the tumors was performed with ^{60}Co. The biodistribution study showed the uptake of the immunoconjugates by the tumor to be 14% after 7 h. At 40 h, the ratio of uptake in tumors to uptake in blood reached a maximum value of 6.2. The administered activities of ^{211}At corresponded to absorbed doses in tumors of 1.35, 2.65, and 3.70 Gy. The value (mean ± SEM) for D37 was 1.59 ± 0.08 Gy. Tumor growth after ^{60}Co external irradiation showed a value for D37 of 7.65 ± 1.0 Gy. The corresponding RBE of ^{211}At irradiation was 4.8 ± 0.7.

Imaging

Different imaging techniques is repeatedly used in the research and gives important additional information regarding for example the distribution of radioactivity in tissues. Below is listed the imaging techniques use by the Targeted Alpha Therapy Group.

Alpha Camera Imaging

This newly developed technique by Tom Bäck makes it possible to image and pin-point the location of the alpha particles emitted by for example ^{211}At and ^{213}Bi in *in vivo* samples, with a resolution of ~20 µm.

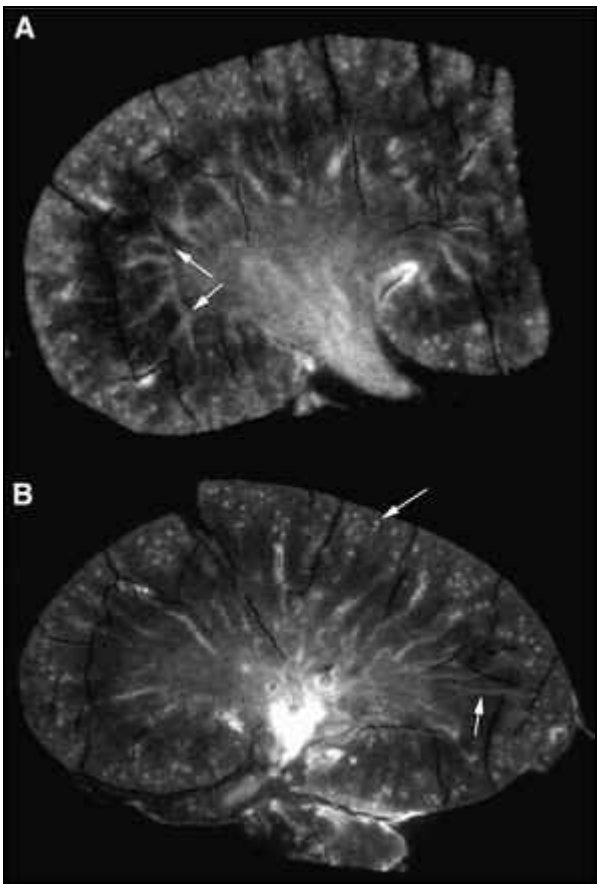

Fig. 1. *Cryosections of Balb/c nu/nu kidneys imaged with the Alpha Camera at 30 min (A) and 2 h (B) after intravenous injection of ^{211}At-IgG trastuzumab. White arrows indicate vascular branches (A) and medullary rays and glomeruli (B).* ***Click image for higher resolution****. J Nucl Med, 2010;51 (10):1616-23.*

Fluorescence Microscopy

This technique has been used when in radiobiological studies when investigationg the appearence of double-strand breaks in irradiated cell nuclei. Breaks are visualized by labeling of gamma-H2AX foci, emerging within minutes at the site of DNA breaks.

Light Microscopy

This technique is used on a regular basis when for example investigating the presence of microscopic tumors in hematoxylin/eosin coloured tissue samples in our therapy studies.

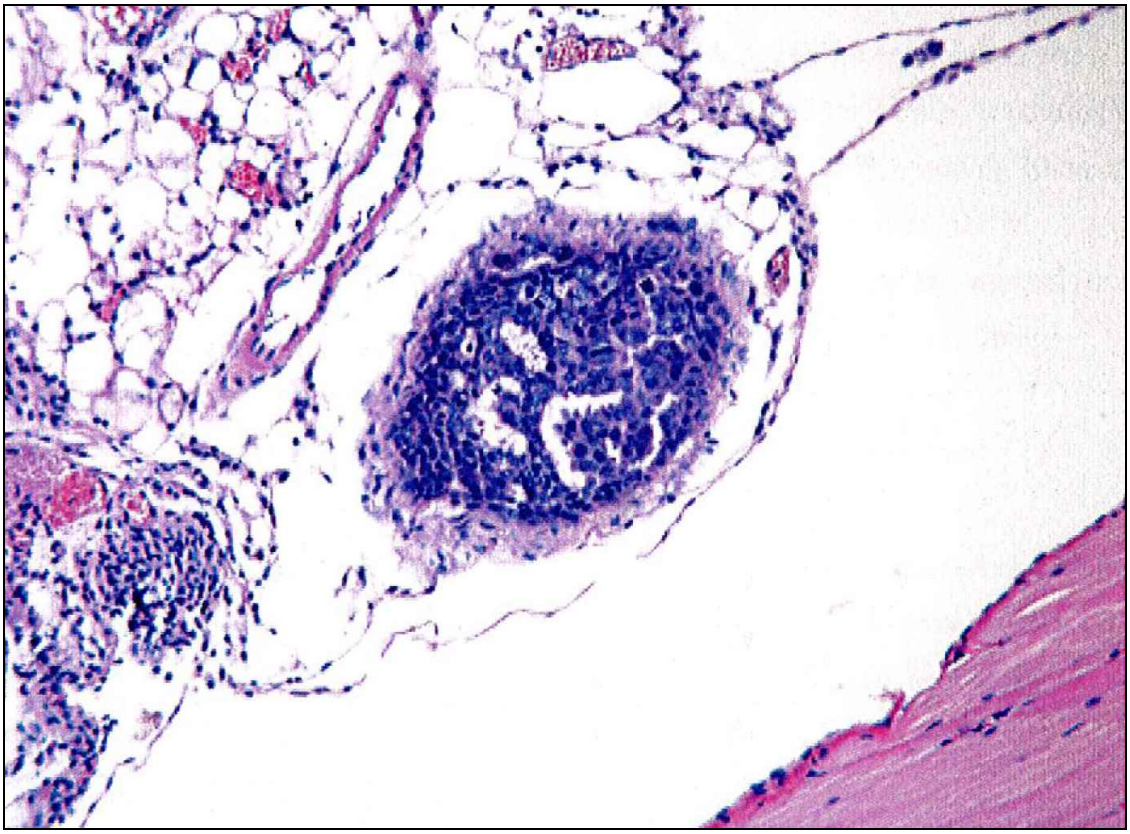

Fig. 2. *Light microscopy image of micrometastasis 2 weeks after intraperitoneal inoculation of ovarian tumor cells (OVCAR-3) in vivo (Balb/c nu/nu). Original magnification x 10.* ***Click image for higher resolution****. Image from Håkan Andersson's PhD thesis in 2000.*

Scanning Electron Microscopy (SEM)

This technique has been used in some studies when for example investigating the relationship between the estimated absorbed dose to differently sized small tumors and the therapeutic efficacy.

Transmission Electron Microscopy (TEM)

This technique has been used occasionally when investigating how the ovarian tumor cells for example are attached to the peritoneal lining during studies of the therapetic efficacy.

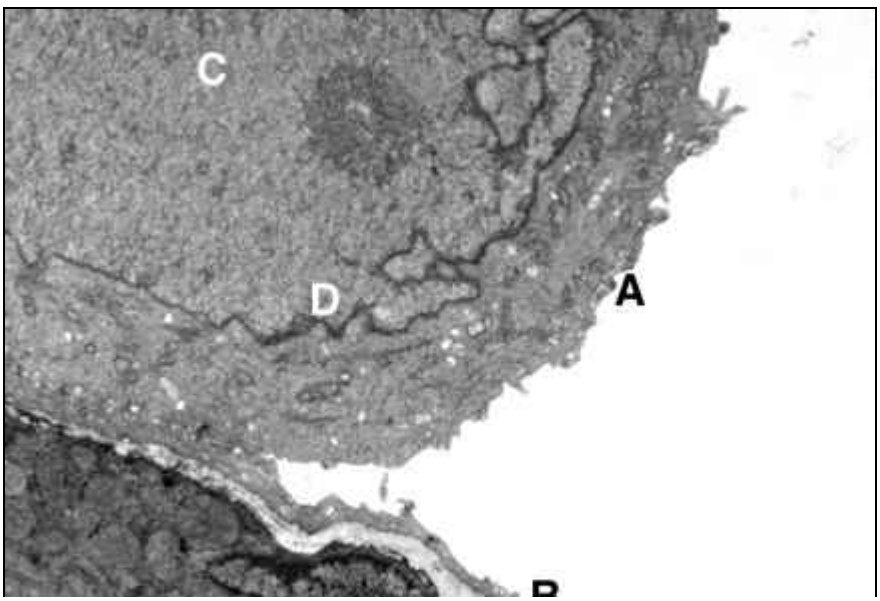

Fig. 3. *TEM image of a tumor cell covered with microvilli (A) adhered to the mesothelial cell layer (B) on peritoneum. The nucleus can also be seen (C), together with its envelope (D). The specimen shown was taken from upper left quadrant of*

abdominal wall from Balb/c nu/nu. ***Click image for higher resolution****. J Nucl Med, 2006;47(8):1238-40.*

Scintigraphy/CT/SPECT-CT

Various standard nuclear-medicine imaging techniqes have been utilized in for example the phase I study to image the localization of radioactivity in the body.

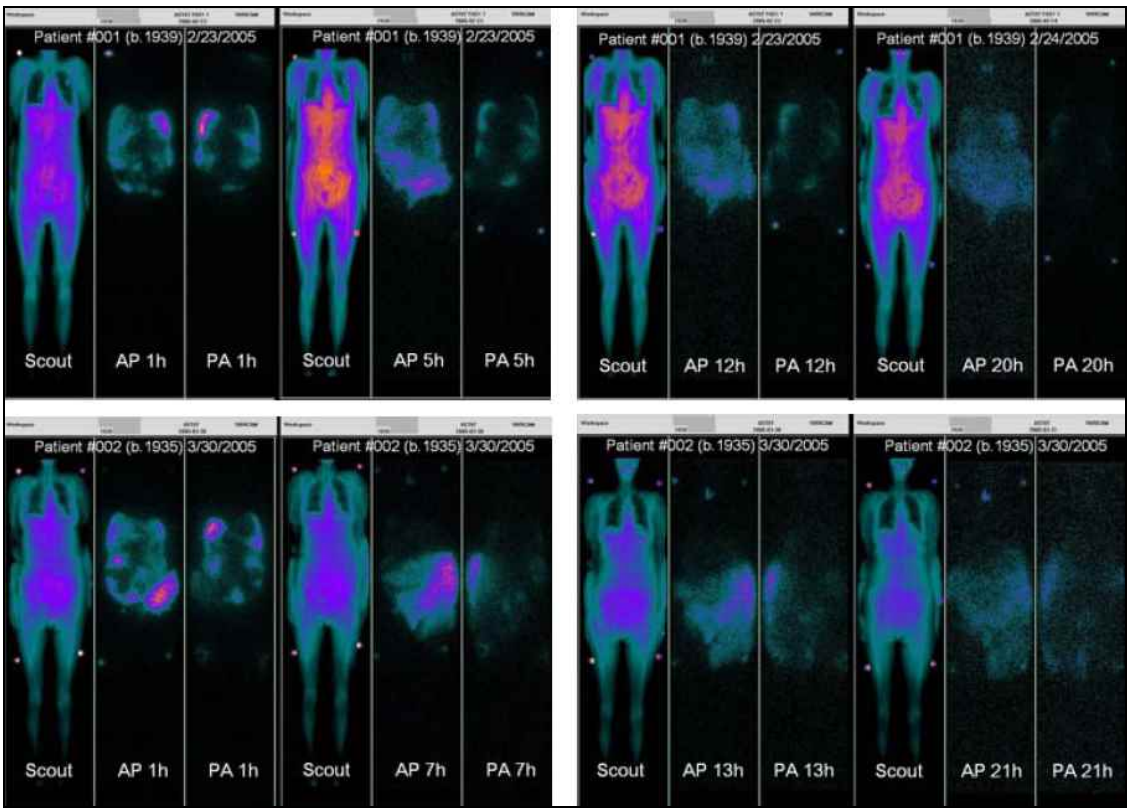

Fig 1. *Gamma-camera images of 2 patients in our phase I study on intraperitoneal infusion of ^{211}At-MX-35 F(ab')2 for ovarian carcinoma. Images show anterior-posterior (AP) and posterior-anterior (PA) views of patients up to 24 h postinfusion.* ***Click image for higher resolution****.*

Automation

After more than 20 years of experience in working with the α-emitting radionuclide Astatine-211 (At-211) the chemistry branch of the TAT-group has begun developing an automatic system for production of At-211-radiopharmaceuticals.

Although manual methods of synthesizing At-211 radiopharmaceuticals can be feasible, they would require expert skills and result in only small scale production. This is why future clinical advancements with At-211 will rely on the possibility of automatic production, similar to the development in PET radiochemistry. An automated system is not only useful for standardizing radiopharmaceutical preparations and increasing radiation safety but also reduces the risk of human error.

Our method is based on the combination of dry distillation to isolate astatine-211 in a chemical useful form and a synthesis module for producing radiopharmaceuticals. These components have been merged into a complete automatic process platform where the unique hardware is controlled by a single computer software.

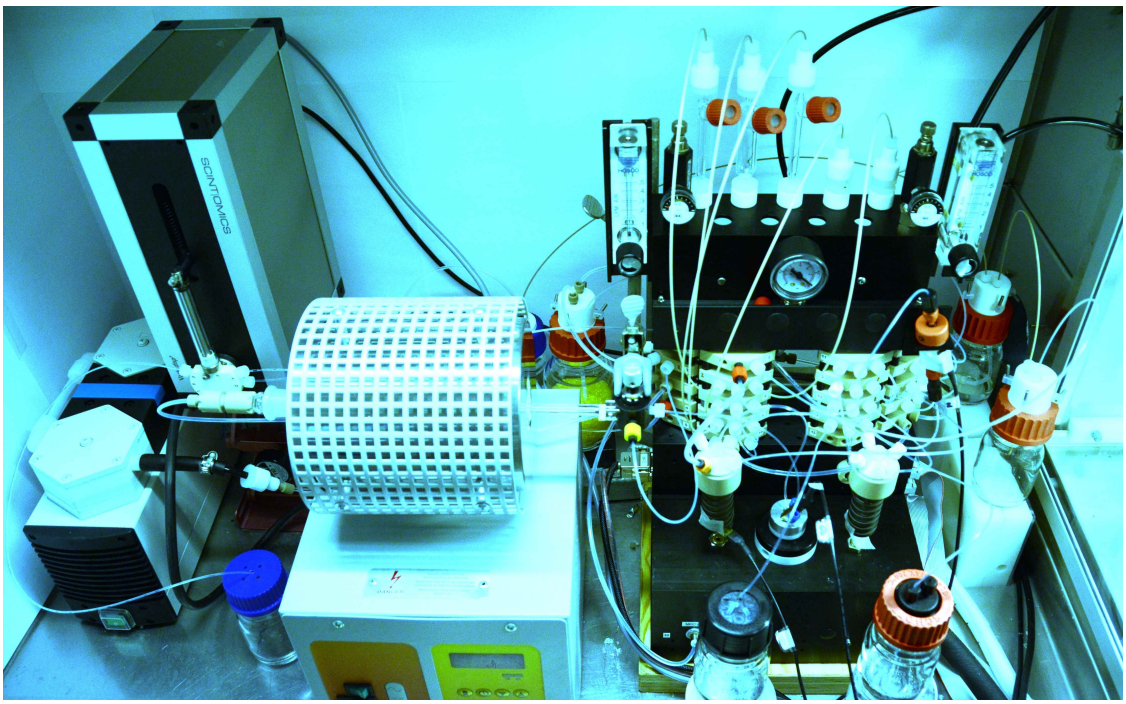

To increase radiation safety, the system is adapted to fit inside a glovebox or a small lead-shielded, hot-cell to minimize exposure to the volatile, radioactive astatine. This compact platform is very versatile as it can accommodate any type of target used for the cyclotron

The Arronax cyclotron characteristics

ARRONAX is an isochronous cyclotron with 4 high hill sectors. The overall size of the cyclotron is of the order of 4m. The working RF frequency is 30.45 MHz with an RF cavity composed of two dees at a voltage of 65 kV.
Table 1 summarises the characteristics of the beam for the four types of particles.

Table 1: ARRONAX cyclotron characteristics

Extracted Particles	Energy range (MeV)	Highest possible current (µAe)	most common current range (µAe)
H+	35 - 70	375 x 2	0.05 - 100 x 2
He2+	70	70	0.07 - 0.1
HH+	35	50	0.1 - 1
D+	15 - 35	50	0.05 - 1.2

The cyclotron has the capacity to send simultaneously proton beams in both opposite beamlines. It is regularly used in this configuration.

For more information, please have a look at http://accelconf.web.cern.ch/AccelConf/IPAC2011/papers/WEPS069.PDF [http://accelconf.web.cern.ch/AccelConf/IPAC2011/papers/WEPS069.PDF]

Laboratories & apparatus

In the controlled area of ARRONAX several laboratories allow the handling of radioactive isotopes safely:

- 2 radiochemistry laboratories (ZCE1 and ZCE2) each containing two fume hoods and glove box.
- 1 cell culture laboratory microscope with a time lapse, a CO2 incubator, a centrifuge, a biological safety cabinet (PSM) and a fume hood
- 1 radiolabeling laboratory equiped with a hot cell and a phospho-imager cyclone.
- 1 metrology room containing three gamma spectrometers with their lead shielding, two alpha spectrometrer,a liquid scintillator, a gas detector alpha / beta total.
- 2 target preparation room containing two electroplating system, a binocular.
- 1 control room containing three quality HPLC which can be coupled to a radioactivity detector or IT-TOF, an UV-visible spectrometer, a GC-MS, an ICP-AES, an electromobility device.
- 1 GMP production lab containing 3 shielded cells.
- 1 sterile GMP production lab containing 5 ht cells equipede with an ionisation chamber.

Access to these laboratories and the materials is possible for external users. To do this, you must make a request to plandemanip@arronax-nantes.fr [mailto:plandemanip@arronax-nantes.fr].

Radionuclide production

As from the beginning of the 2000s, a technological revolution dramatically modified the prospects of nuclear medicine.

This technological revolution was the introduction of PET imaging with 18FDG in the routine practice of nuclear oncology. At the same time a substantial progress has been achieved in radionuclide therapy development as well, especially in radioimmunotherapy and radiopeptide therapy. All these developments open large prospects both in diagnostic imaging and radionuclide therapy with the availability of a lot of carrier molecules which are currently evaluated in preclinical and clinical studies. Beyond oncology, new innovative radiopharmaceuticals are expected to be validated in the coming years, in cardiology and neurology.

In this context, some new needs show up for original and innovative positron, beta- and alpha-emitting radionuclides.

1- PET imaging

For PET imaging, fluorine-18 is undoubtedly the radionuclide of choice, due to its favourable radiophysical characteristics. A lot of new carrier candidates, including FLT, F-MISO, FES, F-choline and F-DOPA, have been clinically evaluated and some of them could be approvedjavascript:toggle_preview();
Mode prévisualisation for a routine use in the coming years. However, the short physical half life (110 minutes) of fluorine-18 requires its production in a cyclotron located at a short distance of each user centre. That's why there is more and more interest for positron-emitting radionuclides with short half-lives but which can be produced in a generator and especially for **[*gallium-68*]** (physical half-life: 68 minutes) for which the father is germanium-68 (with a long half-life of 271 days). Such a generator 68Ge/68Ga has the great advantage to be used for a few months in a nuclear medicine department but germanium-68 needs to be produced in a cyclotron with a high intensity due to its low production yield.

Moreover, fluorinated molecules have a small size and consequently fast kinetics after intravenous injection, which is compatible with the relative short physical half life of fluorine-18. However, for larger carrier molecules, such as antibodies or more generally immunoconstructs, blood kinetics is much slower and maximal tumor accretion is observed relatively late, some days after intravenous injection. This time interval is not compatible with the 110 minutes half-life of fluorine-18. For this new imaging application named immuno-PET, new radionuclides with longer half-lives are needed. **[*Iodine-124*]** is a positron-emitting radionuclide with a physical half-life of 4.2 days which favorably fits with the blood kinetics of antibodies for immuno-PET imaging.

[*Copper-64*] (half-life: 12.7 hours) is another positron-emitting radionuclide of great interest which is also considered for routine production.

Another clinical application which needs some radionuclides with half-lives longer than that of fluorine-18, even for small molecules with fast blood kinetics, is the pre-therapeutic dosimetric calculation. For this application, the innovative approach consists in taking into consideration some pairs of positron- and beta-emitting radionuclides.

Given the present clinical routine use of iodine-131 and yttrium-90 for the labeling of immunoconstructs and peptides, the favorite pairs of radionuclides are iodine-124/iodine-131 and yttrium-86/yttrium-90. However, for the latter pair, a high energy gamma ray emitted at a high rate by yttrium-86 is a real drawback for the routine use of this radionuclide.

Another highly requested pair of radionuclides is copper-64/copper-67 due to the favorable characteristics of both radionuclides.

In cardiology, thallium-201 and technetium-99m MIBI (Cardiolite®) radiopharmaceuticals have been used in clinical practice for some decades, for the diagnosis of myocardial ischemia. However the low energy of the gamma rays emitted by these radionuclides requires an attenuation correction to be introduced which has some limitations. These limitations result in a relative high percentage of false positive results which can lead to some useless invasive coronarography procedures.

[*Rubidium-82*] is a positron-emitting radionuclide which behaves like thallium-201 and is taken-up by the myocardial muscle. The high energy (511 keV) annihilation photons allow to achieve a reliable attenuation correction. Consequently it has been clearly shown that the diagnostic specificity of rubidium-82 imaging is significantly higher than that of thallium-201 or technetium-99m MIBI SPECT imaging. Rubidium-82 has a very short physical half-life (75 sec) and is produced, in a generator, by decay of strontium-82 which has a 25.5 day physical half-life. This very short half-life of rubidium-82 allows to perform both rest and stress imaging tests in less than 30 minutes as compared with a few hours for thallium-201 or technetium-99m MIBI SPECT imaging.

Strontium-82/rubidium-82 generators have been used in the US for more than a decade but currently, the production capability of high activity of strontium-82 is seriously limited in the production centers. ARRONAX cyclotron, with a high energy/high intensity of proton beam will allow to produce up to 600 generators a year.

2- Radionuclide therapy

The three currently used radionuclides for therapy are iodine-131, yttrium-90 and lutetium-177. They cover a range of beta energy which fits well with the range of small tumor sizes which are appropriate for this treatment modality. However iodine-131 emits a relatively high percentage of high energy gamma rays which requires some medical staff radiation safety constraints including some confining of patients in shielded rooms for a few days. These constraints seriously limit the number of patients who could have benefit of radionuclide therapy. Moreover yttrium-90, a high energy beta-emitter, is taken up by bone/bone marrow after release from its chelator coupled to the carrier molecule resulting in bone marrow irradiation which limits the injected activity. Additionally yttrium-90 does not emit gamma rays for pre-therapeutic imaging and yttrium-86 has too high energy gamma rays for routine imaging.

A radionuclide with favorable radiophysical and biological characteristics is **[*copper-67*]** (physical half-life: 61.5 hours) which has been preclinically and clinically evaluated for more than 2 decades. As compared with iodine-131 and yttrium-90, copper-67 has shown the highest therapeutic index in a few clinical studies. However its industrial production has been, up to now, limited by the lack of high energy (70 MeV), high intensity (a few hundreds of microamps) cyclotrons necessary for the production of high activities for clinical studies. ARRONAX cyclotron will be able to produce such high activities.

Finally alpha-emitting radionuclides are being more and more considered for their use in alpha-therapy because of their high LET (Linear Energy Transfer) which gives a high killing effect especially for small clusters of malignant cells. A few alpha-emitting radionuclides are available, including astatine-211, lead-212/bismuth-212 and actinium-225/bismuth-213. ARRONAX cyclotron will produce **[*astatine-211*]** (physical half-life: 7.2 hours) for preclinical and clinical alpha-therapy studies.

Radionuclides priduced byARRONAX

Radionuclide	Target	Nuclear reaction	Cross section (mbarns)	Needed Energy (MeV)
^{64}Cu	Ni	$^{64}Ni(p,n)$	≈ 675	15
^{68}Ge	Ga	$^{69}Ga(p,2n)$	≈ 550	
^{124}I	Te	$^{124}Te(p,n)$	≈ 590	15
^{82}r	RbCl	$^{nat}Rb(p,4n)$	≈ 98	
^{67}Cu	ZnO	$^{68}Zn(p,2p)$	≈ 10	70

Radiobiology

The interaction of ionizing radiation with living matter changes its intrinsic structure (breaking of chemical bonds, recombination ...) differently depending onseveral factors:
- The particle involved
- The linear energy transfer
- The density of energy deposition in the medium
- The total deposited dose.

The cyclotron ARRONAX delivers several types of particles: alpha, deuteron and proton with energies up to 68 MeV.
Dose rates vary between 0.01 and 10 MGy /s allowing us to study and compile data over a wide range of linear energy transfer (LET) and density of energy deposition for each incident ion. These features are unique and complementary to those of other accelerators in France and around the world.

The AX Hall of ARRONAX cyclotron is a room dedicated to experiments. It has several unique features:
- The ability to irradiate using a horizontal beam or a vertical beam
- The possibility, in the vertical beam configuration, to perform on-line time lapse microscopy.
- The possibility to pulse the alpha particle beam (variable inter-pulse duration from 330 ns up to 5 s)

Inside the facility, a cell culture laboratory is present equipped with a PSM, a centrifuge, an incubator, a -80 ° C freezer and various fridges and freezers. A time lapse microscope with controlled atmosphere is available in this room.

Developments in progress:
Innovative tools for dosimetry are being developed:
- The calibration of the optical density of radiosensitive films (including Gafchromic EBT2) as a function of the dose deposited by alpha particles and deuterons will be studied.

- A set of collimators and degraders is being developed in order to obtain spatially uniform beam with minimum energy dispersion.

- A new method for measuring the on-line dose will be implemented based on the measurement of bremsstrahlung emission from the irradiated medium.

- Implementation of time-lapse microscopy in beam.

Teams involved:
Development of radiobiology at ARRONAX is performed by a group of researchers from several laboratories (ARRONAX, CRCNA, ICO and Subatech).

Cross section measurements

Production of radionuclides

The radionuclides that are used for medical applications are generally produced artificially. They are obtained by sending projectiles on targets formed from stable elements in nature.

The choice of the projectile used depends on the decay mode of the radionuclide that is to be produced. For beta + emitting radionuclides, charged particles such as protons will be used, produced by an accelerator. For emitting radionuclides beta-, neutrons, produced in a reactor, are used. For alpha-emitting radionuclides, neutrons from reactors will also be used. Thus we see that accelerators and nuclear reactors are complementary with regard to the production of radionuclides.

The quantity of radionuclides produced during the irradiation of a target is proportional to the number of target nuclei and the flow of the projectile used. The coefficient of proportionality, which contains all the physics of the interaction, is called production cross section. It depends on the energy of the projectile.

To optimize the production of a radionuclide, we must determine the proper energy interval of our projectiles and take into account the fact that for a given projectile energy, several different nuclear reactions are possible. These other nuclear reactions will produce unwanted radioisotopes (contaminants) that must be removed later. It is therefore important during the optimization phase of irradiation parameters to see how we can avoid the production of these contaminants in order to simplify the subsequent work of radiochemical purification.

The production cross sections

This optimization work is done using the production cross sections of the different isotopes.

These cross sections are available, when they are known, in data bases (NNDC). For some reactions, cross sections are not known precisely and it is necessary to measure them again. To this end, a program of cross sections measurement is implemented at Arronax using the "stacked foils » technique.

Research partnerships

It is the policy of Arronax to propose and get involved in research partnerships. Purely academic or academia/industry partnerships are considered when their object is consistent with the original missions of Arronax.
Accordingly, Arronax is currently a partner of the Région Pays de la Loire NucSan (Nuclear Technologies for Health) research project, which, in addition to the Arronax GIP, includes 10 laboratories of Nantes and Angers, and of the "Investissements d'Avenir" laboratory of Excellence IRON (Innovative Radiopharmaceuticals for Oncology and Neurology), which brings together laboratories and clinical centers from Nantes, Angers, Tours, Caen, Toulouse, Orléans, Rennes and Strasbourg.
The ArronaxPlus equipment of excellence of the "Investissements d'Avenir" program another example of scientific and technological consortium, managed by Arronax with the goal of offering a coordinated group of technological platforms, from chemistry to clinical nuclear medicine, to help in the development of radiopharmaceuticals in all medical domains including oncology, cardiology and neurology.
Arronax is also a partner in two government subsidized academia/industry partnership: Theranean and QuantiCardi. These two projects are funded through the FUI (Fonds Unique Interministériel) managed by the Oséo agency:

- **Theranean** (Therapy through Neutron Activation using Nanoparticles) aims at developing a neutron activation device driven by a highly intense 70 MeV proton beam delivered by the Arronax cyclotron to activate holmium nano and microparticles for the treatment of cancer by brachytherapy. It is coordinated by the AAA company (Saint-Génis-Pouilly, France) and involves Subatech, the Nano-H S.A.S. company, the University Claude Bernard Lyon 1, the INSA-MATEIS (CNRS) laboratory, in collaboration with the Hospices Civils de Lyon.
- The objective of the **QuantiCardi project** is the preindustrial development of an integrated solution consisting in innovative components dedicated to the imaging of myocardic perfusion by Positron Emission Tomography (PET) to measure myocardic blood flow and the coronary reserve. A subnormal coronary reserve is symptomatic coronary insufficiency, disease responsible for 30 50% of death by cardiopathy in Europe. The project is headed by Lemer PAX company and involves Keosys, Subatech, IRCCyN-IVC and the CRCNA.

A large collaborative project, aiming at creating a national academic and industrial cluster in molecular radiotherapy, is being developed with Atlanpole Biotherapies in response to the "Projets Structurants des Pôles de Compétivité call for tender of the"Investissements d'Avenir".

history

After submission of a scientific project in 2001, the cyclotron Arronax reached full power on October 25, 2010 and has been operational since 2011.

2001: the scientific file written by Jacques Barbet, Jean-François Chatal, Jacques Martino and Yves Thomas is presented to scientific authorities and potential funders
May 3, 2002: after scientific expertises from CNRS, Inserm, CEA and Universities, the Ministry of Research formalizes a scientific evaluation of the submitted document
2002-2003: A study of technical and economic feasibility, co-funded by the Regional Council of Pays de la Loire and the State (Prefecture) and led by the University Hospital of Nantes, confirms the technical feasibility and more accurately assesses the costs of investment and operation
December 18, 2003: The project, led by the University of Nantes and supported by the Minister Francois Fillon and the President of the Regional Council of Pays de la Loire, Jean-Luc Harousseau, receives a favorable advice of the Interministerial Committee for the Planning and Development of the Territory (CIADT)
July 9, 2004: Jacques Auxiette, newly elected President of the Regional Council of Pays de la Loire, supports and decides to launch the project to be installed on the northern site of the Nantes University Hospital, on land made available by the hospital. The project ownership is delegated by the State to the Region Pays de la Loire during the building period.
End of 2004 : the financial closure of the estimated investment of € 36.9 million is provided with the following distribution
State: € 8.4 million
Region Pays de la Loire: 14.260 M €
European Funds: 7,490 M €
French
Poitou Charente Brittany Regional Council: 0.750 M €
Pays de la Loire Regional Council: 0,500 M €
General Council of Loire Atlantique: 2.00 M €
General Council of Maine et Loire: 0,300 M €
Nantes Métropole: 3.00 M €
Angers Loire Métropole: 0,200 M €

2005: definition of the equipments and award of public contracts
7 December 2006: laying of the first foundation stone
March 2008: delivery of the cyclotron, then assembly, tests and adjustments
November 7, 2008: Inauguration of the cyclotron and Arronax site in the presence of Prime Minister François Fillon, President of Region Jacques Auxiette, Deputy Mayor of Nantes Jean-Marc Ayrault, Mayor and Senator of Saint Herblain Jean-Charles Gautier

Inauguration le 07/11/2008

de gauche à droite:
J. C. Gautier, Sénateur-maire de St Herblain
J. Auxiette, Président du Conseil régional des Pays de la Loire
Y. Lecointe, Président de l'Université de Nantes
J. Martino, Directeur du GIP Arronax
F. Fillon, Premier Ministre

25 October 2010 :: the cyclotron reaches full power for 24 hours
2011: The cyclotron produces Strontium-82 in routine and R/D allows for the production of copper-64, Ge-68, Scandium-44 and radiolysis, radiobiology and physics experients.

The Arronax GIP

From a statutory point of view, Arronax is a « Groupement d'Intérêt Public » (GIP). Arronax is thus a public research institute with a private accounting. It is a kind of mixed economy system that allows it both to cooperate as equal with public research partners and to act as a company with respect to industrial customers (Siret: 13000411200012, DUNS: 295659028).

A GIP is a grouping of several public and private members, linked by a written agreement, approved by the State. Members of the Arronax GIP are the State and the Region Pays de la Loire, large national organizations of research, higher education and research institutions, hospitals. Members are gathered in an Administration Council which elects its president and vice president.

The Arronax GIP is constituted for a period of 25 years, renewable. First, it supports the operation of the cyclotron Arronax (Accelerator for Research in Radiochemistry and Oncology at Nantes AtlantiX), which is a large platform with an international Research and Development objective. The responsibility for management lies with the director of the GIP, who signs research contracts and service contracts with national or international, public or industrial partners.

Staff members working for the GIP are, researchers, engineers, technicians provided by its members, and employees of the GIP. Some counselors, and several members of the partnership laboratories cooperate regularly on the platform. Depending on the time period, the number of staff members is between 30 and 40.

Scientific Board members

The mission of the International Scientific Council of ARRONAX is to advise the management of the GIP in its strategic choices.

It meets once a year in the fall since 2004. It consists 14 members including 4 technical committee members:
■ **Professor Suresh Srivastava**, Professor of Radiology at the Medical School of the State University of New York at Stony Brook, director of Radionuclide and Research Division Radiopharmaceutical (R & RR) of the Medical Department at Brookhaven National Laboratory, Upton, New York (USA), President.
■ **Professor Marion de Jong**, Professor of Nuclear Biology, Erasmus MC, Rotterdam (Netherlands), Vice-President.
■ **Professor Patrick Bourguet** (Centre Eugène Marquis, Rennes), Professor of Biophysics and Nuclear Medicine, University of Rennes 1 (France).
■ **Professor Patrick Cozzone**, Professor of Biophysics at the Faculty of Medicine of Marseille, head of department at the Hospital La Timone, CHU Marseille, Chair of Biophysics at the Institut Universitaire de France, founder and directorof the Centre for Magnetic Resonance Biological and Medical CNRS (France).
■ **Professor Peter Ell**, Nuclear Medicine, Senior Investigator National Institute for Health Research (NIHR) and Professor Emeritus at University College London (UK).
■ **Professor Denis Guilloteau**, professor of pharmaceutical biophysics, Director of Inserm U619 "Dynamics and pathology of brain development," Director of Nuclear Medicine, CHU Bretonneau, Tours (France).
■ **Dr. Ulli Köster**, nuclear physicist, radioisotope production at the Institut Laue Langevin (Grenoble) and ISOLDE (CERN).
■ **Professor Jörg Kotzerke,** Professor of Nuclear Medicine, Director of the Department of Nuclear Medicine, University Hospital of Dresden (Germany).
■ **Dr. Bernard Laune**, Accelerators Physicist , Head of Mission for the Pole IN2P3 Accelerators CEA / CNRS, Technical Coordinator of the Accelerators Division of the Institute of Nuclear Physics of Orsay, Member of the National Programme for Research in Radiation Therapy (France).
■ **Professor Jacques Martino**, nuclear physicist, director of IN2P3 (CNRS), Paris (France).

Additional members from the Technical Committee:
■ **Professor Michel Chérel**, Professor of Biophysics, Pharmacist, Doctor of the University of Nantes, Centre for Research in Cancer Nantes-Angers, Nantes (France).
■ **Dr. Ferid Haddad**, Senior Lecturer at the University of Nantes, Deputy Director of GIP ARRONAX, Doctor of Physics, Subatech, Nantes (Nantes).
■ **Dr. Vincent Metivier**, Assistant Professor at the Ecole des Mines de Nantes, Doctor of Physics, Subatech, Nantes (France)
■ **Docteur Freddy Poirier**,Research ingineer at the CNRS, Doctor in accelerator physics, ARRONAX, Nantes(France).

The Arronax facility

The Arronax plant is installed in a 4000 m^2 building, located 1 rue Aronnax, Saint Herblain, in the suburbs of Nantes, near the north branch of the University Hospital. This building is built on a 10 000 m^2 plot of land in the Bio-Ouest Laënnec technology park.

The building is split into 3 parts:
• A conventional area (blue on plan) comprising offices, a conference room, the cyclotron control-command room, an electrical supply room and standard service areas (heating equipment, ventilation system, compressor, etc.).
• A controlled area (in yellow) in which all nuclear activities are performed. Here are the cyclotron, its reaction shields, its utilities, the various laboratories, storage areas for nuclear waste, target processing areas (hot cells, etc.)
• A technical space (in green), to allow for growth in activity, or for use by partners and R/D consortiums developed by Arronax.

Research units

Aerosol Physics and Metrology Laboratory (LPMA)

The Aerosol Physics and Metrology Laboratory (LPMA) has long been involved in developing aerosol science in France in conjunction with various academic and industrial partners. It is located at the CEA site in Saclay (Essonne, France). It is directed by François Gensdarmes.

Summary

Context and research themes

The LPMA carries out experimental research, studies and technical assessments related to the characterisation of source terms at facilities, in normal and accident situations.

This involves:

- basic research and studies, as well as applied studies, on aerosol physics and metrology, and on air contamination by natural sources, both radioactive and non-radioactive, and anthropogenic sources (formation, physical and chemical changes, and transfer, mainly via containment barriers);
- research and studies on the physics and chemistry of phenomena likely to occur during an accident situation at a nuclear facility;
- applying the results obtained to define, analyse and develop the related measurement devices, especially atmospheric samplers;
- testing devices used to measure radioactive contamination.

Research axes

Main areas

To fulfil its tasks, the LPMA develops knowledge in three main areas :

- Aerosol physics: sources (suspension, nucleation), changes in space and over time (condensation, evaporation, agglomeration, electrical charge) and aerosol deposition (deposition on surfaces, transfer via ducts).
- Aerosol metrology: measuring physical properties (aerodynamics, diffusion, electrical, aggregate morphology) and sampling methods (performance, use strategy).
- Purification of radioactive gases such as iodine and tritium.

Major research topics currently studied at LPMA

- Particle suspension by air flow or by the fall of potentially dispersible materials (powders, contaminated objects, liquids), suspension during dismantling operations.
- Characterisation of aerosols emitted during a fire situation and the suspension of contaminants emitted by materials subject to fire.
- Nanoparticles (characterising emissions, specific metrology, transfer and deposition, containment and filtration)
- Sampling aerosols for workstation monitoring.
- Radon, thoron and decay product metrology.
- Assessing the performance of air contamination monitors.
- Trapping radioactive iodine and tritium on activated carbon and zeolite filters.

Specialties and researchers

Services provided

- Assessment and characterisation of α, β et γ radioactive contamination measurement equipment.
- Verification and calibration of radon measurement instruments.
- Measurement and characterisation of particle releases at industrial facilities.

Researchers

François Gensdarmes, head of laboratory
Sylvain Bondiguel, technician
Sylvain Fauvel, engineer
Guillaume Davenne, technician
Zakaria Mana, engineer
Nathalie Michielsen, research engineer
Céline Monsanglant-Louvet, research engineer

Publications

LEMAC's publications (till 2003) recorded in this website

LPMA's publications (since 2003) recorded in this website

The co-authored book “History and Reviews of Aerosol Science” (2005) includes a chapter on the research carried out by LPMA and its partners between 1980 and 2001.

The table of contents

Contact

Francois Gensdarmes, head of laboratory

IRSN/PSN-RES/SCA
Aerosol Physics and Metrology Laboratory
91191 Gif-sur-Yvette Cedex
France

By phone: +33 (0)1 69 08 55 06

François-Xavier Ouf, engineer
Samuel Peillon, engineer
Sébastien Pontreau, technician
Stéphane Roussel, technician
Audrey Roynette, technician
Philippe Sillon, technician

Facilities and techniques

Facilities

Icare, test bench for performing tests using calibrated radioactive aerosols, with caesium or plutonium markers;

Baccara, test bench for research on the metrology of radon.

Lec, ISO Class 8 dust-monitoring cleanroom.

Bise, air duct for research on the suspension of contaminants by air flow.

Cepia, test chamber for research on the performance of personal and environment aerosol samplers.

Measuring equipment

For aerosol characterisation :

Condensation Nuclei Counter (CNC), Nephelometer and Optical Counters (COP),

Scanning Mobility Particle Sizer (SMPS), Engine Exhaust Particle Size Spectrometer (EEPS), Differential Mobility Spectrometer (DMS),

Diffusion battery, Aerodynamic Particle Sizer (APS), Aerosizer, Electrical Low Pressure and Cascade Impactors (ELPI, Andersen), Coulter Counter,

Tapered Element Oscillating Microbalance (TEOM).

For aerosol generation:

Atomizers, Piezoelectric ceramics, Vibrating Orifices, Rotating brush, Fluidized bed, Vortex Shaker, Voltage pulse generator, Evaporation/condensation generator.

For radioactivity:

MINI 20 proportional counter, □, □ and □ spectrometry, Measurement of the activity concentration of radon

Partnership and research networks

LRGP (CNRS and Nancy University joint laboratory),
CORIA (Rouen University, CNRS and INSA joint laboratory),
LISA (Paris-Est Créteil University, Paris Diderot University and CNRS joint laboratory),
CERTES (Paris-Est Créteil University),
LPGP (Paris-Sud University and CNRS joint laboratory),
INRS,
CEA,
LNE,
AREVA,
EDF,
ONERA

Alpha-emitter Astatine-211; Production and Utilization

Laboratory works and implementation

National Institute of Radiological Sciences (NIRS)
National Institutes for Quantum and Radiological Science and Technology (QST)

Dr. Kotaro NAGATSU

Candidate radionuclides for RNT

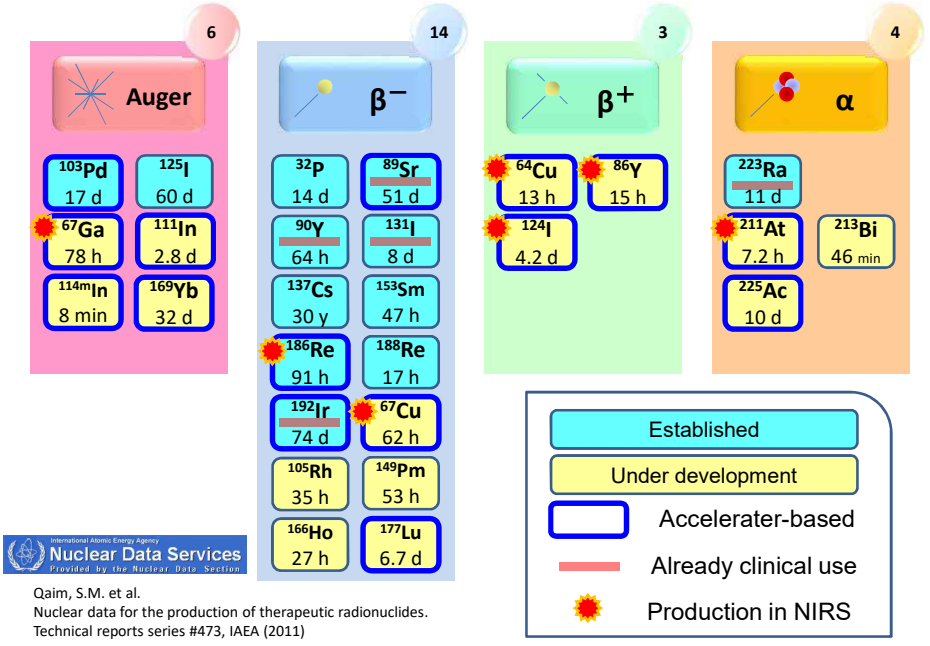

Nuclear Data Services

Qaim, S.M. et al.
Nuclear data for the production of therapeutic radionuclides.
Technical reports series #473, IAEA (2011)

Production; Results

Gamma

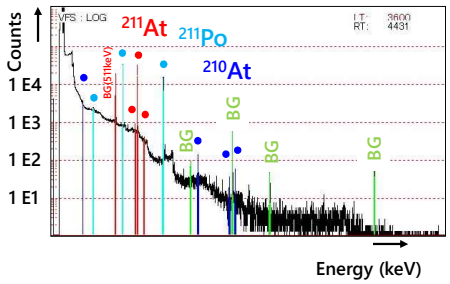

Alpha

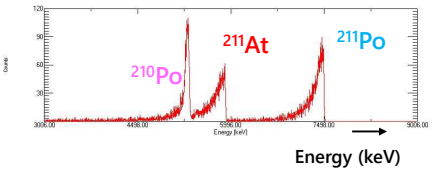

120 h from EOB (~17-$T_{1/2}$ of ^{211}At)

Items	Results
Bombardement	α 28.5 MeV 13 eμA × 2 h
Yield at target	600 μCi/μAh*
Yield	9.5±0.2 mCi**
Purity	>99% (+^{211}Po) (@5 h from EOB)
^{210}At/ ^{211}At	0.0022% @ EOB
^{210}Po mix rate	0.32 nCi/μAh (0.67 ppm of ^{211}At**)
Purification time	~1.5 h

* decay corrected
** decay uncorrected

Recent Condition
12 eμA x 3 h
= 12–14 mCi/ $CHCl_3$ 0.5 cc
@1h EOB

RI Production by Accelerator AVF-930

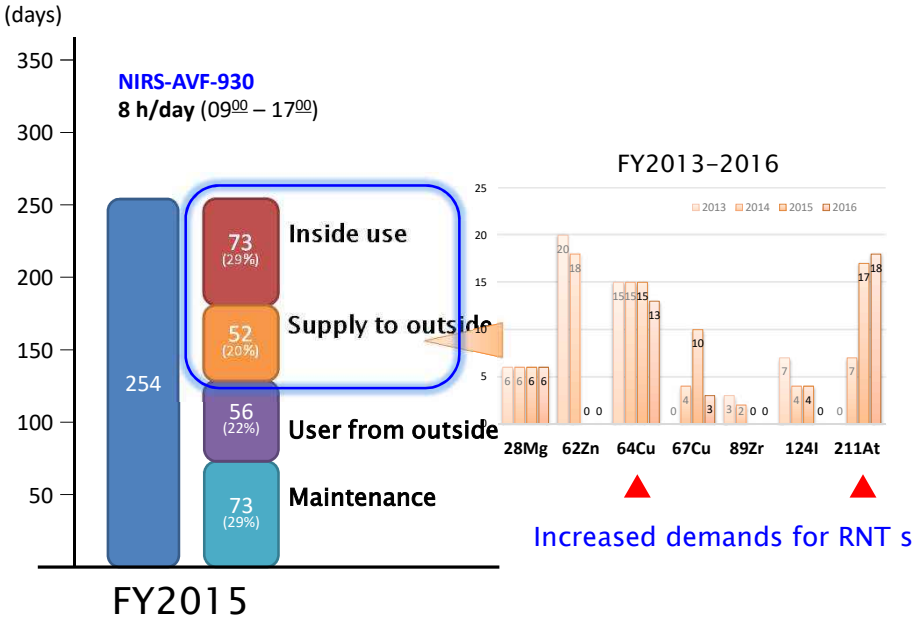

Increased demands for RNT s

Fukushima Medical University
Fukushima Global Medical Science Center
Targeted Alpha Therapy

FMU website

Radionuclide Therapy Ward in Medical Center

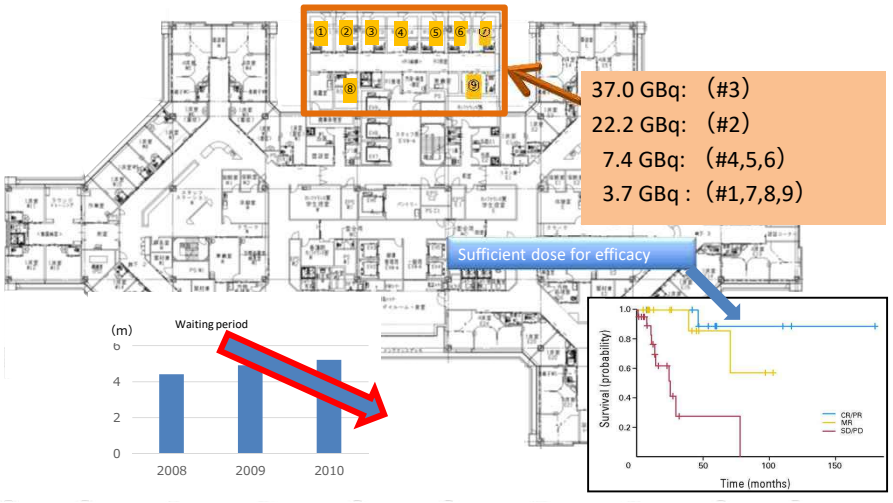

Two cyclotrons for production of radionuclides

HM-20S

Proton	Energy	20 MeV
	Current	150 μA
Deuteron	Energy	10 MeV
	Current	50 μA
Max. Targets		8 (4/Port)
Power		55 kW

MP−30

Proton	Energy	15 - 30 MeV
	Current	100 μA
Deuteron	Energy	16 MeV
	Current	50 μA
Alpha	Energy	32 MeV
	Current	30 μA
Max. Targets		Depend on Requirement
Power		150 kW

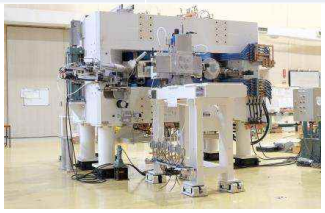

Cyclotron (MP-30, Sumitomo Heavy Industries, Ltd.)

Acceleration energy

Proton	15 - 30 MeV
Deuteron	8 - 15 MeV
Alpha	32 MeV

For Nuclear Reaction of

(p,x) (d,x) (α,x)

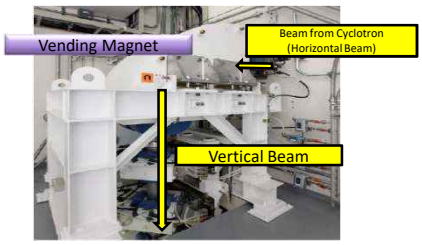

MP-30 Cyclotron

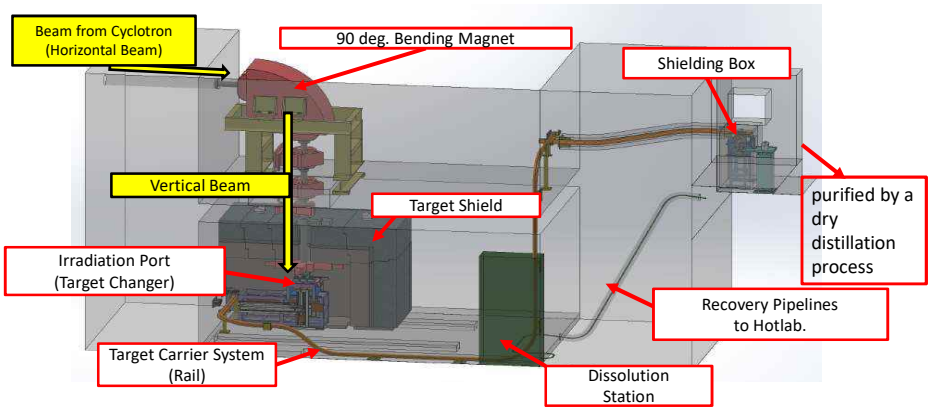

Special Features:

Vertical Irradiation System & Automatic Target Transport System

Preclinical facility for study with radionuclide

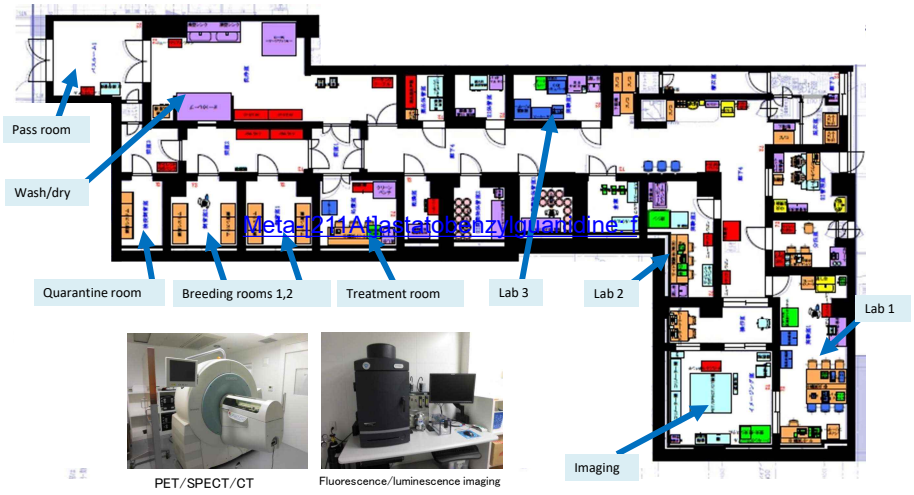

Production group of α-emitter in Europe

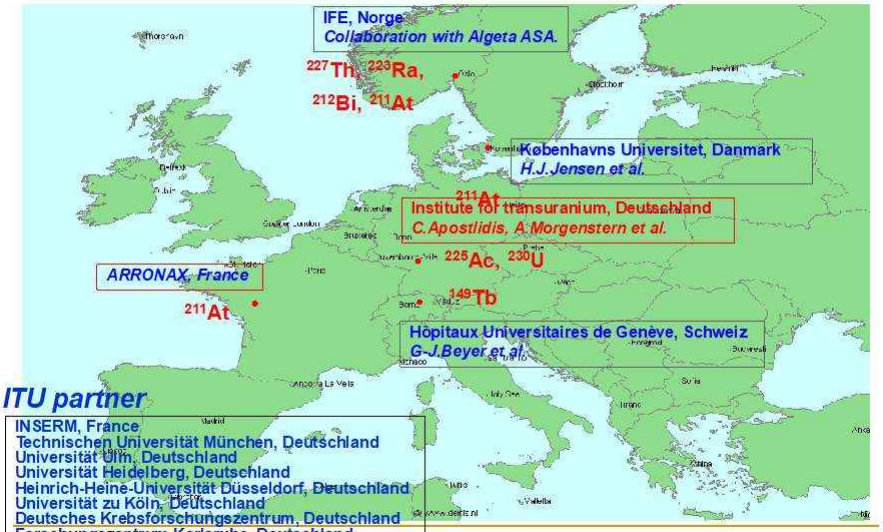

ITU partner

INSERM, France
Technischen Universität München, Deutschland
Universität Ulm, Deutschland
Universität Heidelberg, Deutschland
Heinrich-Heine-Universität Düsseldorf, Deutschland
Universität zu Köln, Deutschland
Deutsches Krebsforschungszentrum, Deutschland
Forschungszentrum Karlsruhe, Deutschland
Universiteit Gent, Belgie
Virga Jesseziekenhuis, Belgie
Universitätsspital Basel, Schweiz

Ruusia, Poland

Production facilities of α-emitter in Japan

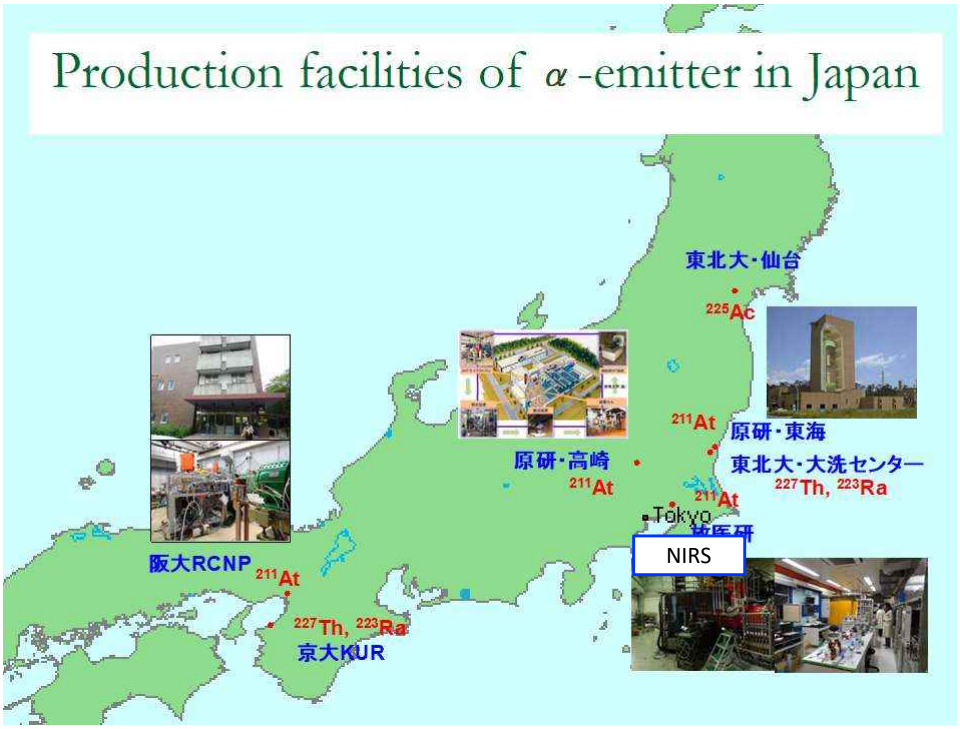

参考文献

[1] 細野眞 （2013） α線内用療法の現状と展望，Isotope News, No.711, 2-7

[2] Dekempeneer, et al. （2016） Targeted alpha therapy using short-lived alpha-particles and the promise of nanobodies as targeting vehicle

[3] 日本アイソトープ協会 （2017） アイソトープ等流通統計 2017（抜粋）

[4] IAEA Technical Report Series No.15-A Basic Toxicity Classification of Radionuclides (1963) （抜粋）

[5] Sophie Poty, et al. Alpha Emitters for Radiotherapy: Basic Radiochemistry to Clinical Studies – Part 2. Journal of Nuclear Medicine, published on March 1, 2018 as doi:10.2967/jnumed.117.204651 (2018)

[6] George Sgouros et al. Radiobiology and Dosimetry of a-Particle Emitters for Targeted Radionuclide Therapy*. THE JOURNAL OF NUCLEAR MEDICINE・Vol. 51・No. 2・February 2010

[7] Guérard F, Gestin JF, Brechbiel MW. Production of [^{211}At]-astatinated radiophamaceuticals and applications in targeted a-particle therapy. Cancer Biotherapy and Radiopharmaceuticals （2013） DOI: 10.1089/cbr.2012.1292

[8] Radioactive waste management. IRSN Thematic series （抜粋）

展望 TENBO

α線内用療法の現状と展望

細野　眞
Hosono Makoto
（近畿大学高度先端総合医療センター）

1　はじめに

放射性同位元素（RI）内用療法（内照射療法，核医学治療）とは非密封放射性核種による内部放射線治療であり，放射性核種を含んだ薬剤を病巣（がん，あるいは良性疾患）に選択的に取り込ませて放射線を照射するものである。英語ではUnsealed radionuclide therapy，Radionuclide therapy，Targeted radionuclide therapyなどと呼ばれることが多い。

従来は，RI内用療法にβ線を放出する核種が主として用いられており（同時にγ線を放出する核種もある），甲状腺機能亢進症・分化型甲状腺癌に対する^{131}I（ヨウ素）は1940年代から臨床に利用されてきた歴史を持つ[1)]。また，褐色細胞腫・神経芽腫など神経内分泌腫瘍に対する^{131}I-MIBG（カテコラミン類似体）も国内外で約30年来用いられてきた[2)]。これらは組織の特異的な取込み機序を応用した古典的かつ優れた分子標的療法と言える。また，転移性骨腫瘍の疼痛緩和療法として向骨性放射性薬剤が1990年前後から世界的に広く使われ，主なものは，^{89}Sr（ストロンチウム，販売名メタストロン），^{153}Sm（サマリウム）-EDTMP（販売名Quadramet）である[3)]。さらに，B細胞性非ホジキンリンパ腫治療薬としてRI標識抗CD20モノクローナル抗体が1990年代に入って登場し，米国で2002年に^{90}Y（イットリウム）-ゼヴァリンが，2003年に^{131}I-Bexxar（ベキサール）が相次いで認可された[4)]。2010年前後からは，ソマトスタチン受容体を発現する神経内分泌腫瘍に対するRI標識ソマトスタチンアナログ治療がPeptide receptor radionuclide therapy（PRRT）として海外で盛んに行われるようになり，^{177}Lu（ルテチウム）-DOTA-[Tyr3]-octreotate（^{177}Lu-DOTATATE）などが代表的な薬剤である[5)]。

現在（2013年6月時点），日本国内で保険収載されている内用療法薬剤は，甲状腺機能亢進症・分化型甲状腺癌に対する^{131}I，固形癌骨転移疼痛緩和の^{89}Sr（2007年保険収載），B細胞性非ホジキンリンパ腫に対する^{90}Y-ゼヴァリン（2008年保険収載）である。

最近，α放出核種であるRadium-223（^{223}Ra，塩化ラジウム-223，Xofigo®，以前はAlpharadinと呼ばれていた）が，転移性骨腫瘍に対する放射性薬剤として登場し，症状を緩和し，骨関連事象（病的骨折など）の出現を遅らせ，生命予後を延長し，さらに副作用の少ない優れた抗腫瘍薬として，欧米での第Ⅲ相臨床試験の結果が2011～12年にかけて報告され，2013年5月15

表 1　臨床利用可能な α 核種の例

核種		半減期	娘核種		崩壊系列	元素分類
^{223}Ra	ラジウム	11.4 日	^{219}Rn		アクチニウム系列	アルカリ土類金属
^{211}At	アスタチン	7.21 時間	^{211}Po	^{207}Bi	アクチニウム系列	ハロゲン
^{212}Bi	ビスマス	60.6 分	^{212}Po	^{208}Tl	トリウム系列	窒素族
^{225}Ac	アクチニウム	10.0 日	^{221}Fr		ネプツニウム系列	アクチノイド
^{213}Bi	ビスマス	45.6 分	^{213}Po	^{209}Tl	ネプツニウム系列	窒素族
^{149}Tb	テルビウム	4.15 時間	^{149}Gd	^{145}Eu	—	ランタノイド

日に米国食品医薬品局（FDA）の承認を得たことから，^{223}Ra を含めた α 放出核種による内用療法に注目と期待が集まるようになった。本稿では，α 放出核種による内用療法について概説する。

2　なぜ α 放出核種による内用療法か

β 放出核種による内用療法が前述のように ^{131}I による甲状腺癌治療，^{90}Y 及び ^{131}I 標識抗体による非ホジキンリンパ腫などにおいて有効であることは議論の余地がないが，様々ながんの治療において内用療法の果たす役割はまだ限定的であると言わざるを得ない。RI 標識抗体による放射免疫療法にしても数多くのがんに対してこの四半世紀試みられたが，いまだに固形癌に対して有効性を確立したものはなく，実用化に至ったのは非ホジキンリンパ腫に対するものだけである。そこで内用療法の有効性を高める研究が精力的に行われ，がんに親和性の高い新規化合物の開発とともに，核種自体についても，様々な物理学的化学的性質を持つ核種が内用療法への応用を試みられ，その中で α 放出核種も取り上げられた[6]。また，世界各地の原子炉や加速器で生成する核種を医療に応用しようという動きも自然なことであった。**表 1** に臨床利用可能な α 核種の例を示す。

α 線の大きな特徴は，高い線エネルギー付与（linear energy transfer：LET）と短い飛程にある。例えば，転移性骨腫瘍治療で用いられている代表的な核種である ^{89}Sr や ^{153}Sm の β 放出核種と α 放出核種である ^{223}Ra を比較すると（**表 2**），^{223}Ra の放射線のエネルギーは ^{89}Sr に比べて数十倍高く，α 線の LET は β 線の LET のほぼ 400 倍（80 keV/μm vs 0.2 keV/μm）である。このように α 線の LET が高いため，DNA 二重鎖切断を起こして損傷の修復がしにくいので，生物学的効果比（RBE）も高く，RBE は用いる指標によって異なる値を示し得るが，α 線の細胞不活化作用に関する RBE は 3.8 であるとの報告がある。なお，ここで留意すべきは，α 線の放射線加重係数が 2007 年 ICRP 勧告等で 20 とされているが，それは放射線防護の見地から設定されている値であり，RBE とはかなり大きく違う点である。α 線の LET が高いことから，酸素増感比（OER）が小さいため低酸素細胞にも有効で，細胞周期依存性が小さいため放射線感受性の低い S 後期細胞にも有効と考えられる。

表 2　向骨性放射性同位元素の物理学的性質[13]

核種	半減期（日）	放出放射線当たりの平均エネルギー（MeV）	組織中の平均飛程（mm）
^{89}Sr	50.5	0.58	2.4
^{153}Sm	1.9	0.22	0.55
^{223}Ra	11.4	27.4*	＜0.10

* 子孫核種の放出エネルギーを含む

また α 線の飛程は非常に短く，例えば ^{223}Ra で 100 μm 以下と，細胞数個分の長さである（**図 1**）。このため α 放出核種が腫瘍にうまく局在すれば，周囲の正常組織の不要な被ばくが少なくなる。その一方で，α 放出核種を腫瘍部位

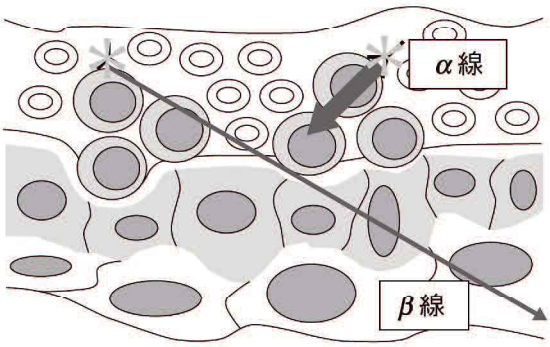

図1　組織中のα線とβ線
α線の飛程は数十μmと標的細胞に留まるが，β線は正常組織にも到達する

に選択的に運ぶドラッグデリバリーの手法が不可欠である。なぜならば，β放出核種の場合ならば，組織内の飛程が数mmあるので腫瘍組織に結合したβ放出核種が，血流や結合部位が少ない腫瘍組織をも照射できる（クロスファイヤー効果）が，α放出核種は飛程の短さゆえに，それを期待できないからである。後述の^{223}Ra（塩化ラジウム-223）はカルシウムと同様に核種そのものが骨に結合して標的部位に照射するが，多くの場合は核種と標的をマッチさせるドラッグデリバリーの手法が不可欠であり，その1つが腫瘍に特異的なモノクローナル抗体に結合し，それを体内に投与し，抗体の力を借りて腫瘍組織まで運搬する放射免疫治療である。1996年にBismuth（ビスマス）-213標識抗CD33抗体が骨髄性白血病に使用されたのが，α放出核種標識抗体がヒトに投与された初めての例とされる[7]。

このような内用療法におけるα放出核種の応用は，外部放射線治療の分野での粒子線の応用にシンクロするとも考えられる。

3　塩化ラジウム-223による骨転移治療の現状

最近，α放出核種である^{223}Ra（塩化ラジウム-223，Xofigo®）が，転移性骨腫瘍に対する抗腫瘍薬としてノルウェーのAlgeta社（www.algeta.com）によって開発された。^{89}Srが骨転移疼痛緩和の対症療法薬であるのに対して，^{223}Raは抗腫瘍薬として生命予後の改善を示す。現在Algeta社とバイエル社とのパートナーシップによって国際市場への導入が進められている。

元素としてラジウムはカルシウム，ストロンチウムと同様のアルカリ土類金属であり，骨に親和性がある。^{223}Ra（半減期11.4日，α：5.716 MeV）は骨代謝の亢進した骨転移部位に集積して，病巣を照射する。そのα線の飛程が組織中で100 μm以下と短いため骨髄の被ばくが少なく，腫瘍に選択的に高い線量を与えることができる。^{223}Raから娘核種の^{219}Rn，^{215}Po，^{211}Pb，^{211}Bi，^{207}Tlと壊変を経て安定核種^{207}Pbに至るまでα線とともにβ線，γ線も放出する（**図2**）。^{223}RaはActinium-227（アクチニウム，半減期21.77年）から取り出すことができ，半減期11.4日と医薬品として製造して世界中に運搬するのにも適し，医療現場でも扱いやすい。

^{223}Ra開発の経緯に関しては，2005年に乳癌と前立腺癌の骨転移症例を対象にした第Ⅰ相臨床試験の結果が報告され[8]，2007年に前立腺癌の骨転移症例を対象にした第Ⅱ相臨床試験の結果が報告された[9]。さらに，2008年から実施された第Ⅲ相臨床試験ALSYMPCA（ALpharadin in SYMptomatic Prostate Cancer）で去勢抵抗性（ホルモン抵抗性）前立腺癌多発骨転移症例における大規模な臨床試験が欧米で実施され，全生存期間を延長し，骨関連事象（病的骨折など）発現までの期間を延長することが2011～12年にかけて公表された[10,11]。報告によれば，全生存期間中央値は^{223}Ra群の14.9か月と全く治療効果のないプラセボ群の11.3か月，骨関連事象発現期間中央値は^{223}Ra群の15.6か月，プラセボ群の9.8か月と^{223}Raによって有意な延長を示した。一方副作用に関しては，α線は生物学的効果が大きいので副作用が強いのではないかとの予想もあるかもしれないが，実際には軽微であり，grade 3～4の好中球減少は1.8%，grade 3～4の血小板減少は4.1%と骨髄抑

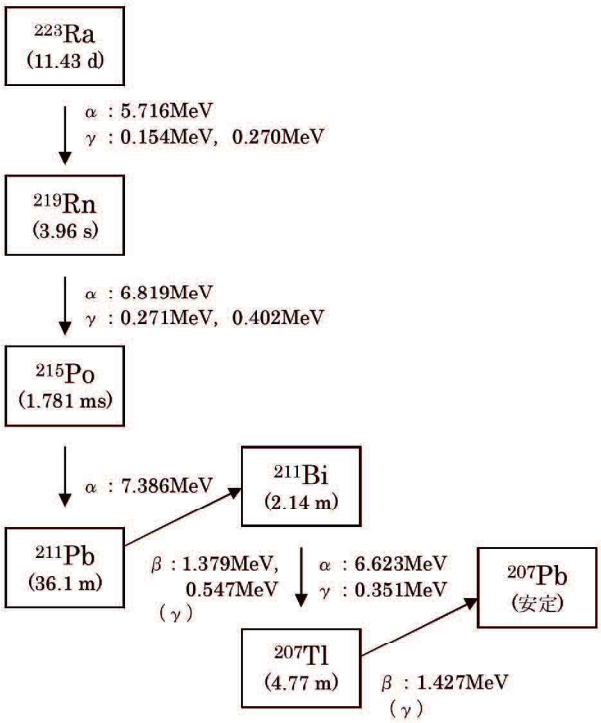

図 2　^{223}Ra 壊変系列

制が軽度にとどまり，ほかには悪心・嘔吐・下痢が主なものであった。この報告を受けて，欧米で去勢抵抗性前立腺癌多発骨転移に対する医薬品としての申請がなされ，米国では 2013 年 5 月 15 日に承認された。今後の展開として，乳癌やその他の固形癌への適応も検討され，また ^{223}Ra と化学療法を併用してより高い治療効果を得ることも考えられている。

α 放出核種である ^{223}Ra の医療の国内導入の可否に関しては，2010 年以前には懐疑的な見方があった。それは，免除レベル取り入れによる法令改正（放射線障害防止法 2005 年 6 月 1 日施行）以前には α 放出核種というだけで，定義数量が 4 群の中で最も厳しい 3.7 kBq（第 1 群）であったり，^{226}Ra（半減期 1,600 年）/^{222}Rn（ラドン，半減期 3.824 日）から半減期が長いのではないかとの連想があったりしたことが原因かもしれない。法令改正前の定義数量（第 1 群）3.7 kBq は，法令改正後は，下限数量 100 kBq となり取り扱いやすくなった。いずれにしても，^{223}Ra はもともと医療法施行規則に基づく告示の別表にも掲載され，医療法の枠内で用いることのできる核種である。

日本核医学会は，ワーキンググループ「α 線を用いたがんの最小侵襲治療法のあり方について」（代表 井上登美夫）において 2008 年頃から α 放出核種の内用療法への応用を検討し[12]，また平成 22 年度厚生労働科学研究費補助金研究「医療放射線の安全確保と有効利用に関する研究」（研究代表者 細野　眞）は，^{223}Ra の有効性と放射線防護の要件を検討して，^{223}Ra を国内医療へ導入するための環境整備を進めた[13]。また ^{223}Ra 内用療法実施において，管理は通常は光子を測定して行うので，^{223}Ra から放出される光子に対するサーベイメータ等の計測器の特性を検討することが重要である[14]。

4　α 線内用療法の展望

α 線内用療法を推進するに当たって幾つかの重要な要素があるが，放射線生物学，核種製造と放射性薬剤合成，線量評価の各分野の研究が代表的なものであろう。

放射線生物学の分野では，α 線の生物学的効果について取り組むべきテーマは多く，^{223}Ra を例にとると，なぜ ^{223}Ra が転移性骨腫瘍に対して効くのかについては解明されていないことも多い。α 線の飛程が組織中で 100 μm 以下であるので，骨の沈着部位から腫瘍細胞に十分に照射されるのかどうかという疑問がある。ある程度はクロスファイヤー効果が寄与しているのであろう。また，α 線照射によって組織中に産生されるサイトカインが直接照射を受けない腫瘍細胞にも作用を与えるという Bystander effect の関与も考えられている。

核種製造と放射性薬剤合成の分野では，加速器や原子炉から効率的に α 放出核種を製造する技術が重要であるのはもちろんであるが，α 放出核種固有の性質，つまり安定核種になるまで複数の壊変を伴い，元素の物理学的化学的性質が遷移するという点に対応して，元素の性質

が変化しても安定にリガンドに結合する手法の開発が不可欠である。通常のキレートでは核種の化合物への安定な結合が得られにくいので，リポソームを使ってα放出核種を化合物に結合させる手法などが試みられつつある[15]。

線量評価として，放射線生物学的な組織内での微細な評価（microdosimetry）が基礎となるが，イメージングに基づいて生体内での核種の分布・動態を確認し[16]，適切な量と種類の放射性薬剤を処方することも，これからの内用療法に不可欠な要素である。今後，個別化医療を実現するためにイメージングを用いた患者さんごとの線量評価が求められるようになるであろう。

このようなα線を含めて内用療法の諸課題について世界中の専門家たちが一堂に会して熱い議論を行っているのが，International Symposium on TArgeted Radiotherapy and Dosimetry（ISTARD）であり，2012年10月のヨーロッパ核医学会（EANM，European Association of Nuclear Medicine，開催地ミラノ）の際に4th ISTARDが同時開催された。2004年，2006年にはそれぞれヘルシンキ，アテネでEANMと合わせて，2009年にはトロントでSNM，Society of Nuclear Medicineと合わせて開催された。最先端の内用療法を知る上で欠かせない学会である。ISTARDには様々な分野の専門家が参加しているが，とりわけ線量評価を担っている医学物理の専門家が存在感を発揮しつつある。

5 まとめ

α線内用療法は，科学の進歩がもたらした新しいがん治療として注目され，その開発や実施には，医療従事者はもちろん，放射線生物学，核種製造と放射性薬剤合成，線量評価などの高度な分野の専門家が密接に連携することが必要であり，産業界や行政を含めた多数の関係者を巻き込む巨大プロジェクトとして，社会に大きなインパクトを与えようとしている。

【謝辞】

本稿の執筆に当たり，α核種の国内医療導入に多大なご尽力をいただいた，横浜市立大学大学院 井上登美夫先生（現 日本核医学会理事長），近畿大学原子力研究所 伊藤哲夫所長，京都医療科学大学 遠藤啓吾学長，日本アイソトープ協会 池渕秀治先生，中村吉秀氏，中村伸貴氏，柳田幸子氏，山田崇裕氏，北岡麻美氏に深謝いたします。

参考文献

1）Higashi, T., Kudo, T., Kinuya, S., Radioactive iodine（131I）therapy for differentiated thyroid cancer in Japan: current issues with historical review and future perspective, *Ann Nucl Med*, **26**, 99−112（2012）
2）Grunwald, F., Ezziddin, S., 131I-metaiodobenzylguanidine therapy of neuroblastoma and other neuroendocrine tumors, *Semin Nucl Med*, **40**, 153−163（2010）
3）Lewington, V.J., Bone-seeking radionuclides for therapy, *J Nucl Med*, **46**（Suppl 1）, 38S−47S（2005）
4）Witzig, T.E., Fishkin, P., Gordon, L.I., Gregory, S.A., Jacobs, S. Macklis, R., McLaughlin, P., Press, O., Zelenetz, A.D., Treatment recommendations for radioimmunotherapy in follicular lymphoma: a consensus conference report, *Leuk Lymphoma*, **52**, 1188−1199（2011）
5）Cremonesi, M., Ferrari, M., Di Dia, A., Botta, F., De Cicco, C., Bodei, L., Paganelli, G., Recent issues on dosimetry and radiobiology for peptide receptor radionuclide therapy, *Q J Nucl Med Mol Imaging*, **55**, 155−167（2011）
6）McDevitt, M.R., Sgouros, G., Finn, R.D., Humm, J.L., Jurcic, J.G., Larson, S.M., Scheinberg, D.A., Radioimmunotherapy with alpha-emitting nuclides, *Eur J Nucl Med*, **25**, 1341−1351（1998）
7）Jurcic, J.G., McDevitt, M.R., Sgouros, G., Ballangrud, A., Finn, R.D., Geerlings, M.W.S., Humm, J.L., Molinet, R., Apostolidis, C., Larson, S.M., Scheinberg, D.A., Targeted alpha particle therapy for myeloid leukemias: a phase I trial of Bismuth-213-HuM195（anti-CD33）, *Blood*, **90**, 504a（1997）
8）Nilsson, S., Larsen, R.H., Fossa, S.D., Balteskard, L., Borch, K.W., Westlin, J.E., Salberg, G., Bruland, O.S., First clinical experience with alpha-emitting

radium-223 in the treatment of skeletal metastases, *Clin Cancer Res*, **11**, 4451–4459 (2005)
9) Nilsson, S., Franzen, L., Parker, C., Tyrrell, C., Blom, R., Tennvall, J., Lennernas, B., Petersson, U., Johannessen, D.C., Sokal, M., Pigott, K., Yachnin, J., Garkavij, M., Strang, P., Harmenberg, J., Bolstad, B., Bruland, O.S., Bone-targeted radium-223 in symptomatic, hormone-refractory prostate cancer: a randomised, multicentre, placebo-controlled phase II study, *Lancet Oncol*, **8**, 587–594 (2007)
10) Lewington, V., Lamey, R., Staudache, K., Vogelzang, N., Radiation safety, tolerability, and survival gain in patients with castration-resistant prostate cancer (CRPC) and bone metastases receiving radium-233 chloride in a double-blind, randomized, phase III trial (ALSYMPCA), *Eur J Nucl Med Mol Imaging*, **39**, S304 (2012)
11) Parker, C., Heinrich, D., O'Sullivan, J.M., Fossa, S.D., Chodacki, A., Demkow, T., Logue, J.P., Seke, M., Widmark, A., Johannessen, D.C., Nilsson, S, Hoskin, P., Solberg, A., James, N.D., Syndikus, I., Cross, A., O'Bryan-Tear, C.G., Garcia-Vargas, J.E., Sartor, A.O., Overall survival benefit and safety profile of radium-223 chloride, a first-in-class alpha-pharmaceutical: Results from a phase III randomized trial (ALSYMPCA) in patients with castration-resistant prostate cancer (CRPC) with bone metastases, *J Clin Oncol*, **30**, abstract 8 (2012)
12) 井上登美夫，渡邉直行，絹谷清剛，並木宣雄，梅田泉，油野民雄，細野眞，荒野泰，鷲山幸信，藤村洋子，α線を用いたがんの最小侵襲治療法のあり方について　ワーキンググループ報告，核医学，**46**，241 (S185) (2009)
13) 細野眞，中村吉秀，柳田幸子，山田崇裕，北岡麻美，中村伸貴，池渕秀治，藤村洋子，ホルモン療法抵抗性前立腺癌の治療に用いられる放射性ラジウム-223の有効性および投与された患者の管理区域からの退出などの放射線防護対策について，平成22年度厚生労働科学研究費補助金（地域医療基盤開発推進研究事業）「医療放射線の安全確保と有効利用に関する研究」分担研究報告書，1–10 (2011)
14) 芳原新也，細野眞，稲垣昌代，任誠雲，森元英夫，花岡宏平，坂口健太，山西弘城，伊藤哲夫，223Ra薬剤の汚染管理に関する測定，*RADIOISOTOPES*, in press (2013)
15) Jonasdottir, T.J., Fisher, D.R., Borrebaek, J., Bruland, O.S., Larsen, R.H., First in vivo evaluation of liposome-encapsulated 223Ra as a potential alpha-particle-emitting cancer therapeutic agent, *Anticancer Res*, **26**, 2841–2848 (2006)
16) Hindorf, C., Chittenden, S., Aksnes, A.K., Parker, C., Flux, G.D., Quantitative imaging of 223Ra-chloride (Alpharadin) for targeted alpha-emitting radionuclide therapy of bone metastases, *Nucl Med Commun*, **33**, 726–732 (2012)

参考文献[２]

EXPERT OPINION ON BIOLOGICAL THERAPY, 2016
VOL. 16, NO. 8, 1035–1047
http://dx.doi.org/10.1080/14712598.2016.1185412

Taylor & Francis
Taylor & Francis Group

REVIEW

OPEN ACCESS

Targeted alpha therapy using short-lived alpha-particles and the promise of nanobodies as targeting vehicle

Yana Dekempeneer[a], Marleen Keyaerts[a,b], Ahmet Krasniqi[a], Janik Puttemans[a], Serge Muyldermans[c], Tony Lahoutte[a,b], Matthias D'huyvetter[a*] and Nick Devoogdt[a*]

[a]Vrije Universiteit Brussel, In Vivo Cellular and Molecular Imaging, Brussels, Belgium; [b]Nuclear Medicine Department, UZ Brussel, Brussels, Belgium; [c]Vrije Universiteit Brussel, Laboratory of Cellular and Molecular Immunology, Brussels, Belgium

ABSTRACT

Introduction: The combination of a targeted biomolecule that specifically defines the target and a radionuclide that delivers a cytotoxic payload offers a specific way to destroy cancer cells. Targeted radionuclide therapy (TRNT) aims to deliver cytotoxic radiation to cancer cells and causes minimal toxicity to surrounding healthy tissues. Recent advances using α-particle radiation emphasizes their potential to generate radiation in a highly localized and toxic manner because of their high level of ionization and short range in tissue.

Areas covered: We review the importance of targeted alpha therapy (TAT) and focus on nanobodies as potential beneficial vehicles. In recent years, nanobodies have been evaluated intensively as unique antigen-specific vehicles for molecular imaging and TRNT.

Expert opinion: We expect that the efficient targeting capacity and fast clearance of nanobodies offer a high potential for TAT. More particularly, we argue that the nanobodies' pharmacokinetic properties match perfectly with the interesting decay properties of the short-lived α-particle emitting radionuclides Astatine-211 and Bismuth-213 and offer an interesting treatment option particularly for micrometastatic cancer and residual disease.

ARTICLE HISTORY
Received 15 January 2016
Accepted 29 April 2016
Published online 19 May 2016

KEYWORDS
Cancer; targeting vehicles; targeted alpha therapy; radionuclide labeling; nanobody; bismuth-213; astatine-211

1. Introduction

1.1. Targeted radionuclide therapy

The evolution of modern medicine during the second half of the twentieth century has improved the clinical outcome of patients with numerous forms of cancer. Today, the treatment of cancer generally consists of surgery, systemic chemotherapy, radiation therapy (including external beam radiation), immunotherapy, antihormone therapy, targeted radionuclide therapy (TRNT). The choice depends upon the location and grade of the tumor and the stage of the disease, as well as the general state of the patient. Presently, tumor reduction by chemotherapy is increasingly being used in combination with surgery in multiple cancer types. Chemotherapy interacts with vital processes of the cell cycle or cell metabolism, thereby stopping or reversing cancer growth. Chemotherapy does not distinguish cancer cells from certain healthy cells, making it a less specific treatment option. External beam radiation is not suited for disseminated disease and immunotherapy often has to deal with specific resistance issues.[1]

The main objective of TRNT is the ability to selectively deliver cytotoxic radiation to cancer cells that causes minimal toxicity to surrounding healthy tissues, using optimized vehicles that deliver a nuclear payload into the tumor cells. TRNT is a growing and favorable treatment option for cancer. Currently, two principal categories can be distinguished. First, there are agents that accumulate naturally in tumor tissue. Examples are Iodine-131 (^{131}I) for the treatment of differentiated thyroid cancer [2] and Strontium-89 (^{89}Sr) and Radium-223 (^{223}Ra) for the treatment of bone metastases.[3,4] ^{131}I and ^{89}Sr are both β^--particle-emitting radionuclides, while ^{223}Ra is an α-particle-emitting radionuclide. The second category includes agents that target tumor-associated antigens that are aberrantly present in malignant tissue. Examples are Yttrium-90 (^{90}Y)- and Lutetium-177 (^{177}Lu)-octreotide as radiolabeled peptides to treat somatostatin-overexpressing neuroblastoma.[5–7] In addition, monoclonal antibodies (mAbs) are also used as vehicles to target tumor-associated antigens and hereby providing a specific internal radiotherapy.[8] The only regulatory-approved radiolabeled mAb is ^{90}Y-ibritumomab to treat non-Hodgkin lymphoma.[9,10]

Thus, a radiopharmaceutical usually consists of two parts: a targeting biomolecule that specifically determines the localization of the radiopharmaceutical and a radionuclide that delivers the mechanism of action through its decay. Today, radiopharmaceuticals are used as either diagnostics for non-invasive imaging through the detection of γ-rays using positron emission tomography (PET) or single-photon emission computerized tomography (SPECT), and/or as therapeutics to deliver radiation to the targeted tumor cells. When

CONTACT Yana Dekempeneer yana.dekempeneer@vub.ac.be Research Cluster Imaging and Physical Sciences (BEFY), In vivo Cellular and Molecular Imaging Lab (ICMI), Vrije Universiteit Brussel (VUB), Campus Jette, Laarbeeklaan 103, B-1090 Jette, Belgium
*These authors contributed equally to this work.

Article highlights

- Due to the short range in tissue and high linear energy transfer of α-particles, targeted alpha therapy (TAT) is ideal for micrometastatic or residual disease
- Nanobodies are the smallest antibody-derived antigen-binding fragments and have superior characteristics compared to classical mAbs and their derived fragments for *in vivo* cell targeting
- Nanobodies are being evaluated intensively as both diagnostic tracers for nuclear imaging and vehicles for TRNT
- The combination of the short-lived α-particle emitters ^{211}At and ^{213}Bi and nanobodies offer new possibilities for their application in TAT, which will most likely be demonstrated by ongoing and planned research work.

The box summarizes key points contained in the article.

radiopharmaceuticals are employed both for diagnosis and therapy, they are referred to as 'theranostic agents.' This combined diagnostic–therapeutic procedure uses a diagnostic test to determine whether a patient may benefit from a specific therapeutic drug, allowing personal, structural, and functional characterization of a tumor during therapy. Moreover, the therapy response could be measured throughout the therapy.

In general, there are three types of radiation that can be used for TRNT: β$^-$-particles, Auger electrons, and α-particles. Each radionuclide is characterized by its own decay properties, tissue range, half-life, and chemistry, proposing the opportunity to adapt the features of the radionuclide to a particular type of cancer and in the long run to the needs of an individual patient.[11] Until now, TRNT has been mainly explored using β$^-$-particle-emitting radionuclides. β$^-$-Particles have a low linear energy transfer (LET) (0.2 keV/μm), producing repairable DNA damage including single- or double-stranded DNA breaks, base chemical modifications, and protein crosslinks. In case of low-LET radiation, like for example β$^-$-particles, the damage caused by direct ionization of the target might only be sublethal, if dosed insufficiently high. Indirect effects caused by reactive oxygen species (ROS) also contribute to the eventual damage. β$^-$-Particles have a relatively long range in tissue (1–10 mm), causing cytotoxic damage in surrounding nontargeted cells, referred to as 'crossfire effect.' This might be useful for the treatment of heterogeneous, bulky tumors, but it has the disadvantage of damaging surrounding normal tissue. Most progress with β$^-$-particle radiation has been made in hematological malignancies, while the progress in epithelial-derived tumors has been slow. One of the shortcomings of low-LET β$^-$-particle-emitters is that much more of the radioactivity need to reach the tumor tissue to effectively kill it, compared to high-LET α-particles. A single α-particle is sufficient to destroy the cell nucleus, as cell death due to the α-radiation is largely independent of oxygenation or active cell proliferation. β$^-$-Particles on the other hand need much more hits at the level of the cell nucleus as they produce sparse ionization and individual DNA lesions, mostly repairable. This disadvantage is one of the reasons for the average success of agents labeled with β$^-$-particle-emitting radionuclides in clinical trials. Theoretically, Auger-electron emitters present multiple advantageous characteristics, making it an attractive candidate for TRNT. Auger emitters have a short effect range (subcellular, order of nanometers), a LET of 4–26 keV/μm, and are able to produce a high level of cytotoxicity due to Auger electron cascades. These cascades, by which electrons, carrying a characteristic kinetic energy, are ejected from atoms in response to a downward transition by another electron in the atom. In contrast to α-radiation, Auger radiation is of low toxicity when decaying outside the cell nucleus, such as in the cytoplasm or outside of cells, and will therefore cause little damage to nontargeted cells. Some studies have shown that Auger electrons can be effective when targeted only to the cell membrane.[12] However, it is generally considered that the radioisotope needs to be delivered close to the cell nucleus in order to be effective, which makes internalization into the cell crucial.[13]

1.2. General considerations of targeted alpha therapy

The selection of the appropriate radionuclide depends on its decay properties, namely the physical half-life and emission characteristics. For the management of bulky and heterogeneous tumors, treatment with β$^-$-particle-emitting radionuclides might be the preferred approach. However, for the eradication of small-volume tumors and small clusters of cancer cells, agents that emit high-energy α-particles would be more beneficial due to their highly specific toxic load to the targeted tumor cells and their short range in tissue. Thus, the main strength of targeted alpha therapy (TAT) is the potential to deliver radiation in a highly localized and toxic manner, because of their high level of ionization produced and short range in tissue.[14] An α-particle consists of a ^{4}He nucleus; therefore, it is much heavier than other subatomic particles emitted from decaying radionuclides and nuclear reactions. The main characteristics of currently available α-particle-emitting radionuclides are summarized in Table 1.[12] With a charge of +2, α-particles are effective ionization agents with a high LET (50–230 keV/μm) at a short range of 50–100 μm in tissue. They induce clusters of DNA damage such as double-stranded DNA breaks and base chemical modifications that evoke a large number of cellular responses and pathways that include apoptosis, autophagy, necrosis, and cell-cycle arrest. This type of damage is difficult to repair by the cell. Moreover, the damage is independent from the generation of indirect ROS, leaving their effectiveness potentially unabated by tumor hypoxia.[12] These characteristics make α-emitters effective in eradicating small clusters or isolated cancerous cells with little exposure to surrounding healthy tissue. Thus, TAT is of high interest for the treatment of micrometastatic and minimal residual disease after surgery. Moreover, the concept of TAT has moved from bench to bedside, with increasing clinical experience in, for example, ovarian cancer, metastatic prostate cancer, gliomas, and acute myeloid leukemia (Table 2). A median survival of 8.9 months could be achieved after intravenous administration of the α-immunoconjugate, Bismuth-213 (^{213}Bi)-cyclic diethylenetriaminepentaacetic acid anhydride (cDTPA)-9.2.27, in patients with metastatic melanoma in a phase I trial.[15] Using TAT to treat metastatic melanoma, α-particles reach the endothelial cell nuclei, causing cell death and leading to capillary closure and interruption of nutritional support to the tumor. If enough capillaries are closed down, the tumor might regress and could even disappear. Thus, this

Table 1. Main characteristics of the currently available α-particle-emitting radionuclides.

Isotope	Daughter isotopes*	Physical half-life	Maximum energy (keV)	Occurrence (%)	Associated emissions
^{211}At	–	7.2 h	5.867	α (41.8%)	α, γ, LEE
	^{211}Po	516 ms	7.450	α (100%)	
^{225}Ac	–	10 days	5.830	α (100%)	α, γ, Auger, β$^-$
	^{221}Fr	4.9 min	6.341	α (100%)	
	^{217}At	32.3 ms	7.069	α (99.98%)/β$^-$ (0.01%)	
	^{213}Bi	45.6 min	6.051	α (2.2%)/ β$^-$(97.8%)	
	^{213}Po	4.2 μs	8.377	α (100%)	
^{213}Bi	–	45.6 min	6.051	α (2.2%)/β$^-$ (97.8%)	α, γ, Auger, β$^-$
	^{213}Po	4.2 μs	8.377	α (100%)	
^{212}Bi	–	61 min	5.870	α (36%)/β$^-$ (64%)	α, γ, Auger, β$^-$
	^{212}Po	298 ns	8.785	α (100%)	
^{227}Th	–	18.72 days	6.038	α (100%)	α, γ, Auger, β$^-$
	^{223}Ra	11.4 days	5.871	α (100%)	
	^{219}Rn	4 s	6.819	α (100%)	
	^{215}Po	1.8 ms	7.386	α (100%)	
	^{211}Bi	2.14 min	6.623	α (99.7%)/β$^-$ (0.3%)	
^{212}Pb	–	10.64 h		β$^-$ (100%)	β$^-$
	^{212}Bi	61 min	5.870	α (36%)/β$^-$ (64%)	α, γ, Auger, β$^-$
	^{212}Po	0.3 μs	8.785	α (100%)	
^{223}Ra	–	11.4 days	5.871	α (100%)	α, γ, Auger, β$^-$
	^{219}Rn	4 s	6.819	α (100%)	
	^{215}Po	1.8 ms	7.386	α (100%)	
	^{211}Bi	2.14 min	6.623	α (99.7%)/β$^-$ (0.3%)	

*Generated α-particle emitter after decay of the conjugated parent.
LEE: Low-energy electron emission; NS: yield not significant.

subtype of TAT targets specifically the vasculature and has been referred to as 'tumor anti-vascular α-therapy (TAVAT).'[16] TAT has been compared to β$^-$-particle-emitting radionuclides in several clinical trials, highlighting their promising therapeutic potential. For example, investigators compared ^{131}I-labeled bisphosphonates with their Astatine-211 (^{211}At)-labeled counterparts for pain relief in patients with bone metastasis.[17] In addition, Henriksen et al. explored the bone-seeking properties of ^{223}Ra and compared it with those of the β$^-$-particle-emitting radionuclide ^{89}Sr.[3] The conclusion of both studies was that α-particle radiation showed a lower toxic effect to the healthy bone marrow compared to β$^-$-particle emitters, which is attributed to the reduced cross-fire effect. This and other studies indicated that the strength and short distance of high-LET α-particles make them more suitable than low-LET β$^-$-particles in particular circumstances. Despite its positive features, the translation of TAT into the clinic has been slow, mainly due to the limited radionuclide availability and the short physical half-life and daughter α-particles of some of the available α-emitters. Furthermore, several other issues concerning α-particle emitters should be addressed as well, which are discussed in the following paragraphs.

1.2.1. Radiolysis

Radiolysis is the dissociation of molecules by nuclear radiation. The magnitude of energy deposits by volume of α-particle emitters is two times greater than that of β$^-$-emitters such as ^{90}Y or ^{131}I. Because of this, the potential impact of radiolysis effects when using α-particles is noticeably higher. Hence, the radiolabeling of certain vectors with an α-particle emitter using high levels of radioactivity while maintaining appropriate biological properties may be challenging.[51] Studies by Zalutsky et al. indeed emphasize the potential importance of radiolysis-mediated effects on the chemistry of α-particle-emitting radiopharmaceuticals and the need to evaluate their labeling chemistry and stability at high doses required for clinical use.[63,64]

1.2.2. The radiation-induced biological bystander effect

The radiation-induced biological bystander effect (RIBBE) is a process whereby nontargeted healthy cells are damaged, not as a result of directly being hit by radiation, but via the radiation-induced death or stress of neighboring cells. As α-particle-emitting radionuclides have a range in tissue that is equivalent to only a few cell diameters, the physical crossfire effect will be limited. To date, the majority of studies of RIBBE have been performed *in vitro* using single-cell or multicellular systems *ex vivo* or in artificial three-dimensional human tissue systems. Boyd et al. demonstrated that cell death in adjacent cells after treatment with α-particle-emitting radionuclides might be enhanced via RIBBE.[65] Furthermore, evidence on the *in vivo* effectiveness of RIBBE has been limited, but new findings indicate that they may affect tumor development in susceptible mouse models. For example, Mancuso et al. demonstrated that DNA double strand breaks and apoptotic cell death could be induced by bystander responses in mouse cerebellum after X-ray exposure of the remainder of the body.[66] Mice were whole-body exposed or irradiated with individual cylindrical lead shields providing protection of heads. Whole-body-irradiated animals developed cerebellar tumors. A high percentage of mice (62%) died of aggressive disease by 23 weeks, with median survival of 14 weeks. Significantly, they also observed a remarkably increased medulloblastoma rate (39%) in lead shielded-irradiated mice, indicating that bystander effects are factual *in vivo* events with carcinogenic potential. However, the underlying mechanisms are incompletely characterized and it remains unclear how processes involving oxidative metabolism and stress-inducible proteins lead to (oxidative) DNA damage in bystander cells.[67]

1.2.3. Distribution of recoil daughters in the body

Another important aspect that should be taken into account is the unstable bond of daughter isotopes upon α-decay due to the different chemical properties of the daughters. This could result in an immediate loss of the daughter atom from the chelating chemistry.[68] In addition, the recoil energy of the recoiling daughters is more than 1000 times higher than the binding energy of any chemical compound, which will lead to the rupture of the chemical bonds of the daughter atom with the targeting vehicle, as well as to the ionization of the surrounding medium. The released daughter isotopes that are often themselves α-emitters might cause substantial harm since they will no longer be bound to the targeting vehicle. Therefore, it is of utmost importance to study the fate of both mother and daughter isotopes. For instance, the biodistribution of the bone-targeting radiopharmaceutical

Table 2. Vehicles used in targeted α-particle therapy in preclinical and clinical settings.

Radionuclide	TAT agent	Indication	Antigen	Reference (preclinical data)	Reference (clinical phase)
^{225}Ac	Anti-CD33 IgG (HuM195)	Leukemia	CD33	[18]	I [19,20]
^{225}Ac	Anti-HER2 IgG (trastuzumab)	Ovarian cancer	HER2	[21]	–
^{227}Th	Anti-HER2 IgG (trastuzumab)	Breast and ovarian cancer	HER2	[22,23]	
^{227}Th	Anti-CD20 IgG (rituximab)	Non-Hodgkin lymphoma	CD20	[24,25]	
^{213}Bi	Anti-CD33 IgG (HuM195)	Leukemia	CD33	[26,27]	I and I/II [28,29]
^{213}Bi	Anti-CD20 IgG (rituximab)	Non-Hodgkin lymphoma	CD20	[30,31]	I [32]
^{213}Bi	Plasminogen activator inhibitor type 2	Breast cancer, pancreatic cancer	Urokinase plasminogen activator receptor	[33–35]	
^{213}Bi	Anti-MUC1 IgG (C595 IgG)	Ovarian cancer, pancreatic cancer	MUC1	[36,37]	
^{213}Bi	Substance P	Glioblastoma	Neurokinin type-1 receptor		0/I [38,39]
^{213}Bi	Anti-NG2 IgG (9.2.27 IgG)	Melanoma	NG2 proteoglycan	[40,41]	I [15,42,43]
^{213}Bi	Anti-CD138 IgG	Multiple myeloma	CD138	[44]	
^{213}Bi	Anti-PSMA IgG (J591 IgG)	Prostate cancer	PSMA	[45]	
^{213}Bi	C6.5K-A scFv, C6.5K-A diabody	Breast and ovarian carcinomas	HER2	[46]	
^{212}Pb/^{212}Bi	Anti-HER2 IgG (TCMC-trastuzumab)	Ovarian cancer	HER2	[47,48]	[48–50]
^{211}At	Chimeric 81C6 IgG	Glioblastoma	Tenascin-C	[51,52]	II [53]
^{211}At	MX35 F(ab')$_2$	Ovarian cancer	NaPi2b	[54]	I [55]
^{211}At	Anti-FRA IgG (Mov18)	Ovarian cancer	Folate receptor alpha	[56]	
^{211}At	Anti-EGFRvIII IgG	Glioblastoma	EGFRvIII	[57]	
^{211}At	Anti-HER2 C6.5 diabody	Breast cancer	HER2	[58]	
^{211}At	$Z_{HER2:342}$ and $(Z_{HER2:4})_2$ affibody molecules	Breast and ovarian carcinomas	HER2	[59]	
^{223}Ra	^{223}Ra-chloride	Skeletal breast and prostate cancer metastases	Hydroxyapatite	[60]	I–III [61,62]

NG2: Neural/glial antigen 2; PSMA: prostate-specific membrane antigen; EGFRvIII: epidermal growth factor receptor variant III.

^{223}Ra, which naturally targets the hydroxyapatite matrix in the bone, has been studied extensively *in vivo*.[3,69] Although the daughter isotopes are not intrinsically bone-seeking, the rapid cascade of α-particle-emitting daughters will deliver high doses to bone metastases. However, their short half-life appears to prevent them from causing major damage to healthy tissue. An *in vivo* study demonstrated that less than 2% of the daughters migrate away from the bone surface within 6 h after administration of ^{223}Ra, and after 3 days, this number has dropped down to less than 1%.[3] Another example is the decay of actinium-225 (^{225}Ac) with the formation of potentially disadvantageous radiotoxic daughter products such as ^{213}Bi. It is critically important to reduce the redistribution of the daughter isotopes to nontarget tissues and to diminish systemic radiotoxic events. Therefore, the ^{225}Ac 'nanogenerator' approach was designed in which the delivery system is engineered to be internalized into the targeted tumor cell.[70] McDevitt and colleagues demonstrated the ability to safely and efficiently use ^{225}Ac as a potent tumor-selective generator in both established solid carcinomas and disseminated cancers.[71] Although these results were very promising, additional development of this modality is warranted to optimize the stability of the nanogenerator to maximize the retention of the tumor while avoiding uptake in healthy organs.

1.2.4. Dosimetry

Radiation dosimetry is the measurement of the absorbed dose delivered by the ionizing radiation and provides a basis for understanding the effects and efficacy of different radiation-based treatments. One of the major impediments of TRNT is the heterogeneous distribution of the radiopharmaceutical in normal and tumor tissues. In the case of α-particle radiation, their short path length and high LET need to be taken into account, posing an enormous challenge on the methods needed for relevant dosimetry.[72] For high-LET irradiation, the effect of a single incident in the nucleus of the cell is so abundant that the variations in absorbed dose (specific energy) to the nucleus can be very large and therefore might be a misleading index of the biologic effect. The clinical quantification of the absorbed doses with the γ-camera is only able to give an estimate about the uptake of the radiopharmaceutical in whole organs and in macroscopic tumors, while quantification of absorbed doses in smaller compartments in organs or microscopic tumors is barely feasible. Thus, small-scale dosimetry or microdosimetry, which takes into account the stochastic nature of energy deposited in small targets, would generate improved dosimetric calculations for α-particle radiation. Due to the limited clinical experience with α-particles to date, unknown maximum tolerable doses in humans are the major issue in TAT. In mice, absorbed doses of α-particle radiation can be calculated in tissues at a macroscopic level (organs and substructures) using Monte Carlo techniques based on fundamental physical principles.[73,74] In addition to that, Bäck and colleagues developed the α-camera, which is a quantitative imaging technique developed to detect α-particles in tissues *ex vivo* at suborgan level, to get a better view on the biodistribution of internal α-radiation on a cellular level.[75] The high-resolution (35 µm or less) α-camera was able to measure the activity distribution on a cellular level by virtue of the short path length of α-particles, making it a promising tool in the evaluation of future TAT.

2. The current developments

2.1. A milestone for TAT: radium-223

Radium (Ra) and polonium (Po) were first described by Marie and Pierre Curie in 1898 while investigating the radioactive

properties of a complex ore, which had radioactive emissions in excess. ^{223}Ra and ^{89}Sr are bone-targeting radiopharmaceuticals with hydroxyapatite ($Ca_5[PO_4]_3OH$) as target, which is an essential component of the inorganic bone matrix. Ra, barium (Ba), Sr, and calcium (Ca) are all chemicals in the alkaline earth metal family on the periodic table and each will localize in the areas of osteoblastic metastases. ^{223}Ra is currently the most commonly used radioisotope for medical therapeutics, showing an increased survival in patients with metastatic castration-resistant prostate cancer [61] and has a half-life of 11.4 days (Table 1). ^{223}Ra is the first α-emitter approved by the US Food and Drug Administration.[76] In addition, ^{223}Ra is the first α-particle-based therapy that results in pain relief and extends survival in patients with progressive castration-resistant prostate cancer and bone metastasis in the absence of visceral metastasis. Thus, ^{223}Ra is naturally incorporated in areas of increased bone turnover in bone metastases.[77] More than 90% of patients with metastatic resistant prostate cancer have radiologic evidence of bone metastases. ^{223}Ra dichloride has been evaluated in two phase I trials and three double-blind phase II trials. The phase III ALSYMPCA (Alpharadin in the Treatment of Patients With Symptomatic Bone Metastases in Castration-Resistant Prostate Cancer) trial showed an improved overall survival of 3 months and pain relief in patients with osseous metastasis.[61] The success of ^{223}Ra as a therapeutic further stimulates TAT-based preclinical and clinical research. In a way, ^{223}Ra could be considered as a game changer in nuclear medicine, as it might facilitate the future use of additional high-LET particle emitters.

2.2. Other promising α-particle-emitting radionuclides

Besides ^{223}Ra, many other α-particle emitters have suitable characteristics for therapeutic applications (Table 2). ^{211}At, ^{213}Bi, lead-212 (^{212}Pb)/bismuth-212 (^{212}Bi), and ^{225}Ac are the most frequently used α-particle-emitting radionuclides in clinical molecular targeting applications to date.[78]

2.2.1. Actinium-225

^{225}Ac is a parent α-particle emitter in a decay cascade that produces three net α-particle isotopes, ^{221}Fr (half-life 4.8 min), ^{217}At (half-life 32.3 ms), and ^{213}Bi (half-life 45.6 min), making it a very effective and potent option for TAT (Table 1). ^{225}Ac has a half-life of 10 days and can be produced by natural decay of ^{233}U in Oak Ridge National Laboratory, USA [79] or by accelerator-based methods in Karlsruhe.[80] However, the latter production of ^{225}Ac also results in the production of ^{227}Ac which decays with a half-life of 21.772 years. The biggest disadvantage concerning ^{225}Ac is its cost, which might reach to $1200/mCi. In addition, the recoiled daughters of ^{225}Ac can do significant damage to healthy tissue when not retained at the tumor site. Encapsulation in a nano-carrier, fast uptake of the α-particle-emitting radionuclides in tumor cells, and local administration are some approaches to minimize toxic effects caused by α-particle-emitting daughters.[68] On the other hand, the relatively long half-life of ^{225}Ac allows a centralized production and shipment of the irradiated targets to further users so that any investigator is able to exploit the power of this α-particle. Furthermore, ^{225}Ac decays to ^{213}Bi, of which the latter also results in a 440 keV γ-ray emission that can be useful for imaging of the therapeutic biodistribution. It should be remarked that it is uncertain whether the measured radioactive decay represents intact radiopharmaceutical or released daughter radioisotopes. Moreover, ^{225}Ac can be conjugated to peptides or antibodies, using an optimized radiochemistry with standard widely available macrocyclic bifunctional chelators.[81,82] *In vivo* experiments showed that the ^{225}Ac complex with 1,4,7,10-tetraazacyclododecane-*N*,*N*′,*N*″,*N*‴-tetra-acetic acid (DOTA) was more stable than the ^{225}Ac complex with 4,7,10,13,16-hexaazacyclohexadecane- *N*,*N*′,*N*″,*N*‴,*N*⁗,*N*⁗′-hexaacetic acid.[70] The biodistribution aspects of ^{225}Ac-labeled mAbs and other carriers, together with their pharmacokinetic properties, radiobiology, and dosimetry, have been reviewed by Miederer et al.[70] A successful phase I trial has demonstrated that a humanized anti-CD33 mAb HuM195 conjugated to ^{225}Ac (Actimab-A) is safe to use at doses ≤0.1 MBq/kg [19] (Table 2).

2.2.2. Bismuth-213

^{213}Bi is most often produced through an ^{225}Ac-generator. The principal drawbacks of using ^{213}Bi are its very short physical half-life of 46 min and limitations regarding availability and cost as for ^{225}Ac. Pippin and colleagues were the first to label ^{213}Bi with mAbs.[83] Moreover, McDevitt and colleagues labeled ^{213}Bi via the bifunctional metal cDTPA complex with a humanized mAb (HuM195) directed against CD33, a glycoprotein expressed on the majority of myeloid leukemia cells.[26] In subsequent studies, the stability of this radiopharmaceutical has been improved to achieve a clinically applicable ^{213}Bi-CHX-A-DTPA-HuM195.[84] A phase I clinical study on 18 patients with acute myelogenous leukemia (AML) or chronic myelomonocytic leukemia showed no significant extramedullary toxicity, although myelosuppression was seen in all patients.[28] The phase I/II trials showed that sequential administration of cytarabine and ^{213}Bi-CHX-A-DTPA-HuM195 was reported to be tolerable and produced remissions in some patients with AML, although myelosuppression was again a common adverse effect.[29] The responses in this high-risk population persisted up to 12 months. In addition, patients with non-Hodgkin lymphoma, malignant melanoma, and glioblastoma have been enrolled in clinical trials with other ^{213}Bi-labeled compounds, showing its relevant potential for TAT (Table 2).

2.2.3. Astatine-211

^{211}At is an α-particle-emitting radionuclide with a physical half-life of 7.2 h and its decay does not result in the production of any relevant daughter isotopes. The first branch decays to ^{211}Po (half-life 526 ms), after which it decays through α-particle radiation to stable ^{207}Pb. In the second branch, ^{211}At α-decays to ^{207}Bi, which then results in stable ^{207}Pb after emission of X-rays. Theoretically, this offers significant advantages for TAT regarding minimal toxicity and quantitative α-particle emission. However, additional clinical research is needed in order to confirm this as a real advantage. The chemical features of ^{211}At are similar to those of iodine, its nearest halogen neighbor, but ^{211}At contrarily also tends to behave as a metalloid. Moreover, the exact behavior of ^{211}At is far from understood due to the limited

knowledge of the chemistry of elemental ^{211}At and the lack of any stable equivalent, which excludes the use of conventional analytical techniques for its characterization.[85] Reasonable yields (0.8–2.5 GBq) of ^{211}At are obtained via the bombardment of natural bismuth targets with α-particles through the ^{209}Bi(α, 2n) ^{211}At nuclear reaction in a cyclotron.[86] The 7.2-h half-life of ^{211}At is well suited for a multistep synthetic procedure. Consequently, a wide variety of tumor-associated antigens that are aberrantly expressed on the cancer cell surface have been targeted by ^{211}At-labeled radiopharmaceuticals.[87,88] To date, ^{211}At has been investigated bound to antibodies, thymidine analogs,[89] biotin analogs,[90] colloids,[91] melanin precursors,[92] substrate carriers,[93] and bisphosphonate complexes.[94] Only two clinical studies have been reported so far with ^{211}At-labeled molecules.[53,55] The first clinical study for the treatment of recurrent brain tumor provides a proof-of-concept for regional targeted radiotherapy with ^{211}At-labeled mAbs.[53] This clinical study demonstrated that the regional administration of ^{211}At-ch81C6 was feasible, safe, and resulted in a possible therapeutic benefit for patients with malignant brain tumors. In the second reported clinical study of ^{211}At using the MX35 F(ab')$_2$, the compound was delivered successfully through intraperitoneal administration without observed toxicity.[55] These two clinical trials showed no subjective toxicity related to the immunoconjugate and the overall outcomes were highly encouraging. However, there are no clinical data on the toxicity of ^{211}At-labeled immunoconjugates after intravenous administration. Further clinical evaluation of ^{211}At-labeled compounds in metastatic tumors or residual disease is warranted.

3. Vehicles for TAT

The attractive feature of TRNT is its adaptable nature. The radionuclide and the targeting vehicle should in principle be matched to each other in the context of the route of administration, disease stage, target accessibility, and site of action. The selection of both the optimal tumor-associated antigen and the targeting vehicle is a crucial step in the development of a new probe for TRNT. The ideal antigen should be overexpressed on cancer cells, while the expression levels on normal, healthy cells should be extremely low.[95] Examples of biomarkers that are targeted in TAT studies are epidermal growth factor receptor variant III, human epidermal growth factor receptor 2 (HER2), folate receptor alpha, tenascin-C, CD20, CD33, and prostate-specific membrane antigen (Table 2). The vehicle molecules should be optimized to provide a high degree of selectivity and specificity toward the target site or 'biomarker.' Below, a section of important vehicles are discussed.

mAbs are Y-shaped proteins that contain two identical *fragment antigen-binding* (Fab) fragments and a *fragment crystallizable* (Fc) region (Figure 1). They are produced by plasma cells (mature, activated B cells) and are recruited by the immune system to identify and destroy foreign objects. Moreover, they have the capacity to bind any potential antigen epitope with high affinity, including tumor-associated biomarkers. Today, a variety of preclinical and clinical investigations were conducted using mAbs labeled with α-particle-emitting radionuclides (Table 2). The melanoma trials (Table 2) using ^{213}Bi-cDTPA-9.2.27 show that solid tumors can be regressed by TAVAT. Moreover, these clinical results demonstrated that TAVAT for melanoma patients were locally efficacious and nontoxic up to 1.4 mCi. In the ^{213}Bi-HuM195 phase I study described above, the authors provided a proof-of-concept for the use of α-particle immunotherapy to treat myeloid leukemia. Although ^{213}Bi-HuM195 was well tolerated and 14 (78%) of 18 patients had reductions in the percentage of bone marrow blasts, myelosuppression was seen in all treated patients.[28] Similarly, myelosuppression and liver function abnormalities were observed in a phase I/II trial investigating antileukemic effects of ^{213}Bi-HuM195 after partial cytoreductive chemotherapy.[29] These toxicities could be explained by the suboptimal pharmacokinetic properties of mAbs as vehicles for TAT. The high molecular weight of mAbs (150 kDa) and the presence of an Fc-region result in a long serum half-life (several days or weeks) and in interactions with Fc-receptors in myeloid and hepatic sinusoidal cells, resulting in higher bone marrow toxicity and accumulation in the liver. Improvement in antibody engineering has led to the development of antibody fragments that are smaller and devoid of Fc, such as 25-kDa single-chain Fv (scFv), Fab (50 kDa), F(ab')$_2$ (110 kDa), diabodies (55 kDa), and minibodies (80 kDa) without compromising their affinity and specificity (Figure 1).[96]

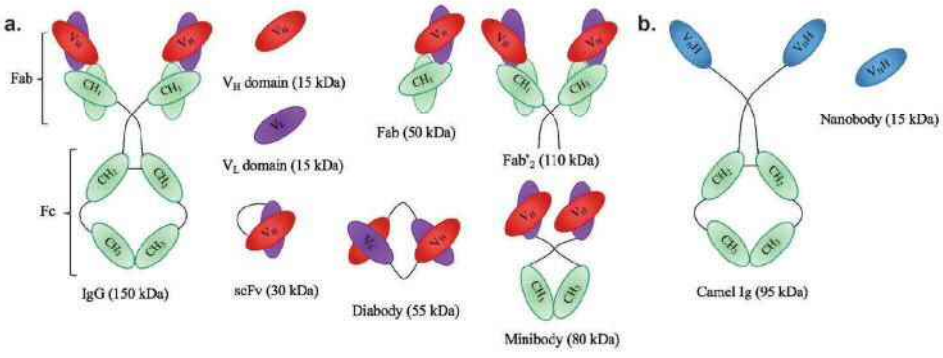

Figure 1. Schematic representation of antibodies and their derived antigen-binding fragments. a. Conventional mAb and the derived Fab, scFv, Fv domains V_L or V_H, Fab'$_2$, minibody and diabody. b. Camelid heavy-chain-only antibody and its V_HH (also known as nanobody).

Smaller engineered mAb derivatives are more rapidly delivered to the tumor and mediate more effective tumor penetration. Because of their smaller size and lack of Fc, they are more rapidly cleared from the circulation, which is indirectly proportional to the level of kidney retention. Therefore, their administration results in fast tumor uptake with high tumor-to-background ratios. One study reported the successful conjugation of ^{213}Bi to anti-HER2 C6.5 scFv and diabody molecules. However, a lack of tumor-specific therapeutic effect was shown, probably resulting from instability of the scFv and diabody molecules *in vivo*.[46] Here, it was concluded that the physical half-life of 45.6 min of ^{213}Bi was too short to allow the systemically administered diabody to specifically localize in an established solid tumor. In a subsequent study, ^{211}At was coupled to the stable *N*-succinimidyl-*N*-(4-[^{211}At] astatophenethyl) succinamate and subsequently conjugated to the C6.5 diabody (Table 2).[58] Here, the somewhat longer physical half-life of ^{211}At matches more closely to the rapid tumor targeting and rather fast systemic clearance of the C6.5 diabody. In the ^{211}At-MX35 F(ab')$_2$ phase I trial, therapeutic doses were reached for the treatment of ovarian cancer.[55] However, 50% of the initial activity concentration of this radionuclide remained in the peritoneal fluids 24 h after injection, indicating a higher toxicity risk related to this immunoconjugate.

Besides antibodies and antibody derivatives, ligands (e.g. folate), synthetic protein scaffolds (e.g. affibodies), and substrate analogs (e.g. peptides) can also be used as targeting agents in order to specifically deliver the toxic radionuclide.[97–99] Affibody molecules are small single domain proteins with a molecular weight of 6.5 kDa that are derived from one of the immunoglobulin binding domains of staphylococcal protein A.[100] Previous research demonstrated that affibody molecules can bind to their targets within minutes after administration. The binding kinetics of affibodies are similar to that of nanobodies, but faster than the larger sized mAb and its derived fragments. With regard to TAT, affibody molecules directed against the membrane protein HER2 ($Z_{HER2:342}$ and the bivalent version $[Z_{HER2:4}]_2$) were radiolabeled with ^{211}At using the precursor *N*-succimidyl-*para*(trimethylstannyl) benzoate. Based on preliminary results, the authors concluded that the labeling chemistry needs to be improved before this strategy can be translated to clinical studies.[59]

So far, significant improvements have been made in the development and application of optimized vehicles for TAT. While these preliminary results are promising, there is still considerable room for improvement, mainly in the development of new coupling chemistries and elucidation and optimization of the *in vivo* biodistribution.

4. Nanobodies: potential vehicles to specifically deliver toxic α-radiation

Recently, there has been a growing interest in the use of nanobodies as vehicles for TRNT. Nanobodies are the smallest, antigen-binding fragments from unique heavy-chain-only antibodies naturally occurring in *Camelidae* (Figure 1).[101] Several applications of nanobodies as *in vivo* diagnostic tracers have been and are currently being developed.[102] Nanobodies have many favorable characteristics as targeted tracers, including high stability in harsh conditions, such as elevated temperatures and extreme pHs offering the potential to use a broader range of radiochemistry methods. Other favorable characteristics include high affinity and specificity for their cognate antigen and facile production (Figure 2(a,b)). As such, nanobodies have been developed as efficient radiotracers directed against a variety of membrane-bound biomarkers [103] in various animal models of cancer,[104–107] inflammation,[108] and cardiovascular diseases [102] using SPECT/PET. Because of their exceptional targeting specificity that is unaffected by labeling with various radionuclides, nanobodies have become valuable vehicles for both nuclear imaging and TRNT.[105–107] Furthermore, nanobodies possess various advantages over mAbs. First, the molecular weight of nanobodies (15 kDa) is one-tenth of that of conventional Abs (150 kDa), making it possible to recognize and bind hidden isotopes. Second, nanobodies have a low immunogenicity because of their rapid blood clearance and high sequence identity to human variable domains of the heavy chain. Furthermore, previous studies by our group demonstrated that nanobodies efficiently penetrate tumor tissues and bind tumor antigens rapidly and specifically *in vivo*.

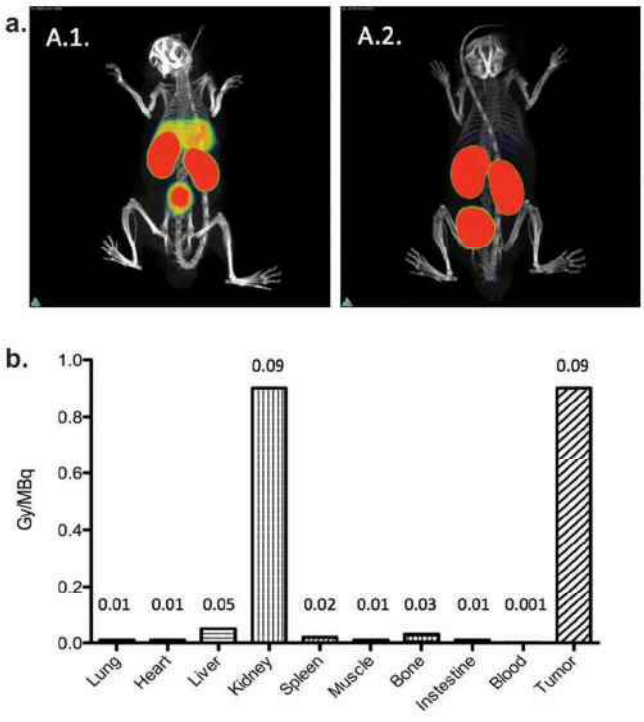

Figure 2. Nanobodies possess numerous advantageous characteristics, including their high antigen specificity (a) and high tumor targeting potential (b). **a.** ^{99m}Tc-labeled-nanobody targeting the complement receptor of the Ig superfamily, CRIg, expressed on Kupffer cells in the liver. 3D-rendered SPECT/micro-CT images of naive wild-type (A.1.) and CRIg$^{-/-}$ mice (A.2.) 1 h after intravenous injection of ^{99m}Tc-labeled-nanobody. Representative images for 3 mice per group are shown. Figures adapted with permission from.[115] **b.** Dosimetry calculation of untagged ^{177}Lu-DTPA-anti-HER2 nanobody coinfused with 150 mg/kg Gelofusin, in HER2^{pos} tumor xenografted mice. Radiolabeling of nanobodies is characterized by significant retention of radioactivity at the kidneys, due to the charged-based aspecific tubular reuptake after glomerular filtration. Figure adapted with permission from.[109].

Meanwhile, there is very little nonspecific binding to other tissues, which, along with the rapid blood clearance, results in high tumor-to-background ratios as early as 1 h after injection.[109] Therefore, the nanobody technology could provide an adequate solution to the off-target toxicity problem caused by long blood circulation, as is observed during mAb-based TRNT. A first-in-human PET study with a GMP-grade HER2-targeting nanobody-based tracer for breast cancer has recently been completed at our university hospital [110] and new clinical trials with nanobodies targeting HER2 and tumor-associated macrophages are planned for 2016. The first clinical study confirmed the fast clearance of nanobodies in patients, with only 10% of the injected activity remaining in the blood at 1 h p.i. (Figure 3(a)). In addition, high tumor-to-background ratios could be observed in 17 out of 19 primary tumors, with mean standard uptake values ranging between 0.7 and 11.8 (Figure 3(b)). Furthermore, the utility of nanobodies as vehicles for TRNT has been investigated in preclinical models using the β^--particle-emitting radionuclide ^{177}Lu. The most relevant *in vivo* study demonstrated that ^{177}Lu-labeled anti-HER2 nanobody efficiently targeted HER2^{pos} s.c. xenografts in a 5-day follow-up study, while radioactivity levels in normal organs were low (Figure 2(b)).[109] Weekly i.v. administrations of ^{177}Lu-labeled anti-HER2 nanobody in mice with small HER2^{pos} tumors completely prevented tumor growth, while tumors grew exponentially in untreated mice or in mice receiving a control, nontargeting nanobody. In addition, TRNT using a ^{177}Lu-labeled anti-5T2 multiple myeloma nanobody led to an inhibition of disease progression in treated mice compared to control animals. [111] These proof-of-concept TRNT studies show that nanobodies display a more beneficial toxicity profile than mAbs and can deliver a specific lethal radiation dose to a developing tumor. The low molecular weight of nanobodies, below the kidney cut-off for glomerular filtration, and the subsequent charged-based nonspecific tubular reuptake result in significant accumulation and retention of radioactivity in the kidneys. To avoid potential kidney-related toxicities, strategies were tested to reduce renal retention. Both the removal of nonessential positively charged amino acids in the nanobody sequence and co-infusion with positively charged amino acids or the plasma expander Gelofusin were able to lower kidney retention significantly. [107,109] Another approach to reduce the kidney retention is to use optimized radiolabeling procedures. For instance, Zalutsky and colleagues labeled an anti-HER2 nanobody with iodine-131 (^{131}I), using the prosthetic group *N*-succinimidyl-4-guanidinomethyl-3-iodobenzoate (SGMIB). SGMIB is a prosthetic group used for antibody and small-protein radioiodination and possesses improved properties as a group that stabilizes ^{131}I and maximizes the retention in tumor cells.[112,113] Remarkably, ^{131}I-SGMIB-anti-HER2-nanobody was not retained in the kidneys, while tumor targeting was maintained. In addition, Zalutsky and coworkers recently labeled an anti-HER2 nanobody with ^{211}At, using this similar residualizing agent, referred to as *N*-succinimidyl-3-[^{211}At]astato-4-guanidinomethylbenzoate (SAGMB).[114] Paired-label biodistribution studies directly compared the *in vivo* behavior of ^{211}At-SAGMB-nanobody to that of its ^{131}I analog SGMIB-nanobody in athymic mice, showing excellent preservation of HER2 binding after ^{211}At labeling in combination with high internalization and optimal tumor uptake. Further investigation of this ^{211}At-SAGMB-nanobody compound is warranted.

5. Conclusion

TAT is an emerging and promising treatment modality that has the ability to specifically kill isolated cancer cells or cell

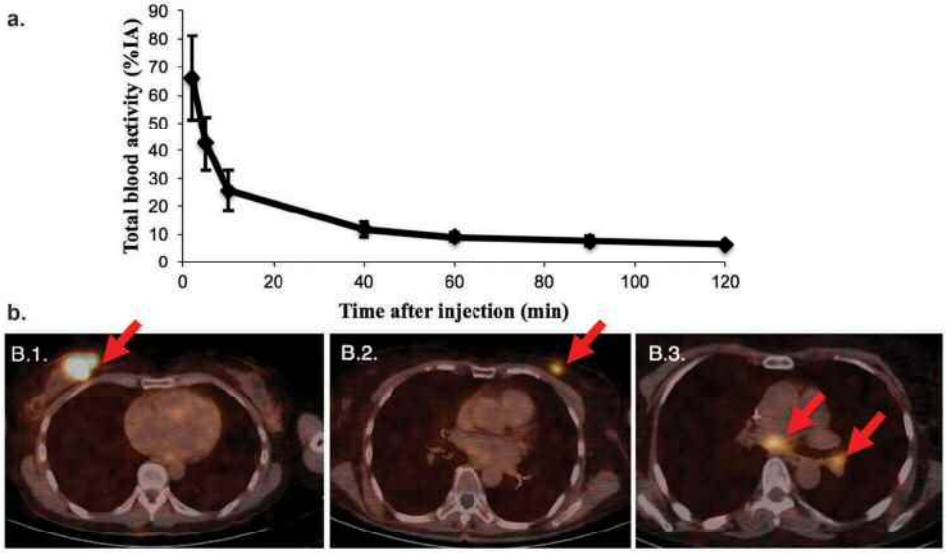

Figure 3. Diagnostic tumor imaging using ^{68}Ga-HER2-nanobody in patients with HER2^{pos}-breast cancer. **a.** Time-activity curve of total blood activity, expressed in % of injected activity (%IA) (n=20). **b.** Fusion PET/CT images of the uptake of ^{68}Ga-HER2-nanobody in breast carcinoma lesions. (B.1.) Patient with the highest tracer uptake (SUVmean 11.8) in a primary breast carcinoma. (B.2.) Patient with moderate tracer uptake in the left breast, which is easily discernable from background (SUVmean 4.9). (B.3.) Patient with invaded lymph nodes in the mediastinum and left hilar region. Lesions are indicated by red arrows. Figures are adapted with permission from.[110].

clusters and might only cause little damage to healthy non-target tumor cells. The combination of preclinical and clinical data affirms the potential of TAT. However, more research is needed to identify the ideal combination of targeting vehicle and α-particle radionuclide, its specific way of linking both, and all this optimized toward specific target expression, disease stage, target accessibility, and site of action.

6. Expert opinion: nanobodies coupled to α-particle-emitting radionuclides in cancer therapy

There is an unmet need to treat minimal residual disease and micrometastatic spread of tumor cells, as the current cancer treatment options like chemotherapy, surgery, and external beam radiotherapy are less effective once the tumor has metastasized. Targeted α-particle therapy or TAT allows, due to the high LET of the associated radioactivity, precise delivery of a highly toxic radiation to target cells with reduced harm to normal untargeted cells in the vicinity. This strategy might be ideal for the treatment of small malignant cell populations that are located in the proximity of essential normal tissue structures and could be used in addition to other existing treatment modalities. Increased production and evaluation of α-particle emitters has improved their availability, enhancing the development for new TATs. Currently, TAT has mainly been explored using mAbs. However, the high molecular weight of mAbs and the presence of the Fc-region result in a long serum half-life and interactions with cells containing Fc-receptors. Consequently, the systemic administration of radiolabeled mAbs results in a prolonged presence of radioactivity in blood and highly perfused organs, and unwanted radiation exposure of nontargeted cells. Unsurprisingly, myelotoxicity has been shown to be a limiting factor in several preclinical and clinical studies. Moreover, the dose delivered to carcinomas is often inadequate, owing to the limited penetration of mAb-based vehicles. Hence, we claim that mAbs are not the ideal vehicles to couple with an α-particle emitter. Ab engineering is an interesting approach to overcome some of the limitations of mAbs. Nanobodies in particular have emerged as excellent Ab fragments, as they exhibit high affinity and specificity, fast diffusion and clearance kinetics *in vivo*, high tumor-to-normal-tissue ratios, and a high stability. Moreover, nanobodies have already proven their value in both diagnostic and therapeutic applications. We believe that nanobodies, with their improved properties compared to full-size mAbs and larger Ab-fragments, could be ideal vehicles for TAT.

A key element in the design of radiopharmaceuticals is attuning the properties of the therapeutic radionuclide with those of the tumor-targeting vehicle. The main goal here is to optimize the vehicle in such a way that it fits the characteristics of the α-particle-emitting radionuclide, resulting in optimal tumor targeting and minimal exposure of normal organs. Due to their half-life in the range of minutes to hours, ^{213}Bi and ^{211}At could be ideal radioactive partners for fast and specific targeting nanobodies. However, both radioisotopes have both their advantages and disadvantages. Currently, the most important limitation of ^{211}At is the limited availability of accelerators that are able to generate the 28 MeV α-particle beam required to produce useful levels of ^{211}At.[86] Therefore, production and supply of sufficient amounts of ^{211}At is still challenging, although over the past few years some progress has been made in the recruitment of new cyclotrons for commercial ^{211}At production. Today, about 30 cyclotrons in the world have the beam characteristics (28 MeV) capable for the production of ^{211}At. Furthermore, Lindegren and colleagues developed a fully automated procedure that enables automatic, reproducible, rapid, high-yield production of clinically relevant amounts of ^{211}At and ^{211}At-labeled radiopharmaceuticals.[116] To date, only two clinical trials have been reported using ^{211}At-labeled molecules (Table 2). In the first clinical trial, the median survival for patients with glioblastoma multiforme, anaplastic astrocytoma, and oligodendroglioma was 54, 52, and 116 weeks after ^{211}At-labeled chimeric antitenascin 81C6 therapy.[53] In the second phase I study, ovarian cancer patients were injected with ^{211}At-MX35 F(ab')$_2$. Intraperitoneal administration of this immunoconjugate showed that it was possible to achieve therapeutic absorbed doses (15.6 ± 1.0 mGy/[MBq/L]) in the peritoneal peritoneum, where the microscopic tumor clusters are situated, without significant toxicity.[55]

Targeting vehicles can be astatinated via a variety of prosthetic groups.[85] However, many prosthetic groups fail to deliver relevant amounts of astatinated end product, as well as proper *in vivo* stability. In addition, automatable chemistries with high radiochemical yields are yet to be developed. Therefore, many ^{211}At-labeled compounds labeled have been abandoned in the past. To this, a more in-depth understanding of the chemistry of ^{211}At is required to provide future, useful astatinated radiopharmaceuticals. The production of ^{213}Bi is more straightforward, through the actinium-225/bismuth-213 generator system. However, the use of ^{213}Bi has been limited by the availability of ^{225}Ac. In numerous clinical studies, ^{213}Bi ($t_{1/2}$ = 46 min) has shown to be effective to treat patients with malignant melanoma, metastatic breast cancer, prostate cancer, pancreatic cancer, and other metastatic diseases. The labeling of targeting vehicles with ^{213}Bi is generally performed using straightforward chelating agents such as DTPA and DOTA. In addition, ^{213}Bi decays via a branched pathway by α and β emissions to stable ^{209}Bi, leading to low toxicity due to the minimal recoil energy the daughter experience upon α-decay. However, the short half-life of ^{213}Bi might eventually limit its clinical applicability, as relevant therapeutic doses of ^{213}Bi need to be available on a regular basis. Based on these characteristics and on the corresponding features of nanobodies, we claim that nanobodies are ideal for radiolabeling with short-lived radionuclides such as ^{211}At and ^{213}Bi.

α-Particle recoiling daughter isotopes pose serious problems during TAT as they can do significant harm to healthy tissue when they are not retained at the tumor site. Different approaches to limit the distribution of recoiling daughter isotopes have been found such as encapsulation in a nano-carrier and fast internalization of the α-particle inside the tumor cells. In general, monovalent nanobodies only show limited degree of internalization inside tumor cells after binding. However, it has been shown that internalization can be stimulated by the development of multivalent nanobody constructs, which

would augment the amount of α-particles trapped inside the tumor cell.[117]

In order to become valuable, some aspects concerning nanobody-based TAT need to be considered.[1] In general, nanobody targeting is characterized by only moderate absolute uptake in tumor tissue (compared to longer circulating mAbs) and fast blood clearance. To this, it will be important to assess the maximum dose that can be delivered to target tissues. The fast clearance and very specific way of targeting of nanobodies allows repeated injections. In the past, we have shown that therapeutic doses can be reached through fractionated administration using ^{177}Lu-labeled nanobodies.[109,111] We therefore believe that therapeutic TAT doses will be achieved by means of repeated administration. The high LET of α-particles will have their beneficial effect on tumor tissues, but can in parallel cause toxicity in tissues with elevated uptake or retention. It is known that nanobodies can interact with the negatively charged lumen of kidney tubuli during filtration from blood. It is therefore of upmost importance to assess the effect of nanobody-TAT at the level of the kidneys. Based on previous published work, there are several countermeasures that can be taken to reduce renal retention of radiolabeled nanobodies. Kidney retention can be reduced significantly by removal of the nanobodies' amino-acid tag or through co-infusion with the plasma expander Gelofusin and positively charged amino acids.[107,109] In addition, it has been shown that the linker between radioisotope and targeting vehicle can have a dramatic influence on the degree of kidney retention. Recently, anti-HER2 nanobodies were radiolabeled with ^{131}I using the prosthetic group SGMIB. It was shown that while the retention in tumor cells was maintained, a complete absence of kidney retention was observed.[112] Interestingly, this exact prosthetic group can be used for astatination of nanobodies. The short path length of α-particles causes a heterogenous distribution in both tumor and tissues, which can lead to very localized toxicity (suborgan or subtissue level). Novel methods that allow micro- and small-scale dosimetry will be essential to realistically estimate dosimetry of TAT-based radiopharmaceuticals. Emerging strategies include the recent development of the α-camera that allows *ex vivo* imaging of α-particle deposits at a cellular level.

In conclusion, the superior characteristics of α-particle emitters ^{213}Bi and ^{211}At as toxic payload and nanobodies as targeting vehicles offer exciting possibilities in TAT. We therefore expect that the pairing of short-lived α-particle emitters and fast and specific targeting nanobodies will show their potential in the future.

Declaration of interests

Y Dekempeneer is supported by a personal grant from Kom op tegen Kanker, and the authors have received funding from the IWT and Research Foundation Flanders (FWO). T Lahoutte, M D'huyvetter and N Devoogdt are co-founders of Camel-IDS. The authors have no other relevant affiliations or financial involvement with any organization or entity with a financial interest in or financial conflict with the subject matter or materials discussed in the manuscript. This includes employment, consultancies, honoraria, stock ownership or options, expert testimony, grants or patents received or pending, or royalties.

ORCID

Serge Muyldermans http://orcid.org/0000-0002-3678-3575
Nick Devoogdt http://orcid.org/0000-0001-9220-4833

References

Papers of special note have been highlighted as:
• of interest
•• of considerable interest

1. Restifo NP, Smyth MJ, Snyder A. Acquired resistance to immunotherapy and future challenges. Nat Rev Cancer. 2016 ;16 (2):121–126. Nature Publishing Group.
2. Middendorp M, Grünwald F. Update on recent developments in the therapy of differentiated thyroid cancer. Semin Nucl Med. 2010 ;40 (2):145–152. Elsevier Inc.
3. Henriksen G, Fisher DR, Roeske JC, et al. Targeting of osseous sites with alpha-emitting 223Ra: comparison with the beta-emitter 89Sr in mice. J Nucl Med. 2003;44(2):252–259.
4. Van Dodewaard-de Jong J, Oprea-Lager D, Hooft L, et al. Radiopharmaceuticals for palliation of bone pain in patients with castration-resistant prostate cancer metastatic to bone: a systematic review. Eur Urol. 2015. European Association of Urology.
5. Kwekkeboom DJ, Mueller-Brand J, Paganelli G, et al. Overview of results of peptide receptor radionuclide therapy with 3 radiolabeled somatostatin analogs. J Nucl Med. 2005;46(1):62S– 6S.
6. Valkema R, Pauwels S, Kvols L, et al. Survival and response after peptide receptor radionuclide therapy with [90Y-DOTA0,Tyr3] octreotide in patients with advanced gastroenteropancreatic neuroendocrine tumors. Semin Nucl Med. 2006;36(2):147–156.
7. De Jong M, Valkema R, Jamar F, et al. Somatostatin receptor-targeted radionuclide therapy of tumors: preclinical and clinical findings. Semin Nucl Med. 2002;32(2):133–140.
8. Koppe MJ, Postema EJ, Aarts F, et al. Antibody-guided radiation therapy of cancer. Cancer Metastasis Rev. 2005;24(4):539–567.
9. Ghobrial I, Witzig T. Radioimmunotherapy: a new treatment modality for B-cell non-Hodgkin's Lymphoma. Oncology (Williston Park). 2004;18(3):623–630.
10. Chamarthy MR, Williams SC, Moadel RM. Radioimmunotherapy of non-Hodgkin's lymphoma: from the "magic bullets" to "radioactive magic bullets. Yale J Biol Med. 2011;84(4):391–407.
11. Volkert WA, Goeckleler WF, Ehrhardt GJ, et al. Therapeutic radionuclides: production and decay property considerations. J Nucl Med. 1991;32(1):174–185.
12. Pouget JP, Navarro-Teulon I, Bardiès M, et al. Clinical radioimmunotherapy-the role of radiobiology. Nat Rev Clin Oncol. 2011;8 (12):720–734.
13. Buchegger F, Perillo-Adamer F, Dupertuis YM, et al. Auger radiation targeted into DNA: a therapy perspective. Eur J Nucl Med Mol Imaging. 2006;33(11):1352–1363.
14. Mulford DA, Scheinberg DA, Jurcic JG. The promise of targeted α-particle therapy. J Nucl Med. 2005;46:199–205.
15. Allen B, Singla A, Rizvi S, et al. Analysis of patient survival in a Phase I trial of systemic targeted α-therapy for metastatic melanoma. Immunotherapy. 2011;3(9):1041–1050.
16. Allen BJ, Raja C, Rizvi S, et al. Tumour anti-vascular alpha therapy: a mechanism for the regression of solid tumours in metastatic cancer. Phys Med Biol. 2007;52(13):L15–9.
17. Larsen RH, Murud KM, Akabani G, et al. 211At-and 131I-labeled bisphosphonates with high in vivo stability and bone accumulation. J Nucl Med. 1999;40:1197–1204.
18. Miederer M, McDevitt MR, Sgouros G, et al. Pharmacokinetics, dosimetry, and toxicity of the targetable atomic generator, 225Ac-HuM195, in nonhuman primates. J Nucl Med. 2004;45(1):129–137.
19. Jurcic JG, Rosenblat TL, McDevitt MR. Phase I trial of the targeted alpha-particle nano-generator actinium-225 (225Ac)-lintuzumab (anti-CD33; HuM195) in acute myeloid leukemia (AML). J Clin Oncol. 2011;29:Abstract 6516.
20. Jurcic J, Ravandi F, Pagel JM, et al. Phase I trial of the targeted alpha-particle nano-generator actinium-225 (225Ac)-lintuzumab

(anti-CD33) in combination with low-dose cytarabine (LDAC) for older patients with untreated acute myeloid leukemia (AML). Blood. 2013;122(21):1460–1460.
21. Borchardt PE, Yuan RR, Miederer M, et al. Targeted actinium-225 in vivo generators for therapy of ovarian cancer. Cancer Res. 2003;63 (16):5084–5090.
22. Heyerdahl H, Abbas N, Brevik EM, et al. Fractionated therapy of HER2-expressing breast and ovarian cancer xenografts in mice with targeted alpha emitting 227Th-DOTA-p-benzyl-trastuzumab. PLoS One. 2012;7:8.
23. Heyerdahl H, Abbas N, Sponheim K, et al. Targeted alpha therapy with ovarian cancer in nude mice 227Th-trastuzumab of intraperitoneal. Curr Radiopharm. 2013;6(2):106–116.
24. Melhus KB, Larsen RH, Stokke T, et al. Evaluation of the binding of radiolabeled rituximab to CD20-positive lymphoma cells: an in vitro feasibility study concerning low-dose-rate radioimmunotherapy with the α -emitter 227 Th. Cancer Biother Radiopharm. 2007;22 (4):469–479.
25. Dahle J, Jonasdottir TJ, Heyerdahl H, et al. Assessment of long-term radiotoxicity after treatment with the low-dose-rate alpha-particle-emitting radioimmunoconjugate 227Th- rituximab. Eur J Nucl Med Mol Imaging. 2010;37(1):93–102.
26. McDevitt M, Nikula T, Finn R. Bismuth labeled antibodies for therapy of leukemias, lymphomas, and carcinomas: preclinical studies. Tumor Target. 1996;2(Abstract):182.
27. Schwartz J, Jaggi JS, O'Donoghue JA, et al. Renal uptake of bismuth-213 and its contribution to kidney radiation dose following administration of actinium-225-labeled antibody. Phys Med Biol. 2011;56(3):721–733.
28. Jurcic JG, Larson SM, Sgouros G, et al. Targeted alpha particle immunotherapy for myeloid leukemia. Blood. 2002;100(4):1233–1239.
• **The first proof-of-concept for systemic-targeted alpha immunotherapy in humans using a monoclonal antibody as targeting vehicle.**
29. Rosenblat TL, McDevitt MR, Mulford DA, et al. Sequential cytarabine and α-particle immunotherapy with bismuth-213–lintuzumab (HuM195) for acute myeloid leukemia. Clin Cancer Res. 2010;16 (21):5303–5311.
30. Heeger S, Moldenhauer G, Egerer G, et al. Conventional and pretargeted radioimmunotherapy using bismuth-213 to target and treat non-Hodgkin lymphomas expressing CD20: a preclinical model toward optimal consolidation therapy to eradicate minimal residual disease. Blood. 2010;116(20):4231–4239.
31. Roscher M, Hormann I, Leib O, et al. Targeted alpha-therapy using [Bi-213] anti-CD20 as novel treatment option for radio-and chemoresistant non-Hodgkin lymphoma cells. Oncotarget. 2013;4 (2):218–230.
32. Heeger S, Moldenhauer G, Egerer G. Alpha-radioimmunotherapy of B-lineage non-Hodgkin's lymphoma using 213Bi-labelled anti-CD19-and anti-CD20-CHX-A"-DTPA conjugates. Abstr Pap Am Chem Soc. 2003;225:U261.
33. Song EY, Abbas Rizvi SM, Qu CF, et al. Pharmacokinetics and toxicity of213Bi-labeled PAI2 in preclinical targeted alpha therapy for cancer. Cancer Biol Ther. 2007;6(6):898–904.
34. Allen BJ, Tian Z, Rizvi SMA, et al. Preclinical studies of targeted alpha therapy for breast cancer using 213Bi-labelled-plasminogen activator inhibitor type 2. Br J Cancer. 2003;88(6):944–950.
35. Qu CF, Song EY, Li Y, et al. Pre-clinical study of 213Bi labeled PAI2 for the control of micrometastatic pancreatic cancer. Clin Exp Metastasis. 2005;22(7):575–586.
36. Song EY, Qu CF, Rizvi SMA, et al. Bismuth-213 radioimmunotherapy with C595 anti-MUC1 monoclonal antibody in an ovarian cancer ascites model. Cancer Biol Ther. 2008;7(1):76–80.
37. Qu CF, Songl YJ, Rizvi SMA, et al. In vivo and in vitro inhibition of pancreatic cancer growth by targeted alpha therapy using 213Bi-CHX.A"-C595. Cancer Biol Ther. 2005;4(8):848–853.
38. Cordier D, Forrer F, Bruchertseifer F, et al. Targeted alpha-radionuclide therapy of functionally critically located gliomas with 213Bi-DOTA-[Thi8, Met (O2) 11]-substance P: a pilot trial. Eur J Nucl Med Mol Imaging. 2010;37(7):1335–1344.
39. Morgenstern A, Krolicki L, Kunikowska J, et al. Targeted alpha therapy of glioblastoma multiforme: first clinical experience with 213Bi-substance P. J Nucl Med. 2014;55(supplement 1):390–390.
40. Rizvi SMA, Allen BJ, Tian Z, et al. In vitro and preclinical studies of targeted alpha therapy (TAT) for colorectal cancer. Color Dis. 2001;3 (5):345–353.
41. Li Y, Wang J, Abbas Rizvi SM, et al. In vitro targeting of NG2 antigen by 213Bi-9.2.27 α-immunoconjugate induces cytotoxicity in human uveal melanoma cells. Investig Ophthalmol Vis Sci. 2005;46 (12):4365–4371.
42. Raja C, Graham P, Abbas Rizvi S, et al. Interim analysis of toxicity and response in phase 1 trial of systemic targeted alpha therapy for metastatic melanoma. Cancer Biol Ther. 2007;6(6):846–852.
43. Allen BJ, Raja C, Rizvi S, et al. Intralesional targeted alpha therapy for metastatic melanoma. Cancer Biol Ther. 2005;4(12):1318–1324.
44. Fichou N. Single-dose anti-CD138 radioimmunotherapy: bismuth-213 is more efficient than lutetium-177 for treatment of multiple myeloma in a preclinical model. Front Med. 2015;2(76):1–11.
45. Li Y, Tian Z, Rizvi SMA, et al. In vitro and preclinical targeted alpha therapy of human prostate cancer with Bi-213 labeled J591 antibody against the prostate specific membrane antigen. Prostate Cancer Prostatic Dis. 2002;5(1):36–46.
46. Adams GP, Shaller CC, Chappell LL, et al. Delivery of the α-emitting radioisotope bismuth-213 to solid tumors via single-chain Fv and diabody molecules. Nucl Med Biol. 2000;27(4):339–346.
47. Tan Z, Chen P, Schneider N, et al. Significant systemic therapeutic effects of high-LET immunoradiation by 212Pb-trastuzumab against prostatic tumors of androgen-independent human prostate cancer in mice. Int J Oncol. 2012;40(6):1881–1888.
48. Yong K, Brechbiel M. Application of 212Pb for Targeted α-particle Therapy (TAT): pre-clinical and mechanistic understanding through to clinical translation. AIMS Med Sci. 2015;2(3):228–245.
49. Meredith R, Torgue J, Shen S, et al. Dose escalation and dosimetry of first-in-human α radioimmunotherapy with 212Pb-TCMC-trastuzumab. J Nucl Med. 2014;55(10):1636–1642.
50. Meredith RF, Torgue J, Azure MT, et al. Pharmacokinetics and imaging of 212Pb-TCMC-trastuzumab after intraperitoneal administration in ovarian cancer patients. Cancer Biother Radiopharm. 2013;29(1):12–18.
51. Zalutsky MR, Garg PK, Friedman HS, et al. Labeling monoclonal antibodies and F (ab ') 2 fragments with the a-particle-emitting nuclide astatine-211: Preservation of immunoreactivity and in vivo localizing capacity. Proc Natl Acad Sci. 1989;86(18): 7149–7153.
52. Zalutsky MR, Stabin MG, Larsen RH, et al. Tissue distribution and radiation dosimetry of astatine-211-labeled chimeric 81C6, an α-particle-emitting immunoconjugate. Nucl Med Biol. 1997;24 (3):255–261.
53. Zalutsky MR, Reardon DA, Akabani G, et al. Clinical experience with α-particle–emitting 211At: treatment of recurrent brain tumor patients with 211At-labeled chimeric antitenascin monoclonal antibody 81C6. J Nucl Med. 2007;49(1):30–38.
54. Elgqvist J, Andersson H, Bäck T, et al. Fractionated radioimmunotherapy of intraperitoneally growing ovarian cancer in nude mice with 211 At-MX35 F (ab') 2: therapeutic efficacy and myelotoxicity. Nucl Med Biol. 2006;33(8):1065–1072.
55. Andersson H, Cederkrantz E, Bäck T, et al. Intraperitoneal α-particle radioimmunotherapy of ovarian cancer patients: pharmacokinetics and dosimetry of 211At-MX35 F (ab') 2—a phase I study. J Nucl Med. 2009;50(7):1153–1160.
56. Andersson H, Lindegren S, Bäck T, et al. The curative and palliative potential of the monoclonal antibody MOv18 labelled with 211At in nude mice with intraperitoneally growing ovarian cancer xenografts-a long-term study. Acta Oncol (Madr). 2000;39(6):741–745.
57. Reist CJ, Foulon CF, Alston K, et al. Astatine-211 labeling of internalizing anti-EGFRvIII monoclonal antibody using N-succinimidyl 5-[211 At] astato-3-pyridinecarboxylate. Nucl Med Biol. 1999;26 (4):405–411.

58. Robinson MK, Shaller C, Garmestani K, et al. Effective treatment of established human breast tumor xenografts in immunodeficient mice with a single dose of the α-emitting radioisotope astatine-211 conjugated to anti-HER2/neu diabodies. Clin Cancer Res. 2008;14(3):875–882.
59. Steffen A-C, Almqvist Y, Chyan M-K, et al. Biodistribution of 211At labeled HER-2 binding affibody molecules in mice. Oncol Rep. 2007;17(5):1141–1147.
60. Henriksen G, Breistol K, Bruland OS, et al. Significant antitumor effect from bone-seeking, alpha-particle-emitting (223)Ra demonstrated in an experimental skeletal metastases model. Cancer Res. 2002;62(11):3120–3125.
61. Parker C, Nilsson S, Heinrich D, et al. Alpha emitter radium-223 and survival in metastatic prostate cancer. N Engl J Med. 2013;369 (3):213–223.
62. Nilsson S, Larsen RH, Fosså SD, et al. First clinical experience with alpha-emitting radium-223 in the treatment of skeletal metastases. Clin Cancer Res. 2005;11(12):4451–4459.
63. Pozzi OR, Zalutsky MR. Radiopharmaceutical chemistry of targeted radiotherapeutics, part 2 : radiolytic effects of 211At alpha-particles influence N-succinimidyl 3-211At-astatobenzoate synthesis. J Nucl Med. 2005;46(8):1393–1400.
64. Pozzi OR, Zalutsky MR. Radiopharmaceutical chemistry of targeted radiotherapeutics, Part 3: alpha-particle-induced radiolytic effects on the chemical behavior of 211At. J Nucl Med. 2007;48(7):1190–1196.
65. Boyd M, Sorensen A, McCluskey AG, et al. Radiation quality-dependent bystander effects elicited by targeted radionuclides. J Pharm Pharmacol. 2008;60(8):951–958.
66. Mancuso M, Pasquali E, Leonardi S, et al. Oncogenic bystander radiation effects in patched heterozygous mouse cerebellum. Proc Natl Acad Sci. 2008;105(34):12445–12450.
67. Havaki S, Kotsinas A, Chronopoulos E, et al. The role of oxidative DNA damage in radiation induced bystander effect. Cancer Lett. 2015;356(1):43–51. Elsevier Ireland Ltd.
68. De Kruijff R, Wolterbeek H, Denkova A. A critical review of alpha radionuclide therapy—how to deal with recoiling daughters? Pharmaceuticals. 2015;8(2):321–336.
69. Lewis B, Chalhoub E, Chalouhy C, et al. Radium-223 in bone-metastatic prostate cancer: current data and future prospects. Oncology (Williston Park). 2015;29(7):483–488.
• **Manuscript describes the successful alpha emitter ^{223}Ra that has been approved by the US Food and Drug Administration (FDA).**
70. Miederer M, Scheinberg DA, McDevitt MR. Realizing the potential of the actinium-225 radionuclide generator in targeted alpha particle therapy applications. Adv Drug Deliv Rev. 2008;60(12):1371–1382.
71. McDevitt MR, Ma D, Lai LT, et al. Tumor therapy with targeted atomic nanogenerators. Science. 2001;294:1537–1541.
72. Sgouros G, Roeske JC, Mcdevitt MR, et al. MIRD pamphlet no. 22 - radiobiology and dosimetry of alpha- particle emitters for targeted radionuclide therapy. J Nucl Med. 2010;51(22):311–328.
73. Huang C-Y, Oborn BM, Guatelli S, et al. Monte Carlo calculation of the maximum therapeutic gain of tumor antivascular alpha therapy. Med Phys. 2012;39(3):1282–1288.
74. Huang CY, Guatelli S, Oborn BM, et al. Microdosimetry for targeted alpha therapy of cancer. Comput Math Methods Med. 2012;2012.
75. Bäck T, Jacobsson L. The alpha-camera: a quantitative digital autoradiography technique using a charge-coupled device for ex vivo high-resolution bioimaging of alpha-particles. J Nucl Med. 2010;51 (10):1616–1623.
76. FDA Approves Xofigo for Advanced Prostate Cancer [Internet]. 2013. Available from: http://www.fda.gov/NewsEvents.
77. Bruland ÒS, Nilsson S, Fisher DR, et al. High-linear energy transfer irradiation targeted to skeletal metastases by alpha-emitter 223Ra: adjuvant or alternative to conventional modalities? Clin Cancer Res. 2006;12(21):6250–6257.
78. Wadas TJ, Pandya DN, Solingapuram Sai KK, et al. Molecular targeted α-particle therapy for oncologic applications. Am J Roentgenol. 2014;203:253–260.
79. McDevitt MR, Sgouros G, Finn RD, et al. Radioimmunotherapy with alpha-emitting nuclides. Eur J Nucl Med. 1998;25(9):1341–1351.
80. Apostolidis C, Molinet R, McGinley J, et al. Cyclotron production of Ac-225 for targeted alpha therapy. Appl Radiat Isot. 2005;62 (3):383–387.
81. McDevitt MR, Ma D, Simon J, et al. Design and synthesis of 225Ac radioimmunopharmaceuticals. Appl Radiat Isot. 2002;57:841–847.
82. Maguire WF, McDevitt MR, Smith-Jones PM, et al. Efficient 1-step radiolabeling of monoclonal antibodies to high specific activity with 225Ac for α-particle radioimmunotherapy of cancer. J Nucl Med. 2014;55(9):1492–1498.
83. Pippin CG, Gansow OA, Brechbiel MW, et al. Recovery of Bi-213 from an Ac-225 cow: application to the radiolabeling of antibodies with Bi-213. Chemists' Views of Imaging Centers. Springer US. 1995;315–322.
84. McDevitt MR, Finn RD, Ma D, et al. Preparation of (alpha)-emitting (213) Bi-labeled antibody constructs for clinical use. J Nucl Med. 1999;40(10):1722.
85. Guérard F, Gestin J-F, Brechbiel MW. Production of (211At)-astatinated radiopharmaceuticals and applications in targeted α-particle therapy. Cancer Biother Radiopharm. 2013;28(1):1–20.
86. Zalutsky MR, Pruszynski M. Astatine-211: production and availability. Curr Radiopharm. 2011;4(3):177–185.
•• **Paper describes the potential advantages of ^{211}At for targeted α-particle therapy.**
87. Zalutsky MR, Vaidyanathan G. Astatine-211-labeled radiotherapeutics an emerging approach to targeted alpha-particle radiotherapy. Curr Pharm Des. 2000;6(14):1433–1455.
88. Zalutsky MR, Zhao X, Alston KL, et al. High-level production of α-particle–emitting 211At and preparation of 211At-labeled antibodies for clinical use. J Nucl Med. 2001;42(10):1508–1516.
89. Vaidyanathan G, Larsen RH, Zalutsky MR. 5-[211At] Astato-2'-deoxyuridine, an α-particle-emitting endoradiotherapeutic agent undergoing DNA incorporation. Cancer Res. 1996;56(6):1204–1209.
90. Foulon CF, Alston KL, Zalutsky MR. Astatine-211-labeled biotin conjugates resistant to biotinidase for use in pretargeted radioimmunotherapy. Nucl Med Biol. 1998;25(2):81–88.
91. Bloomer WD, McLaughlin WH, Neirinckx RD, et al. Astatine-211–tellurium radiocolloid cures experimental malignant ascites. Science. 1981;212(4492):340–341.
92. Link EM, Carpenter RN. 211At-methylene blue for targeted radiotherapy of human melanoma xenografts: treatment of micrometastases. Cancer Res. 1990;50(10):2963–2968.
93. Vaidyanathan G, Zalutsky MR. No-carrier-added meta-[123 I] iodobenzylguanidine: synthesis and preliminary evaluation. Nucl Med Biol. 1995;22(1):61–64.
94. Murud KM, Larsen RH, Bruland OS, et al. Influence of pretreatment with 3-amino-1-hydroxypropylidene-1, 1-bisphosphonate (APB) on organ uptake of 211 At and 125 I-labeled amidobisphosphonates in mice. Nucl Med Biol. 1999;26(7):791–794.
95. Larson SM, Carrasquillo JA, Cheung N-KV, et al. Radioimmunotherapy of human tumours. Nat Rev Cancer. 2015;15(6):347–360. Nature Publishing Group.
96. Holliger P, Hudson PJ. Engineered antibody fragments and the rise of single domains. Nat Biotechnol. 2005;23(9):1126–1136.
97. Müller C, Schibli R. Prospects in folate receptor-targeted radionuclide therapy. Front Oncol. 2013;3:249.
98. Vergote I, Leamon CP. Vintafolide: a novel targeted therapy for the treatment of folate receptor expressing tumors. Ther Adv Med Oncol. 2015;7(4):206–218.
99. Dong C, Liu Z, Wang F. Peptide-based radiopharmaceuticals for targeted tumor therapy. Curr Med Chem. 2014;21(1):139–152.
100. Löfblom J, Feldwisch J, Tolmachev V, et al. Affibody molecules: engineered proteins for therapeutic, diagnostic and biotechnological applications. FEBS Lett. 2010;584(12):2670–2680. Federation of European Biochemical Societies.

101. Hamers-Casterman C, Atarhouch T, Muyldermans S, et al. Naturally occurring antibodies devoid of light chains. Nature. 1993;363 (6428):446–448.
102. De Vos J, Devoogdt N, Lahoutte T, et al. Camelid single-domain antibody-fragment engineering for (pre)clinical in vivo molecular imaging applications: adjusting the bullet to its target. Expert Opin Biol Ther. 2013;13(8):1149–1160.
103. D'Huyvetter M, Xavier C, Caveliers V, et al. Radiolabeled nanobodies as theranostic tools in targeted radionuclide therapy of cancer. Expert Opin Drug Deliv. 2014;131(12):1–16. Informa UK, Ltd.
104. Huang L, Gainkam LOT, Caveliers V, et al. SPECT imaging with 99mTc-labeled EGFR-specific nanobody for in vivo monitoring of EGFR expression. Mol Imaging Biol. 2008;10(3):167–175.
105. Vaneycken I, Govaert J, Vincke C, et al. In vitro analysis and in vivo tumor targeting of a humanized, grafted nanobody in mice using pinhole SPECT/micro-CT. J Nucl Med. 2010;51(7):1099–1106.
106. Vaneycken I, Devoogdt N, Van Gassen N, et al. Preclinical screening of anti-HER2 nanobodies for molecular imaging of breast cancer. Faseb J. 2011;25(7):2433–2446.
107. Tchouate Gainkam LO, Caveliers V, Devoogdt N, et al. Localization, mechanism and reduction of renal retention of technetium-99m labeled epidermal growth factor receptor-specific nanobody in mice. Contrast Media Mol Imaging. 2011;6(2):85–92.
108. Schoonooghe S, Laoui D, Van Ginderachter JA, et al. Novel applications of nanobodies for in vivo bio-imaging of inflamed tissues in inflammatory diseases and cancer. Immunobiology. 2012;217 (12):1266–1272. Elsevier GmbH.
109. D'Huyvetter M, Vincke C, Xavier C, et al. Targeted radionuclide therapy with A 177Lu-labeled anti-HER2 nanobody. Theranostics. 2014;4(7):708–720.
• **First paper that describes the successful nanobody-based targeted radionuclide therapy of HER2^{pos} cancer.**
110. Keyaerts M, Xavier C, Heemskerk J, et al. Phase I study of 68Ga-HER2-nanobody for PET/CT assessment of HER2 expression in breast carcinoma. J Nucl Med. 2015;57(1):27–33.
•• **The first clinical trial with ^{68}Ga-labeled anti-HER2 nanobody in HER2^{pos} breast carcinoma (EudraCT number 2012-001135-31).**
111. Lemaire M, D'Huyvetter M, Lahoutte T, et al. Imaging and radioimmunotherapy of multiple myeloma with anti-idiotypic nanobodies. Leukemia. 2014;28(2):444–447.
112. Pruszynski M, Koumarianou E, Vaidyanathan G, et al. Improved tumor targeting of anti-HER2 nanobody through N-succinimidyl 4-guanidinomethyl-3-iodobenzoate radiolabeling. J Nucl Med. 2014;55(4):650–656.
•• **Successful radioiodination of an anti-HER2 nanobody with SGMIB as the residualizing agent.**
113. Choi J, Vaidyanathan G, Koumarianou E, et al. N-succinimidyl guanidinomethyl iodobenzoate protein radiohalogenation agents: influence of isomeric substitution on radiolabeling and target cell residualization. Nucl Med Biol. 2014;41 (10):802–812.
114. Choi J, Vaidyanathan G, Koumarianou E, et al. A 211At-labeled nanobody for α-particle therapy of HER2-expressing cancers. J Nucl Med. 2015;56(Supplement 3):171.
115. Zheng F, Put S, Bouwens L, et al. Molecular imaging with macrophage CRIg-targeting nanobodies for early and preclinical diagnosis in a mouse model of rheumatoid arthritis. J Nucl Med. 2014;55 (5):824–829.
116. Aneheim E, Albertsson P, Bäck T, et al. Automated astatination of biomolecules – a stepping stone towards multicenter clinical trials. Sci Rep. 2015;5:12025. Nature Publishing Group
117. Oliveira S, Schiffelers RM, Van Der Veeken J, et al. Downregulation of EGFR by a novel multivalent nanobody-liposome platform. J Control Release. 2010;145(2):165–175. Elsevier B.V.

２ アイソトープ Supply of Radioisotopes

2.1 アイソトープの供給量 Amounts of Radioisotopes Supplied

2.1.1 おもな非密封アイソトープの供給量の推移（核種別，年度別）
Amounts of Major Unsealed Radioisotopes§ Supplied in Fiscal 2012-2016

（単位Unit：MBq）

核種 Nuclide ＼ 年度 Year	2012	2013	2014	2015	2016
^{3}H Total	230,198	262,603	148,831	210,084	415,415
（標識化合物 ^{3}H-Labeled compound）	230,197	188,601	148,829	210,081	415,413
^{14}C Total	77,391	86,604	129,476	67,834	37,840
（標識化合物 ^{14}C-Labeled compound）	77,391	86,604	118,355	67,832	37,839
^{18}F	29,970	41,070	37,555	50,750	38,170
^{22}Na	122	171	74	122	818
^{32}P Total	113,024	96,418	73,030	68,456	52,664
（標識化合物 ^{32}P-Labeled compound）	69,264	62,632	54,296	42,583	52,647
^{33}P Total	12,230	11,188	9,166	8,155	3,435
（標識化合物 ^{33}P-Labeled compound）	4,220	3,602	4,763	5,250	3,435
^{35}S Total	56,649	51,670	38,915	38,522	28,965
（標識化合物 ^{35}S-Labeled compound）	53,134	49,561	36,658	36,154	28,964
^{45}Ca	1,222	815	963	815	561
^{51}Cr	31,943	32,737	23,562	20,787	24,236
^{54}Mn	108	71	75	56	37
^{55}Fe	335	777	296	222	296
^{57}Co	168	371	249	235	149
^{59}Fe	298	538	463	186	166
^{60}Co	7	32	9	6	8
^{63}Ni	28	37	9	0	2
^{65}Zn	66	104	108	23	54
^{67}Ga	518	703	1,083	1,130	999
^{68}Ge	3,488	4,255	2,447	3,330	2,072
^{75}Se	226	7	44	11	4
^{85}Kr	211,650	214,260	226,508	4,840	70,892
^{85}Sr	420	364	212	268	134
^{86}Rb	592	148	121	74	148
^{89}Sr	458	160	149	141	1
^{90}Sr	6	13	32	21	9
^{90}Y	20,572	7,363	4,403	6,505	3,885
^{99}Mo	148,000	175,750	236,874	155,400	156,325
^{99m}Tc	99,561	78,494	63,399	64,870	42,290
^{109}Cd	10	6	21	3	12
^{111}In	10,915	12,765	11,396	13,886	11,259
^{123}I	16,440	12,710	24,919	56,410	77,004
^{125}I Total	77,832	71,950	61,978	65,890	46,132
（標識化合物 ^{125}I-Labeled compound）	4,236	4,007	3,892	4,184	46,126
^{131}I	17,432	20,397	15,355	15,591	21,519
^{134}Cs	41	9	5	26	8
^{137}Cs	251	246	248	159	141
^{177}Lu	370	370	-	-	-
^{201}Tl	666	353	333	639	1,036
その他 Others	76	69	119	71	194
合 計 Total	1,163,283	1,185,598	1,112,427	855,518	1,036,880
供給先事業所数 Number of users	503	488	428	417	391

§ Radionuclide/Labeled Compounds, Radiopharmaceuticals for research puropose

2.1.2 おもな非密封アイソトープの供給量（核種別，機関別）2016年度

Amounts of Major Unsealed Radioisotopes§ Supplied in Fiscal 2016 (by Organization)

（単位Unit：MBq）

核種 Nuclide ＼ 機関 Organization	総数 Total	医療機関 Hospital and Clinic	教育機関 Educational Institution	研究機関 Research Institute	民間企業 Private Company	その他の機関 Others
^{3}H	415,415	19,086	305,054	62,057	29,218	0
^{14}C	37,840	0	1,234	34,522	2,084	-
^{18}F	38,170	925	6,105	12,580	18,005	555
^{22}Na	818	-	89	729	-	-
^{32}P	52,664	351	26,206	21,242	4,643	222
^{33}P	3,435	-	794	2,641	-	-
^{35}S	28,965	-	21,687	6,975	303	-
^{45}Ca	561	-	518	43	-	-
^{51}Cr	24,236	259	9,259	6,744	7,900	74
^{54}Mn	37	-	37	-	-	0
^{55}Fe	296	-	259	37	-	-
^{57}Co	149	-	130	19	-	-
^{59}Fe	166	-	55	92	-	19
^{60}Co	8	-	-	3	1	4
^{63}Ni	2	-	-	2	-	-
^{65}Zn	54	-	43	11	-	-
^{67}Ga	999	148	851	-	-	-
^{68}Ge	2,072	925	-	-	1,147	-
^{75}Se	4	-	-	4	-	-
^{85}Kr	70,892	-	-	-	70,892	-
^{85}Sr	134	-	59	75	-	-
^{86}Rb	148	-	74	74	-	-
^{89}Sr	1	-	-	0	1	0
^{90}Sr	9	-	1	7	1	0
^{90}Y	3,885	-	2,405	1,480	-	-
^{99}Mo	156,325	5,550	115,625	24,050	9,250	1,850
^{99m}Tc	42,290	-	24,790	16,650	110	740
^{109}Cd	12	-	10	2	-	-
^{111}In	11,259	148	5,661	5,106	-	344
^{123}I	77,004	62,789	12,069	2,035	111	-
^{125}I	46,132	269	10,961	15,172	19,730	-
^{131}I	21,519	-	3,108	3,971	14,070	370
^{134}Cs	8	-	1	7	-	-
^{137}Cs	141	-	43	98	0	0
^{201}Tl	1,036	148	666	-	222	-
その他 Others	194	-	19	175	0	0
合　計 Total	1,036,880	90,598	547,813	216,603	177,688	4,178

§ Radionuclide/Labeled Compounds, Radiopharmaceuticals for research puropose

参考文献[４]抜粋

TABLE I

RADIONUCLIDES ARRANGED IN ORDER OF THEIR MOST RESTRICTIVE $(MPC)_a$ VALUE

HIGH TOXICITY

Pa^{231}, Cf^{249}, Th-Nat, Pu^{239}, Pu^{240}, Pu^{242}, Th^{232}, Pu^{238}, Ac^{227}, Th^{230}, Np^{237}, Th^{228}, Am^{241}, Am^{243}, Cm^{243}, Cm^{245}, Cm^{246}, Cf^{250}, Cf^{252}, Cm^{244}, U^{232}, Ra^{226}, Ra^{228}, Sm^{147}, U-Nat, Nd^{144}, U^{238}, Pu^{241}, Pb^{210}, U^{230}, U^{233}, U^{234}, U^{235}, U^{236}, Cm^{242}, Th^{227}, Po^{210}, Ra^{223}, Sr^{90}.

MEDIUM TOXICITY

Upper Sub-Group A

Ra^{224}, Pa^{230}, Bk^{249}, I^{129}, Eu^{154}, Ru^{106}, Ce^{144}, Bi^{210}, At^{211}, Na^{22}, Co^{60}, Ag^{110m}, I^{126}, I^{131}, Cs^{134}, Eu^{152}(13yr), Cs^{137}, Bi^{207}, Pb^{212}, Ac^{228}, In^{114m}, Sb^{124}, Ta^{182}, Cl^{36}, Sc^{46}, Sb^{125}, Ir^{192}, Tl^{204}, Ca^{45}, Mn^{54}, Y^{91}, Zr^{95}, Sr^{89}, Cd^{115m}, In^{115}, Te^{127m}, Te^{129m}, I^{133}, Ba^{140}, Tb^{160}, Tm^{170}, Hf^{181}, Th^{234}.

Lower Sub-Group B

P^{32}, V^{48}, Fe^{59}, Co^{58}, Ni^{63}, Zn^{65}, Rb^{86}, Rb^{87}, Tc^{99}, Cd^{109}, Sn^{113}, Pm^{147}, Sm^{151}, Os^{185}, Hg^{203}, As^{76}, Y^{90}, Zr^{97}, Nb^{95}, Ru^{103}, Ag^{105}, Sn^{125}, Cs^{135}, Eu^{155}, Gd^{153}, Bi^{212}, K^{42}, As^{74}, Se^{75}, Sr^{85}, Nb^{93m}, Zr^{93}, Te^{125m}, Te^{132}, I^{135}, La^{140}, Tm^{171}, W^{181}, W^{185}, Na^{24}, Sc^{48}, Mn^{52}, Y^{93}, Tc^{97m}, Sb^{122}, Ce^{141}, Pr^{142}, Re^{183}, Ir^{194}, Bi^{206}, Ca^{47}, Co^{57}, Ga^{72}, Br^{82}, Cd^{115}, Te^{131m}, Cs^{136}, Pr^{143}, Ho^{166}, Re^{188}, Pa^{233}, Mo^{99}, Ce^{143}, Dy^{166}, Tc^{96}, Ag^{111}, I^{132}, Nd^{147}, Pm^{149}, Re^{186}, Au^{198}, Tl^{202}, S^{35}, Sr^{91}, Os^{143}, Zn^{69m}, As^{73}, As^{77}, Sr^{92}, Y^{92}, Tc^{97}, Pd^{109}, Ba^{131}, Sm^{153}, Eu^{152}(4.2h), Gd^{159}, Er^{169}, W^{187}, Os^{191}, Ir^{190}, Pt^{193}, Rn^{220}, Rn^{222}, * Sc^{47}, Mn^{56}, Ni^{59}, Ni^{65}, Kr^{87}, Ru^{105}, Rh^{105}, I^{134}, Er^{171}, Yb^{175}, Lu^{177}, Re^{187}, Pt^{191}, Pt^{197}, Au^{196}, Np^{239}, Si^{31}, Fe^{55}, Pd^{103}, Te^{127}, Au^{199}, Hg^{197m}, Tl^{200}, Tl^{201}, Be^{7}, A^{41}, Cu^{64}, Hg^{197}, Th^{231}, Nd^{149}, Ru^{97}, In^{115m}, Pb^{203}, Cl^{38}, Dy^{165}, Cr^{51}, F^{18}, C^{14}, Kr^{85m}, Te^{129}, Xe^{135}, Cs^{131}.

LOW TOXICITY

H^{3}, Zn^{69}, Ge^{71}, Nb^{97}, In^{113m}, Cs^{134m}, Pt^{193m}, Pt^{197m}, Tc^{99m}, Co^{58m}, Kr^{85}, Xe^{133}, Os^{191m}, Xe^{131m}, Y^{91m}, Sr^{85m}, Tc^{96m}, Rh^{103m}, A^{37}.

* The figure used for this isotope is the same as that given in Basic Safety Standards for Radiation Protection [3].

参考文献[５]

Journal of Nuclear Medicine, published on March 1, 2018 as doi:10.2967/jnumed.117.204651

Alpha Emitters for Radiotherapy: Basic Radiochemistry to Clinical Studies – Part 2

Running title: Alpha Emitters for Radiotherapy

Sophie Poty[1], Lynn C. Francesconi[2,3], Michael R. McDevitt[1,4], Michael J. Morris[5],

Jason S. Lewis[1,6]

[1]*Department of Radiology and the Program in Molecular Pharmacology, Memorial Sloan Kettering Cancer Center, New York, NY, USA*
[2]*Department of Chemistry, Hunter College, New York, NY, USA*
[3]*The Graduate Center of the City University of New York, New York, NY, USA*
[4]*Department of Radiology, Weill Cornell Medical College, New York, NY, USA*
[5]*Department of Medicine, Memorial Sloan Kettering Cancer Center, New York, NY, USA*
[6]*Departments of Radiology and Pharmacology, Weill Cornell Medical College, New York, NY, USA*

Correspondence: Jason S. Lewis, PhD, 1275 York Avenue, New York, NY 10065, USA. Phone: 646-888-3038, FAX: 646-422-0408, Email: lewisj2@mskcc.org

First author: Sophie Poty, PhD, 1275 York Avenue, New York, NY 10065, USA. Phone: 646-888-3080, FAX: 646-422-0408, Email: potys@mskcc.org

Word count: 5845

Disclaimer: The authors have nothing to disclose.

Financial support: The authors gratefully acknowledge the Radiochemistry and Molecular Imaging Probe core, which was supported in part by the NIH/NCI Cancer Center Support Grant P30 CA008748. We gratefully acknowledge Mr. William H. and Mrs. Alice Goodwin and the Commonwealth Foundation for Cancer Research and The Center for Experimental Therapeutics of Memorial Sloan Kettering Cancer Center (JSL) and the fellowship from the François Wallace Monahan Fellowship from the JLM Benevolent Fund (SP).

Key words: Radiotherapy, Alpha Emitters, Radiochemistry, Clinical Trials

Learning Objectives: On successful completion of this activity, participants should be able to (1) match α-emitters to potential vectors or targets of interest; (2) highlight the potential of α-emitters in preclinical work; and (3) identify the current clinical uses of α-emitters and the importance of clinical trial design for broader application of α-therapy.

Abstract: The use of radioactive sources to deliver cytotoxic ionizing radiation to disease sites dates back to the early 20th century, with the discovery of radium and its physiological effects. Alpha-emitters are of particular interest in the field of clinical oncology for radiotherapy applications. The first part of this review explored α-emitting radionuclides' basic radiochemistry, high cell-killing potency, and availability, together with hurdles such as radiolabeling methods and daughter redistribution. The second part of this review will give an overview of the most promising and current uses of α-emitters in preclinical and clinical studies.

The short particle range and high linear energy transfer of alpha-emitting radionuclides complement the large particle range and low energy transfer of β-particles. These physical characteristics allow α-particles to deposit the great majority of their energy in the area surrounding the desired targeted tumor cells (< 100 μm), enabling them to kill isolated tumor cells. Alpha-emitting radionuclides are therefore of particular interest for the treatment of systemic disease such as leukemia or lymphoma but also minimal disseminated disease composed of small clusters or isolated tumor cells. The past few years have also seen the preclinical and/or clinical use of alpha-emitters for the treatment of solid primary and metastatic disease such as glioblastoma or castration-resistant prostate cancer (CRPC) (*1,2*). Six α-emitters are currently under investigation in preclinical and clinical studies using either their intrinsic targeting properties or targeted alpha-therapy (TAT) strategies. Antibodies, peptides, and small molecules have been successfully conjugated to α-particle emitters; however, few of these α-conjugates have been translated to the clinic for evaluation.

For basic physical characteristics of the described alpha-emitters, the authors would like to refer the readers to Part 1 of this review.

PRECLINICAL EVALUATION (PUBLISHED OVER THE LAST 10 YEARS)

The design of preclinical studies plays an important role in the success and translation of α-therapy to the clinical stage (Fig. 1). The following section presents a selection of preclinical studies with strong translational potential.

Systemic cancers: Lymphoma and leukemia

CD20 is a well-known target for the treatment of B-cell lymphoma. Despite its intermediate half-life, ^{211}At has been conjugated to an anti-CD20 monoclonal antibody and evaluated in two lymphoma models: a subcutaneous tumor xenograft and a disseminated model (*3*). High total doses (1.78 MBq) of ^{211}At-anti-CD20 radioimmunotherapy (RIT) demonstrated moderate attenuation in tumor growth in a subcutaneous xenograft model. In contrast, a 0.55 MBq total dose resulted in complete disease eradication in 70% of the animals with the disseminated lymphoma model (Fig. 2A) (*3*). Following the 0.55 MBq total dose, universally lethal toxicity was observed within five days with severe weight loss and petechiae. This study highlights the different potential of α-therapy depending on tumor cell accessibility.

The longer-lived α-emitting radioisotope, ^{227}Th, was originally conjugated to antibodies such as trastuzumab and anti-CD20 mAb (rituximab), demonstrating significant tumor growth delay and prolonged survival in breast, ovarian, and lymphoma models (*4,5*). Long-term toxicity (up to 1 year) was assessed in mice with human lymphoma Raji xenografts (*6*). A 1000 kBq/kg dosage for [^{227}Th]Th-rituximab resulted in significant body weight decrease with temporary white blood cell and platelet count drops (*6*). The MTD was determined to be between 600-1000 kBq/kg with a maximum absorbed dose to the bone marrow between 2.1-3.5 Gy (*6*).

Reducing non-specific toxicity and hematotoxicity using the pretargeting method was investigated. Pretargeted α-RIT using an anti-CD20 single-chain variable region (scFv)-streptavidin construct and a [^{213}Bi]Bi-DOTA-biotin was reported by Park *et al.* to treat non-Hodgkin lymphoma (*7*). A favorable biodistribution profile was obtained using the pretargeting method with specific tumor uptake of 16.5% ± 7.0% injected dose per gram at 90 minutes post-injection (Fig. 2B) (*7*). A therapy study with injections of up to 29.6 MBq (total dose) of [^{213}Bi]Bi-DOTA-Biotin exhibited dose-dependent tumor response (*7*). Three

mice out of 10 achieved complete remission with the highest dose and only one showed signs of early toxicity, losing approximately 10% of its body weight. The median survival for the 22.2 MBq [^{213}Bi]Bi-DOTA-Biotin total dose group was 90 days compared to 19 days for untreated mice (*7*).

The anti-CD33 antibody, lintuzumab (HuM195), has a long history of TAT applications for the treatment of acute myeloid leukemia (AML) and the clinical use of this agent will be discussed later in this review. Preclinically, it was first conjugated to ^{213}Bi and ^{225}Ac, and more recently conjugated to ^{227}Th (*8*). In this study, complete tumor regression up to 20 days was observed in an AML xenograft model with a dose of 700 kBq/kg of ^{227}Th-RIT (*8*).

Metastatic prostate cancer

The external domain of prostate-specific membrane antigen (PSMA) is a major target of interest for TAT. McDevitt et al. successfully conjugated ^{213}Bi to J591, an anti-PSMA monoclonal antibody, and demonstrated the ability of the developed α-RIT to improve median tumor-free survival together with reduction of prostate specific antigen (PSA) levels in mice with intramuscular LNCaP xenografts (*9*). The past decade has also seen the development of numerous small molecule PSMA inhibitors to diagnose and treat prostate cancer. The actinium-225 conjugate will be described later in the clinical section of this review. An ^{211}At-labeled small PSMA inhibitor conjugate was recently evaluated in PSMA-positive mice models, showing significant tumor growth delay and improved survival (*10*). Long-term toxicity (up to 12 months) revealed nephropathy to be the dose-limiting effect, and the maximum tolerated dose (MTD) was set to be 37 kBq total dose in immunocompetent CD1 mice (*10*).

Radium-223 is a particularly interesting radionuclide due to its bone-seeking properties and its antitumor effects were demonstrated in animal models (*11*). Validation of this radionuclide in both preclinical and clinical studies is extensive, leading to the commercialization and use of this radioisotope in men with metastatic prostate cancer. We will, therefore, focus our interest on the clinical studies performed with this α-emitter in the clinical section below.

Disseminated intraperiteonal disease

Lead-212 (β-emitter), the decay daughter of ^{224}Ra and parent of ^{212}Bi (α-emitter), is widely exploited as an α-particle nanogenerator. ^{212}Pb was first validated preclinically when conjugated to trastuzumab to treat disseminated human epidermal growth factor receptor 2 (HER-2) positive peritoneal disease; its clinical application will be discussed in the next section (*12*). The contribution of internalization in HER-2 TAT in terms of efficacy was compared to a non-internalizing ^{212}Pb-labeled anti-carcinoembryonic antigen 35A7 antibody (*13*). A-431 intraperiteonal xenografted mice that express both HER-2 (low level) and carcinoembryonic antigen (high level) were injected with the same activity of both radioimmunoconjugates. Absorbed dose calculations revealed higher dose to the tumor in the case of the non-internalizing antibody [^{212}Pb]Pb-35A7 (35.5 Gy) compared to the internalizing [^{212}Pb]Pb-trastuzumab (27.6 Gy) (*13*). However, the trastuzumab conjugate led to an unexpected longer mean survival (> 130 days) (*13*). This study demonstrates the advantage of internalizing antibodies for therapy of small-volume xenograft tumors but also highlights the need for microdosimetry studies. With ^{212}Pb α-therapy of disseminated intraperitoneal disease well established, the Brechbiel group developed α-therapy targeting HER-1 (also referred to as epidermal growth factor receptor) to provide another possibility or treatment combination for patients with residual tumor tissue following debulking

surgery, micrometastatic disease, or disseminated peritoneal disease. Cetuximab was therefore radiolabeled with ^{212}Pb and total doses of 370-740 MBq were well tolerated by mice with minimal toxicity (*14*).

Emerging targets of interest – targeting the tumor microenvironement

CD70 belongs to the tumor necrosis factor superfamily and together with CD27L, plays an important role in T-cell signaling. It is overexpressed on T and B-cell lymphomas as well as on several types of solid tumors (i.e., renal cell carcinoma, ovarian and pancreatic adenocarcinoma, breast and colon cancer). CD-70 is notably a promising target for immunotherapy and was also investigated by Hagemann *et al.* for ^{227}Th-TAT (*15*). Mice bearing human renal cell carcinoma 789-O subcutaneous xenografts experienced complete growth inhibition with doses as low as 50 kBq/kg (*15*). Decreased circulating neutrophils, lymphocytes, and total white blood cells as compared to the control group indicated myelosuppression in the treated mice (Fig. 2C). However, this toxicity was transient and mice recovered by day 114 (*15*).

Targeting the tumor microenvironment such as the tumor vasculature and the neovascular endothelium are interesting targets for α-therapy. [^{225}Ac]Ac-E4G10 antibody-conjugate, which targets monomeric vascular endothelial cadherin, recently demonstrated inhibition of tumor growth and improved survival in a high-grade glioblastoma mouse model (*1*). Mechanistic studies highlighted the tumor blood-brain barrier microenvironment remodeling by dual depletion of endothelial and perivascular cells (*16*). Even though more than 20% of injected dose per gram of tissue of [^{225}Ac]Ac-E4G10 was observed in the liver after 10 days post-treatment, no liver toxicity was reported (*1*).

Integrins play an important role in tumor angiogenesis and their blockade can result in inhibition of tumor growth or metastasis. Among them, $\alpha_v\beta_3$ antagonists demonstrate

strong potential for the treatment of cancer. A DOTA-(RGDyK) peptide conjugate radiolabeled with ^{225}Ac displays high affinity for $\alpha_v\beta_3$ integrin (*17*). Cerenkov imaging performed in U87mg xenografted mice upon injection of 1.9 MBq (total dose) of the radiolabeled peptide, showed tumor, liver, and kidneys uptake. *Ex vivo* imaging confirmed the biodistribution (Fig. 2D) (*17*). Cerenkov radiation is observed with a wide range of medical isotopes, including ^{225}Ac (*18*). Since α-particles travel with low velocity, ^{225}Ac Cerenkov emissions are postulated to result from the β-decay of ^{213}Bi, ^{209}Tl, and ^{209}Pb. A therapy study using three different doses based on [^{225}Ac]Ac-DOTA-(RGDyK) MTD (0.04 MBq; 1 MTD, 0.5 MTD, and 0.25 MTD) showed high blood urea nitrogen retention in all cohorts, suggesting kidney impairment (*17*).

ALPHA VS. BETA STUDIES

The following studies compare the efficacy of α-particle therapy to β-particle therapy. ^{225}Ac-labeled anti-rat HER-2/neu mAb (7.16.4) efficacy was compared to ^{213}Bi and ^{90}Y conjugates to treat breast cancer lung metastasis (Fig. 3A) (*19*). Injection of the MTD resulted in improved median survivals: 50 days for the [^{90}Y]Y-7.16.4 group and 61 days for the [^{213}Bi]Bi-7.16.4 group. Of a total 12 mice, 8 achieved long-term survival (up to one year) in the [^{225}Ac]Ac-7.16.4-treated group (*19*). Alpha-therapy superiority compared to beta-therapy was attributed to the local α-radiation dose delivery vs. the β-particle energy that was mostly deposited outside of the metastasis. Due to the pharmacokinetics of the antibody-radioconjugates, >90% of the ^{213}Bi-conjugate decay occurred before reaching its target. The longer physical half-life of ^{225}Ac together with the emission of 4 net α-particles per decay therefore resulted in higher absorbed doses, which explains the longer survival of the ^{225}Ac-treated mice. Slow but significant release of ^{225}Ac daughters resulted in long-term renal toxicity (Fig. 3B) (*19*).

Peptide receptor radionuclide therapy using the somatostatin analog DOTATOC radiolabeled with ^{225}Ac and ^{177}Lu also compared α to β therapeutic potential (*20*). Equitoxic doses of the α- and β-emitter radiopharmaceuticals were determined using comparative cytotoxicity assessment and a factor of approximately 700 was applied between the ^{225}Ac- and ^{177}Lu-conjugates. The degree of DNA double-strand breaks was determined using quantification of γH2AX levels. The overall percentage of cells with γH2AX foci was significantly higher in tumors treated with 48 kBq (total dose) of [^{225}Ac]Ac-DOTATOC (35%) than those treated with 30 MBq (total dose) of [^{177}Lu]Lu-DOTATOC (21%) (Fig. 3C) (*20*). This observation was consistent with a delayed exponential tumor growth of 25 days with [^{225}Ac]Ac-DOTATOC vs. 21 days with [^{177}Lu]Lu-DOTATOC (Fig. 3D) (*20*).

Alpha-particle emitters have substantial therapeutic potential due to their ability to generate higher levels of double-DNA strand breaks compared to β-particle. However, alpha versus beta studies can be biased by the use of α-emitters with long half-lives and numerous alpha-emitting progeny that increase the tumor-absorbed dose. Dosimetric considerations, even though challenging with α-emitters, should be a parameter of choice for the determination of the administered activity in such comparative studies. Moreover, parameters such as the tumor size, hypoxia or the intratumoral radiopharmaceutical distribution should be considered.

In the clinic, the choice between α- or β-therapy is currently dependent on the patient tumor burden and previous response to β-therapy. Alpha-therapy is currently only offered at late disease stage and the efficacy of this therapy is still unknown at earlier disease stages (*21*). Comparison of the therapeutic potentials of alpha vs. beta therapy for clinical applications would therefore be premature at this moment. Further evaluation of α-therapy

is required at early stage disease but also in combination with current standard of care or new therapeutic approaches such as inhibition of DNA repair pathways (e.g. PARP inhibitors) (*21*). Cocktail approaches of α- and β-therapy should also be evaluated due to the complementary nature of their particle range.

CLINICAL EVALUATION

To our knowledge, 62 clinical trials were registered on clinicaltrials.gov using alpha emitters; among them, 52 involved [^{223}Ra]Ra-dichloride (Table 1) utilizing the bone-seeking properties of radium. This last section will focus on clinical achievement and evolution of the most notable clinical studies performed with α-emitting radionuclides.

Advanced myeloid leukemia: from [^{213}Bi]Bi-Lintuzumab to [^{225}Ac]Ac-Lintuzumab

In a phase I dose escalation trial, a humanized anti-CD33 mAb, HuM195 (lintuzumab) that targets myeloid leukemia cells was radiolabeled with ^{213}Bi (*22*). The choice of an α-emitting radionuclide was justified by the significant toxicities, particularly prolonged myelosuppression, observed in previous studies using β-particle emitters. Eighteen patients with primary refractory or relapsed advanced myeloid leukemia (AML) were treated with 10.4-37.0 MBq/kg (*22*). Although all patients developed transient myelosuppression (recovery time of 22 days), no extramedullary toxicity was observed. Of the evaluable patients, 93% showed a reduction in peripheral blood leukemia cells and 78% showed a reduction in bone marrow blasts. However, no patient achieved complete remission (*22*), likely because of the patients' large tumor burden (up to 10^{12} cells). Partial cytoreduction of the tumor burden prior to the ^{213}Bi treatment was evaluated in a phase I/II trial with sequential treatment with cytarabine (200 mg/m^2/d) and [^{213}Bi]Bi-HuM195

(18.5-46.3 MBq/kg) (*23*). A decrease in marrow blasts was reported for all dose levels and a ^{213}Bi dose-response relationship with remission was observed for doses ≥ 37 MBq/kg (*23*).

Actinium-225 was next considered as an alternative therapeutic radioisotope to ^{213}Bi in order to take advantage of the greater cytotoxic potential and significantly longer half-life of ^{225}Ac. [^{225}Ac]Ac-HuM195 was subsequently evaluated in a Phase I study with relapsed or refractory patients AML (*24*). Doses between 18.5-148 kBq/kg were administered. Redistribution of daughters in the kidneys was anticipated, but no evidence of radiation-induced nephrotoxicity was seen. Peripheral blasts were eliminated in 63% of the patients but only at doses of 37 kBq/kg or higher. Bone marrow blast reduction was observed in 67% of patients (*24*). A phase I/II study in AML patients currently evaluates the MTD and efficacy of the combination of low-dose cytarabine and [^{225}Ac]Ac-HuM195. Preliminary results recommend a 74 kBq/kg/fraction dose for the phase II study in order to limit prolonged myelosuppression (*25*). Patients receiving [^{225}Ac]Ac-HuM195 have also been administered furosemide and spironolactone in order to prevent potential radiation-induced renal toxicity (*25,26*). Furosemide has since been discontinued as it was causing dehydration in some patients. However, without furosemide, there has been no renal toxicity observed in patients receiving [^{225}Ac]Ac-HuM195.

Neuroendocrine tumors: [^{213}Bi]Bi-DOTATOC for β-radiation-refractory tumors

Kratochwil and colleagues performed a first-in-human study using a somatostatin analogue TAT, [^{213}Bi]Bi-DOTATOC, as a therapeutic option for patients with refractory neuroendocrine tumors that were pretreated with β-emitting [^{90}Y]Y/[^{177}Lu]Lu-DOTATOC (*27*). Patients with progressive advanced neuroendocrine tumors with liver metastasis were treated with intraarterial infusions, and one patient with bone carcinosis was treated with a systemic infusion (Fig. 4A). [^{213}Bi]Bi-DOTATOC was administered in cycles with

increasing activities (1.0-4.0 GBq, total dose) every two months. All patients showed long-lasting anti-tumor responses, highlighting the ability of [^{213}Bi]Bi-DOTATOC to overcome β-radiation resistance. Renal toxicity was minimized due to a protocol developed with the β-emitting particle radiopeptide therapy, including lysine, arginine, and Gelofusine administration (*27*).

HER2-expressing ovarian carcinoma: [^{212}Pb]Pb-TCMC-Trastuzumab

The biodistribution, pharmacokinetics, and safety of [^{212}Pb]Pb-TCMC-trastuzumab in patients with HER2-expressing ovarian cancer with malignancies mainly confined to the periteonal cavity that progressed after multiple therapies were assessed in a first-in-human study by Meredith et al (*28*). A single intraperitonal injection of [^{212}Pb]Pb-TCMC-trastuzumab (7.4 MBq/m^2) following a 4 mg/kg intravenous injection of trastuzumab (*28*) was first evaluated followed by a dose escalation study (7.4-21.1 MBq/m^2) (*29*). Furosemide and spirolactone were administered as renal protective agents. Minimal radiopharmaceutical redistribution out of the peritoneal cavity and no significant myelosuppression was observed (*28*). However, no patient met criteria for a partial response (*29*).

Metastatic castration-resistant prostate cancer: from [^{223}Ra]Ra-dichloride to [^{225}Ac]Ac-DOTA-PSMA

With 52 clinical trials registered on clinicaltrial.gov, the use of [^{223}Ra]Ra-dichloride (Alpharadin or Xofigo®) has impacted the therapeutic landscape of α-radiation therapy. Approximately 80% of the clinical trials involve prostate cancer and 35% employ a combination of drugs and [^{223}Ra]Ra-dichloride. First clinical experiments with [^{223}Ra]Ra-dichloride (46-250 kBq/kg) performed on prostate and breast cancer patients reported

pain relief and reduction in alkaline phosphatase (*30*). ALSYMPCA, a phase III, randomized, double-blind, placebo-controlled trial aimed to evaluate the efficacy and safety of [^{223}Ra]Ra-dichloride (50 kBq/kg every 4 weeks for a total of 6 cycles) vs. placebo plus standard of care in symptomatic CRPC patients (*31*). Overall survival was significantly longer with [^{223}Ra]Ra-dichloride: 14.9 months compared to 11.3 months with the placebo (Fig. 4B) (*31*). These primary results led to the FDA approval of [^{223}Ra]Ra-dichloride to treat CRPC in May 2013. Prolonged time to increase total alkaline phosphatase and prostate-specific antigen (PSA) was also observed (*32*). [^{223}Ra]Ra-dichloride is well tolerated, minimally toxic and patients reported significant improvement in quality of life (*32*); however, it does not target soft tissue disease or the circulating component of the disease (late manifestations).

Another promising α-therapeutic option for metastatic CRPC employs a small urea-based PSMA inhibitor (*2*) already used in the clinic for prostate cancer positron emission tomography (PET) imaging (*33*) and β-therapy (*34*). While promising, this β-therapy is ineffective in about 30% of patients and contraindicated for patients with diffuse red marrow infiltration. ^{225}Ac was considered to overcome β-resistance and reduce hematologic toxicity. Two metastatic CRPC patients in challenging clinical situations first received [^{225}Ac]Ac-PSMA-617 (100 kBq/kg, bimonthly) as salvage therapy after the validation of PSMA-positive tumor phenotype by [^{68}Ga]Ga-PSMA-11 PET/CT scans (*2*). Both patients showed complete response (Fig. 4C) with a drop of PSA levels below the measurable level. Xerostomia was reported in the two patients (*2*). A larger study with 14 mCRPC patients identified the best compromise between toxicity and antitumor response (*35*). A treatment activity of 100 kBq/kg was determined to be tolerable with significant antitumor activity (*35*). Though, a solution to preserve the salivary glands should be investigated. [^{225}Ac]Ac-PSMA-617 offers the major advantage of targeting metastases in any tissue and could

therefore be used as a complementary option to [^{223}Ra]Ra-dichloride therapy. Shortage of ^{225}Ac, however, remains a challenge and limits the evaluation of ^{225}Ac-TAT in large studies.

INTEGRATING ALPHA-THERAPY INTO CURRENT AND FUTURE CLINICAL PARADIGMS:

The future of alpha-therapy lies in the resolution of hurdles mentioned in Part 1 of this review, that is to say availability, production concerns and issues associated with daughter redistribution. Solutions to these issues are currently being investigated and should facilitate the broader development of α-emitter radiotherapy with larger, randomized, prospective clinical studies that would ultimately result in more meaningful efficacy and toxicity evaluation.

The future of alpha-therapy also lies in the proper design of clinical trials and the incorporation of this mode of therapy into current standard of care or in combination with new therapeutic approaches. An irony of the current status of [^{223}Ra]Ra-dichloride is that despite the completion of early-phase studies and ALSYMPCA, the optimal dose and duration of therapy is still not known. Currently, a randomized phase II trial (NCT02023697) examines men with mCRPC with two or more skeletal metastases under three separate treatment arms; standard [^{223}Ra]Ra-dichloride regimen (55 kBq/kg, FDA approved), a high-dose regimen (88 kBq/kg, every month for six months), and an extended duration regimen (55 kBq/kg injections, every month for 12 months). This study will complement a completed smaller single-arm study (NCT01934790) in which patients who had received a six-month course of [^{223}Ra]Ra-dichloride underwent another six months of the drug at standard doses (55 kBq/kg per month). Preliminary data on 44 patients reveals that 66% of patients completed re-treatment with an excellent safety profile (*36*). The clinical impact of additional treatments still needs to be defined.

The optimization of [^{223}Ra]Ra-dichloride treatment is also explored in combination with tumor-targeting therapy such as androgen receptor (AR) axis-directed therapy. A randomized phase III trial (NCT02043678) compares the androgen biosynthesis inhibitor abiraterone acetate and prednisone with abiraterone, prednisone and [^{223}Ra]Ra-dichloride in men with mCRPC who had not received cytotoxic chemotherapy. The Independent Data Monitoring Committee recommended that this trial be unblinded when it observed an imbalance in fractures and deaths, favoring treatment with abiraterone/prednisone alone (*37*). At this time, the details of these data are pending, but for now clinicians are increasingly cautious about treating men with early mCRPC with the combination of abiraterone, prednisone, and [^{223}Ra]Ra-dichloride.

The combination of [^{223}Ra]Ra-dichloride with chemotherapy is also being explored in men with mCRPC. [^{223}Ra]Ra-dichloride has been tested in a phase Ib/IIa study (NCT01106352) in combination with docetaxel (step-down dose 60 mg/m^2). Patients were randomized to either the combination arm or to docetaxel on a 2:1 basis. PSA declines of over 50% occurred in 61% of patients in the combination arm and 54% in the docetaxel arm. Sustained suppression was also apparent in the Kaplan-Meier analysis, with a significantly longer time to PSA progression in favor of the combination (6.6 vs 4.8 months; P=.0198) (*38*). A number of newer trials are exploring [^{223}Ra]Ra-dichloride as an adjunct to boost other treatment effects, such as PARP inhibitor (i.e., olaparib (*39*) or niraparib (NCT03076203)), or as an immune adjuvant leveraging the abscopal effect to enhance the impact of immunotherapy ([^{223}Ra]Ra-dichloride in combination with PD-L1 inhibitor atezolizumab (NCT02814669)). Combinations of tumor and bone targeting offer a promise of amplifying the effects of treatment beyond the host compartment of bone and would allow patients with visceral metastases to receive [^{223}Ra]Ra-dichloride, which at the present time, is not permissible in the US. Dual tumor and bone targeting is also possible with

tumor-directed α-emitters ([^{225}Ac]Ac-PSMA-617), although formal dose-finding prospective studies for these agents are still needed, in which the optimal dose and treatment intervals are defined, and toxicity mitigation strategies (in particular for xerostomia) are developed.

CONCLUSION

Studies described in this review demonstrate that α-emitting radionuclides have the potential to be excellent therapeutic candidates and, along with β-particle therapy, can expand the options for therapy. Alpha-emitting radionuclides are currently considered at late disease stages as an alternative choice when resistance to β-therapy is observed or when the patient presents with extended bone marrow disease; however, applications in earlier disease stages should be evaluated. Together Part 1 and Part 2 of this review give a broad overview of α-emitters from basic radiochemistry to clinical use. The future of α-radiotherapy is dependent on numerous factors; Part 1 highlights hurdles and new approaches for a wider use of α-emitting radionuclides, and Part 2 highlights the importance of clinical trials design for a proper determination of α-therapy optimal dose and incorporation into standard of care protocols.

References

1. Behling K, Maguire WF, Lopez Puebla JC, et al. Vascular targeted radioimmunotherapy for the treatment of glioblastoma. *J Nucl Med.* 2016;57:1576-1582.

2. Kratochwil C, Bruchertseifer F, Giesel FL, et al. ^{225}Ac-PSMA-617 for PSMA-targeted a-radiation therapy of metastatic castration-resistant prostate cancer. *J Nucl Med.* 2016;57:1941-1944.

3. Green DJ, Shadman M, Jones JC, et al. Astatine-211 conjugated to an anti-CD20 monoclonal antibody eradicates disseminated B-cell lymphoma in a mouse model. *Blood.* 2015;125:2111-2119.

4. Dahle J, Bruland OS, Larsen RH. Relative biologic effects of low-dose-rate alpha-emitting ^{227}Th-rituximab and beta-emitting ^{90}Y-tiuexetan-ibritumomab versus external beam X-radiation. *Int J Radiat Oncol.* 2008;72:186-192.

5. Heyerdahl H, Krogh C, Borrebaek J, Larsen A, Dahle J. Treatment of HER2-expressing breast cancer and ovarian cancer cells with alpha particle-emitting ^{227}Th-trastuzumab. *Int J Radiat Oncol.* 2011;79:563-570.

6. Dahle J, Jonasdottir TJ, Heyerdahl H, et al. Assessment of long-term radiotoxicity after treatment with the low-dose-rate alpha-particle-emitting radioimmunoconjugate ^{227}Th-rituximab. *Eur J Nucl Med Mol Imaging.* 2010;37:93-102.

7. Park SI, Shenoi J, Pagel JM, et al. Conventional and pretargeted radioimmunotherapy using bismuth-213 to target and treat non-Hodgkin lymphomas expressing CD20: a preclinical model toward optimal consolidation therapy to eradicate minimal residual disease. *Blood.* 2010;116:4231-4239.

8. Hagemann UB, Wickstroem K, Wang E, et al. In vitro and in vivo efficacy of a novel CD33-targeted Thorium-227 conjugate for the treatment of acute myeloid leukemia. *Mol Cancer Ther.* 2016;15:2422-2431.

9. McDevitt MR, Barendswaard E, Ma D, et al. An alpha-particle emitting antibody ([^{213}Bi]J591) for radioimmunotherapy of prostate cancer. *Cancer Res.* 2000;60:6095-6100.

10. Kiess A, Minn IL, Vaidyanathan G, et al. (2*S*)-2-(3-(1-Carboxy-5-(4-[^{211}At]astatobenzamido)pentyl)ureido)-pentanedioic acid for PSMA-targeted alpha-particle radiopharmaceutical therapy. *J Nucl Med.* 2016;57:1569-1575.

11. Larsen RH, Saxtorph H, Skydsgaard M, et al. Radiotoxicity of the alpha-emitting bone-seeker ^{223}Ra injected intravenously into mice: histology, clinical chemistry and hematology. *In vivo.* 2006;20:325-331.

12. Milenic DE, Garmestani K, Brady ED, et al. Alpha-particle radioimmunotherapy of disseminated peritoneal disease using a ^{212}Pb-labeled radioimmunoconjugate targeting HER2. *Cancer Biother Radio.* 2005;20:557-568.

13. Boudousq V, Bobyk L, Busson M, et al. Comparison between internalizing anti-HER2 mAbs and non-internalizing anti-CEA mAbs in alpha-radioimmunotherapy of small volume peritoneal carcinomatosis using ^{212}Pb. *PLoS One.* 2013;8:e69613.

14. Milenic DE, Baidoo KE, Kim YS, Brechbiel MW. Evaluation of cetuximab as a candidate for targeted alpha-particle radiation therapy of HER1-positive disseminated intraperitoneal disease. *mAbs.* 2015;7:255-264.

15. Hagemann UB, Mihaylova D, Uran SR, et al. Targeted alpha therapy using a novel CD70 targeted thorium-227 conjugate in in vitro and in vivo models of renal cell carcinoma. *Oncotarget.* 2017;8:56311-56326.

16. Behling K, DiGialleonardo V, Maguire WF, et al. Remodelling the vascular microenvironment of glioblastoma with alpha-particles. *J Nucl Med.* 2016;57:1771-1777.

17. Pandya DN, Hantgan R, Budzevich MM, et al. Preliminary therapy evaluation of ^{225}Ac-DOTA-c(RGDyK) demonstrates that cerenkov radiation derived from ^{225}Ac daughter

decay can be detected by optical imaging for in vivo tumor visualization. *Theranostics.* 2016;6:698-709.

18. Ruggiero A, Holland JP, Lewis JS, Grimm J. Cerenkov luminescence imaging of medical isotopes. *J Nucl Med.* 2010;51:1123-1130.

19. Song H, Hobbs RF, Vajravelu R, et al. Radioimmunotherapy of breast cancer metastases with alpha-particle emitter ^{225}Ac: comparing efficacy with ^{213}Bi and ^{90}Y. *Cancer Res.* 2009;69:8941-8948.

20. Graf F, Fahrer J, Maus S, et al. DNA double strand breaks as predictor of efficacy of the alpha-particle emitter Ac-225 and the electron emitter Lu-177 for somatostatin receptor targeted radiotherapy. *PLoS One.* 2014;9:e88239.

21. Fendler WP, Cutler C. More alpha than beta for prostate cancer? *J Nucl Med.* 2017;58:1709-1710.

22. Jurcic JG, Larson SM, Sgouros G, et al. Targeted alpha particle immunotherapy for myeloid leukemia. *Blood.* 2002;100:1233-1239.

23. Rosenblat TL, McDevitt MR, Mulford DA, et al. Sequential cytarabine and alpha-particle immunotherapy with bismuth-213-lintuzumab (HuM195) for acute myeloid leukemia. *Clin Cancer Res.* 2010;16:5303-5311.

24. Jurcic JG, Rosenblat TL. Targeted alpha-particle immunotherapy for acute myeloid leukemia. *Am Soc Clin Oncol Educ Book.* 2014:e126-131.

25. Jurcic JG, Levy MY, Park JH, et al. Phase I Trial of Targeted alpha-particle therapy with Actinium-225 (Ac-225)-Lintuzumab and low-dose cytarabine (LDAC) in patients age 60 or older with untreated acute myeloid leukemia (AML). *Blood.* 2016;128:4050.

26. Jaggi JS, Seshan SV, McDevitt MR, Sgouros G, Hyjek E, Scheinberg DA. Mitigation of radiation nephropathy after internal alpha-particle irradiation of kidneys. *Int J Radiat Oncol Biol Phys.* 2006;64:1503-1512.

27. Kratochwil C, Giesel FL, Bruchertseifer F, et al. ^{213}Bi-DOTATOC receptor-targeted alpha-radionuclide therapy induces remission in neuroendocrine tumours refractory to beta radiation: a first-in-human experience. *Eur J Nucl Med Mol Imaging.* 2014;41:2106-2119.

28. Meredith RF, Torgue J, Azure MT, et al. Pharmacokinetics and imaging of ^{212}Pb-TCMC-trastuzumab after intraperitoneal administration in ovarian cancer patients. *Cancer Biother Radio.* 2014;29:12-17.

29. Meredith R, Torgue J, Shen S, et al. Dose escalation and dosimetry of first-in-human alpha radioimmunotherapy with ^{212}Pb-TCMC-trastuzumab. *J Nucl Med.* 2014;55:1636-1642.

30. Nilsson S, Larsen RH, Fossa SD, et al. First clinical experience with alpha-emitting radium-223 in the treatment of skeletal metastases. *Clin cancer Res.* 2005;11:4451-4459.

31. Parker C, Nilsson S, Heinrich D, et al. Alpha emitter radium-223 and survival in metastatic prostate cancer. *N Engl J Med.* 2013;369:213-223.

32. Sartor O, Coleman R, Nilsson S, et al. Effect of radium-223 dichloride on symptomatic skeletal events in patients with castration-resistant prostate cancer and bone metastases: results from a phase 3, double-blind, randomised trial. *Lancet Oncol.* 2014;15:738-746.

33. Afshar-Oromieh A, Holland-Letz T, Giesel FL, et al. Diagnostic performance of ^{68}Ga-PSMA-11 (HBED-CC) PET/CT in patients with recurrent prostate cancer: evaluation in 1007 patients. *Eur J Nucl Med Mol Imaging.* 2017;44:1258-1268.

34. Brauer A, Grubert LS, Roll W, et al. ^{177}Lu-PSMA-617 radioligand therapy and outcome in patients with metastasized castration-resistant prostate cancer. *Eur J Nucl Med Mol Imaging.* 2017;44:1663-1670.

35. Kratochwil C, Bruchertseifer F, Rathke H, et al. Targeted alpha-therapy of metastatic castration-resistant prostate cancer with ^{225}Ac-PSMA-617: dosimetry estimate and empiric dose finding. *J Nucl Med.* 2017;58:1624-1631.

36. Sartor O, Heinrich D, Mariados N, et al. Re-treatment with radium-223: first experience from an international, open-label, phase I/II study in patients with castration-resistant prostate cancer and bone metastases. *Ann. Oncol.* 2017;28:2464-2471.

37. http://www.prnewswire.com/news-releases/phase-iii-trial-of-radium-ra-223-dichloride-in-combination-with-abiraterone-acetate-and-prednisoneprednisolone-for-patients-with-metastatic-castration-resistant-prostate-cancer-unblinded-early-300564844.html.

38. Morris MJ, Loriot Y, Fizazi K, et al. Effects of radium-223 (Ra-223) with docetaxel versus docetaxel alone on bone biomarkers in patients with bone-metastatic castration-resistant prostate cancer (CRPC): A phase I/IIa clinical trial. *J Clin Oncol.* 2017;35(suppl 6S; abstract 154).

39. Mateo J, Carreira S, Sandhu S, et al. DNA-repair defects and olaparib in metastatic prostate cancer. *N Engl J Med.* 2015;373:1697-1708.

40. Zalutsky MR, Reardon DA, Akabani G, et al. Clinical experience with alpha-particle emitting ^{211}At: treatment of recurrent brain tumor patients with ^{211}At-labeled chimeric antitenascin monoclonal antibody 81C6. *J Nucl Med.* 2008;49:30-38.

41. Andersson H, Cederkrantz E, Back T, et al. Intraperitoneal alpha-particle radioimmunotherapy of ovarian cancer patients: pharmacokinetics and dosimetry of ^{211}At-MX35 F(ab')2--a phase I study. *J Nucl Med.* 2009;50:1153-1160.

42. Cederkrantz E, Andersson H, Bernhardt P, et al. Absorbed doses and risk estimates of ^{211}At-MX35 F(ab')2 in intraperitoneal therapy of ovarian cancer patients. *Int J Radiat Oncol.* 2015;93:569-576.

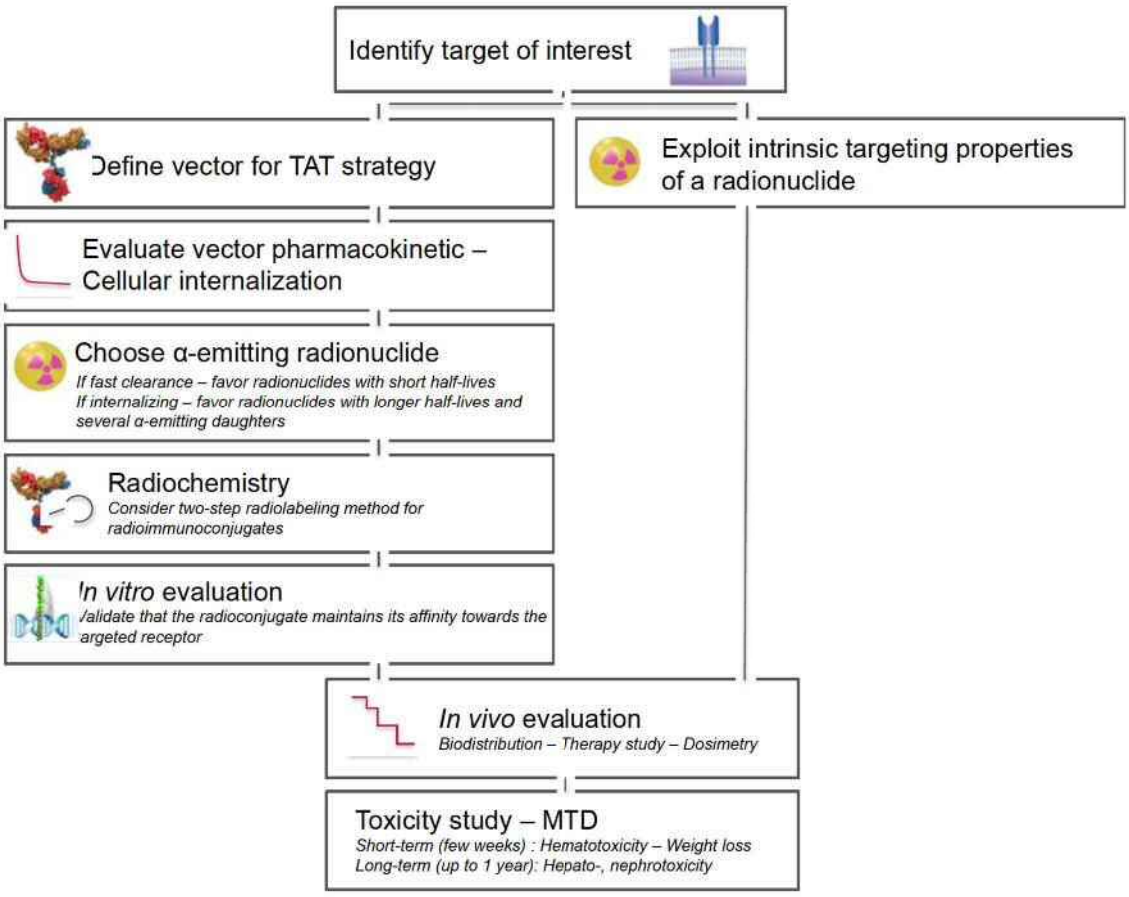

Figure 1. Preclinical study design flow chart. MTD: Maximum Tolerated Dose; TAT: Targeted α-therapy.

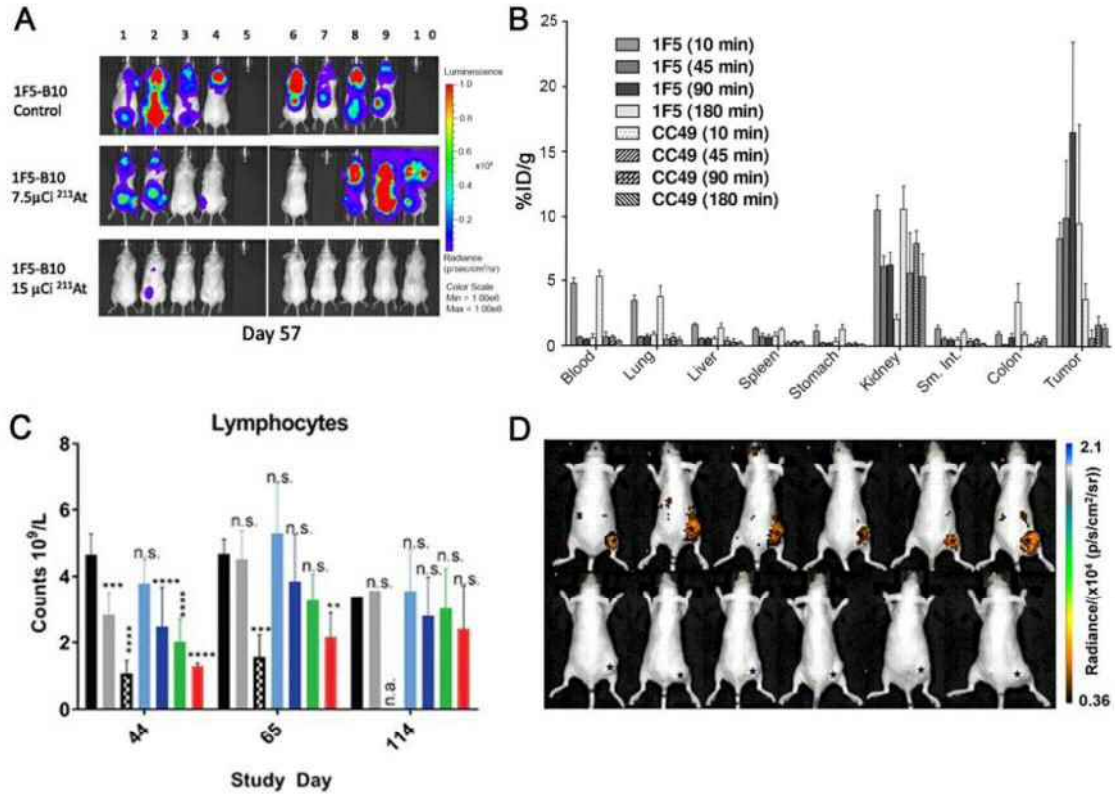

Figure 2. Preclinical studies, potency, imaging, and pitfalls of α-therapy. A) Bioluminescence imaging of [^{211}At]At-B10-1F5 (anti-CD20) RIT in Granta-519^{Luc}, a minimal residual disease model of lymphoma. Animals were treated on day 6 with 278 kBq (7.5 µCi) or 555 kBq (15 µCi) and received 1x10^7 bone marrow cells intravenously from syngeneic donors two days after treatment (*3*). B) Biodistribution of [^{213}Bi]Bi-DOTA-biotin after pretargeting RIT with 1F5(scFv)4-streptavidin (anti-CD20) and CC49(scFv)4-streptavidin (negative control) (*7*). C) Transient lymphocytes decrease after CD70-targeted ^{227}Th-conjugate (TTC) therapy indicative of myelosuppression (*15*). D) Cerenkov imaging acquired 24 h post-injection of [^{225}Ac]Ac-DOTA-c(RGDyK) in U87MG tumor-bearing mice. Top images show efficient tumor accumulation; bottom images show reduced tumor uptake upon blockage and demonstrate the specificity of the radiotherapy for $\alpha_v\beta_3$ integrin (*17*). Reprinted with permission.

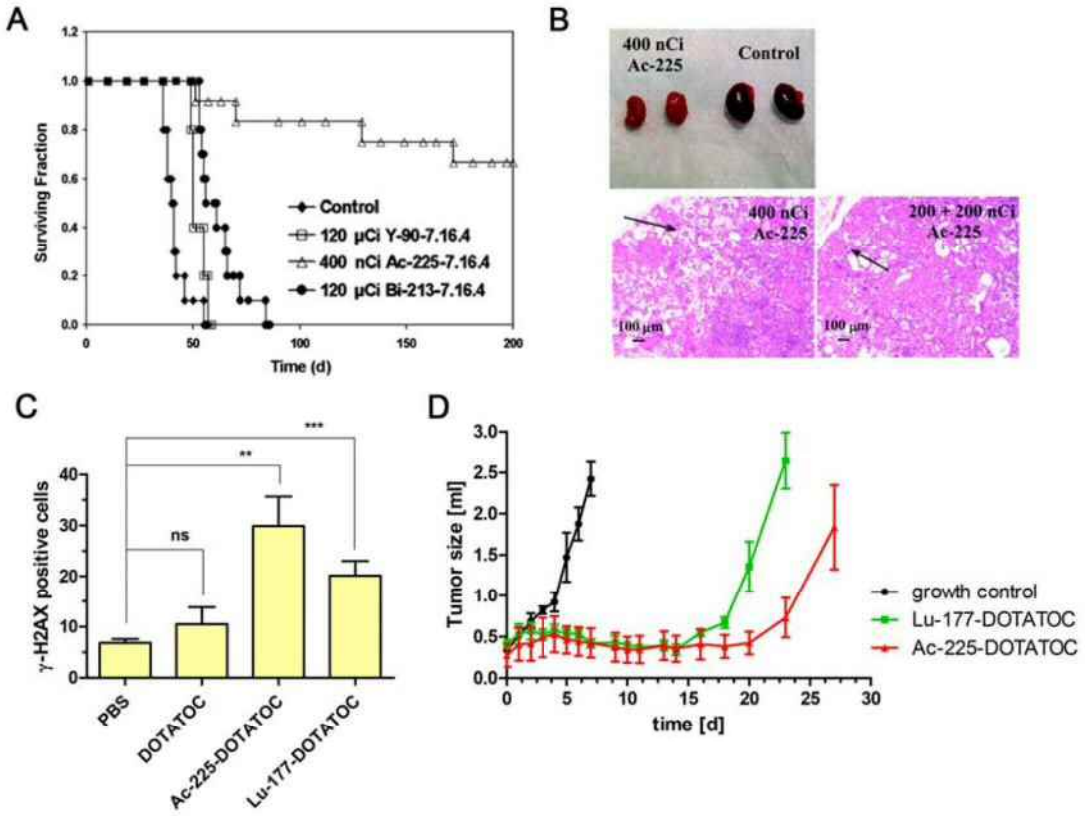

Figure 3. Preclinical alpha vs. beta studies. A) Kaplan-Meier survival curves of *neu*-N transgenic mice treated with 14.8 kBq (400 nCi) of ^{225}Ac-7.16.4, 4.4 MBq (120 µCi) of [^{213}Bi]Bi-7.16.4, and 4.4 MBq (120 µCi) of [^{90}Y]Y-7.16.4, three days after intravenous injection of 1x10^{5} NT2.5 cells (*19*). B) *Top*, Photographs of kidneys from a *neu*-N mouse surviving one year after treatment with 14.8 kBq (400 nCi) of [^{255}Ac]Ac-7.16.4 compared to a healthy *neu*-N mouse. *Bottom*, H&E staining of kidneys from *neu*-N mice surviving one year after treatment with 14.8 kBq (400 nCi) (*middle*) and 7.4 + 7.4 kBq (200 + 200 nCi) of [^{225}Ac]Ac-7.16.4 (*right*). Arrows indicate collapse of cortical tissue due to loss of tubular epithelium in the kidney cortex (*19*). C) Quantification of γH2AX-positive cells after immunofluorescent staining of DNA DSBs in AR42J tumors following treatment with 47 kBq of [^{225}Ac]Ac-DOTATOC, 30 MBq of [^{177}Lu]Lu-DOTATOC, 1 µg of DOTATOC (unlabelled), or PBS(*20*). D) Tumor size measurement showing growth delay after treatment with equitoxic doses of [^{225}Ac]Ac-DOTATOC (44 kBq) and [^{177}Lu]Lu-DOTATOC (34 MBq) (*20*). Reprinted with permission.

Radiopharma-ceutical and dosage	Target and study population	Features and outcome	Dose-limiting observations and toxicity	Ref.
[^{211}At]At-ch81C6	Tenascin	Phase I and II: Feasibility, safety, and efficacy	No grade 3 or higher toxicity	(*40*)
71-347 MBq	18 patients with primary or metastatic brain tumor	Overall survival of 54.1 weeks vs. 23 weeks for glioblastoma patients		
[^{211}At]At-MX35 F(ab')$_2$	Sodium-dependent phosphate transport protein 2b	Phase I: Pharmacokinetic and dosimetry	With 200 MBq/mL, effective dose of 2.6 Sv (lifelong lethal cancer risk of 10%)	(*41,42*)
22.4-101 MBq/L	Women with complete clinical remission after second-line chemotherapy of recurrent ovarian cancer	Estimated absorbed dose to peritoneal 15.6 ± 1.0 mGy/(MBq/L)		
[^{213}Bi]Bi-DOTATOC	Somatostatin receptors	First-in-human	Moderate acute hematologic and chronic kidney toxicities	(*27*)
1.0-4.0 GBq	Patients with progressive neuroendocrine tumors	Long-lasting tumor response. Remission of tumors refractory to β-radiation.		
[^{213}Bi]Bi-HuM195	CD-33	Phase I: Dose escalation	Transient myelosuppression	(*22*)
10.36-37.0 MBq/kg	Primary refractory or relapsed AML	Reduction in peripheral blood leukemia cells and bone marrow blasts		
[^{225}Ac]Ac-HuM195	CD-33	Phase I: Dose escalation	Myelosuppresion	(*24*)
18.5-148 kBq/kg	Patients with AML	MTD of 111 kBq/mL bone marrow and peripheral blast reduction		
[^{225}Ac]Ac-PSMA-617	PSMA	First-in-human	Xerostomia	(*2*)
100 kBq/kg	2 patients with metastatic CRPC	Complete response on PET imaging and PSA level below measurable levels		
[^{227}Th]Th-epratuzumab BAY1862864	CD-22	Phase I: Dose escalation, determination of MTD		
Starting dose: 1.4 MBq	Patients with relapsed or refractory CD-22 positive non-Hodgkin's lymphoma	Currently recruiting: NCT02581878		
[^{223}Ra]Ra-dichloride	Intrinsic bone-seeking properties	Phase III: ALSYMPCA Overall survival and time to disease progression		(*31,32*)
50 kBq/kg	Symptomatic CRPC	Overall survival of 14.9 months vs. 11.3 months		
[^{212}Pb]Pb-trastuzumab	HER2	Phase I: Safety and tolerability		(*29*)
7.4-21.1 MBq/m^2	Progressive ovarian carcinoma after multiple therapy	Few tumor volume decreases		

Table 1. Examples of clinical evaluation of α-therapy.

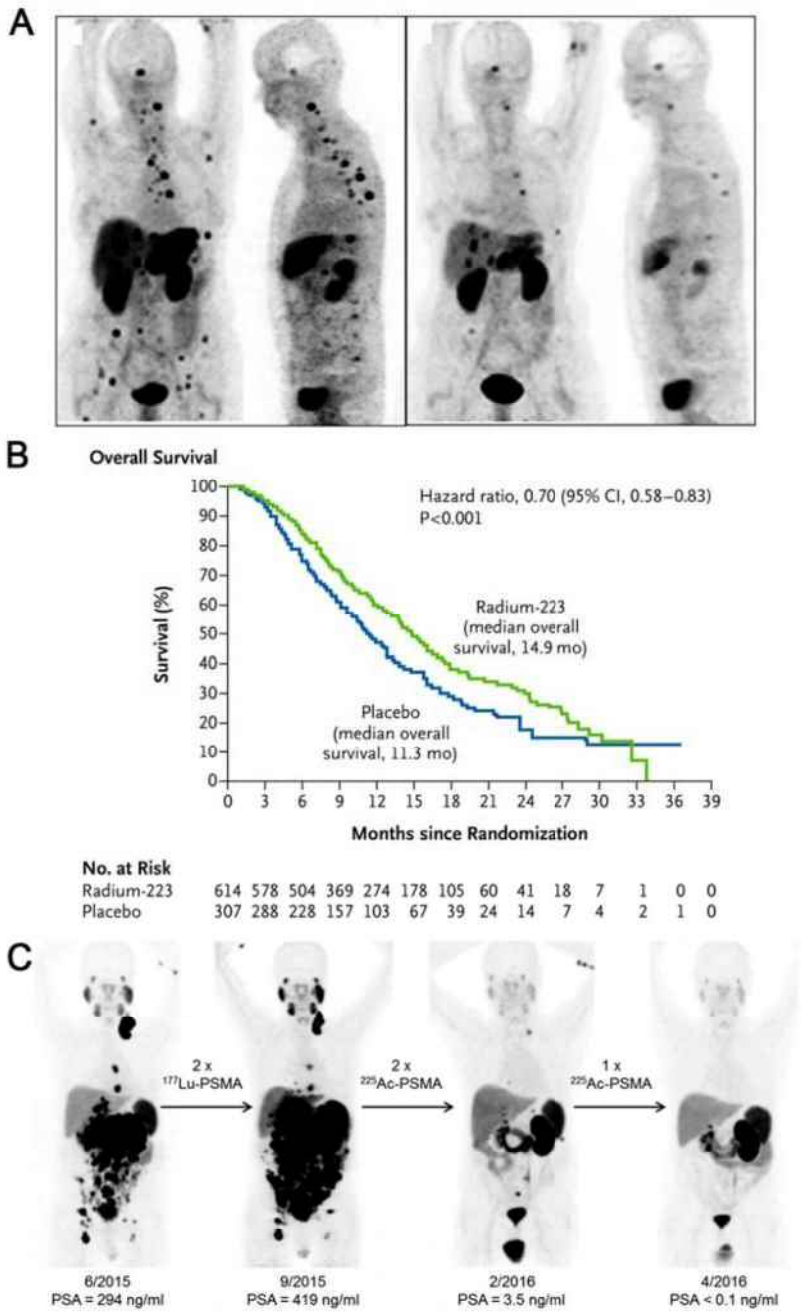

Figure 4. Clinical application of α-radiotherapy. A) *Left*, [^{68}Ga]Ga-DOTATOC PET maximum intensity projection of a neuroendocrine tumor patient showing an extensive tumor burden in the liver as well as disseminated bone marrow metastases. *Right*, significant reduction of the liver metastases after administration of 10.5 GBq of [^{213}Bi]Bi-DOTATOC into the common hepatic artery (*27*). B) Kaplan-Meier estimates of overall survival of patients with symptomatic CRPC following treatment with ^{223}Ra-dichloride as compared to the placebo group (*31*). C) Evolution of [^{68}Ga]Ga-PSMA-11 PET/CT scans of a patient with metastatic CRPC showing extended periteonal carcinomatosis and liver metastases. After two cycles of [^{177}Lu]Lu-PSMA-617, the patient showed disease progression and was offered [^{225}Ac]Ac-PSMA-617. After three cycles of ^{225}Ac-TAT, PET/CT indicated complete response and PSA level dropped to immeasurable levels (*2*). Reprinted with permission.

JNM The Journal of NUCLEAR MEDICINE

Alpha Emitters for Radiotherapy: Basic Radiochemistry to Clinical Studies – Part 2

Sophie Poty, Lynn C Francesconi, Michael Robert McDevitt, Michael J. Morris and Jason S. Lewis

J Nucl Med.
Published online: March 1, 2018.
Doi: 10.2967/jnumed.117.204651

The Journal of Nuclear Medicine is published monthly.
SNMMI | Society of Nuclear Medicine and Molecular Imaging
1850 Samuel Morse Drive, Reston, VA 20190.
(Print ISSN: 0161-5505, Online ISSN: 2159-662X)

SNMMI SOCIETY OF NUCLEAR MEDICINE AND MOLECULAR IMAGING

SPECIAL CONTRIBUTION

MIRD Pamphlet No. 22 (Abridged): Radiobiology and Dosimetry of α-Particle Emitters for Targeted Radionuclide Therapy*

George Sgouros[1], John C. Roeske[2], Michael R. McDevitt[3], Stig Palm[4], Barry J. Allen[5], Darrell R. Fisher[6], A. Bertrand Brill[7], Hong Song[1], Roger W. Howell[8], and Gamal Akabani[9]

In collaboration with the SNM MIRD Committee: Wesley E. Bolch, A. Bertrand Brill, Darrell R. Fisher, Roger W. Howell, Ruby F. Meredith, George Sgouros (Chair), Barry W. Wessels, and Pat B. Zanzonico

[1]Department of Radiology and Radiological Science, Johns Hopkins University, Baltimore, Maryland; [2]Department of Radiation Oncology, Loyola University Medical Center, Maywood, Illinois; [3]Departments of Medicine and Radiology, Memorial Sloan-Kettering Cancer Center, New York, New York; [4]Dosimetry and Medical Radiation Physics Section, International Atomic Energy Agency, Vienna, Austria; [5]Centre for Experimental Radiation Oncology, St. George Cancer Centre, Kogarah, Australia; [6]Radioisotopes Program, Pacific Northwest National Laboratory, Richland, Washington; [7]Department of Radiology, Vanderbilt University, Nashville, Tennessee; [8]Division of Radiation Research, Department of Radiology, New Jersey Medical School Cancer Center, University of Medicine and Dentistry of New Jersey, Newark, New Jersey; and [9]Department of Nuclear Engineering, Texas A&M University, College Station, Texas

The potential of α-particle emitters to treat cancer has been recognized since the early 1900s. Advances in the targeted delivery of radionuclides and radionuclide conjugation chemistry, and the increased availability of α-emitters appropriate for clinical use, have recently led to patient trials of radiopharmaceuticals labeled with α-particle emitters. Although α-emitters have been studied for many decades, their current use in humans for targeted therapy is an important milestone. The objective of this work is to review those aspects of the field that are pertinent to targeted α-particle emitter therapy and to provide guidance and recommendations for human α-particle emitter dosimetry.

Key Words: α-particle emitters; human α-particle emitter dosimetry; targeted α-particle emitter therapy

J Nucl Med 2010; 51:311–328
DOI: 10.2967/jnumed.108.058651

Several reviews have been published on the topic of α-particle–emitting radionuclides, which have been the subject of considerable investigation as cancer therapeutics (*1–8*). In the context of targeted therapy, α-particle emitters have the advantages of high potency and specificity. These advantages arise from the densely ionizing track and short path length of the emitted positively charged helium nucleus in tissue. The practical implication of these features, as well as the distinction between α-particles and the more widely used β-particle emitters for targeted radionuclide therapy, is that it is possible to sterilize individual tumor cells solely from self-irradiation with α-particle emitters. This is generally not possible with β-particle emitters given achievable antibody specific activity, tumor-cell antigen expression levels, and the need to avoid prohibitive toxicity (*5*). These attributes combine to provide the fundamental strength and rationale for using α-particle–emitting radionuclides for cancer therapy. Current approaches to cancer treatment are largely ineffective once the tumor has metastasized and tumor cells are disseminated throughout the body. There is also increasing evidence that not all tumor cells are relevant targets for effective tumor eradication and that sterilization of a putative subpopulation of a small number of tumor stem cells may be critical to treatment efficacy (*9*). The eradication of such disseminated tumor cells, or of a subpopulation of tumor stem cells, requires a systemic targeted therapy that is minimally susceptible to chemo- or radioresistance, is potent enough to sterilize individual tumor cells and microscopic tumor cell clusters (even at a low dose-rate and low oxygen tension), and exhibits an acceptable toxicity profile (*10*). α-Particle–emitting radionuclides address this critical need. To accomplish these goals, a reliable, cost-effective source of α-particle emitters is needed for research and development and for routine use in clinical practice. Improved chemical labeling and stability will be needed to achieve the desired biodistribution and associated dose distribution necessary for successful therapy with acceptable acute and long-term toxicities. These limitations have slowed the development and clinical use of α-emitter targeted therapy relative to the use of β- and Auger-electron–emitting radionuclides.

Received Sep. 29, 2008; revision accepted Jun. 29, 2009.
For correspondence or reprints contact: George Sgouros, Department of Radiology and Radiological Science, CRB II 4M61/1550 Orleans St., School of Medicine, Johns Hopkins University, Baltimore, MD 21231.
E-mail: gsgouros@jhmi.edu
*Unabridged version of this document is available at: http://interactive.snm.org/index.cfm?PageID=1110&RPID=2199&FileID=144234.

The first clinical trial of an α-particle emitter in radiolabeled antibody therapy used ^{213}Bi conjugated to the antileukemia antibody HuM195 and was reported in 1997 (*11,12*), 4 years after ^{213}Bi was first suggested for therapeutic use (*13*). This trial was followed by a human trial of the antitenascin antibody 81C6 labeled with the α-emitter ^{211}At in patients with recurrent malignant glioma (*14*). In addition to these 2 antibody-based trials, a clinical trial of unconjugated ^{223}Ra against skeletal metastases in patients with breast and prostate cancer was recently completed (*15*). More recently, a patient trial of ^{211}At targeting ovarian carcinoma has been initiated (*16*). Future trials of α-emitters are anticipated using antibodies labeled with ^{211}At or ^{213}Bi and directed against tumor neovasculature (*17–19*). A conjugation methodology for ^{225}Ac was recently described (*20*), and a phase I trial of this radionuclide with the antileukemia antibody HuM195 in leukemia patients has recently been initiated (*21*). Table 1 summarizes clinical trials involving α-particle–emitting radiopharmaceuticals.

This report focuses on α-emitter dosimetry as it relates to human use in targeted therapy. A review of α-particle radiobiologic studies is provided with a focus on the radiobiology of α-emitters that are relevant to targeted therapy in humans. Closely related to the radiobiology of α-emitters is the concept of relative biological effectiveness (RBE), which is also reviewed. The dosimetry of α-emitters has been addressed in a large number of publications. The criteria for microdosimetry, the different approaches for performing such calculations, and selected studies in which such calculations have been performed are briefly described.

TABLE 1. Summary of Recently Reported Clinical Trials Using α-Particle Emitters

Radionuclide	Delivery vehicle	Type of cancer	Comments	Reference
^{211}At	Antitenascin IgG	Glioblastoma multiforme	Ongoing phase I trial using surgical cavity injection of labeled antitenascin IgG; median survival of 60 wk; 2 patients with recurrent glioblastoma multiforme survived nearly 3 y	*14*
	MX35 F(ab′)$_2$	Ovarian carcinoma	Ongoing phase I trial using MX35 F(ab′)$_2$; bone marrow and peritoneal absorbed doses of 0.08 and 8 mGy/MBq, respectively	*16*
^{213}Bi	Anti-CD33 IgG	Myelogenous leukemia (acute or chronic)	Phase I completed with no toxicity, substantial reduction in circulating and bone marrow blasts; phase I/II in cytoreduced patients, 4 of 23 patients at very high risk showed lasting complete response (up to 12 mo)	*11,21*
	Antineurokinin receptor peptide	Glioblastoma	Two patients treated with ^{213}Bi; 1 with oligodendroglioma treated by distillation in resection cavity alive more than 67 mo	*148*
	Anti-CD20 IgG (rituximab)	Relapsed or refractory non-Hodgkin lymphoma	Phase I study with 9 patients treated to date	*149*
	9.2.27 IgG	Melanoma	Sixteen patients; intralesional administration led to massive tumor cell kill and resolution of lesions; significant decline in serum marker melanoma-inhibitory-activity protein at 2 wk after treatment	*150*
^{223}Ra	$RaCl_2$	Skeletal breast and prostate cancer metastases	Phase IA dose-escalation studies completed involving single-dose infusion of 46–250 kBq/kg in 25 patients with no dose-limiting hematologic toxicity; phase IB study in 6 patients to evaluate repeated injections (2 or 5 fractions) totaling up to 250 kBq/kg; phase II randomized trial in 33 patients with metastatic breast or prostate cancer treated with external beam plus saline or 4 times 50 kBq/kg dose of ^{223}Ra at 4-wk intervals; shows significant (−66%) decrease in bone alkaline phosphatase compared with placebo and 15 of 31 patients with prostate-specific antigen decrease > 50% from baseline vs. 5 of 28 in control group	*151,152*
^{225}Ac	Anti-CD33 IgG	Acute myelogenous leukemia	Phase I trial, ongoing, at first dose-level of 18.5 kBq/kg (0.5 μCi/kg); 1 of 2 patients had elimination of peripheral blasts and reduction in marrow blasts	*21*

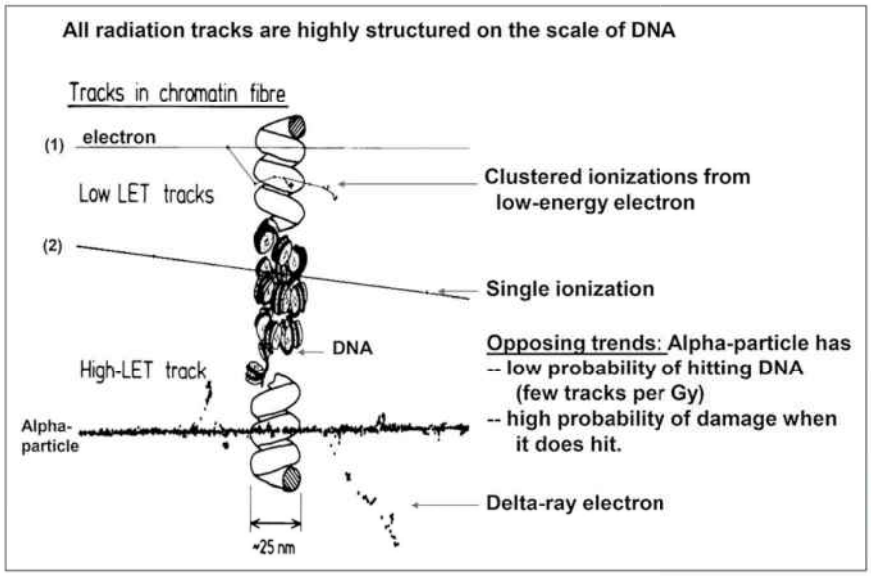

FIGURE 1. Illustration of difference in ionization density between low- and high-LET tracks. (Reprinted with permission of (*153*).)

Therapeutic nuclear medicine is already a highly multidisciplinary field. Therapy with α-particle emitters is easily one of the more multidisciplinary endeavors within this enterprise. This review is intended to provide the necessary background including the physics and dosimetry perspective to aid in the design, conduct, and analysis of clinical trials using α-emitting radiotherapeutics.

α-PARTICLE RADIOBIOLOGY

Interest in α-particle–emitting radionuclides for cancer therapy is driven by the physical and radiobiologic properties of α-particles as compared with those of photons and electrons (Fig. 1). The energy deposited along the path of an α-particle per unit path length is shown in Figure 2. As shown in the figure, the energy deposition along the path, or linear energy transfer (LET), of an α-particle can be 2 or 3 orders of magnitude greater than the LET of β-particles emitted by radionuclides such as ^{131}I and ^{90}Y.

One of the first studies demonstrating the biologic effects of heavy charged particles was by Raymond Zirkle in 1932 (*22*). He examined the effect of polonium α-particles on cell division in fern spores and showed a much greater biologic effect when the spore nucleus was placed in the Bragg peak of the α-particle track, compared with the plateau region of the track (*23*). Much of the subsequent radiobiology of α-particles was established in a series of seminal studies performed by Barendsen et al. in the 1960s (*24–32*). These studies first demonstrated the now familiar and accepted features of α-particle irradiation. A subsequent series of studies on the mutation and inactivation

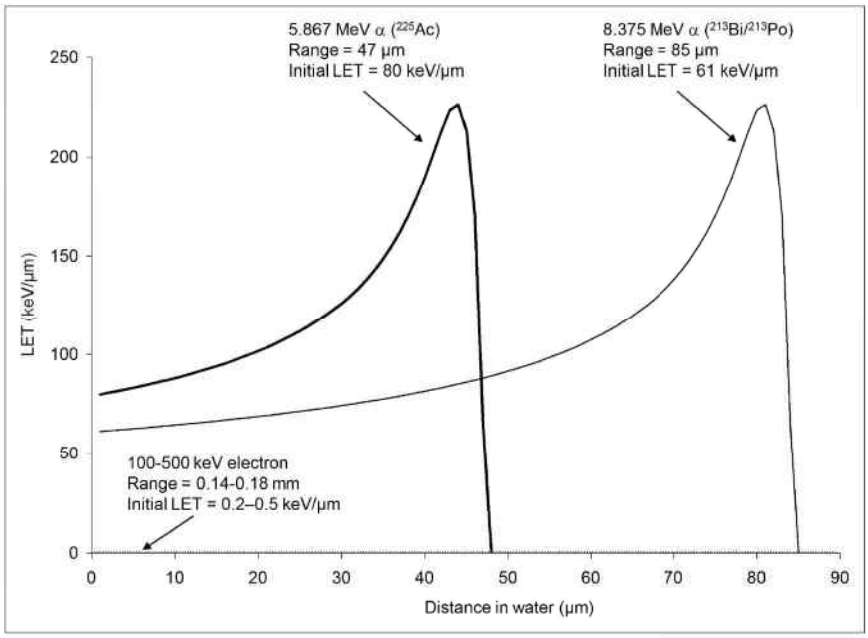

FIGURE 2. LET vs. distance traveled in tissue for α-particles with 2 different initial kinetic energies. α-Particles emitted with lower initial energy are closer to their Bragg peak and, therefore, start out with higher LET. LET of electrons with initial energy of 100–500 keV is also shown at bottom of plot for comparison. (Plot generated using data from (*108*).)

of 3 different mammalian cell types exposed to helium, boron, or nitrogen ions spanning LET values in the range of 20–470 keV·μm^{-1} was key in evaluating the various biophysical models that had been posited to explain low- versus high-LET effects (*33–36*). The work was also instrumental in providing both the experimental results and the biophysical analysis to help understand the RBE-versus-LET relationship established by Barendsen. The biophysical analysis in the last paper of the series (*33*) provided compelling theoretic support for the concept of 2 types of radiation-induced cellular inactivation. The first type is that due to the accumulation of multiple events that can be repaired at low doses (i.e., sublethal damage) but that saturate the cellular repair mechanisms at higher doses. This type of inactivation yields the characteristic linear-quadratic dose–response curve for low-LET radiation, corresponding to a small number, approximately 3–9 (i.e., ~100–300 eV) ionizations in a distance of about 3 nm associated with a low probability of producing lethal lesions. The second type of inactivation arises from a single lethal event for high-LET radiation. In this case, a larger number of ionizations, more than 10, over the 3-nm distance depositing more than 300 eV produces lethal lesions with a high probability. It is important, however, to remember that these studies were performed using external beams of α-particles in which the incident α-particles were generally orthogonal to an α-permeable surface on which the cells were cultured as a monolayer of adherent cells.

As initially demonstrated experimentally by Fisher et al. (*37*), and then theoretically by Humm et al. (*38*), and most recently by Kvinnsland et al. (*39*), the spatial distribution of α-particle emitters has an important impact on the absorbed dose distribution and, correspondingly, on the slope of the cell-survival curve. Neti and Howell recently provided experimental evidence of a lognormal cellular uptake of ^{210}Po citrate among a cell population uniformly exposed to the radiochemical and showed that this distribution can substantially alter the cell survival curve (*40*). Although many of the results obtained from the external-beam studies (summarized in Table 2) are generally applicable regardless of the α-particle distribution, specific parameters such as the average number of α-particle traversals to induce a lethal event or the D_0 value (i.e., the absorbed dose required to reduce cell survival to 0.37) are highly sensitive to experimental factors such as the geometry of the cells, the thickness or diameter of the cell nucleus, the distribution of DNA within the nucleus (i.e., the phase of the cell cycle), and the number and spatial distribution of the α-particle sources relative to the target nuclei.

The distinction between DNA double-strand breaks (DSBs) caused by a single high-LET track versus DNA damage caused by multiple low-LET tracks is illustrated in Figure 3. This basic observation underpins almost all the radiobiology of α-particles.

TABLE 2. α-Particle Beam Findings That Are Also Applicable to Internally Administered α-Particle Emitters

No.	Finding
1	RBE > 1 for cell sterilization, chromosomal damage/cancer induction relative to low-LET radiation
2	Reduced susceptibility to modulation by radiosensitizers and radioprotectors
3	Reduced capacity to repair sublethal damage
4	Higher induction of DNA DSBs at low total absorbed doses
5	Monoexponential surviving fraction curve after uniform irradiation (absence of a shoulder)

Traversals Required for Cell Kill

The average number of α-particle nuclear traversals required to kill a cell, as measured by loss of the subsequent ability to form a colony, ranges from as low as 1 (*41*) to as high as 20 (*42*). If bystander effects are included, the lower end of the range would include 0. The variability in this value when bystander effects are not considered arises because of the high sensitivity of this determination to the geometry of the cell and the nucleus during irradiation and also the LET of the incident α-particles and the LET distribution within the nucleus.

Quoting from a publication of Raju et al. (*43*), "The notion that a cell will be inactivated by the passage of a single α particle through a cell nucleus prevailed until Lloyd and her associates (*42*) demonstrated that 10 to 20 5.6 MeV α particles were required to induce one lethal lesion in flattened C3H 10T1/2 cells. Studies by Bird, et al. (*44*) showed that approximately four ^{3}He ions were required to pass through the cell nucleus to induce one lethal lesion in V79 cells at the G_1/S-phase border, cells in late S phase required five to eight ^{3}He ions. Todd, et al. (*45*) investigated the effect of 3.5 MeV α particles on synchronized T-1 cells, and observed that approximately one α particle out of four to five traversing a cell nucleus is effective in inducing one lethal lesion. Roberts and Goodhead (*46*) estimated that one out of six 3.2 MeV α-particle traversals through a C3H 10T1/2 cell nucleus is lethal. Barendsen (*47*) concluded that the probability of inactivation per unit track length of high-LET α particles is approximately 0.08 μm^{-1} for both T-1 and C3H 10T1/2 cells consistent with the results of Roberts and Goodhead for C3H10T1/2 cells (*46*)." In a study comparing high-LET effects of Auger versus α-particle emitters, Howell et al. found that about 9 decays of ^{210}Po were required to reduce cell survival to 37% (D_0) when it was distributed between the cytoplasm and nucleus of V79 cells; the energy deposited in the cell nucleus corresponds to about 2 complete (maximum chord length) traversals of the cell nucleus (*48*). In a murine lymphoma cell line, approximately 25 cell-bound α-particle–emitting ^{212}B immunoconjugates were required to reduce clonogenic

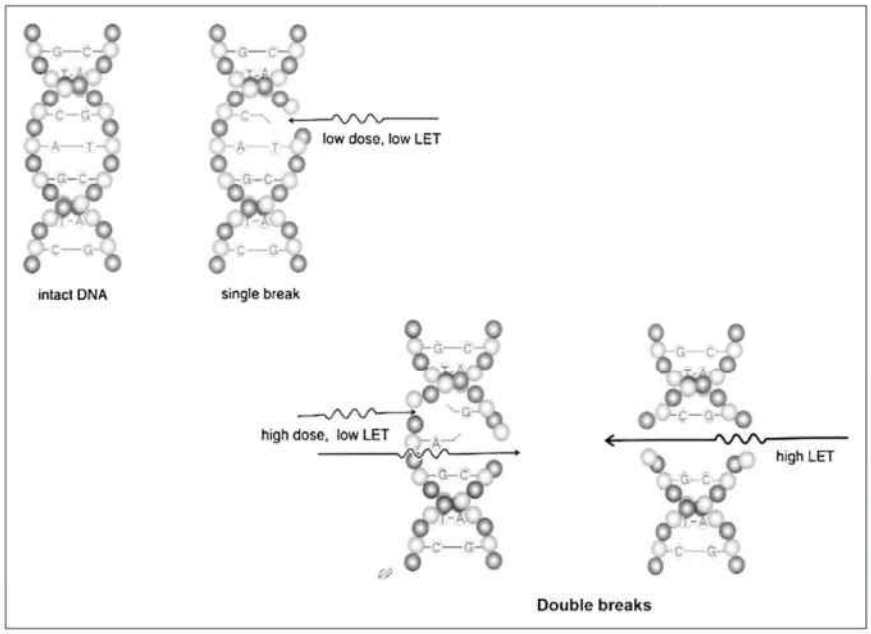

FIGURE 3. Single high-LET track has high probability of yielding DNA DSB, whereas probability of DSB induction with low-LET tracks becomes comparable only at higher absorbed doses. (Reprinted with permission of (*154*).)

survival by 90% (*49*). The theoretic efficiency of DSB production when an α-particle passes through DNA was examined by Charlton et al. (*50*) and was found to be surprisingly low; approximately one eighth of 10-MeV α-particles passing through a 54-nucleotide section of DNA produce a DSB. One passage in 4 of 1.2-MeV α-particles produces a DSB.

Barendsen's estimate of the inactivation probability per unit track length and Goodhead et al.'s determination of the number of lethal lesions per micrometer track through the nucleus (*33*) suggest another approach for estimating inactivation probability. Along these lines, Charlton and Turner introduced the total α-particle path length (or chord length) through the nucleus as a useful parameter (*51*). This was used to derive λ, the mean free path between lethal events for α-particles traveling through nuclei. Drawing from an extensive compilation of experimental data, the investigators found that this parameter ranged from 1.5 to 64.4 μm. As expected, λ was found to be dependent on the LET (Fig. 4). An inactivation probability per unit track length through the nucleus has also been used in a model describing radiation-induced cellular inactivation and transformation. By incorporating aspects of a state vector model for carcinogenesis (*52*) into the inactivation/transformation model, Crawford-Brown and Hofmann (*53*) have described a model that successfully predicts both cell survival and transformation after irradiation by α-particles of different LETs at absorbed doses below 1 Gy. This model was used to examine the impact on model predictions of including a correlation between initiation of cellular transformation and cellular inactivation. At absorbed doses greater than 1 Gy, a significant difference was observed in the predicted probability that a cell is transformed and survives.

Cell Survival Curve

Cell survival curves (i.e., surviving fraction, SF, vs. absorbed dose, D) for low-LET radiation such as x-rays exhibit an initial "shoulder" that is thought to reflect the repair of radiation damage. This type of cell survival curve can be represented by the linear-quadratic equation

$$SF = e^{-\alpha D - \beta D^2}. \qquad \text{Eq. 1}$$

The parameters α and β are, respectively, sensitivity per unit dose (D) and per unit dose squared (D^2). As the absorbed dose exceeds a certain threshold level, presumably

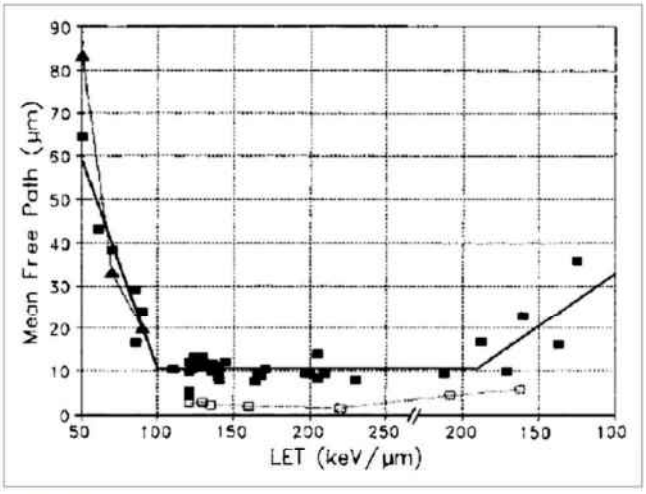

FIGURE 4. Dependence of mean free path on LET. LET is plotted (e.g., from 200 to 100 keV/μm after 250 keV/μm) so that stopping powers on low-energy side of Bragg peak can be identified. (Reprinted with permission of (*51*).)

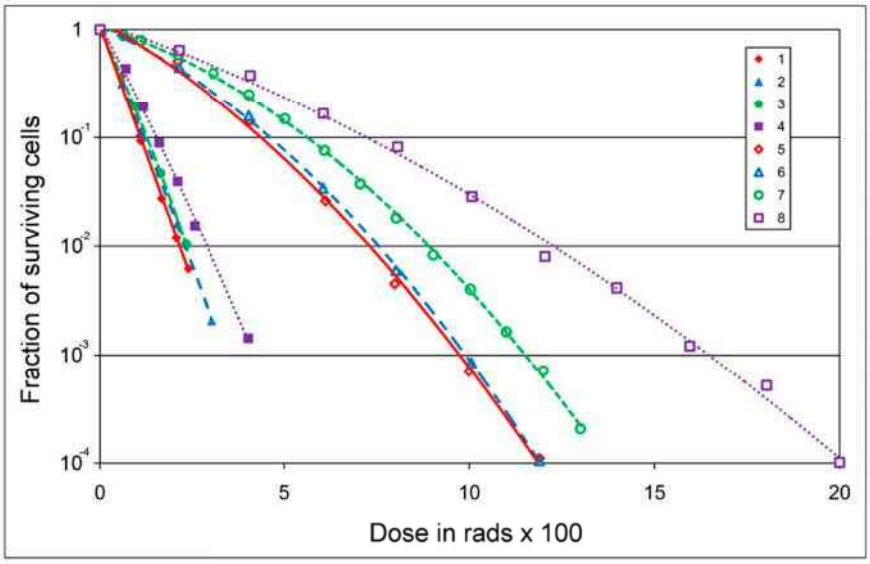

FIGURE 5. Survival curves obtained with ^{210}Po α-particles (1–4) or 250-kVp x-rays (5–8) and with different cell lines: R_1 cells derived from rhabdomyosarcoma of rat (1 and 8), subline of human kidney cell line T_1 with mean chromosome number of 121 (2 and 5), subline of T_1 with 62 chromosomes (3 and 6), and subline of T_1 with 63 chromosomes (4 and 7). (Adapted from (*155*).)

the dose at which the radiation damage repair rate is reduced relative to the rate of induced damage, the relationship between surviving fraction and absorbed dose approaches log-linearity. As shown in Figure 5, the cell survival curve for α-particle radiation is log-linear at low as well as high absorbed doses; that is, it does not exhibit a shoulder region, reflecting the reduced capability of cells to repair α-particle damage. The equation describing this is

$$SF = e^{-D/D_0}, \qquad \text{Eq. 2}$$

with the parameter D_0 equal to the absorbed dose required to yield a surviving fraction of 37%. The log-linear aspect of cell survival curves after α-particle irradiation reflects a reduced repair capacity, not the absence of repair. That α-particle damage is repaired has been demonstrated by several studies, as described in the "Radiomodulation" section. Repair of damage is not inconsistent with single-event lethality and a log-linear survival curve. The key distinction is whether death is a result of accumulated damage or of a single event. Cell survival curves that exhibit an initial shoulder reflect cell death that results from the accumulation of damage, whereas log-linear cell survival curves reflect cell death arising from a single event, without the need to accumulate damage. In both situations, repair is possible.

Oxygen Effect

In addition to dose rate, the influence of oxygen concentration has long been recognized as an important factor in the response of cells to radiation (*54,55*). Figure 6 demonstrates that this effect is strongly influenced by the LET of the radiation. The oxygen enhancement ratio (OER), or relative radiosensitivity of cells to oxygen concentration, is 1 for charged particles with an LET greater than 140 keV/μm (*24*). The initial LET of 4- to 8-MeV α-particles typical of the α-emitters of interest in targeted α-emitter therapy ranges from 110 to 61 keV/μm. The OER values in this LET range are 1.3 to 2.1. Because the LET of the emitted α-particles increases well beyond the 140 keV/μm threshold for OER = 1 as the Bragg peak is approached, the ability of α-particles to overcome radioresistance due to hypoxia will depend on the spatial distribution of the α-emitters relative to the hypoxic region. The ability to overcome hypoxia, noted above, is strictly radiobiologic. There are studies suggesting that hypoxia may alter the phenotype of the cell via cell signaling pathways associated with increased concentrations of hypoxia-inducible factor 1α, leading to a cell phenotype that is inherently more resistant to radiation and other cytototoxic agents, including chemotherapeutics (*56*). The classic OER effect has been explained as a free radical–mediated effect in which the presence of oxygen "fixes" free radical–induced damage, thereby making repair of the damage more difficult (*57*). In this case, the reduced OER effect with α-particle radiation may be explained by the

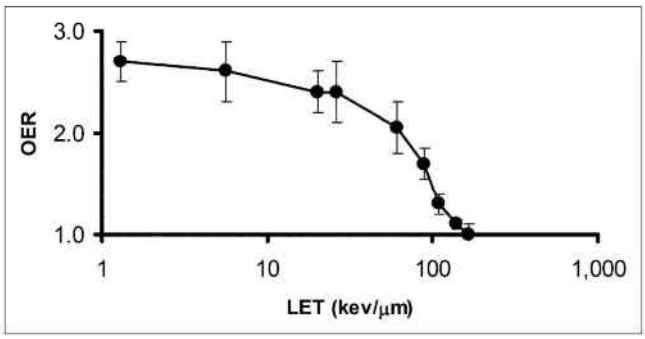

FIGURE 6. OER as function of LET. OER was measured using cultured human kidney-derived cells incubated in air or nitrogen. α-Particles of different energies generated by cyclotron or 250-kVp x-rays (average LET ≈ 1.3 keV/μm) were used. (Data replotted from (*24*).)

preponderance of oxygen-independent direct DNA damage (vs. oxygen-dependent indirect, i.e., free radical–mediated, DNA damage) characteristic of α-particles.

Dose Rate

The influence of absorbed dose rate on cell survival for low-LET emissions is well established. As the dose rate is lowered and the exposure time extended, the biologic effect of a given dose is generally reduced (*58*). The primary explanation for this effect is that lower dose rates provide a greater time interval for DNA damage repair. Because high-LET damage is not easily repaired, dose rate or even dose fractionation should not impact cellular survival. Barendsen examined changes in survival after α-particle irradiation over a dose-rate range of 0.5–100 rad/min, and no dose-rate effect was observed (*26*).

Oncogenesis

Although not of prime concern in cancer therapy, a much higher incidence of cancer induction is associated with α-particle irradiation (*59*). Accordingly, the radiation weighting factor for α-particles is 20, meaning that a committee review of the relevant experimental and human data has determined that per unit absorbed dose, α-particles are associated with a 20-fold greater risk of cancer induction than is a similar absorbed dose of photons or β-particles (*60*). A review of human and animal data related to cancer risk estimates has called the value of 20 into question for bone cancer and leukemia risk, particularly at low absorbed doses (*61*). Consideration of dose to target cells on bone surfaces as opposed to the average bone dose gives an RBE for bone cancer risk of 3–12. The authors (*61*) noted that these estimates may also change since there is evidence that bone cancer risk may be best assessed by calculating dose to a 50-μm layer of marrow adjacent to the endosteal bone surface as opposed to a single 10-μm layer as currently assumed. Likewise, a factor of 2 to 3 is more consistent with the experimental data for leukemia induction. All these estimates are based on α-particle emitters not projected for use in targeted α-emitter therapy. The few studies that have been performed to examine carcinogenesis of the short-lived α-emitters of interest in targeted α-emitter therapy have used ^{211}At. Neoplastic changes, predominately papillary carcinomas in various organs, were seen in a few animals but not more than what was expected for untreated mice. Brown and Mitchell (*62*) reported a 13% incidence of plasmocytoma in tumor-bearing mice of the same strain 13–21 mo after treatment with 200–750 kBq of 6-^{211}At-astato-2-methyl-1,4-naphthoquinol bis(diphosphate salt). The frequency of low-grade B-cell non-Hodgkin lymphoma was high but similar to that of the control population. A high incidence of pituitary adenomas and mammary tumors has been seen in rats treated with ^{211}At (*63,64*). These tumors, however, were partially attributed to secondary effects associated with a hormonal imbalance resulting from thyroid or ovarian tissue compromise.

Fractionation

The fundamental rationale for fractionation in external-beam radiotherapy is based on the differential repair capacity of most normal organs compared with most tumors. This is expressed in terms of early versus late responding tissues, corresponding to high versus low α/β ratios (*65*). Fractionation tends to spare normal organs without a reduced efficacy against tumors. As shown in Figure 7, this is not the case with high-LET radiation (*26*). Cultured cells derived from human kidneys showed the same surviving fraction for a single total absorbed dose of α-particle radiation or the same total dose delivered in 2 equal fractions, separated by 12 h. For the same cell line, similar results have been observed when the total dose was delivered in 3 equal fractions at 4, 8, and 12 h after cell plating (*25*). Extension of the biologically effective dose formalism to account for RBE effects has also demonstrated that fractionation is theoretically not likely to confer a normal tissue-sparing effect for high-LET radiation (*66*). Similar conclusions may be drawn for the chronic, exponentially decreasing dose rates delivered by internally administered α-particle emitters.

Radiomodulation

Few examples of agents that can modulate α-particle radiation–induced damage have been reported. In the early 1960s, Barendsen et al. compared the radioprotective effects of cysteamine and glycerol (*25*). The surviving fraction of T_1 (human kidney–derived) cells increased by a factor of 3.7 for 250-kVp x-irradiation and only 1.2 for

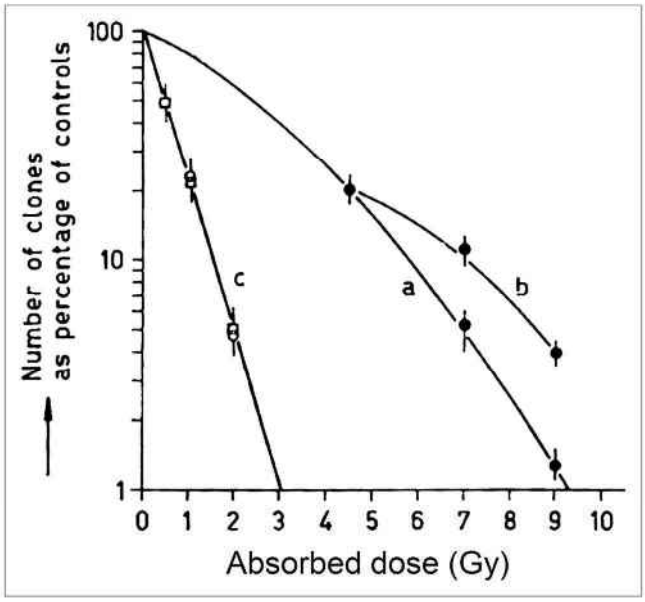

FIGURE 7. Effect of fractionation on cell survival: cell survival curve obtained with single doses of 200-kV x-rays (a), curve obtained when 200-kV x-ray doses are separated by 12 h (4.5 Gy, then 2.5 or 4.5 Gy) (b), and curve obtained with 3.4-MeV α-particles (c). In (c), circles correspond to single exposure, and squares to 2 equal exposures separated by 12 h. (Adapted from (*26*).)

^{210}Po α-particle radiation. Similar results were observed with glycerol; cell survival was increased by 2.0 and 1.2 for 250-kVp x-rays and ^{210}Po α-particles, respectively. Qualitatively consistent but quantitatively different results have been obtained with the radiosensitizer Wortmannin. This irreversible and potent inhibitor of DNA-dependent protein kinase is involved in the nonhomologous end-joining DNA repair pathway invoked in the repair of DNA DSBs (*67*). In V79 Chinese hamster cells, Wortmannin led to a 3- to 4-fold increase in genotoxic damage, as measured by the induction of micronuclei. High-LET irradiation, as delivered by a boron neutron-capture reaction, leading to the release of α-particles with an average energy of 2.3 MeV, yielded an increase in micronucleus induction of approximately 2-fold. This finding suggests that the more complex double-strand damage induced by high-LET radiation is a substrate of the nonhomologous end-joining pathway (*68,69*). In vivo studies in mouse testes have shown that soybean oil, *S*-(2-aminoethyl)isothiuronium bromide hydrobromide, and cysteamine afford some protection against the cytotoxic effects of 5.3-MeV α-particles emitted by ^{210}Po (*70–73*). When spermatogonial cell survival was used as the biologic endpoint, dose modification factors of 2.2, 2.4, and 2.6, respectively, were obtained. No modification of the spermatogonial response to α-particles was observed when dimethyl sulfoxide or vitamin C was used (*74,75*).

That DNA damage and its repair are at the core of α-emitter radiobiologic effects is supported by many years of experimental and theoretic work. It is important, however, to keep in mind that all the foundation work regarding the radiobiology of α-emitters was performed well before modern molecular biology came into existence. In light of the remarkable and far-reaching gains in our understanding of the molecular mechanisms involved in cancer genesis, the cellular response to radiation, and DNA single and DSB repair, a reexamination of α-particle radiobiology using modern tools is warranted.

RBE

The biologic effect of ionizing radiation is influenced by the absorbed dose, the dose rate, and the quality of radiation. Radiation quality is characterized by the spatial distribution of the energy imparted and by the density of ionizations per unit path length, referred to as the LET or stopping power of a charged particle (*22,60*). Depending on the effect considered, greater ionization density along a track will increase the probability of inducing a biologic effect. Compared with electrons and β-particles, α-particles exhibit a high density of ionization events along their track (*76*). Electrons and β-particles that are emitted by radionuclides generally range in energy from several megaelectron volts to as low as several kiloelectron volts, with corresponding LET values ranging from about 0.1 to 1 keV/μm (β-particles actually are characterized by a spectrum of energies; the bottom end of the spectrum is zero). The exception to these is Auger electrons, which have energies as low as several electron volts and corresponding LET values as high as 25 keV/μm. α-Particles emitted by radionuclides range in energy from 2 to 10 MeV, with initial LET values ranging from 60 to 110 keV/μm. A given tissue-absorbed dose resulting from α-particles, therefore, is likely to yield considerably greater biologic effects (again depending on the effect being considered) than the same absorbed dose delivered by typical electrons or β-particles. To account for differences in energy deposition pattern exhibited by different quality radiations, the concept of RBE has been established. An authoritative review of this concept, its derivation, and appropriate application has been published by the International Commission on Radiological Protection (ICRP) (*60,77*), and the reader is encouraged to consult this source for additional information. In radiobiology, RBE equals the ratio of absorbed doses of 2 types of radiation that produce the same specified biologic effect.

RBE Defined

RBE is calculated as the absorbed dose of a reference radiation (e.g., x-rays, γ-rays, β-particles), $D_r(x)$, required to produce a biologic effect, x, divided by the absorbed dose of the test radiation, $D_t(x)$, required to produce the same biologic effect:

$$RBE(x) = \frac{D_r(x)}{D_t(x)}. \qquad \text{Eq. 3}$$

RBE is thus an experimentally determined value defined for a particular biologic effect and therefore for a particular biologic system.

The experimentally determined value can be influenced by the variability of the biologic system across different laboratories. This issue has been examined for studies in vitro (*78*). The methodology used for calculating the absorbed dose of the 2 radiation types will also impact the result. Ideally, this should not be the case. The methodology used should provide the true absorbed dose value or specific energy distribution ("Case for Microdosimetry" section) to the relevant biologic target for both the test and the reference radiations. In practice, however, this is a challenge even for studies in vitro (*79*). In the setting of human α-particle emitter dosimetry, consistency and reproducibility will be as important as accuracy. This issue is discussed in greater detail in "Recommendations for Dosimetry of Deterministic Effects" section.

The fact that the RBE is related to the pattern of ionizing energy deposition along a particle track leads to a third factor that will impact the results. The RBE for a particular radiation type will also depend on the initial emission energy of the particle (i.e., how close the particle is to the end of its track [the Bragg peak]). This factor has been examined by Charlton et al. (*80*) and Howell et al. (*81*). In the studies by Howell et al., a uniform distribution of decays was assumed to calculate the D_0 for 7 α-emitting

isotopes covering a wide range of initial energies. Using the D_0 obtained for x-rays for the cell line used in the α-emitter calculations, a linear relationship between RBE and initial α-particle energy was obtained over an initial α-energy ranging from 5 to 8.5 MeV. The straight line was given by RBE = 2.9–0.167E_i, where E_i is the initial α-particle energy in megaelectron volts. This is an approximate scaling of the equation derived from in vivo experimental data by Howell et al. (*81*). In addition to effects related to the Bragg peak, nonuniform biodistribution of the α-emitters also leads to microdosimetric effects that impact RBE and the slope of the cell-survival curve (*37–39*).

If the reference radiation yields a dose–response relationship that is not log-linear for the biologic system examined, the RBE value will depend on the specific biologic quantitative endpoint selected (e.g., D_{50}, D_{37} (= D_0), D_{10}, etc., which determines whether the comparison falls in the shoulder or in the log-linear region of a dose–response or survival curve). The type of biologic endpoint (e.g., survival, mutation) and the dose rates of the test and reference radiations will also influence the RBE value. Strictly speaking, the test radiation should be delivered in a manner identical to that of the reference radiation (e.g., chronic or acute). However, acute externally administered x- and γ-rays are often used as the reference radiation when RBE values are determined for internally administered radionuclides. Given the often-sizeable difference in biologic responses to acute-versus-chronic low-LET radiation, the dose rate at which the reference radiation is delivered can impact the resulting RBE (*48*). The dose-rate pattern delivered by radiopharmaceuticals is generally well represented by multicomponent exponential functions. Howell et al. have delivered such patterns with external beams of ^{137}Cs γ-rays (*82*). This approach was used to study the bone marrow response to exponentially decreasing dose rates of ^{137}Cs γ-rays (*83*). The response of granulocyte–macrophage colony-forming cells in the marrow to decreasing dose rates with half-times ranging from 62 h to ∞ (i.e., constant dose rate) were studied and compared with the response to acute exposures. Mean lethal doses for chronic irradiation were up to 40% higher than those for acute exposures. Thus, care must be taken when comparing RBE values based on different reference radiations.

Based on a review of experimental literature, an RBE value of between 3 and 5 was recommended for cell killing by a panel convened by the Department of Energy in 1996 (*84*). Because human studies using α-particle emitters have yet to be analyzed for deterministic effects, an RBE of 5 was recommended for projecting the possible deterministic biologic effects associated with an estimated α-particle absorbed dose.

RBE, Q, and w_R

The discussion thus far has focused on RBE. RBE is occasionally confused with quality factors, Q, and radiation weighting factors, w_R. This confusion reflects the historical evolution of RBE which was originally defined as relative biological efficiency and intended to apply to both radiobiology (deterministic effects) and protection (stochastic effects). As currently recommended by the ICRP, however, RBE is not to be used directly in radiation protection but only as a starting quantity to derive the radiation weighting factor w_R, which replaced the quality factor Q in the most recent ICRP recommendations (*85,86*). The RBE values used to arrive at w_R relate to stochastic endpoints such as cancer induction, rather than deterministic endpoints such as normal-tissue toxicity and tumor cell sterilization in cancer therapy patients. The ICRP radiation weighting factor for α-particles is 20. This value, intended only for stochastic effects caused by α-particle irradiation, is based on animal experiments and from analysis of historical α-emitter exposures. In contrast to RBE values, weighting factors are not directly measured values but rather are consensus recommendations of the ICRP (*60*).

The radiation weighting factor w_R is a unitless factor that converts average absorbed dose (in units of grays) to equivalent dose in an organ or tissue. The SI unit for equivalent dose is referred to by the special name *sievert.* The sievert is not a unit in the conventional sense but is intended to indicate that the absorbed dose value has been adjusted to reflect a biologic risk that is associated with stochastic effects. Although the sievert is often used in the context of deterministic effects, this use is not strictly correct because the ICRP has stipulated that the sievert should be used only to designate the risk of incurring stochastic biologic effects such as cancer. The ICRP has reported on RBE for deterministic effects (RBE_M), but no special name has been chosen by the ICRP for the product of absorbed dose and a factor such as RBE that specifically reflects similar scaling for a deterministic effect (*77*).

α-PARTICLE DOSIMETRY

Radiation dosimetry offers a means for standardizing and comparing the efficacy of different radiation-based treatments. It provides a logical basis for understanding the effects that various radiation qualities have on biologic matter. For α-particle emitters, accurate dosimetry calculations require knowledge of the activity distribution as a function of time at the cellular and subcellular levels (*87*). Furthermore, an accurate representation of the geometry at this level is also required. For in vitro experiments (i.e., cell survival studies), the activity distribution is straightforward, consisting of uptake on the surface or within the cell, along with a known fraction in the surrounding solution. In these experiments, the cell and nucleus can be approximated as concentric spheres, the dimensions of which can easily be measured. However, for clinical applications, these idealizations give way to complex activity and tissue geometries. In these cases, modeling the 3-dimensional geometry of a spheroid (*88,89*) or using microscopic data from tissue biopsy samples (*90*) can provide information on the target

geometry. Determining the activity distribution, however, remains difficult. Autoradiography (*91*) may provide a snapshot of the activity distribution at a single instance in time. However, the determination of the activity as a function of time may require mathematic modeling (*92–94*) of the carrier molecules as they diffuse through tissue and bind to markers on cell surfaces. Ideally, such modeling should be validated using animal model measurements in vivo.

Case for Microdosimetry

There are 2 methods for calculating the energy deposited by individual α-particles. One method uses the MIRD formalism to calculate the average dose to the target (cell nucleus) for a variety of source compartments (cell surface, cytoplasm, and nucleus). Extensive tables have been produced for various combinations of α-particle–emitting radionuclides and cellular geometries (*95,96*). The basis for using mean absorbed dose is related to the biologic properties of low-LET radiations such that a large number, often several thousands, of statistically independent radiation deposition events in a single cell nucleus is required to induce a demonstrable biologic effect. In such a case, the statistical variation of the energy imparted to different cell nuclei is minimal. In contrast, for high-LET irradiation, such as α-particles, the effect of even a single event in the cell nucleus is so great that the mean absorbed dose can be a misleading index of biologic effect. This is due to several reasons. Foremost is that the number of α-particles that traverse a cell nucleus is often few, and therefore stochastic variations become important. In addition, the path of the α-particle through the cell nucleus is also critical. An α-particle that crosses directly through a cell nucleus will deposit a large amount of energy, whereas one that merely grazes the surface will deposit little or no energy. Thus, a second method for α-particle dosimetry—microdosimetry—takes into account the stochastic nature of energy deposited in small targets. The fundamental quantities in classic microdosimetry are specific energy (energy per unit mass) and lineal energy (energy per unit path length through the target) (*97*). Microdosimetry was originally proposed by Rossi (*98*) to explain the stochastic nature of energy deposited in matter by external ionizing radiation. It has subsequently been adapted to the case of internally deposited α-particle emitters (*99–101*).

Microdosimetric Techniques

Microdosimetric spectra may be calculated using either analytic or Monte Carlo methods (*102*). Analytic methods use convolutions (via Fourier transforms) of the single-event spectrum to calculate multievent distributions (*98*). The single-event spectrum represents the pattern of specific energy depositions for exactly 1 α-particle hit. Kellerer developed a method to efficiently determine the multiple-event spectrum through the use of Fourier transforms (*103*). Although analytic codes are computationally efficient, they are often limited to simple source–target geometries because the single-event spectrum must be known for each source–target configuration. Monte Carlo codes offer greater flexibility than analytic methods and can simulate a wide variety of geometries and source configurations. Idealizations are often made to simplify the coding and reduce calculation time. In nearly all Monte Carlo codes, α-particles are assumed to travel in straight lines. This approximation is valid for α-particles having energies less than 10 MeV (*97*). In addition, the range of δ-rays (energetic electrons originating from the α-particle track that cause secondary ionizations in the vicinity of the track) and the width of the α-particle track (~100 nm) are often ignored because the targets that are studied (i.e., cell nucleus) are much larger than these dimensions (*104*). The rate of α-particle energy loss is characterized by the stopping power. These data for a variety of media can be obtained from the literature (*105–108*). Inherent in the stopping-power formulation is the continuous slowing-down approximation. As the name implies, this approximation assumes that α-particles lose energy continuously as they traverse matter. Thus, the calculated specific energy imparted depends on the choice of stopping powers used.

Criterion for Adopting Microdosimetry

The rationale for microdosimetry was outlined by Kellerer and Chmelevsky (*109*). They suggested that the stochastic variations of energy deposited within the target must be considered when the relative deviation of the local dose exceeds 20%. For example, a small cell nucleus with a diameter of 5 μm irradiated by α-particles would require an average dose of at least 100 Gy for the relative deviations to be less than the 20% threshold. Thus, the necessity for microdosimetric methods will depend on the source distribution, the target size and shape, and the expected mean dose. For small average doses (such as those expected by nontargeted tissues) microdosimetry may be important in characterizing the pattern of energy deposition and in understanding how this pattern relates to clinical outcomes. However, in tumor, where the mean dose may be large, a microdosimetric treatment may not be necessary.

Microdosimetry Implementation Techniques

Although microdosimetry has increased our understanding of stochastic patterns of energy deposition by α-particles in both simple and complex geometries and has made it possible to explain in vitro observations, application to clinical practice has been limited because time-dependent activity distributions at the subcellular level are complex and not well characterized in vivo. Roeske and Stinchcomb (*110*) described a technique for determining dosimetric parameters that are important in α-particle dosimetry. These parameters consist of the average dose, SD of specific energy, and the fraction of cells receiving zero hits. The individual values are determined using tables of the "S" value (*111*), and the first and second moments of the single-event spectra. The average dose is determined by

multiplying the S value by the cumulated activity within the source compartment. Dividing the average dose by the first moment of the single-event spectrum yields the average number of hits. Subsequently, the fraction of cells receiving zero hits (or any number of hits) can be determined using the average number of hits and the Poisson distribution. The SD is the product of the average number of hits and the second moment of the single-event spectrum. Individual moments may be determined using either analytic methods or Monte Carlo calculations. Stinchcomb and Roeske (*112*) have produced tables of the S value and the individual moments for several geometries and source configurations appropriate for α-particle therapy. These tables were also used in the analysis of cell survival after α-particle irradiation (*112*).

Applications of Microdosimetry

Early applications of microdosimetry were performed to assess the probability of cancer induction after exposure to α-emitters. These exposures were generally not intended for therapeutic purposes, and carcinogenesis was of concern. In one such application, the specific energy distributions for plutonium oxide in dog lung were calculated. The calculations accounted for the size distribution of the inhaled aerosol and the associated deposition probabilities in the lung for various particle sizes. The distribution of target sites; the probability of an α-particle intersecting a target site; and the range, energy loss, straggling characteristics, and δ-ray production of α-particle tracks were also considered. The analysis provided an improved understanding of the relationship between dose, as described by microdosimetric specific energy spectra, and response, as measured by the incidence of lung tumors in beagle dogs (*113*).

In radioimmunotherapy, microdosimetry has been used in several α-particle applications. These applications can be broadly characterized as theoretic studies of simple cellular geometries, experimental analysis of cell survival after α-particle irradiation, and the microdosimetry of realistic geometries such as multicellular spheroids and bone marrow. The work in each of these categories will be discussed separately.

Roesch (*99*) described an approach for calculating microdosimetric spectra. Fisher et al. (*37*) subsequently applied this approach to several geometries that have therapeutic application, including sources distributed on and within individual cells, sources distributed within spheric clusters of cells, and sources located in cylinders (i.e., blood vessels) that deposited energy within spheric cell nuclei a short distance away. These calculations showed the number of α-particle emissions originating from cell surfaces that would be needed to inactivate cancer cells with high efficiency. The basic geometries that described the spatial distribution of α-emitters relative to the spatial distribution of target spheres have served as the basis of those used in several theoretic studies. In one such study, Humm (*114*) used a Monte Carlo method with a model of cell survival to estimate the surviving fraction of cells located outside a capillary and cells located within a tumor with uniformly distributed ^{211}At. Although the mean dose was similar for these 2 types of geometries, there was a significant variation in the expected cell survival due to the differences in the specific energy spectra. In particular, the fraction of cells receiving no α-particle hits increased with distance from the capillary (due to the short range of the α-particles). The surviving fraction versus mean specific energy was biexponential. That is, for low doses, the slope of this curve was similar to that of a uniformly irradiated tumor. However, with increasing doses, the curve was less steep and asymptotically approached a value corresponding to the fraction of nonhit cells. Building on the previous analysis, Humm and Chin (*38*) analyzed how specific energy spectra are affected by cell nucleus size, binding fraction, cell volume fraction, and nonuniform binding. Their results indicated that nonuniform distributions of α-particle emitters can result in expected survival curves that deviate significantly from the classic monoexponential curves produced by a uniform, external source of α-particles. In these studies, although the inherent cell sensitivity (z_o) was held constant, the slope of the cell survival curve as a function of absorbed dose to the medium was highly dependent on the source configuration. Furthermore, simulations in which cells were more uniformly irradiated resulted in steeper cell survival curves than those in which the distribution of α-emitters was highly heterogeneous. The effects of cell size and shape on expected cell survival were further studied by Stinchcomb and Roeske (*115*). In their analysis, the cell and nucleus were assigned various shapes ranging from spheres to ellipsoids where the ratio of the major-to-minor axis was varied from 1 to 5 while the volume of the nucleus was held constant. Separately, the dimensions of the nucleus were varied while the shape was held constant. Calculations of specific energy spectra and resulting cell survival demonstrated that the expected surviving fraction was not a strong function of the target shape, provided the volume was fixed. However, significant variations in cell survival were observed as the volume of the nucleus was varied. More recently, Aubineau-Laniece et al. developed a Monte Carlo code to simulate cylindric geometries as a model for bronchial airway bifurcations (*116*). In a series of reports on α-particles from radon progeny, Fakir et al. (*117–119*) demonstrated that for uniform surface emissions, there were significant variations in cellular energy deposition. Larger variations in the hit frequencies and energy deposited were observed when a nonuniform distribution of activity was also considered. Palm et al. (*120*) examined the microdosimetric effects of daughter products from ^{211}At. Separate simulations were performed assuming the daughter products decayed at the site of ^{211}At emission or that they diffused away from the site. Based on an analysis of experimental data, the ^{210}Po daughter product seemed to diffuse from the decay site, decreasing the energy deposited

in the cell nucleus by a factor of 2. All these studies illustrate the need to accurately model the source–target geometry. Moreover, approximations, such as using mean values, may impact both the specific-energy spectrum and subsequent calculation of cell survival (*39*).

Application to Cellular Clusters

Single-cell survival analyses after α-particle irradiation has also been extended to multicellular clusters. Charlton (*89*) described a multicellular spheroid model and simulated α-particle energy deposition events within individual cell nuclei. A cell survival model that takes into account the effects of varying LET (*51*) was combined with the distribution of α-particle tracks throughout cells within the spheroid. Simulating a uniform source distribution (average 1 decay per cell, 50% cell packing), this analysis demonstrated that cell survival decreased significantly (from 57% to 37%) as the spheroid diameter increased from 75 to 225 μm. The number of hits per cell also increased in larger spheroids when longer-ranged α-particle emitters were considered. Cell survival subsequently decreased from 46% to 26% in 200-μm-diameter spheroids as the packing fraction was increased from 40% to 70% (also with 1 decay per cell). The decrease in cell survival was due to the increased crossfire dose as the packing fraction was increased. In a separate simulation, the total number of decays per spheroid was kept constant while a small fraction of cells (20%) was assumed not to take up any activity. This process simulated the effects of cells that lacked a specific targeting moiety. It is interesting to note that the unlabeled fraction did not significantly alter the expected cell survival. In these studies, the specific energy distribution is highly nonuniform and varies with depth below the spheroid surface. Thus, a single dose or specific-energy distribution is not representative of that through the entire tumor. By combining the specific-energy distribution with cell survival models, it is possible to gain insight into those factors that will influence the therapeutic efficacy of a particular targeting approach. However, most of these cell survival models do not take into account second-order processes such as the bystander effect that may play an important role in modeling cellular clusters and micrometastases. Refinement of these models is currently an active area of research (*121,122*).

Application to Bone Marrow

Bone marrow is often the dose-limiting organ in radioimmunotherapy. The dosimetry of bone marrow is difficult because of its complex geometry and the presence of tissue inhomogeneities. Thus, idealized models, as have been used in the previous studies, must be replaced by more realistic geometries. The work to date on estimating specific energy spectra for bone marrow has focused largely on using histologic samples obtained from humans or animal models. Akabani and Zalutsky (*90*) obtained histologic samples of beagle bone marrow and manually measured chord length distributions. Using a Monte Carlo program, they calculated the single-event specific energy distribution for sources both in the extracellular fluid and on the surface of red marrow cells. These single-event distributions were combined with a model of cell survival. This analysis demonstrated that activity concentrated on the cell surface resulted in significantly greater cell killing than did activity in the extracellular fluid. The effect of LET on the survival of human hematopoietic stem cells in various geometries was studied by Charlton et al. (*80*). These geometries were determined from human marrow samples obtained from cadavers. Microdosimetric spectra and cell survival were calculated for 3 different source–target geometries: isolated cells labeled on their surfaces, a nontargeted distribution of decays in an extended volume, and nontargeted decays in marrow with 36% of the marrow volume occupied by fat. Two different radionuclides, ^{149}Tb and ^{211}At, were considered. These simulations indicated that for targeted decays ^{149}Tb was 5 times more effective than ^{211}At when compared on a hit-by-hit basis. This enhancement was due to the lower energy of ^{149}Tb resulting in a higher LET of the incident α-particles. Those authors also concluded that cell survival was a function of the position of the decay relative to the cell nucleus. Using a model similar to that of Charlton et al. (*80*), Utteridge et al. (*123*) considered the risk of the development of secondary malignancies (i.e., leukemia) from α-particles. This risk may be important in evaluating the future therapeutic application of α-particles in patients who have an excellent prognosis. Three α-emitting radionuclides were considered on the basis of the relative range (short, medium, and long) of the particle. In this analysis, the authors calculated the fraction of cells that are hit and would survive (as these would potentially cause secondary malignancies). They determined that the lowest fraction occurred for low energies and the highest fraction occurred for the highest-energy α-particle emitter.

RECOMMENDATIONS FOR DOSIMETRY OF DETERMINISTIC EFFECTS

Beyond providing a rational basis for a starting administered activity value for a phase I study, dosimetry has an important role in guiding clinical trial design to help maximize the likelihood of a successful, minimally toxic implementation. This is particularly important because α-emitter targeted therapy has the potential to be both highly effective and also quite toxic. Which of these 2 aspects emerges in a therapeutic trial will depend on having an understanding of the physical and biologic factors that impact response and toxicity. It is essential that clinical trials investigating targeted α-particle therapy be rationally designed; otherwise, there is the risk that α-emitters may be abandoned before they have been properly tested in the clinic.

This increased importance of dosimetric analysis is coupled with a greater difficulty in obtaining the human data necessary to perform dosimetry. In contrast to most

targeted therapy trials to date, collection of biodistribution data for dosimetry from pretreatment imaging studies will not be possible for most α-particle–emitting radionuclides with therapeutic potential. This places a greater emphasis on preclinical studies and extrapolation of results obtained from such studies to the human. Several of the α-emitting radiotherapeutics decay to α-emitting daughters whose distribution may not be that of the carrier. Aside from understanding the biodistribution and dosimetry of the α-emitter–labeled carrier, therefore, the biodistribution and dosimetry of the daughter must also be considered (*124–131*).

In this section, the focus of the discussion and the recommendations that are made are specific to deterministic effects.

Recommendations

After stability and radiochemical purity of the radiopharmaceutical have been established and an appropriate target identified, the following progression of studies is proposed. Elements of these recommendations have also been described elsewhere (*132–134*).

1. Determine cellular targeting kinetics and properties.
   A. Determine number of sites per cell and fraction of cells expressing target.
   B. Determine distribution of binding sites per cell among the targeted cells.
   C. Determine binding and dissociation constants for cell targeting (e.g., antibody affinity).
   D. Determine internalization rate and fraction internalized.
   E. Determine fate of internalized radionuclide.
   F. Determine median lethal dose in targeted versus nontargeted cells.
   G. Determine cell-level dosimetry for targeted and nontargeted cells.

2. Perform animal (xenograft or transgenic) model studies.
   A. Evaluate maximum tolerated administered activity.
   B. Identify likely dose-limiting organs.
   C. Collect macroscopic (whole-organ) pharmacokinetics.
   D. Collect microscopic (e.g., by autoradiography or optical imaging) biodistribution in dose-limiting organs.
   E. Evaluate stability of the radiopharmaceutical in vivo.
   F. Evaluate efficacy at maximum tolerated administered activity.
   G. Perform cell- and organ-level dosimetry for the animal model.

3. Extrapolate data obtained in steps 1 and 2 to the human to arrive at initial activity for a phase I study.
   A. Develop and fit a pharmacokinetic model to data obtained in steps 1 and 2.
   B. Replace model parameter values with estimated human values; simulate biodistribution in humans.
   C. Use model-derived biodistribution to estimate absorbed dose to dose-limiting organs identified in step 2B.

4. Assess radiopharmaceutical distribution during the phase I study.
   A. Image (if possible).
   B. Collect and count blood samples.
   C. Collect, count, and autoradiograph biopsy samples (if practical).

If there are concerns (not addressed by animal studies) about possible renal, urinary bladder wall, or gastrointestinal toxicity related to the localization of activity in luminal contents versus the organ wall:

   D. Collect and count urine samples.
   E. Collect and count fecal samples.

Steps 1–3 are general guidelines. The primary objective is to collect adequate preclinical data so as to have an understanding of the α-emitters' likely biodistribution and kinetics in humans. This objective is particularly important because pretherapy patient imaging will not be possible. It is essential that this approach not be seen as mandatory for moving α-emitter–labeled radiopharmaceuticals to the clinic; in particular, step 3 may be replaced by a projected conservative (worst-case) scenario analysis or by a direct translation of small-animal pharmacokinetics to the human using standard methods to adjust for differences in body size and organ mass (*135*). The autoradiography proposed in steps 2D and 4C will clearly be subject to the practical constraint of α-emitter half-life. For short-lived α-emitters, microscopic imaging of fluorescently tagged agents may be a viable alternative to autoradiography in animal models.

Conventional Versus Cell-Level Dosimetry. In most cases, a microdosimetric analysis will not be necessary for targeted therapy applications because the activity level administered and mean absorbed doses to targeted cells are larger than in the cases described here and the resulting stochastic deviation is expected to be substantially less than 20%. In such cases, standard dosimetry methods may be applied (*111,136*). The standard approach to dosimetry calculations has been described by the MIRD Committee (*111*). In this formalism, the absorbed dose to a target volume from a source region is given as the total number of disintegrations in the source region multiplied by a factor (the S value) that provides the absorbed dose to a target volume per disintegration in the source region. The sum of these products across all source regions gives the total absorbed dose to the target. MIRD cellular S values have been published for cell level dosimetry calculations for situations in which the number of disintegrations in different cellular compartments can be measured or modeled (*95*). With these S values, the absorbed dose to the nucleus may be calculated from α-particle emissions uniformly distributed on the cell surface, in the cytoplasm, or in the nucleus.

Conventional Dosimetry for Organs and Tumors. Estimation of the average absorbed dose to a particular normal organ or tumor volume is based on the assumption that the radioactivity is uniformly distributed in the organ and that

the energy deposited by the emitted α-particles is also distributed uniformly within the organ. With some exceptions (*137–141*), the cross-organ dose from α-particle and electron emissions can be assumed negligible for human organ and tumor dosimetry. Care is required in applying S values for α-emitters because α-emitters may have multiple decay pathways and multiple radioactive daughters that should be considered. For example, S values for ^{213}Bi will not include the emissions from the ^{213}Po daughter, which has a 4-μs half-life and contributes 98% of the α-particles emitted by ^{213}Bi decay (the remaining 2% come from decay of ^{213}Bi itself). This consideration and also the importance of separately accounting for absorbed dose due to electron and photon emissions from that due to α-particles requires that the dosimetry calculations be based on absorbed fraction calculations rather than on S values. The methodology is described by the following equations (presented using the recently published updated MIRD schema) (*142*):

$$D_\alpha(r_T, T_D) = \tilde{A}(r_S, T_D) \cdot \frac{\sum_i \Delta_i^\alpha \phi(r_T \leftarrow r_S; E_i^\alpha)}{M(r_T)}, \quad \text{Eq. 4}$$

$$D_e(r_T, T_D) = \tilde{A}(r_S, T_D) \cdot \frac{\sum_i \Delta_i^e \phi(r_T \leftarrow r_S; E_i^e)}{M(r_T)}, \quad \text{Eq. 5}$$

$$D_{ph}(r_T, T_D) = \frac{\sum_{r_S} \left(\tilde{A}(r_S, T_D) \cdot \sum_i \Delta_i^{ph} \phi(r_T \leftarrow r_S; E_i^{ph}) \right)}{M(r_T)}, \quad \text{Eq. 6}$$

$$D_{RBE}(r_T, T_D) = RBE_\alpha \cdot D_\alpha(r_T, T_D) + RBE_e \cdot D_e(r_T, T_D) + RBE_{ph} \cdot D_{ph}(r_T, T_D), \quad \text{Eq. 7}$$

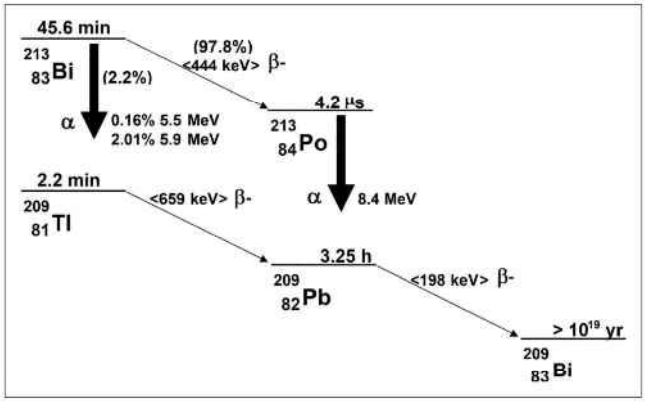

FIGURE 8. Decay scheme for ^{213}Bi.

where $D_x(r_T, T_D)$ is absorbed dose to the target region, r_T, from emission type x, over the dose integration period, T_D; $D_{RBE}(r_T, T_D)$ is RBE-weighted dose to the target region, r_T; r_T and r_S are the target and source region (or tissue), respectively; $\tilde{A}(r_T, T_D)$ is time-integrated activity or total number of nuclear transitions in the target region, r_T; $M(r_T)$ is the mass of the target region; Δ_i^x is mean energy emitted per nuclear transition for the ith emission of particle type x (alpha, electron, or photon); $\phi(r_T \leftarrow r_S; E_i^X)$ is the fraction of energy emitted per nuclear transition in the source region, r_S, that is absorbed in the target region, r_T, by the ith emission of particle type x that is emitted with initial energy E; and RBE_α, RBE_e, *and* RBE_{ph} are RBEs for α-particles (α), electrons (e), and photons (ph), respectively ($RBE_e = RBE_{ph} = 1$).

The total number of nuclear transitions in a particular tissue or region is typically obtained by longitudinal imaging, or counting tissue samples for radioactivity. Values for the Δ_i's are obtained from decay-scheme tabulations published for each radionuclide (*143*). The absorbed fraction for each decay type, ϕ, must be calculated from tabulations of absorbed fractions for the particular tissue geometry. In almost all cases, non–cell-level dose calculations, the absorbed fractions for α-particles,

TABLE 3. Electron Emissions Considered in Absorbed Dose Calculations

	Electrons					
Isotope	Energy (keV)	Isotope % per disintegration	Effective % per disintegration	Mean energy (keV/disintegration)	Δ^e (Gy-kg/Bq-s)	Electron range (mm)
^{213}Bi	200	0.20	0.20	0.40	6.41E−17	0.5
^{213}Bi	347	2.55	2.55	8.85	1.42E−5	1.4
^{213}Bi	423	0.40	0.40	1.69	2.71E−16	1.9
^{213}Bi (β)	**444**	**97.80**	**97.80**	**434.23**	**6.96E−14**	2.1
^{209}Tl (β)	659	100.00	2.20	14.50	2.32E−15	4.2
^{209}Pb (β)	**198**	**100.00**	**100.00**	**198.00**	**3.17E−14**	0.5
Sum				657.67	1.05E−13	

Mean energy and range values are listed for β-emissions. Dominant contributors to electron absorbed dose are shown in bold.

TABLE 4. α-Particle Emissions Considered in Absorbed Dose Calculations

	α-Particles					
Isotope	Energy (keV)	Isotope % per disintegration	Effective % per disintegration	Mean energy (keV/disintegration)	Δ^{α} (Gy-kg/Bq-s)	α-range (μm)
^{213}Bi	5,549	0.16	0.16	8.88	1.42E−15	42.0
^{213}Bi	5,869	2.01	2.01	117.97	1.89E−14	45.5
^{213}Po	7,614	0.003	0.003	0.22	3.58E−17	66.0
^{213}Po	8,375	100.00	97.80	8,190.75	1.31E−12	75.6
Sum				8,317.82	1.33E−12	

can be assumed equal to 1; the absorbed fractions for electrons are likewise usually assumed equal to 1. A description of the methods used to calculate these values is beyond the scope of this review but are provided in the references (*141,144,145*), one of which (*141*), in particular, describes absorbed fractions that are tabulated by α-particle energy for bone marrow trabeculae. For α-emitters that decay via a branched decay scheme, as in ^{213}Bi, for example (Fig. 8), it is important to account for the relative yield of each branch in determining the total energy emitted by each type of emission (i.e., the Δ_i's). In the case of ^{213}Bi, Tables 3 and 4 summarize the electron and α-particle emissions. The tables illustrate how to tally the total electron and α-particle energy. As shown, 2.2% of ^{213}Bi decays results in ^{209}Tl with the emission of an α-particle; the initial energy of the emitted α-particle is either 5.5 or 5.8 MeV, with the probability of each given by the yields shown in Table 2. In the remaining 97.8% of decays, ^{213}Bi decays to ^{213}Po with the emission of a β-particle. ^{213}Po itself decays rapidly via the emission of an 8.4-MeV α-particle to ^{209}Pb, which in turn decays to ^{209}Bi with the emission of a 198-keV β-particle. The exercise illustrates that a careful accounting of emissions is required in tallying the energy emitted per disintegration of the administered α-emitter, even when the decay scheme is relatively simple as for ^{213}Bi. Although outside the scope of this review, the photon S values (Table 5) can be calculated on the basis of tabulations of photon absorbed fractions to different source–target organ combinations and photon energies (*146*).

Units

The issue of identifying the most appropriate dosimetry quantities and units is particularly important for α-emitters because, as noted earlier, there can be confusion regarding the calculation of dosimetry quantities that relate to stochastic versus deterministic effects. It is incorrect to assign the unit sievert to the quantity defined by Equation 7. The sievert is not a unit in the conventional sense but, rather, is intended to indicate that the absorbed dose value has been scaled to reflect a biologic risk that is associated with stochastic effects. Although the product of deterministic RBEs and absorbed dose in grays has been referred to as a sievert, this is not strictly correct because sievert should be used only to designate the risk of incurring stochastic biologic effects such as cancer. No special named unit has been widely adopted to reflect a dose value that has been multiplied by an RBE and that specifically reflects the magnitude of deterministic effects. The MIRD Committee has proposed that the barendsen (Bd) be defined as the special named unit for the product of deterministic RBE and absorbed dose and has published a commentary to this effect (*147*). To avoid confusion during the transition period, the MIRD Committee recommends that the 3 absorbed dose values, for α-, electron, and photon emissions, be provided separately and reported in the absorbed dose unit, gray. This removes any ambiguity as to interpretation of reported absorbed doses for α-emitter therapy applications.

Daughters

The example provided above is for an α-emitter with a relatively simple decay scheme. Each disintegration of the parent ^{213}Bi leads to a single α-particle emission; there are no long-lived α-emitting daughters. This is not the case for the longer-lived α-emitters ^{223}Ra, ^{225}Ac, and ^{227}Th, which decay via α-emitting daughters. Because emission of an α-particle by the parent atom leads to a 50- to 100-nm recoil of the resulting daughter, daughter atoms may not remain conjugated to the molecular carrier. In the most complex scenario, the biologic distribution of the daughter will depend on the site of parent decay (*124*). In practice, the biologic distribution of long-lived daughters tends to be dominated by the chemical fate of the daughter atom. For example, ^{213}Bi, the longest-lived daughter of ^{225}Ac, concentrates in the kidneys. Likewise, ^{223}Ra, the daughter of ^{227}Th, localizes to bone. Dosimetry calculations for such radionuclides must, therefore, account for the biodistribution of both the parent and all daughters.

TABLE 5. Individual Photon S Factors and Summed Photon S Factor Used for ^{213}Bi Photon Dosimetry (*25*)

Isotope	Photon energy (keV)	S factor (Gy/MBq-s)
^{213}Bi	440	5.78E−11
^{213}Bi	79	9.84E−13
^{209}Tl	117	1.60E−12
^{209}Tl	467	6.71E−12
^{209}Tl	1,566	2.37E−11
Sum = $S_{WB \leftarrow WB}$		9.08E−11

ACKNOWLEDGMENT

We thank David E. Charlton for providing guidance, vigorous discussions, and for his critical reading of the manuscript.

REFERENCES

1. Bloomer WD, McLaughlin WH, Lambrecht RM, et al. ^{211}At radiocolloid therapy: further observations and comparison with radiocolloids of ^{32}P, ^{165}Dy, and ^{90}Y. *Int J Radiat Oncol Biol Phys.* 1984;10:341–348.
2. Macklis RM, Kinsey BM, Kassis AI, et al. Radioimmunotherapy with alpha-particle emitting immunoconjugates. *Science.* 1988;240:1024–1026.
3. Zalutsky MR, Vaidyanathan G. Astatine-211-labeled radiotherapeutics: an emerging approach to targeted alpha-particle radiotherapy. *Curr Pharm Des.* 2000;6:1433–1455.
4. McDevitt MR, Ma D, Lai LT, et al. Tumor therapy with targeted atomic nanogenerators. *Science.* 2001;294:1537–1540.
5. McDevitt MR, Sgouros G, Finn RD, et al. Radioimmunotherapy with alpha-emitting nuclides. *Eur J Nucl Med.* 1998;25:1341–1351.
6. Mulford DA, Scheinberg DA, Jurcic JG. The promise of targeted α-particle therapy. *J Nucl Med.* 2005;46(suppl 1):199S–204S.
7. Jurcic JG. Antibody therapy for residual disease in acute myelogenous leukemia. *Crit Rev Oncol Hematol.* 2001;38:37–45.
8. Wilbur DS. Potential use of alpha-emitting radionuclides in the treatment of cancer. *Antibody Immunoconjugates Radiopharm.* 1990;4:85–97.
9. Wicha MS. Cancer stem cells and metastasis: lethal seeds [commentary]. *Clin Cancer Res.* 2006;12:5606–5607.
10. Sgouros G, Song H. Cancer stem cell targeting using the alpha-particle emitter, ^{213}Bi: mathematical modeling and feasibility analysis. *Cancer Biother Radiopharm.* 2008;23:74–81.
11. Jurcic JG, Larson SM, Sgouros G, et al. Targeted alpha particle immunotherapy for myeloid leukemia. *Blood.* 2002;100:1233–1239.
12. Jurcic JG, McDevitt MR, Sgouros G, et al. Targeted alpha-particle therapy for myeloid leukemias: a phase I trial of bismuth-213-HuM195 (anti-CD33) [abstract]. *Blood.* 1997;90:2245.
13. Geerlings MW, Kaspersen FM, Apostolidis C, van der Hout R. The feasibility of ^{225}Ac as a source of alpha-particles in radioimmunotherapy. *Nucl Med Commun.* 1993;14:121–125.
14. Zalutsky MR, Reardon DA, Akabani G, et al. Clinical experience with alpha-particle emitting ^{211}At: treatment of recurrent brain tumor patients with ^{211}At-labeled chimeric antitenascin monoclonal antibody 81C6. *J Nucl Med.* 2008;49:30–38.
15. Nilsson S, Larsen RH, Fossa SD, et al. First clinical experience with alpha-emitting radium-223 in the treatment of skeletal metastases. *Clin Cancer Res.* 2005;11:4451–4459.
16. Hultborn R, Andersson H, Back T, et al. Pharmacokinetics and dosimetry of ^{211}At-MX35 F(AB')(2) in therapy of ovarian cancer: preliminary results from an ongoing phase I study [abstract]. *Cancer Biother Radiopharm.* 2006;21:395.
17. Kennel SJ, Mirzadeh S, Eckelman WC, et al. Vascular-targeted radioimmunotherapy with the alpha-particle emitter ^{211}At. *Radiat Res.* 2002;157:633–641.
18. Kennel SJ, Mirzadeh S. Vascular targeted radioimmunotherapy with ^{213}Bi: an alpha-particle emitter. *Nucl Med Biol.* 1998;25:241–246.
19. Akabani G, McLendon RE, Bigner DD, Zalutsky MR. Vascular targeted endoradiotherapy of tumors using alpha-particle-emitting compounds: theoretical analysis. *Int J Radiat Oncol Biol Phys.* 2002;54:1259–1275.
20. McDevitt MR, Ma D, Simon J, Frank RK, Scheinberg DA. Design and synthesis of ^{225}Ac radioimmunopharmaceuticals. *Appl Radiat Isot.* 2002;57:841–847.
21. Jurcic JG, McDevitt MR, Pandit-Taskar N, et al. Alpha-particle immunotherapy for acute myeloid leukemia (AML) with bismuth-213 and actinium-225 [abstract]. *Cancer Biother Radiopharm.* 2006;21:396.
22. Zirkle RE. Some effects of alpha radiation upon plant cells. *J Cell Comp Physiol.* 1932;2:251–274.
23. Brown A, Suit H. The centenary of the discovery of the Bragg peak. *Radiother Oncol.* 2004;73:265–268.
24. Barendsen GW, Koot CJ, van Kerson GR, Bewley DK, Field SB, Parnell CJ. The effect of oxygen on the impairment of the proliferative capacity of human cells in culture by ionizing radiations of different LET. *Int J Radiat Biol.* 1966;10:317–327.
25. Barendsen GW, Walter HMD. Effects of different ionizing radiations on human cells in tissue culture. IV. Modification of radiation damage. *Radiat Res.* 1964;21:314–329.
26. Barendsen GW. Modification of radiation damage by fractionation of dose anoxia + chemical protectors in relation to LET. *Ann N Y Acad Sci.* 1964;114(A1):96–114.
27. Barendsen GW. Impairment of the proliferative capacity of human cells in culture by alpha-particles with differing linear-energy transfer. *Int J Radiat Biol Relat Stud Phys Chem Med.* 1964;8:453–466.
28. Barendsen GW, Walter HMD, Bewley DK, Fowler JF. Effects of different ionizing radiations on human cells in tissue culture. III. Experiments with cyclotron-accelerated alpha-particles and deuterons. *Radiat Res.* 1963;18:106.
29. Barendsen GW. Dose-survival curves of human cells in tissue culture irradiated with alpha-, beta-, 20-kv x- and 200-kv x-radiation. *Nature.* 1962;193:1153.
30. Barendsen GW, Beusker TLJ. Effects of different ionizing radiations on human cells in tissue culture. I. Irradiation techniques and dosimetry. *Radiat Res.* 1960;13:832–840.
31. Barendsen GW, Beusker TLJ, Vergroesen AJ, Budke L. Effect of different ionizing radiations on human cells in tissue culture. II. Biological experiments. *Radiat Res.* 1960;13:841–849.
32. Barendsen GW, Vergroesen AJ. Irradiation of human cells in tissue culture with alpha-rays, beta-rays and x-rays [abstract]. *Int J Radiat Biol Relat Stud Phys Chem Med.* 1960;2:441.
33. Goodhead DT, Munson RJ, Thacker J, Cox R. Mutation and inactivation of cultured mammalian cells exposed to beams of accelerated heavy ions. IV. Biophysical interpretation. *Int J Radiat Biol Relat Stud Phys Chem Med.* 1980;37:135–167.
34. Munson RJ, Bance DA, Stretch A, Goodhead DT. Mutation and inactivation of cultured mammalian cells exposed to beams of accelerated heavy ions. I. Irradiation facilities and methods. *Int J Radiat Biol Relat Stud Phys Chem Med.* 1979;36:127–136.
35. Thacker J, Stretch A, Stephens MA. Mutation and inactivation of cultured mammalian cells exposed to beams of accelerated heavy ions. II. Chinese hamster V79 cells. *Int J Radiat Biol Relat Stud Phys Chem Med.* 1979;36:137–148.
36. Cox R, Masson WK. Mutation and inactivation of cultured mammalian cells exposed to beams of accelerated heavy ions. III. Human diploid fibroblasts. *Int J Radiat Biol Relat Stud Phys Chem Med.* 1979;36:149–160.
37. Fisher DR, Frazier ME, Andrews TK Jr. Energy distribution and the relative biological effects of internal alpha emitters. *Radiat Prot Dosimetry.* 1985;13:223–227.
38. Humm JL, Chin LM. A model of cell inactivation by alpha-particle internal emitters. *Radiat Res.* 1993;134:143–150.
39. Kvinnsland Y, Stokke T, Aurlien E. Radioimmunotherapy with alpha-particle emitters: microdosimetry of cells with a heterogeneous antigen expression and with various diameters of cells and nuclei. *Radiat Res.* 2001;155:288–296.
40. Neti PVSV, Howell RW. Log normal distribution of cellular uptake of radioactivity: implications for biologic responses to radiopharmaceuticals. *J Nucl Med.* 2006;47:1049–1058.
41. Munro TR. Relative radiosensitivity of nucleus and cytoplasm of Chinese hamster fibroblasts. *Radiat Res.* 1970;42:451–470.
42. Lloyd EL, Gemmell MA, Henning CB, Gemmell DS, Zabransky BJ. Cell survival following multiple-track alpha particle irradiation. *Int J Radiat Biol Relat Stud Phys Chem Med.* 1979;35:23–31.
43. Raju MR, Eisen Y, Carpenter S, Inkret WC. Radiobiology of alpha particles. III. Cell inactivation by alpha particle traversals of the cell nucleus. *Radiat Res.* 1991;128:204–209.
44. Bird RP, Rohrig N, Colvett RD, Geard CR, Marino SA. Inactivation of synchronized Chinese hamster V79 cells with charged-particle track segments. *Radiat Res.* 1980;82:277–289.
45. Todd P, Wood JCS, Walker JT, Weiss SJ. Lethal, potentially lethal, and nonlethal damage induction by heavy-ions in cultured human-cells. *Radiat Res.* 1985;104(suppl):S5–S12.
46. Roberts CJ, Goodhead DT. The effect of ^{238}Pu alpha-particles on the mouse fibroblast cell line C3H 10T1/2: characterization of source and RBE for cell survival. *Int J Radiat Biol Relat Stud Phys Chem Med.* 1987;52:871–882.
47. Barendsen GW. LET dependence of linear and quadratic terms in dose-response relationships for cellular-damage: correlations with the dimensions and structures of biological targets. *Radiat Prot Dosimetry.* 1990;31:235–239.
48. Howell RW, Rao DV, Hou DY, Narra VR, Sastry KSR. The question of relative biological effectiveness and quality factor for auger emitters incorporated into proliferating mammalian cells. *Radiat Res.* 1991;128:282–292.
49. Macklis RM, Lin JY, Beresford B, Atcher RW, Hines JJ, Humm JL. Cellular kinetics, dosimetry, and radiobiology of alpha-particle radioimmunotherapy: induction of apoptosis. *Radiat Res.* 1992;130:220–226.
50. Charlton DE, Nikjoo H, Humm JL. Calculation of initial yields of single-strand and double-strand breaks in cell-nuclei from electrons, protons and alpha-particles. *Int J Radiat Biol.* 1989;56:1–19.

51. Charlton DE, Turner MS. Use of chord lengths through the nucleus to simulate the survival of mammalian cells exposed to high LET alpha-radiation. *Int J Radiat Biol.* 1996;69:213–217.
52. Crawford-Brown DJ, Hofmann W. A generalized state-vector model for radiation-induced cellular transformation. *Int J Radiat Biol.* 1990;57:407–423.
53. Crawford-Brown DJ, Hofmann W. Correlated hit probability and cell transformation in an effect-specific track length model applied to in vitro alpha irradiation. *Radiat Environ Biophys.* 2001;40:317–323.
54. Holthusen H. Articles on the biology of radiation effects: analysis on nematode eggs. *Pflugers Arch Gesamte Physiol Menschen Tiere.* 1921;187:1–24.
55. Thomlinson RH, Gray LH. The histological structure of some human lung cancers and the possible implications for radiotherapy. *Br J Cancer.* 1955;9:539–549.
56. Unruh A, Ressel A, Mohamed HG, et al. The hypoxia-inducible factor-1 alpha is a negative factor for tumor therapy. *Oncogene.* 2003;22:3213–3220.
57. Ewing D, Powers EL. Oxygen-dependent sensitization of irradiated cells. In: Meyn RE, Withers HR, eds. *Radiation Biology in Cancer Research.* New York, NY: Raven Press; 1979:143–168.
58. Hall EJ. *Radiobiology for the Radiologist.* Philadelphia, PA: JB Lippincott Co.; 1994:118.
59. Machinami R, Ishikawa Y, Boecker BB. The international workshop on health effects of Thorotrast, radium, radon and other alpha-emitters, 1999 [preface]. *Radiat Res.* 1999;152(suppl):S1–S2.
60. International Commission on Radiological Protection. *Relative Biological Effectiveness (RBE), Quality Factor (Q), and Radiation Weighting Factor (w_R).* Philadelphia, PA: Elsevier; 2004. ICRP publication 92.
61. Harrison JD, Muirhead CR. Quantitative comparisons of cancer induction in humans by internally deposited radionuclides and external radiation. *Int J Radiat Biol.* 2003;79:1–13.
62. Brown I, Mitchell JS. The development of a [At-211]-astatinated endoradiotherapeutic drug: Part IV—late radiation effects. *Int J Radiat Oncol Biol Phys.* 1998;40:1177–1183.
63. Durbin PW, Asling CW, Johnston ME, et al. The induction of tumors in the rat by astatine-211. *Radiat Res.* 1958;9:378–397.
64. Yokoro K, Kunii A, Furth J, Durbin PW. Tumor induction with astatine-211 in rats: characterization of pituitary tumors. *Cancer Res.* 1964;24:683–688.
65. Hall EJ, Brenner DJ. The radiobiology of radiosurgery: rationale for different treatment regimes for AVMs and malignancies. *Int J Radiat Oncol Biol Phys.* 1993;25:381–385.
66. Dale RG, Jones B. The assessment of RBE effects using the concept of biologically effective dose. *Int J Radiat Oncol Biol Phys.* 1999;43:639–645.
67. Takata M, Sasaki MS, Sonoda E, et al. Homologous recombination and non-homologous end-joining pathways of DNA double-strand break repair have overlapping roles in the maintenance of chromosomal integrity in vertebrate cells. *EMBO J.* 1998;17:5497–5508.
68. Oliveira NG, Castro M, Rodrigues AS, et al. Wortmannin enhances the induction of micronuclei by low and high LET radiation [erratum]. *Mutagenesis.* 2003;18:217.
69. Oliveira NG, Castro M, Rodrigues AS, et al. Wortmannin enhances the induction of micronuclei by low and high LET radiation. *Mutagenesis.* 2003;18:37–44.
70. Harapanhalli RS, Narra VR, Yaghmai V, et al. Vitamins as radioprotectors in vivo. II. Protection by vitamin A and soybean oil against radiation-damage caused by internal radionuclides. *Radiat Res.* 1994;139:115–122.
71. Narra VR, Harapanhalli RS, Goddu SM, Howell RW, Rao DV. Radioprotection against biological effects of internal radionuclides in vivo by S-(2-aminoethyl)isothiouronium bromide hydrobromide (AET). *J Nucl Med.* 1995;36:259–266.
72. Rao DV, Howell RW, Narra VR, Govelitz GF, Sastry KSR. In-vivo radiotoxicity of DNA-incorporated ^{125}I compared with that of densely ionizing alpha-particles. *Lancet.* 1989;2:650–653.
73. Rao DV, Narra VR, Howell RW, Lanka VK, Sastry KSR. Induction of sperm head abnormalities by incorporated radionuclides: dependence on subcellular distribution, type of radiation, dose rate, and presence of radioprotectors. *Radiat Res.* 1991;125:89–97.
74. Goddu SM, Narra VR, Harapanhalli RS, Howell RW, Rao DV. Radioprotection by DMSO against the biological effects of incorporated radionuclides in vivo: comparison with other radioprotectors and evidence for indirect action of Auger electrons. *Acta Oncol.* 1996;35:901–907.
75. Narra VR, Harapanhalli R, Howell RW, Sastry KSR, Rao DV. Vitamins as radioprotectors in vivo. I. Protection by vitamin C against internal radionuclides in mouse testes: implications to the mechanism of damage caused by the Auger effect. *Radiat Res.* 1994;137:394–399.
76. Wright HA, Magee JL, Hamm RN, Chatterjee A, Turner JE, Klots CE. Calculations of physical and chemical-reactions produced in irradiated water containing DNA. *Radiat Prot Dosimetry.* 1985;13:133–136.
77. International Commission on Radiological Protection. *RBE for Deterministic Effects.* Philadelphia, PA: Elsevier; 1990. ICRP publication 58.
78. Schwartz JL, Rotmensch J, Atcher RW, et al. Interlaboratory comparison of different alpha-particle and radon sources: cell survival and relative biological effectiveness. *Health Phys.* 1992;62:458–461.
79. Jostes RF, Hui TE, James AC, et al. In vitro exposure of mammalian cells to radon: dosimetric considerations. *Radiat Res.* 1991;127:211–219.
80. Charlton DE, Utteridge TD, Allen BJ. Theoretical treatment of human haemopoietic stem cell survival following irradiation by alpha particles. *Int J Radiat Biol.* 1998;74:111–118.
81. Howell RW, Goddu SM, Narra VR, Fisher DR, Schenter RE, Rao DV. Radiotoxicity of gadolinium-148 and radium-223 in mouse testes: relative biological effectiveness of alpha-particle emitters in vivo. *Radiat Res.* 1997;147:342–348.
82. Howell RW, Goddu SM, Rao DV. Design and performance characteristics of an experimental cesium-137 irradiator to simulate internal radionuclide dose rate patterns. *J Nucl Med.* 1997;38:727–731.
83. Goddu SM, Bishayee A, Bouchet LG, Bolch WE, Rao DV, Howell RW. Marrow toxicity of ^{33}P-versus ^{32}P-orthophosphate: implications for therapy of bone pain and bone metastases. *J Nucl Med.* 2000;41:941–951.
84. Feinendegen LE, McClure JJ. Meeting report: Alpha-emitters for medical therapy—Workshop of the United States Department of Energy, Denver, Colorado, May 30–31, 1996. *Radiat Res.* 1997;148:195–201.
85. 1990 recommendations of the International Commission on Radiological Protection. *Ann ICRP.* 1991;21:1–201.
86. Radiation protection in medicine: ICRP publication 105. *Ann ICRP.* 2007;37:1–63.
87. Neti PVSV, Howell RW. Biological response to nonuniform distributions of ^{210}Po in multicellular clusters. *Radiat Res.* 2007;168:332–340.
88. Goddu SM, Rao DV, Howell RW. Multicellular dosimetry for micrometastases: dependence of self-dose versus cross-dose to cell nuclei on type and energy of radiation and subcellular distribution of radionuclides. *J Nucl Med.* 1994;35:521–530.
89. Charlton DE. Radiation effects in spheroids of cells exposed to alpha emitters. *Int J Radiat Biol.* 2000;76:1555–1564.
90. Akabani G, Zalutsky MR. Microdosimetry of astatine-211 using histological images: application to bone marrow. *Radiat Res.* 1997;148:599–607.
91. Humm JL, Macklis RM, Bump K, Cobb LM, Chin LM. Internal dosimetry using data derived from autoradiographs. *J Nucl Med.* 1993;34:1811–1817.
92. Baxter LT, Jain RK. Transport of fluid and macromolecules in tumors. IV. A microscopic model of the perivascular distribution. *Microvasc Res.* 1991;41:252–272.
93. Jain RK, Baxter LT. Mechanisms of heterogeneous distribution of monoclonal antibodies and other macromolecules in tumors: significance of elevated interstitial pressure. *Cancer Res.* 1988;48:7022–7032.
94. Sgouros G. Plasmapheresis in radioimmunotherapy of micrometastases: a mathematical modeling and dosimetrical analysis. *J Nucl Med.* 1992;33:2167–2179.
95. Goddu SM, Howell RL, Bouchet LG, Bolch WE, Rao DV. *MIRD Cellular S Values.* Reston VA: Society of Nuclear Medicine; 1997.
96. Goddu SM, Howell RW, Rao DV. Cellular dosimetry: absorbed fractions for monoenergetic electron and alpha particle sources and S-values for radionuclides uniformly distributed in different cell compartments. *J Nucl Med.* 1994;35:303–316.
97. Polig E. Localized alpha-dosimetry. In: Eberg M, Howard A, eds. *Current Topics in Radiation Research.* Vol 13. Amsterdam, The Netherlands: Elsevier; 1978:189–327.
98. Rossi HH. Microdosimetric energy distribution in irradiated matter. In: Attx FH, Roesch WC, eds. *Radiation Dosimetry.* Vol 1. New York, NY: Academic Press; 1968.
99. Roesch WC. Microdosimetry of internal sources. *Radiat Res.* 1977;70:494–510.
100. Fisher DR. The microdosimetry of monoclonal antibodies labeled with alpha emitters. In: Schlafke-Stelson AT, Watson EE, eds. *Fourth International Radiopharmaceutical Dosimetry Symposium.* Oak Ridge, TN: Oak Ridge Associated Universities; 1986:26–36.
101. Stinchcomb TG, Roeske JC. Analysis of survival of C-18 cells after irradiation in suspension with chelated and ionic bismuth-212 using microdosimetry. *Radiat Res.* 1994;140:48–54.
102. Stinchcomb TG, Roeske JC. Analytic microdosimetry for radioimmunotherapeutic alpha emitters. *Med Phys.* 1992;19:1385–1393.
103. Kellerer AM. Analysis of patterns of energy deposition: a survey of theoretical relations in microdosimetry. In: Ebert HG, ed. *Proceedings of the Second*

Symposium on Microdosimetry. Brussels, Belgium: Commission of European Communities; 1970:107–134.
104. Olko P, Booz J. Energy deposition by protons and alpha-particles in spherical sites of nanometer to micrometer diameter. *Radiat Environ Biophys*. 1990;29:1–17.
105. Ziegler JF, Biersack JP, Littmark U. *The Stopping and Range of Ions in Matter*. New York, NY, Pergamon Press; 1985.
106. Ziegler JF. The stopping and range of ions in solids (*Stopping and Range of Ions in Matter*, Vol. 1). New York, NY: Pergamon; 1985.
107. Bichsel H. *Stopping Powers of Fast Charged Particles in Heavy Elements*. Springfield, VA: U.S. National Technical Information Service; 1992. NIST report IR-4550.
108. International Commission on Radiation Units and Measurements. *Stopping Powers and Ranges for Protons and Alpha Particles*. Bethesda, MD: ICRU; 1993. ICRU publication 49.
109. Kellerer AM, Chmelevsky D. Criteria for applicability of LET. *Radiat Res*. 1975;63:226–234.
110. Roeske JC, Stinchcomb TG. Dosimetric framework for therapeutic alpha-particle emitters. *J Nucl Med*. 1997;38:1923–1929.
111. Loevinger R, Budinger TF, Watson EE. *MIRD Primer for Absorbed Dose Calculations*. Revised ed. New York, NY: Society of Nuclear Medicine; 1991.
112. Stinchcomb TG, Roeske JC. Values of "S," <z1>, and <(z1)2> for dosimetry using alpha-particle emitters. *Med Phys*. 1999;26:1960–1971.
113. Fisher DR. Specific energy distributions for alpha emitters in the dog lung. *Ann Occup Hyg*. 1988;32(suppl 1):1095–1104.
114. Humm JL. A microdosimetric model of astatine-211 labeled antibodies for radioimmunotherapy. *Int J Radiat Oncol Biol Phys*. 1987;13:1767–1773.
115. Stinchcomb TG, Roeske JC. Survival of alpha particle irradiated cells as a function of the shape and size of the sensitive volume (nucleus). *Radiat Prot Dosimetry*. 1995;62:157–164.
116. Aubineau-Laniece I, Pihet P, Winkler R, Hofmann W, Charlton DE. Monte Carlo code for microdosimetry of inhaled alpha emitters. *Radiat Prot Dosimetry*. 2002;99:463–467.
117. Fakir H, Hofmann W, Aubineau-Laniece I. Modelling the effect of non-uniform radon progeny activities on transformation frequencies in human bronchial airways. *Radiat Prot Dosimetry*. 2006;121:221–235.
118. Fakir H, Hofmann W, Aubineau-Laniece I. Microdosimetry of radon progeny alpha particles in bronchial airway bifurcations. *Radiat Prot Dosimetry*. 2005;117:382–394.
119. Fakir H, Hofmann W, Caswell RS, Aubineau-Laniece I. Microdosimetry of inhomogeneous radon progeny distributions in bronchial airways. *Radiat Prot Dosimetry*. 2005;113:129–139.
120. Palm S, Humm JL, Rundqvist R, Jacobsson L. Microdosimetry of astatine-211 single-cell irradiation: role of daughter polonium-211 diffusion. *Med Phys*. 2004;31:218–225.
121. Iyer R, Lehnert BE. Alpha-particle-induced increases in the radioresistance of normal human bystander cells. *Radiat Res*. 2002;157:3–7.
122. Azzam EI, de Toledo SM, Gooding T, Little JB. Intercellular communication is involved in the bystander regulation of gene expression in human cells exposed to very low fluences of alpha particles. *Radiat Res*. 1998;150:497–504.
123. Utteridge TD, Charlton DE, Allen BJ. Monte Carlo modeling of the effects of injected short-, medium- and longer-range alpha-particle emitters on human marrow at various ages. *Radiat Res*. 2001;156:413–418.
124. Hamacher KA, Sgouros G. A schema for estimating absorbed dose to organs following the administration of radionuclides with multiple unstable daughters: a matrix approach. *Med Phys*. 1999;26:2526–2528.
125. Fisher DR, Sgouros G. Dosimetry of radium-223 and progeny. In: Stelson AT, Stabin MG, Sparks RB, eds. *Proceedings of the Sixth International Radiopharmaceutical Dosimetry Symposium*. Gatlinburg, TN: U.S. Department of Energy and Oak Ridge Associated Universities; 1999:375–391.
126. Sgouros G. Long-lived alpha emitters in radioimmunotherapy: the mischievous progeny. *Cancer Biother Radiopharm*. 2000;15:219–221.
127. Miederer M, McDevitt MR, Sgouros G, Kramer K, Cheung NK, Scheinberg DA. Pharmacokinetics, dosimetry, and toxicity of the targetable atomic generator, ^{225}Ac-HuM195, in nonhuman primates. *J Nucl Med*. 2004;45:129–137.
128. Hamacher KA, Den RB, Den EI, Sgouros G. Cellular dose conversion factors for alpha-particle-emitting radionuclides of interest in radionuclide therapy. *J Nucl Med*. 2001;42:1216–1221.
129. Muller WA. Studies on short-lived internal alpha-emitters in mice and rats. II. ^{227}Th. *Int J Radiat Biol Relat Stud Phys Chem Med*. 1971;20:233–243.
130. Dahle J, Borrebaek J, Melhus KB, et al. Initial evaluation of ^{227}Th-p-benzyl-DOTA-rituximab for low-dose rate alpha-particle radioimmunotherapy. *Nucl Med Biol*. 2006;33:271–279.
131. Dahle J, Borrebaek J, Jonasdottir TJ, et al. Targeted cancer therapy with a novel low dose rate alpha-emitting radioimmunoconjugate. *Blood*. 2007;110:2049–2056.
132. Siegel JA, Thomas SR, Stubbs JB, et al. MIRD pamphlet no. 16: techniques for quantitative radiopharmaceutical biodistribution data acquisition and analysis for use in human radiation dose estimates. *J Nucl Med*. 1999;40(suppl):37S–61S.
133. Sgouros G. Treatment planning for internal emitter therapy: methods, applications and clinical implications. In: Schafke-Stelson AT, Watson EE, eds. *Proceedings of the 6th International Radiopharmaceutical Dosimetry Symposium, May 7–10, 1996, Gatlinburg, TN*. Oak Ridge, TN: Oak Ridge Associated Universities; 1996:13–24.
134. Sgouros G. Radioimmunotherapy of micrometastases. In: Riva P, ed. *Cancer Radioimmunotherapy: Present and Future*. Newark, NJ: Harwood Academic Publishers; 1998:191–207.
135. Kirschner AS, Ice RD, Beierwaltes WH. Radiation dosimetry of ^{131}I-19-iodocholesterol: the pitfalls of using tissue concentration data [reply]. *J Nucl Med*. 1975;16:248–249.
136. Sgouros G, Ballangrud AM, Jurcic JG, et al. Pharmacokinetics and dosimetry of an alpha-particle emitter labeled antibody: ^{213}Bi-HuM195 (anti-CD33) in patients with leukemia. *J Nucl Med*. 1999;40:1935–1946.
137. Patton PW, Rajon DA, Shah AP, Jokisch DW, Inglis BA, Bolch WE. Site-specific variability in trabecular bone dosimetry: considerations of energy loss to cortical bone. *Med Phys*. 2002;29:6–14.
138. Bolch WE, Patton PW, Rajon DA, Shah AP, Jokisch DW, Inglis BA. Considerations of marrow cellularity in 3-dimensional dosimetric models of the trabecular skeleton. *J Nucl Med*. 2002;43:97–108.
139. Shah AP, Patton PW, Rajon DA, Bolch WE. Adipocyte spatial distributions in bone marrow: implications for skeletal dosimetry models. *J Nucl Med*. 2003;44:774–783.
140. Shah AP, Rajon DA, Patton PW, Jokisch DW, Bolch WE. Accounting for beta-particle energy loss to cortical bone via paired-image radiation transport (PIRT). *Med Phys*. 2005;32:1354–1366.
141. Watchman CJ, Jokisch DW, Patton PW, Rajon DA, Sgouros G, Bolch WE. Absorbed fractions for alpha-particles in tissues of trabecular bone: considerations of marrow cellularity within the ICRP reference male. *J Nucl Med*. 2005;46:1171–1185.
142. Bolch WE, Eckerman KF, Sgouros G, Thomas SR. MIRD pamphlet no. 21: a generalized schema for radiopharmaceutical dosimetry—standardization of nomenclature. *J Nucl Med*. 2009;50:477–484.
143. Eckerman KF, Endo A. *MIRD: Radionuclide Data and Decay Schemes*. Reston, VA: Society of Nuclear Medicine; 2007.
144. Snyder WS, Fisher HL, Ford MR, Warner GG. Estimates of absorbed fractions for monoenergetic photon sources uniformly distributed in various organs of a heterogeneous phantom. *J Nucl Med*. 1969;10(suppl):7–52.
145. Bouchet LG, Jokisch DW, Bolch WE. A three-dimensional transport model for determining absorbed fractions of energy for electrons within trabecular bone. *J Nucl Med*. 1999;40:1947–1966.
146. Snyder WS, Ford MR, Warner GG. *MIRD Pamphlet No. 5, Revised: Estimates of Specific Absorbed Fractions for Photon Sources Uniformly Distributed in Various Organs of a Heterogeneous Phantom*. New York, NY: Society of Nuclear Medicine; 1978.
147. Sgouros G, Howell RW, Bolch WE, Fisher DR. MIRD commentary: proposed name for a dosimetry unit applicable to deterministic biological effects—the Barendsen (Bd). *J Nucl Med*. 2009;50:485–487.
148. Kneifel S, Cordier D, Good S, et al. Local targeting of malignant gliomas by the diffusible peptidic vector 1,4,7,10-tetraazacyclododecane-1-glutaric acid-4,7,10-triacetic acid-substance P. *Clin Cancer Res*. 2006;12:3843–3850.
149. Heeger S, Moldenhauer G, Egerer G, et al. Alpha-radioimmunotherapy of B-lineage non-Hodgkin's lymphoma using ^{213}Bi-labelled anti-CD19-and anti-CD20-CHX-A"-DTPA conjugates [abstract]. *Abstracts of Papers of the American Chemical Society*. 2003;225:U261.
150. Allen BJ, Raja C, Rizvi S, et al. Intralesional targeted alpha therapy for metastatic melanoma. *Cancer Biol Ther*. 2005;4:1318–1324.
151. Bruland OS, Nilsson S, Fisher DR, Larsen RH. High-linear energy transfer irradiation targeted to skeletal metastases by the alpha-emitter Ra-223: adjuvant or alternative to conventional modalities? *Clin Cancer Res*. 2006;12(suppl):6250S–6257S.
152. Nilsson S, Franzen L, Parker C, et al. Bone-targeted radium-223 in symptomatic, hormone-refractory prostate cancer: a randomised, multicentre, placebo-controlled phase II study. *Lancet Oncol*. 2007;8:587–594.
153. Goodhead DT. Talk 23, Alpha Emitters, from Session 6, Effects from Specific Sources of Internal Radiation. Presented at: CERRIE Workshop; July 21–23, 2003; Oxford, U.K.
154. Powsner RA, Powsner ER. *Essentials of Nuclear Medicine Physics*. Malden MA: Blackwell Science, Inc.; 1998.
155. Cole A, ed. *Theoretical and Experimental Biophysics*. New York, NY: Marcel Dekker, Inc.; 1967.

JNM The Journal of NUCLEAR MEDICINE

MIRD Pamphlet No. 22 (Abridged): Radiobiology and Dosimetry of α-Particle Emitters for Targeted Radionuclide Therapy

George Sgouros, John C. Roeske, Michael R. McDevitt, Stig Palm, Barry J. Allen, Darrell R. Fisher, A. Bertrand Brill, Hong Song, Roger W. Howell and Gamal Akabani

J Nucl Med. 2010;51:311-328.
Published online: January 15, 2010.
Doi: 10.2967/jnumed.108.058651

The Journal of Nuclear Medicine is published monthly.
SNMMI | Society of Nuclear Medicine and Molecular Imaging
1850 Samuel Morse Drive, Reston, VA 20190.
(Print ISSN: 0161-5505, Online ISSN: 2159-662X)

SNMMI SOCIETY OF NUCLEAR MEDICINE AND MOLECULAR IMAGING

参考文献[7]

CANCER BIOTHERAPY AND RADIOPHARMACEUTICALS
Volume 28, Number 1, 2013

DOI: 10.1089/cbr.2012.1292

Review

Production of [^{211}At]-Astatinated Radiopharmaceuticals and Applications in Targeted α-Particle Therapy

François Guérard,[1] Jean-François Gestin,[2] and Martin W. Brechbiel[1]

Abstract

^{211}At is a promising radionuclide for α-particle therapy of cancers. Its physical characteristics make this radionuclide particularly interesting to consider when bound to cancer-targeting biomolecules for the treatment of microscopic tumors. ^{211}At is produced by cyclotron irradiation of ^{209}Bi with α-particles accelerated at ~28 MeV and can be obtained in high radionuclidic purity after isolation from the target. Its chemistry resembles iodine, but there is also a tendency to behave as a metalloid. However, the chemical behavior of astatine has not yet been clearly established, primarily due to the lack of any stable isotopes of this element, which precludes the use of conventional analytical techniques for its characterization. There are also only a limited number of research centers that have been able to produce this element in sufficient amounts to carry out extensive investigations. Despite these difficulties, chemical reactions typically used with iodine can be performed, and a number of biomolecules of interest have been labeled with ^{211}At. However, most of these compounds exhibit unacceptable instability *in vivo* due to the weakness of the astatine–biomolecule bond. Nonetheless, several compounds have shown high potential for the treatment of cancers *in vitro* and in several animal models, thus providing a promising basis that has allowed initiation of the first two clinical studies.

Key words: α-immunotherapy, Astatine-211, radiolabeling

Introduction

While β^--emitters have proven their usefulness in the therapy of localized macroscopic cancerous tumors, limited successes have been obtained in the case of microscopic and disseminated cancers. The disappointing results are explained by the relatively long path length of the β^--particles in tissue (several millimeters), leading to the loss of most of the deposited energy in healthy tissues when the tumor being treated is too small. In contrast, α-particle emitters are promising radionuclides for the treatment of such small tumors. When such a radionuclide is conjugated to a suitable targeting agent, the short path length of the α-particles (~25–100 μm), in association with their high energy (~4–8.5 MeV), makes them highly efficient at eradicating small clusters or isolated cancerous cells with a reduced dose deposited to the surrounding healthy tissues. Such radiopharmaceuticals are of high interest for the treatment of disseminated micrometastasis, diseases consisting of monocellular cancer cells such as lymphoma and leukemia, or in the case of residual disease after surgical debulking. Among the hundred α-particle emitters known, a limited number of radionuclides exhibit characteristics that have been considered as potentially suitable for therapeutic applications (^{225}Ac, ^{211}At, ^{212}Bi, ^{213}Bi, ^{223}Ra, ^{149}Tb, ^{227}Th, and ^{212}Pb as an *in vivo* generator of ^{212}Bi, see Table 1). All have been the object of increasing attention in recent years, and several have reached different stages of clinical evaluation while production and availability of the radionuclides and their labeling chemistry issues are being overcome with varying levels of success.[1]

Among these radionuclides, ^{211}At exhibits particularly favorable characteristics, with a 7.2-hour half-life suitable to

[1]Radioimmune and Inorganic Chemistry Section, Radiation Oncology Branch, NCI, NIH, Bethesda, Maryland.
[2]Centre de Recherche en Cancérologie Nantes-Angers (CRCNA), Université de Nantes, Inserm, UMR 892, Institut de Recherche Thérapeutique de l'Université de Nantes, Nantes Cedex 1, France.

Address correspondence to: Martin W. Brechbiel; Radioimmune and Inorganic Chemistry Section, Radiation Oncology Branch, NCI, NIH; 10 Center Drive, MSC-1002, Rm B3B69, Bethesda, MD 20892-1002
E-mail: **martinwb@mail.nih.gov**

Table 1. Characteristics of α-Emitting Radionuclides of Potential Interest for the Therapy of Cancers

Nuclide	*Half-life*	*Decays*	*Energy α (MeV)*	*Production*	*Clinical trial status*
^{225}Ac	10 days	4 α, 2 β^-	5.1–8.4	^{233}U decay/cyclotron	First phase I ongoing
^{211}At	7.2 hours	1 α, 1 EC	5.9 or 7.4	Cyclotron	Two phase I published
^{212}Bi	61 minutes	1 α, 1 β^-	6.1/7.8	^{228}Th decay/^{224}Ra generator	Preclinical
^{213}Bi	46 minutes	1 α, 2 β^-	6.0/8.4	^{225}Ac generator	Phase I/II
^{223}Ra	11.4 days	4 α, 2 β^-	5.7–7.5	^{227}Ac generator	Phase I/II/III
^{149}Tb	4.1 hours	1 α, EC	4.0	Accelerator	Preclinical
^{227}Th	18.7 days	5 α, 2 β^-	5.7–7.5	^{227}Ac generator	Preclinical
^{212}Pb/^{212}Bi[a]	10.6 hours	1 α, 2 β^-	6.1/7.8	^{224}Ra generator	First phase I ongoing

[a]Although ^{212}Pb is not an α-particle emitter, it is included in this table for its considerations in several studies as an *in vivo* generator of the α-particle emitter ^{212}Bi. See Yong and Brechbiel[2] for a definition of the concept.

the kinetics of full antibodies or other biomolecules that require several hours to reach an optimal tumor-to-blood dose ratio. Furthermore, with 100% of its decay leading to the production of an α-particle, high efficiency of the treatments and limited toxicity are expected at relatively low doses. However, the introduction of ^{211}At-based radiopharmaceuticals into clinics has been slowed by difficulties related to the production and availability of the radionuclide, the limited knowledge of the chemistry of elemental astatine, the lack of stability of the astatine–biomolecule bond, and concerns about the potential toxicity of α-radiation on humans.

In this review, the characteristics of ^{211}At and its methods of production and purification for radiolabeling purposes are presented. The different aspects of its chemistry as well as the strategies for the radiolabeling of biomolecules are also described. Finally, the latest advances in the use of ^{211}At-based radiopharmaceuticals in radiotherapy of cancers from the *in vitro* studies to the very first clinical trials that have been published recently are presented.

^{211}At: Characteristics and Production

The 85th element in the periodic table classification was first produced in 1940 when Corson irradiated ^{209}Bi with a beam of α-particles accelerated to 32 MeV.[3] Expected by Mendeleïev to be below the element iodine (and named ekaiodine at that time), it is the only halogen without a stable isotope, which is why its discoverers named it astatine, from the Greek word αστατος (astatos = unstable).

Astatine exists on the Earth in very small quantities (estimated to be a few milligrams in the whole Earth's crust) by some decay branches of ^{235}U, ^{238}U, and ^{232}Th, which actually makes it the rarest natural element.[4] There are 32 astatine isotopes known: ^{191}At and all the rest from ^{193}At to ^{223}At. Their half-lives range from 125 nanoseconds for ^{213}At up to 8.1 hours for ^{210}At, and most of them are α-particle emitters. Among these isotopes, only ^{211}At exhibits physical characteristics that are reasonably adapted for targeted radiotherapy.

The most relevant characteristics of the radionuclide are summarized below, and the reader is referred to the Gmelin Handbook of Inorganic Chemistry on Astatine for an exhaustive review of the topic.[5]

Physical properties

The disintegration of ^{211}At follows a branched decay scheme with a 7.21 hours half-life (Fig. 1). One branch leads to ^{207}Bi by emission of an α-particle. ^{207}Bi, with a 33.9 year half-life, decays to ^{207}Pb via electron capture. The other decay branch occurs via electron capture and leads to the 516 milliseconds half-life radionuclide ^{211}Po, which in turn decays to stable ^{207}Pb by emission of an α-particle. The result of these decay pathways is 100% α-particle emission during the decay of ^{211}At (5.87 and 7.45 MeV in 42% and 58% of the decays, respectively). Concerns have been raised regarding the fate of the ^{211}Po decay during targeted radiotherapy. Palm et al. investigated the influence of the diffusion of ^{211}Po on the dose absorbed by isolated cells in suspension.[6] They estimated that the diffusion distance from the initial ^{211}At nucleus bound to the cell reduces the absorbed dose by a factor of 2 in this model. Part of the deposited dose may indeed be lost from the target in case of dispersed cells, but this phenomenon might be reduced in cell cluster environments, where the dose could be deposited toward a neighboring malignant cell. Also, as noted by the authors of the study, cellular localization may reduce the diffusion of ^{211}Po depending upon the viscosity of the tissue. Another concern is the fate of ^{207}Bi with its long half-life (32.9 years), and the potential issues due to its uptake in the bone, liver, and kidneys. However, 347 MBq of ^{211}At, which is the highest dose that has been administered to a human, leads to only 310 kBq of ^{207}Bi, making its potential toxicity negligible.

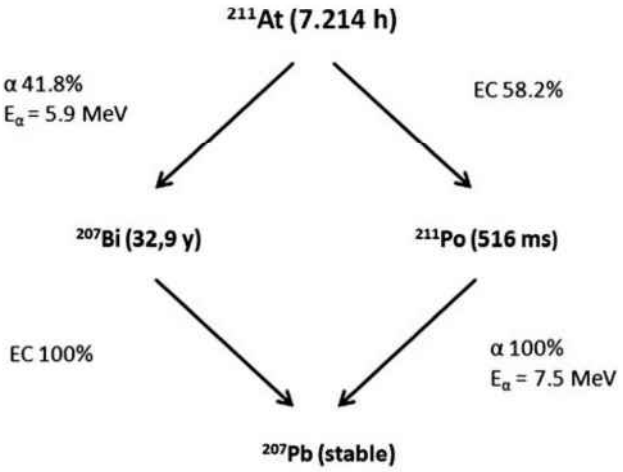

FIG. 1. Simplified decay scheme of ^{211}At.

Also, another interesting characteristic is the emission of X-rays during the decay to ^{211}Po. With energies between 77 and 92 keV, these X-rays can be easily monitored by γ-detectors classically used in laboratory or clinical centers. This combination of emission and instrumentation makes detection relatively easy and useful for *in vivo* monitoring by SPECT imaging.[7]

Production

^{211}At is produced by irradiation of natural bismuth (^{209}Bi) following the nuclear reaction: ^{209}Bi(α, 2n)^{211}At. Other production methods have been investigated, such as the production of a ^{211}Rn/^{211}At generator by irradiation of ^{209}Bi with ^{7}Li,[8] or by fusion of ^{9}Li with ^{208}Pb.[9] However, these alternative methods remain anecdotal with respect to the production of medical research quantities of the radionuclide.

^{211}At production is possible for α-beam energies ranging from 21 to more than 40 MeV, with a maximum cross-section observed for 31 MeV (Fig. 2). However, at this level of energy, ^{210}At is also produced. This 8.1-hour half-life isotope exhibits characteristics that are not compatible with pharmaceutical applications because of its decay into the long half-life ^{210}Po (138.2 days), which is highly toxic, especially to the bone marrow.[10] Production of ^{210}Po is also observed from 26.7 MeV beam energies. Nonetheless, the presence of this isotope after irradiation is generally irrelevant due to an efficient isolation of ^{211}At from the target and impurities during the purification process. For these reasons, the beam energy is generally controlled to 28–29 MeV to limit formation of ^{210}At while maintaining acceptable yields of ^{211}At. However, only a limited number of cyclotrons in the world are able to generate α-beam energies beyond 25 MeV, which strongly limits the availability of this radionuclide.[11]

Another limitation to consider is the low melting point of the irradiated material (Bismuth mp = 272°C) and its low thermal conductivity (k = 7.9 W m^{-1} K^{-1}). Together, with the relatively high volatility of astatine (337°C), this potentially leads to vaporization of the produced activity due to overheating of the target during the irradiation. Solutions have been developed to limit this overheating issue, such as cooling systems using cold gas and water during irradiation, or the use of an irradiation angle that spreads the beam over a larger impact surface on the bismuth. Furthermore, the bismuth is deposited as a thin layer on a material with a better thermal conductivity to enhance cooling. Aluminum has frequently been used as backing material (k = 250 W m^{-1} K^{-1}), although some reports make reference to the use of copper (k = 390 W m^{-1} K^{-1}).

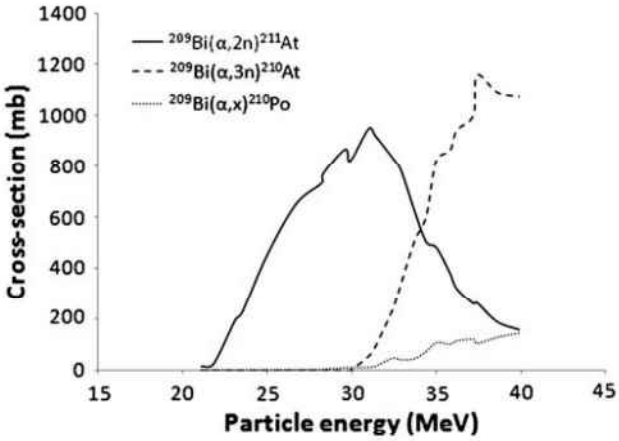

FIG. 2. Cross-section of the irradiation of ^{209}Bi as a function of the alpha particles energy. Plotted from the experimental data from Hermanne et al.[12]

Purification

After irradiation, the target contains the initial ^{209}Bi, traces of ^{210}Po, and the desired ^{211}At activity, which must be obtained in solution with the highest purity. Two methods are described to harvest ^{211}At: dry distillation that is probably the most widely used or liquid extraction that requires dissolution of the target in an acidic solution.

Dry distillation. In this method, the target is placed in a furnace and heated above the boiling point of astatine. The boiling points of bismuth and polonium being 1564°C and 962°C, respectively, the furnace temperature is generally set to 650°C–900°C. During the distillation, while the bismuth and the polonium melt and stay on the support, the volatile astatine is carried away by a stream of gas (generally nitrogen or argon) and trapped at the outlet. The astatine activity can be obtained by bubbling that stream of gas directly into the solvent of choice, or it can be captured in capillary tubing cooled in dry ice/ethanol placed at the outlet.[13] In the latter case, the activity is subsequently dissolved in the solvent of choice (Fig. 3). With this kind of system, the astatine activity is collected in the trap in 20–30 minutes with recovery yields up to 80%.

Wet extraction. This alternative procedure consists of dissolution of the target in concentrated nitric acid. After evaporation of the nitric acid, the residue containing the bismuth and the astatine is dissolved in dilute nitric acid and extracted with di-isopropyl ether, which is the most efficient and practical solvent for this purpose.[14,15] With this method, the astatine activity is obtained in high yields (~90%) in ~1 hour with high radionuclidic purity. The advantage of this

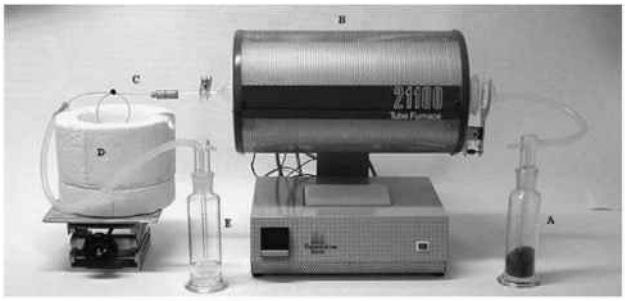

FIG. 3. Example of a typical furnace used for the distillation of ^{211}At. (A) Gas inlet with desiccant. (B) Furnace heated to 650°C–900°C. (C) Capillary trap cooled in (D) a dry ice/ethanol bath. It can be replaced by a cooled bubbler containing the solvent of interest. (E) Gas-wash bottle containing a reducing agent such as $Na_2S_2O_5$ to trap traces of astatine that would escape from the capillary. Reprinted by permission from Lindegren et al[13].

technique over dry distillation is that it makes use of simple and cheap materials. Moreover, harvesting yields are obtained with an excellent reproducibility. However, the choice of extraction solvent is reduced to di-isopropyl ether or analogous solvents that can limit radiochemistry work. Furthermore, some nitric acid is extracted into the organic phase in concentrations that are not negligible, and that can cause side reactions during the radiolabeling chemistry. Nonetheless, it has been demonstrated that biomolecules can be radiolabeled efficiently using standard procedures with ^{211}At recovered with this method.[16]

Chemical Properties of Astatine

Despite more than 70 years of research on astatine, its chemistry is still not clearly established. The main reason is the fact that no stable isotope exists, the most stable isotope being ^{210}At with a half-life of only 8.1 hours. The highest reported activity produced is 6.59 GBq (which corresponds to 0.087 μg of ^{211}At).[17] These amounts preclude the use of standard analysis techniques such as nuclear magnetic resonance, mass spectrometry (although some experiments have been reported[18]), UV, IR, or X-rays. Furthermore, with the astatine being obtained in highly dilute solutions, traces of unavoidable contaminants in solution can become competitive species and cause side reactions. Another impediment to the understanding of astatine chemistry is the lack of cyclotrons to produce this element leading to a reduced number of research laboratories able to run experiments.[11] Despite these obstacles, a relatively clear idea of some of the chemical properties of astatine has been established by analogy with its closest element in the periodic table of the elements, iodine. However, in its positive oxidation states, astatine exhibits many properties specific to metal ions. While almost identical to iodine in the At(−I) state, it is, in some respects, also comparable to silver in the At(+I) state, and close to polonium in its higher oxidation states.

In this section, the inorganic and organic chemistry of astatine is covered. Radiolabeling approaches for biomolecules of interest are also discussed as well as the issue of the limited *in vivo* stability of some ^{211}At-radiolabeled compounds.

Inorganic chemistry of astatine

Six oxidation states have been identified or hypothesized with varying degrees of certainty: −I, 0, +I, +III, +V, and +VII. These forms of astatine were determined at low concentration with chemistry techniques that can be used at a tracer level such as co-precipitation, liquid extraction, or electromigration experiments, with the knowledge of iodine chemistry as a guide. Most of the descriptions of the oxidation states presented below rely on works by Johnson et al.,[19] Appelman,[20] Visser and Diemer,[21,22] and Dreyer et al.[23–25] Also, more exhaustive information can be found in the DOE-Sponsored Nuclear Science Series monogram by Ruth et al.[26]

At(−I). The (−I) oxidation state is probably the most clearly established form of astatine with a strong similarity with iodide. It is obtained in the presence of reducing agents such as SO_3^{2-}, Zn^0, or cysteine, which form the astatide species (At^-). It is characterized by electromigration at the anode or by co-precipitation with AgI, TlI, or PbI_2, and is stable over a wide pH range. The astatide anion exhibits soft base characteristics, similar to iodide. It forms stable complexes with soft cations such as Hg^{2+}, Rh^{3+}, or Ir^{3+}. Pruszyński et al.[27] investigated the complexation of astatide in the presence of mercury nitrate in aqueous solution. Interestingly, the complex formed, assumed to be Hg(OH)At, exhibited a higher stability than the iodinated analog.[27] Similarly, complexes have been prepared with rhodium (III) and iridium (III), and chelated in a macrocyclic agent bearing soft donors sulfur atoms (Fig. 4).[28] These compounds could lead to an interesting approach for the radiolabeling of biomolecules if they exhibit acceptable *in vivo* stability.

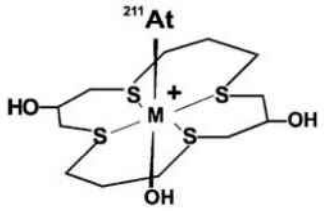

FIG. 4. ^{211}At-M(16-S4-diol) complex, with M = Rh(III) or Ir(III).

At(0). This oxidation state of astatine, also denoted At^0, remains unresolved, mainly because of its highly irreproducible behavior. It is hypothesized that astatine is obtained as At_2 in the gas phase (such as during the distillation process), but in solution, At_2 or the radical $At^\bullet$ is highly unlikely at this level of dilution. Recombination with impurities or other species of the solvent is supposed to occur very rapidly. At^0 has often been referred to as the species that does not exhibit mobility in an electric field. It is supposed to be in the AtX form (with X = HSO_4, NO_3, OAc, etc.) and extracted from an aqueous medium by organic solvents as $AtXL_n$ (n depending on the solvent L used). Also, At^0 was observed to co-precipitate with elemental Ag or Tl.

At(+I). This oxidation state can be obtained under moderately oxidizing conditions (i.e., dilute $HClO_4$ or $H_2Cr_2O_7$) in the At^+ form in acidic medium, or AtO^- in alkaline medium. In the cationic form, it exhibits a relatively weak electrophilic behavior similarly to I^+. Characteristics similar to metals are also observed, with a cationic form stable toward hydrolysis in acidic medium, unlike the other halogens. Denoted $At(\theta)^+$, this cationic form of astatine exhibits the characteristics of a soft acid with an affinity for soft-base ligands (I^-, CN^-, and SCN^-) similar to Ag^+, as demonstrated by the stability of the interhalogen complexes according to the following sequence[29]:

$$AtCl_2^- < AtBr_2^- < AtI_2^-$$

Several pseudohalogen ligands such as SCN^-, N_3^- or $C(CN_3)^-$, with lower stability than AtI_2^-, have also been investigated.[30] Better results were obtained with selenoureas and thioureas with complexes assumed to be in the $At(L_2)$ form (Fig. 5).[31,32] Soft-donor ligands containing phosphorus have also been considered. However, their use seems unlikely for medical applications because of the reductive properties of these ligands at pH > 2, leading to the reduction of At^+ to At^- (Fig. 5).[33]

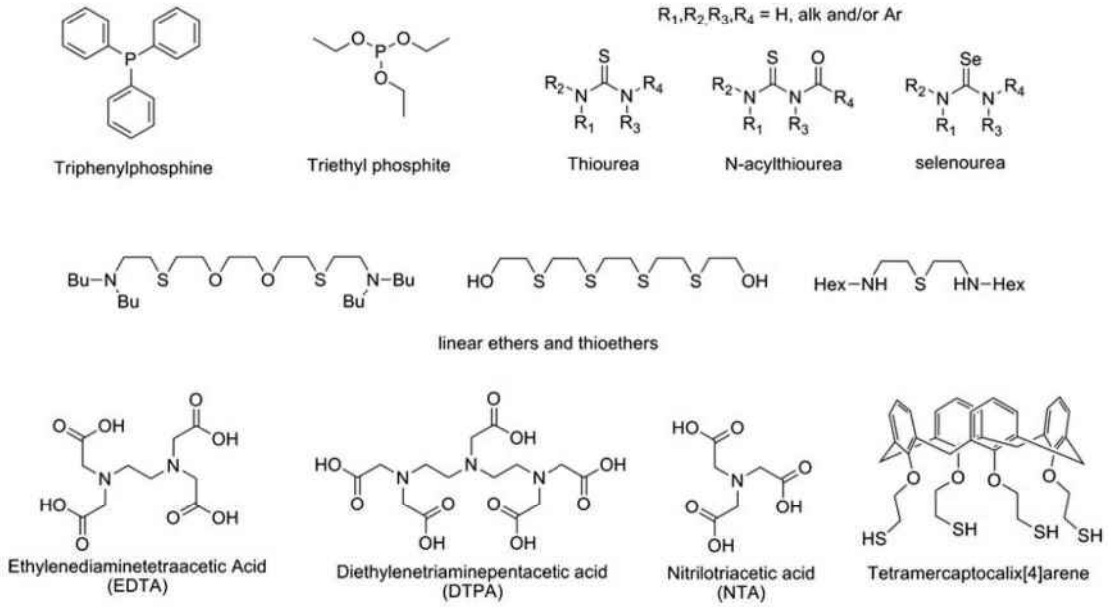

FIG. 5. Organic ligands investigated for the complexation of ^{211}At discussed in the text.

The metalloid-like behavior of astatine led Milesz et al. to study well-known chelating agents for the sequestration of metals such as EDTA,[34] DTPA,[35] or NTA[36] (Fig. 5). The feasibility of radiolabeling an antibody with ^{211}At complexed to DTPA has been demonstrated, but the *in vivo* stability was too low for biomedical applications.[37] While the proof of concept of astatine as a metal for radiolabeling an antibody has been demonstrated, polyaminocarboxylates do not appear to be appropriate for the soft-cation At^+ due to the presence of only hard-donor atoms in their structure (nitrogen and negatively changed oxygen). According to the cited studies, soft donors should be more appropriate for complexation of At^+. This was confirmed by a comparative study of linear nitrogen-, oxygen-, and sulfur-containing ligands, with better results being obtained with the sulfur-containing compounds (Fig. 5).[38] However, no chelating agents stable enough for biomedical applications have been reported yet, the most recent example of the use of ^{211}At in the At^+ form being a sulfur-containing calixarene, which exhibited a weak *in vivo* stability (Fig. 5).[39]

At(III). This oxidation state is obtained in the presence of stronger oxidizing agents such as $S_2O_8^{2-}$ or H_2O_2. However, it is difficult to obtain in a pure form, and is often associated with At^+ in proportions dependent upon experimental conditions. It has been described as a component in anionic ($AtOX_2^-$ and AtX_4^-), neutral [XAtO, $At(OH)_3$, $At(OH)X_2$, or AtX_3], and cationic forms ($AtSO_4^+$ and $AtCrO_4^+$). This form of astatine behaves similarly to At^+, however, as a harder acid with higher affinity for harder bases such as Cl^-, NO_3^-, or SO_4^{2-}. Recent examples of the investigation of this species are limited to a comparative study of the complexation of the At(I) and the At(III) species with thiocyanate and calixarene ligands.[40]

At(V). Obtained as AtO_3^- in strong oxidizing conditions (Ce^{IV}, $NaBiO_3$, hot $S_2O_8^{2-}$, or IO_4^-), it is characterized by coprecipitation with $AgIO_3$, $Ba(IO_3)_2$, or $Pb(IO_3)_2$. No complexation chemistry has been reported yet, but a relatively hard acid behavior can be expected.

At(VII). Many studies have reported the inability to demonstrate the formation of this high oxidation state of astatine, even under the strongest oxidizing conditions. Although preparation of AtO_4^- by use of xenon fluoride in hot NaOH has been reported,[41] its existence remains highly hypothetical.

In conclusion for this section, it must be kept in mind that none of the forms of astatine presented above have actually been definitely established, but rather that some of them seem to be in good agreement with the observed reactivity. Furthermore, extreme caution must be used in the experiments to obtain reproducible results. The purity of the solutions used is a primary factor influencing the results, but clearly, elapsed time also plays an important role in the behavior of astatine as demonstrated by studies by Pozzi and Zalutsky.[42] Indeed, evolution of the oxidation state of astatine in solution has been observed over time. This evolution has been attributed to the high ionizing energy emitted by the α-particles in the medium. As a consequence, oxidizing species such as peroxides can be generated, leading to evolution of astatine to higher oxidation states. On the other hand, it was also hypothesized that solvents such has methanol could be radiolyzed into reducing species (such as hydrogen or formaldehyde) that can reduce At^+ into At^-. These phenomena can highly influence the results of the complexation chemistry of astatine as well as the organic chemistry discussed that follows below.

The organic chemistry of astatine

While the inorganic chemistry of astatine is difficult to comprehend, in part because of its dual behavior between halogen and metalloid, its organic chemistry appears to be

Table 2. Phenyl- and Alkyl-Halogen Bond Energies (kJ/mol)

X	*Phenyl-X*	*Alkyl-X*
F	523	444
Cl	398	339
Br	335	285
I	268	222±12
At	197±20	163±12

Data from Coenen et al.[44]

closer to halogens, and reactions typically used with iodine are generally applicable to the formation of C–At bonds.[43] However, given the tendency of the carbon–halogen bond energy to decrease from the lighter to the heavier halogens, the bonding of At has been mostly limited to sp2 carbons (preferentially aromatic carbons) rather than sp3 carbons, whose resulting bond energies are too weak to provide sufficient stability for biomedical applications (see Table 2).

The reactions employed are similar to the ones used for labeling with radioiodine. They are generally optimized to accelerated procedures required by the relatively short half-life of ^{211}At. Synthetic approaches have been considered with nucleophilic At^- in halogen exchange or dediazoniation processes, but also with electrophilic At^+ in direct aromatic electrophilic substitution (EAS) or in demetallation reactions (Fig. 6). Alternatively, boron–astatine bonds in boron cages with improved stability have been the subject of several investigations recently.

In most cases, At^- is formed in the presence of sodium sulfite, while At^+ is often obtained with hydrogen peroxide, peracetic acid, or *N*-chlorosuccinimide, the latter being the most commonly employed. Advantages and drawbacks of each synthetic approach are discussed in the following sections.

Halogen exchange. Because of the higher nucleofugal character of iodine over the lighter halogens, this reaction is generally performed on iodinated derivatives. Examples are described for substitution on alkyl carbons, but they are unusual because of the weakness of the C_{alkyl}–At bond and the resulting low interest in these compounds for biomedical applications. Aromatic nucleophilic substitution is generally preferred, and while iodinated compounds with which the reaction is facilitated are often the starting material, bromoaryls can be advantageously used to facilitate the chromatographic purification; thanks to the higher difference in polarity between them and the astatinated compounds.

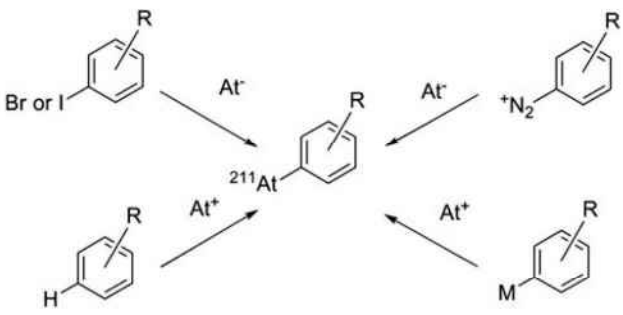

FIG. 6. Main reaction pathways used for the formation of a C–At bond.

The advantages of this approach are the rapidity of the reaction and good radiochemical yields that can be obtained. However, because of the high temperatures required, its use is restrained to substrates tolerant of relatively harsh conditions. Catalysts such as crown ethers or Cu(I) can be used to promote the reaction (see examples in Table 3). However, the effective specific activity that may be achieved through this route remains low.

Dediazoniation. Diazonium salts are widely used in organic synthesis for the derivatization of aromatic rings, including halogenations. In standard organic synthesis, this reaction is performed with an excess of halogen to limit the competing reaction of water with the diazonium leading to the phenol derivative. Because of the high dilution of astatine involved, it seems unlikely to obtain a good radiochemical yield by this method. Indeed, reactions with radioiodine have been shown to work, but with low yields (max 15%). However, much better results have been obtained on identical compounds with ^{211}At (up to 90%).[48] This difference in reactivity can be explained by looking at the dediazoniation mechanisms. Indeed, two modes of cleavage of the C–N bond can occur: heterolytic cleavage leading to the formation of an aryl cation, or homolytic cleavage leading to an aryl radical (Fig. 7). As suggested by Meyer et al.,[49] the homolytic pathway seems more likely. Because of its higher polarizability, astatine has a higher propensity to form a stable complex with the diazonium than iodine. For the same reason, astatine also has a higher propensity to cede an electron to form a radical that is able to recombine with the aryl radical according to the following sequence:

$$ArN_2^+ + At^- \rightarrow (ArN_2^+\, At^-) \rightarrow Ar\bullet + N_2At\bullet \rightarrow ArAt + N_2$$

The use of this approach is marginal due to the harsh conditions required (oxidative and acidic media) for the preparation of the diazonium, thus limiting the method to less-sensitive substrates. Furthermore, a high proportion of side-products, often precipitated in the medium, makes purification and isolation of the product difficult. Examples of astatinated compounds obtained by this approach are uncommon (see Table 4).

Direct EAS. Hydrogen substitution on aromatic rings has been investigated by several research groups to understand the mechanisms of introduction of astatine on protein (which differ from iodine, see next section). Thus, it was demonstrated that the astatination of tyrosine requires conditions that are denaturing for proteins (T=160°C in the presence of an oxidizing agent),[51] highlighting the fact that direct radiolabeling of antibodies on tyrosine residues as it is performed with radioiodine is unlikely with astatine.

Only a limited number of biomolecules were obtained using direct EAS because of the harsh conditions required for this chemistry. One of the most interesting examples of such procedure is the preparation of methylene blue astatide (which was shown to accumulate in melanoma). It was obtained in 15 minutes at 100°C in the presence of sodium persulfate as oxidizing agent, with a 68% radiolabeling yield.[52] However, because of the high amounts of starting material required, the specific activity is very low, and purification is necessary.

TABLE 3. EXAMPLES OF ASTATINATED COMPOUNDS OBTAINED VIA A HALOGEN EXCHANGE REACTION

Compound	*Reaction conditions*	*Yield*	*Ref.*
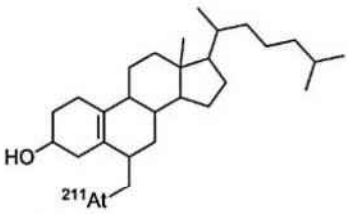 6-[^{211}At]-astatomethyl-19-norcholest-5(10)-en-3β-ol	Prepared from the iodinated derivative in 10 minutes at 70°C in the presence of a crown ether.	80%	45
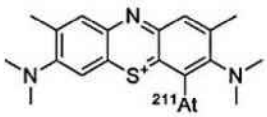 methylene blue astatide	Prepared from the iodinated derivative in 5 minutes at 80°C in the presence of a crown ether.	71%±16%	46
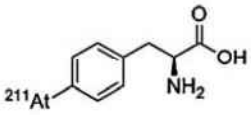 4-[^{211}At]-astato-L-phenylalanine	Prepared from the iodinated derivative in 60 minutes at 120°C in the presence of Cu(I)	67%–80%	47

Demetallation. Electrophilic substitution of At^+ on an organometallic precursor is currently the most widely used reaction. It exhibits many advantages over direct EAS because of the high reactivity of the carbon–metal bond leading to high yields in mild conditions, thereby allowing its use on a wide variety of substrates. Furthermore, high specific activities can be obtained.

Organomercuric compounds were the first precursors to be studied that allowed the introduction of ^{211}At with high yields on various compounds.[53,54] However, the presence of highly toxic traces of mercury in the final compound, even after purification, hampered their use for pharmaceutical purposes. Metals from group IV of the periodic table have been preferred, especially Boron, Silicon, and Tin. Organotin compounds are the most interesting because of the weakness of the carbon–metal bond, making the tin group an excellent leaving group (see Table 5). Furthermore, tin precursors are easily introduced on a large variety of compounds by well-established synthetic approaches.

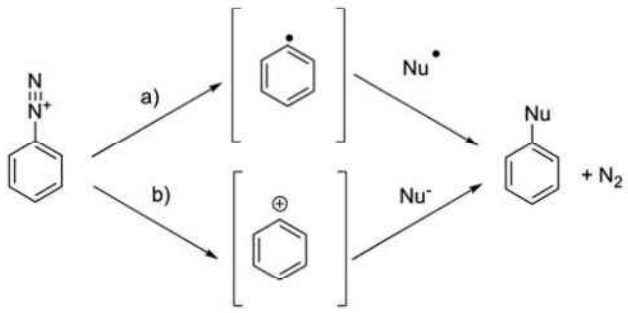

FIG. 7. Two possible dediazoniation pathways: (a) homolytic cleavage and (b) heterolytic cleavage.

Even with toxicity, several orders of magnitude lower than mercury compounds, organotin compounds remain highly toxic molecules that must be separated efficiently from the desired astatinated compound. While high-performance liquid chromatography can be used to remove the tin precursor with a relatively high efficiency, other methods have been developed that achieve a very low level of tin in the final compounds, such as the use of a precursor grafted on a polymer support. This method simplifies the purification process and highly limits the amount of liberated tin. For example, *meta*-[^{211}At]astatobenzylguanidine (MABG), a molecule with potential clinical applications in the treatment of neuroblastoma, was synthesized via a solid-supported tin precursor with good yields and low levels of tin in the final product ([Sn] < 1 ppm) (Fig. 8).[55]

Organotin precursors have become the most widely used method for the introduction of ^{211}At on biomolecules. Many examples describe the radiolabeling of proteins with *N*-succinimidyl astatobenzoate (SAB), a prosthetic group prepared from the tin precursor, as well as a variety of small molecules (see Table 6). Because of its lower toxicity, the tributyltin derivatives seem more appropriate for pharmaceutical applications than the trimethyltin, especially since no significant differences in the reactivity are detectable.[56]

The B–At bond in boron clusters. Because of the higher dissociation energy of the B–I bond compared to C–I (381 ± 21 kJ/mol and 222 ± 12 kJ/mol, respectively), the use of boron clusters such as decaborate, dodecaborate and carborane has been considered recently to improve the stability of antibodies labeled with ^{211}At. Carboranes, containing both

Table 4. Examples of Astatinated Compounds Obtained Via Dediazoniation

Compound	Reaction conditions	Yield	Ref.
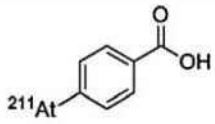 4-[^{211}At]-astatobenzoic acid	Obtained by heating at 50°C until end of nitrogen evolution	70%–85%	48
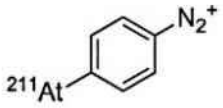 4-[^{211}At]-astatobenzenediazonium	^{211}At reacted with the bisdiazonium in the presence of a protein for 1 hour at 20°C. The second diazonium reacts with tyrosines on the protein.	50%–55% of activity on the protein	50

boron and carbon atoms, are particularly interesting for the functionalization of biomolecules because of their orthogonal reactivity. While the CHs are weak acids (pKa ranging from 22 to 27, depending on position) that can be deprotonated to generate a nucleophile, the borons are reactants toward electrophiles, and many reactions characteristic to aromatic carbons can be considered.[60] These characteristics were used to prepare various structures radiolabeled with ^{211}At with excellent radiolabeling efficiency (yields up to 90% in < 10 minutes, see Fig. 9).[61] Their advantages and drawbacks for the radiolabeling of proteins are discussed in the next section.

Astatination and stability of biomolecules of interest

Since the first studies of astatinated biomolecules, concerns about the lack of *in vivo* stability of the At–biomolecule bond have been raised.[62] Release of free astatine *in vivo* (assumed to be in the form of At^-) leading to irradiation of nontargeted tissues can occur dramatically depending on the nature of the molecules considered and on the radiolabeling method employed. As defined in several animal studies, astatide has a similar behavior to iodide with a high uptake in the thyroid and stomach. However, unlike iodide, significant uptake is also observed in the spleen and lungs (Fig. 10). This phenomenon could be attributed to the *in vivo* oxidation of At^- into At^+, as it was observed that preinjection of thiocyanide (known to form complexes with At^+) decreased astatine uptake in these organs, and that preinjection of periodate, known to oxidize At^- to At^+, increased the uptake in the lung and spleen.[63]

Several animal studies have highlighted the toxicity of free $^{211}At^-$, with damage observed to various organs, especially the thyroid and the ovaries, and development of cancerous tumors due to the ionizing radiation, and to the disturbance of the endocrine system.[64,65] In a long-term study by McLendon et al.,[66] the LD_{10} of [^{211}At]-astatide was found to be 0.56 MBq (15.1 μCi) in B6C3F$_1$ mice with 37.8% weight difference versus saline control and 0.28 MBq (7.7 μCi) in BALB/c (nu/nu) mice with 9.44% weight difference versus controls at the 0.37 MBq (10 μCi) dose 1 year after injection. Histological analyses revealed that damage to the bone marrow, testes, heart, spleen, and stomach increased with the injected dose.[66]

To avoid toxicity issues, a highly stable radiolabeled compound must be achieved. Studies with promising astatinated compounds have been hampered because of their insufficient stability *in vivo*. Depending on the class of biomolecule considered, different levels of stability are observed. There is a tendency for the smaller molecules, which are more rapidly metabolized, to release free astatine more extensively.

Protein-based carriers. Thanks to the increasing number of successful applications of radioimmunotherapy (RIT) in the treatment of cancers over the last 30 years; antibodies and their derivatives have quickly become the vectors of choice for ^{211}At.[67] The half-life of ^{211}At seems reasonably long enough to fit the kinetics of antibodies or their fragments. The first astatination studies using well-known methods for radioiodination of proteins were disappointing. In 1975, Aaij et al. demonstrated that it was possible to directly astatinate by using electrophilic ^{211}At (using chloramine-T or H_2O_2 as oxidizing agent), without denaturation of the protein.[68] The products of this direct labeling procedure were later

Table 5. Carbon–Metal Bond Characteristics (Hydrogen Included for Comparison)

Element M	Electronegativity	Covalent radius (Å)	Energy of the C–M bond (kJ/mol)	% Ionicity of the C–M bond
H	2.20	0.37	418.8	2
B	2.01	0.79	372.7	6
Si	1.74	1.18	301.5	16
Sn	1.72	1.40	226.1	16
Hg	2.00	1.50	113.1	6

Data from Coenen et al.[44]

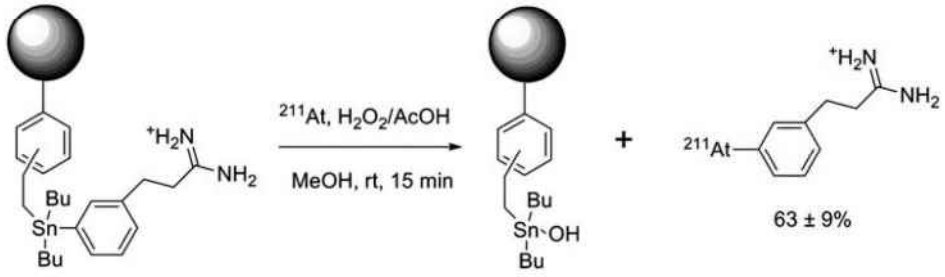

FIG. 8. Synthesis of *meta*-[^{211}At]astatobenzylguanidine (MABG) via a supported tin precursor.[55]

demonstrated to be unstable *in vivo*, as free ^{211}At was released.[69] This instability was first attributed to the weakness of the At–C bond, with astatination assumed to occur on the same sites as for the radioiodination, that is, tyrosine and histidine residues (this kind of bonding having shown to be unstable in previous studies[70]), but later, Visser et al. demonstrated in a series of reports that the conditions employed did not allow the introduction of ^{211}At on tyrosine and histidine.[53,71] Based on their observations, they hypothesized that astatine reacted with the cysteine residues of the proteins when using the direct radiolabeling approach.[72] Consequently, the weak At–S bond formed is easily hydrolyzed *in vivo*, resulting in release of free astatide. These early investigations led to the conclusion that unlike iodine, astatine could not be used in direct radiolabeling procedures of proteins, and that development of prosthetic groups for indirect radiolabeling analogous to those developed for radioiodination would be necessary.

The first stably astatinated proteins were obtained via three-step procedures by production of astatobenzoic acid in a first step, followed by activation of the carboxyl moiety to a mixed anhydride. This activated astatinated compound was then conjugated to the protein in the last step. Animal studies of bovine serum albumin labeled with this method indicated a low uptake of ^{211}At in the stomach, thyroid, spleen, and intestine compared to free ^{211}At in mice.[73] This methodology was improved and simplified by Zalutsky and Narula[74] with the development of an aromatic organotin precursor bearing an activated ester as the conjugation moiety. With a precursor activated for conjugation, this time-saving and more efficient procedure became a standard for radiolabeling proteins with radiolabeling of various antibodies in ~2 hours in sufficient yields to support production of clinical trial doses (Fig. 11).

While initially performed in chloroform in the presence of *N*-chlorosuccinimide with good radiochemical yields (up to 90%),

TABLE 6. EXAMPLES OF TIN PRECURSORS USED FOR THE RADIOLABELING WITH ^{211}AT

Tin precursor	*Radiolabeling conditions*	*Yield*	*Ref.*
 4-tributylstannyl-*N*-piperidinoethyl-benzamide	25 minutes at rt in the presence of chloramine T in EtOH/$CHCl_3$/AcOH	74%	57
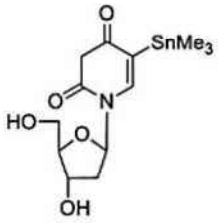 5-(trimethylstannyl)-2'-deoxyuridine	Ultrasounds 15–20 seconds in the presence of H_2O_2 in $CHCl_3$/AcOH	85%–90%	58
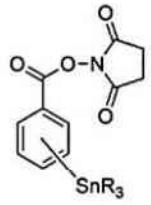 *N*-succinimidyl trialkylstannylbenzoate	Radiolabeling in chloroform or methanol in the presence of a variety of oxidizers. Most of the astatinated proteins were labeled via this prosthetic group.	Up to 90% depending on the conditions used	59

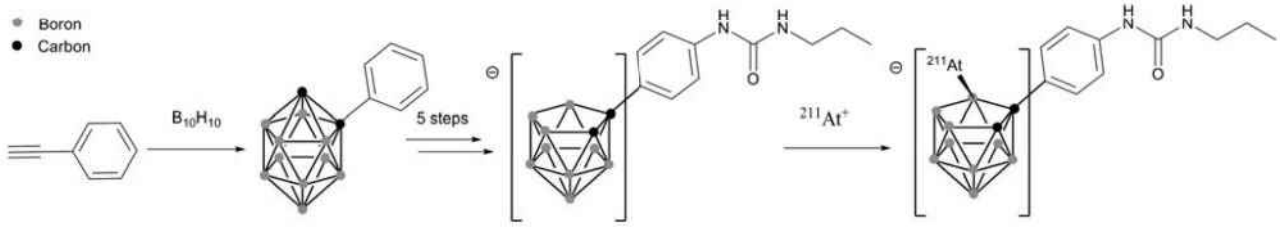

FIG. 9. Preparation of a *nido*-carborane precursor and its radiolabeling with $^{211}At^{+}$.[61]

radiolabeling the organotin precursor exhibited decreasing yields at higher activities. In a study by Pozzi and Zalutsky,[75] this phenomenon was attributed to radiolysis of the chloroform when exposed to high radiation doses of ^{211}At, leading to free-radical chlorination reaction capable of competing with astatine during the electrophilic substitution. A comparison study of different solvents determined methanol as the optimal solvent among chloroform, benzene, and methanol for the production of SAB at high levels of activity.[75]

With the improved stability provided by SAB, clinical translation became feasible as demonstrated by the first clinical study with astatinated ch81C6 antitenascin antibody for the treatment of glioma published recently by Zalutsky et al.[76] Despite the notable *in vivo* stability using of SAB for most of the full antibodies studied, several reports have highlighted the lack of stability for more rapidly metabolized proteins. This phenomenon is observed with rapidly internalized antibodies that are exposed to accelerated metabolization due to additional catabolic processes occurring in the cells, such as the lysosomal proteolysis. To resolve this issue, positively charged prosthetic groups such as pyridine carboxylate or guanidinomethylbenzoate derivatives were developed with the purpose of retaining the positively charged astatinated catabolites inside the tumor cell.[77,78] The conjugation of *N*-succinimidyl 3-[^{211}At]-4-astato-guanidinomethyl benzoate to monoclonal antibody L8A4 known to be internalized in cells expressing the anti-epidermal growth factor (EGF) receptor variant III interestingly resulted with uptake in the spleen, lungs, and thyroid similar to the radioiodinated counterpart.

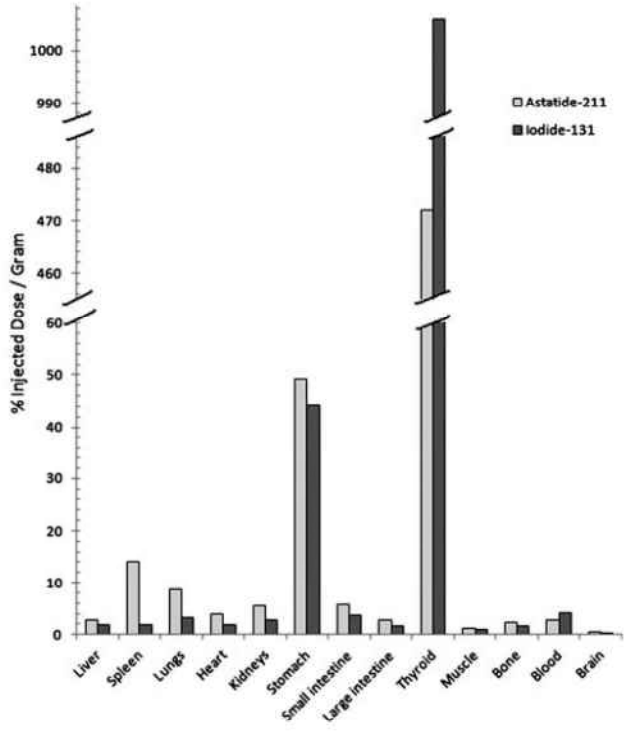

FIG. 10. Uptake of ^{211}At and ^{131}I in normal mice 1 hour postdual injection of [^{211}At]astatide and [^{131}I]iodide. Chart plotted with data from Larsen et al.[63]

The main concerns have been for antibody fragments such as Fab or $F(ab')_2$, which are extensively deastatinated *in vivo* when radiolabeled with SAB, as demonstrated by the significant uptake of activity in the thyroid, stomach, spleen, and lung compared to their radioiodinated counterparts (Fig. 12).[79,80] Several approaches, mostly based on structural modifications of the SAB, have been considered to improve the stability. They have consisted either of increasing the electronic density of the aromatic ring of the prosthetic group to strengthen the C–At bond (e.g., addition of electron donor groups and suppression of electron withdrawing group[56,81,82]), or by the addition of hindering groups such as a methyl in the vicinity of the ^{211}At atom, which was proposed to sterically hinder dehalogenation mechanisms[83] (see examples in Fig. 13). However, limited successes were obtained, except in the case of methyl-SAPS, which appears to improve the *in vivo* characteristics of the antibodies investigated. However, none of these compounds seems to be a real final solution to the stability issue with antibody fragments.

Alternatives to astatoaryl derivatives, boron cages, were proposed more recently by Wilbur et al.[61] with promising results (see structure in Fig. 9—previous section). In a series of reports, it was first demonstrated with small molecules that *nido*-carboranyls are much more stable than aryls toward deastatination.[61] These interesting results led the authors to investigate the radiolabeling of a Fab' antibody fragment with selected *nido*-carboranes and *closo*-decaborate derivatives and to compare them to the classic radiolabeling results obtained from using SAB.[84] It was demonstrated that the first advantage of the boron derivatives over the SAB was the possibility of direct astatination of the antibody fragment. With a modification of the Fab' by conjugation to the boron clusters before radiolabeling, it was possible to reach astatination yields up to 75% in only one step, in 10 minutes. Then, biodistribution studies in mice indicated the superiority of the radiolabeling via the boron cages with a significantly lower uptake of ^{211}At in the thyroid, stomach, spleen, and lungs. The best results were obtained with the *closo*-decaborate derivatives, but significant uptake in the liver and

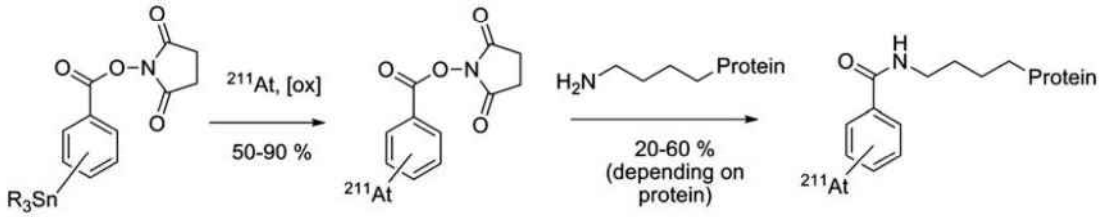

FIG. 11. Standard indirect labeling procedure for the astatination of proteins via the preparation of succinimidyl astatobenzoate (SAB).

kidneys were observed, suggesting that modifications to the boron cage or to the linkers are necessary. Studies by this research group are ongoing to solve this issue, such as the investigation of cleavable linkers to increase the clearance rate from these organs.[85,86]

Peptide/biotin carriers. Because of the relatively short half-life of ^{211}At, smaller biomolecules have been considered as better carriers for targets that are not quickly accessible to full antibodies. This includes peptides that exhibit fast kinetics, or biotin derivatives for pretargeting strategies. Octreotide has been a peptide of interest investigated by Vaidyanathan et al.[87] for targeting somatostatin receptors. In an initial article, they demonstrated that it was possible to radiolabel octreotide via a two-step procedure by conjugation to SAB. Further studies were performed with an octreotide premodified with

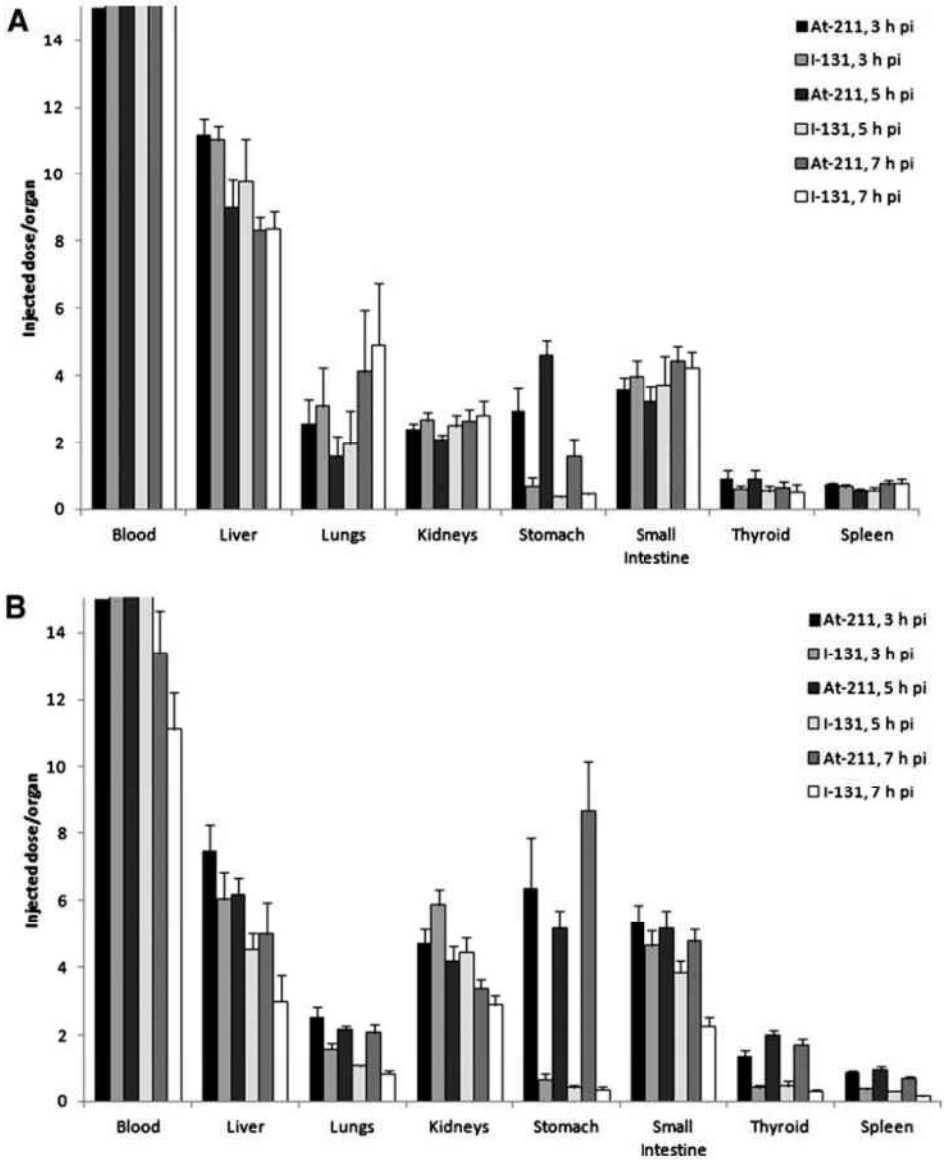

FIG. 12. Comparative biodistribution of [^{211}At]-astatinated and [^{131}I]-iodinated full antibody C110 IgG **(A)** with its F(ab')$_2$ fragment **(B)** in mice. Charts plotted from data by Garg et al.[80]

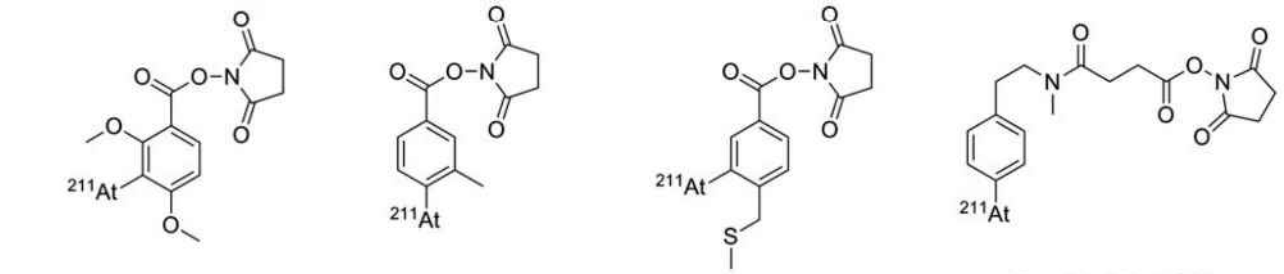

FIG. 13. Modified prosthetic groups based on the SAB structure.[56,81–83]

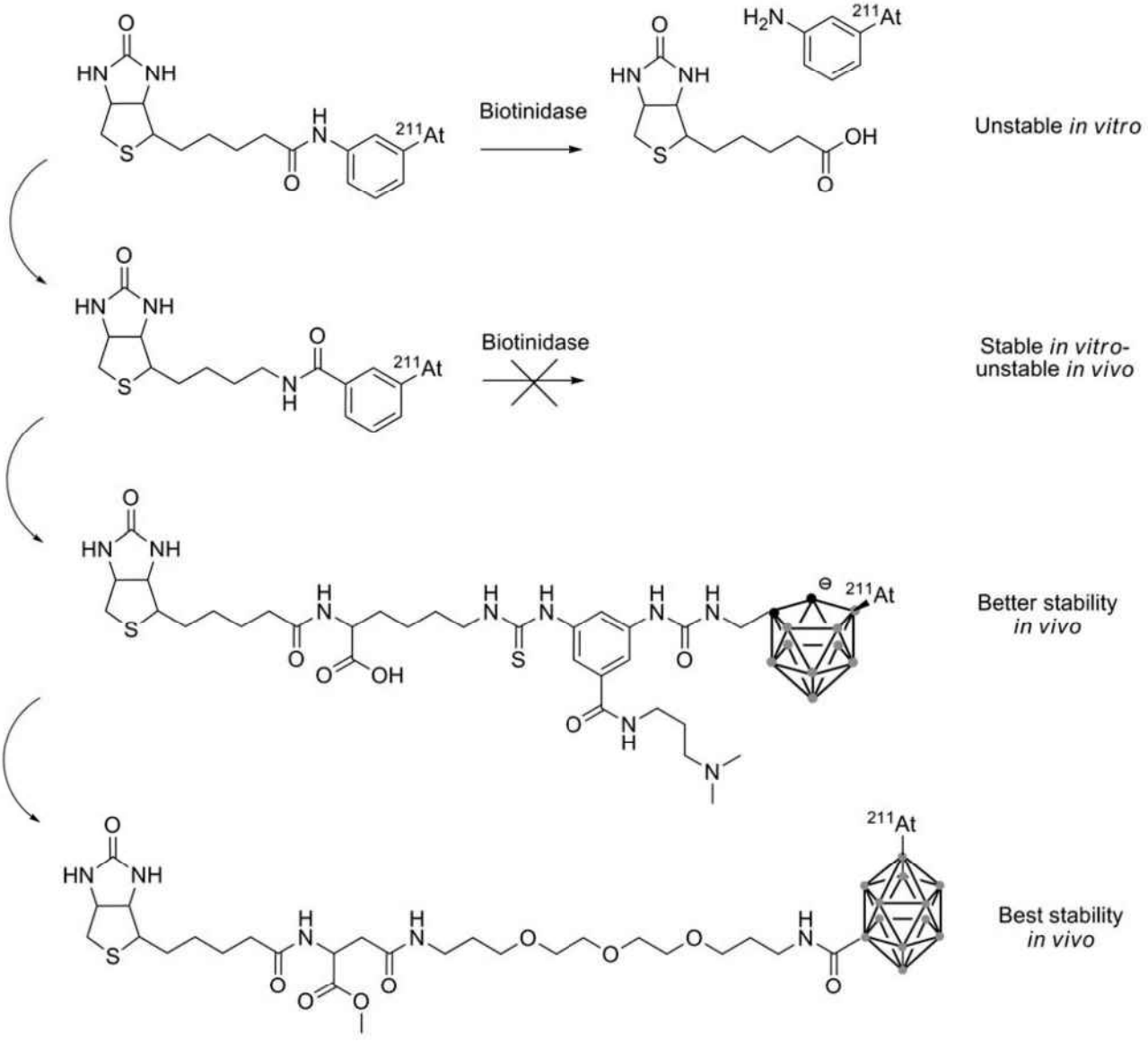

FIG. 14. Successive improvements to the biotin to increase the astatination stability.[91–94]

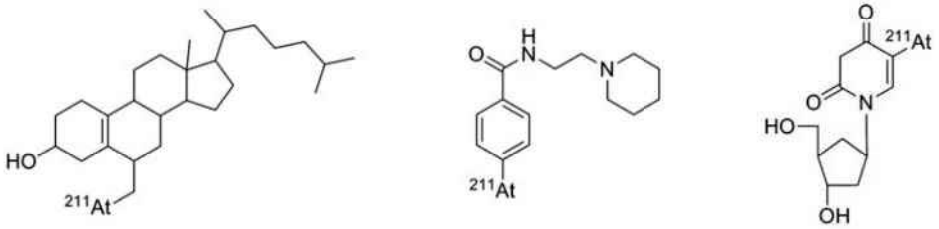

FIG. 15. Examples of small astatinated molecules unstable *in vivo*.[45,57,58]

guadininomethyl trimethylstannylbenzoate for direct radiohalogenation of the peptide. Assays indicated an excellent binding to the somatostatin receptor *in vitro*. No biodistribution study was performed with the astatinated octreotide, but the results obtained with the radioiodinated counterpart, although good in tumor-binding properties, unfortunately demonstrated an elevated uptake of the peptide in the liver and in the kidneys. These results precluded the use of this compound for i.v. administration, although its use in locoregional administration for targeting of medulloblastoma was suggested.[88] Later improvements were attempted by glycosylation of the octreotide that met with limited success on improving binding properties and pharmacokinetics.[89] Nevertheless, while astatination of the octreotide derivatives cited above was demonstrated, no data on the *in vivo* stability are available, and instability of the SAB-like compound would be expected for this kind of rapidly internalized compound.

Several reports relate the use of astatinated biotin for pretargeting (for general details on pretargeting, see Lesch et al.[90]). Initial studies by Foulon et al.[91] described direct astatination of biotin preconjugated to a trialkylstannylaniline moiety. However, the resulting astatinated compound was unstable when incubated in murine serum.[91] The same instability was observed with the radioiodinated counterpart, and analysis of the catabolites led the authors to conclude that cleavage of the amide bond occurred *in vitro* due to a biotinidase enzyme. This issue was resolved by reversing the position of the nitrogen and the carbonyl of the amide bond to avoid the action of the biotinidase (see Fig. 14), and provided high stability of the astatinated compound in murine serum.[92] Unfortunately, biodistribution studies indicated release of the astatine with significant uptake in the lungs, stomach, and thyroid. Thereafter, modifications using the promising boron cages developed by Wilbur et al.[93] provided a higher *in vivo* stability with a *nido*-carborane compared to the aryl compounds. While biodistribution studies indicated that deastatination was still occurring (but at a lower level than with aryl derivatives), latest results suggest that *closo*-decaborate(2−) is the most promising group for a strong stabilization of the astatination of biotin derivatives (see Fig. 14).[94]

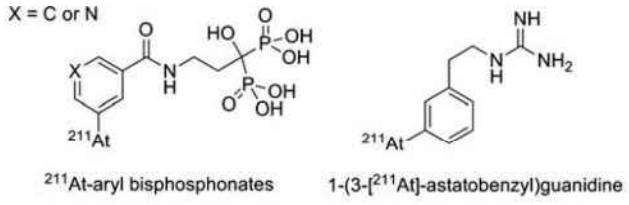

FIG. 16. Small molecules stable *in vivo*.[98,99]

Alternatively, Lindegren's group investigated biotinylated polylysines conjugated to SAB in a pretargeting strategy. In the first study, the poly-L-lysines had molecular weights of 13, 38, and 363 kDa with excellent avidin binding *in vitro*. As expected, biodistribution studies indicated that the smaller compound was rapidly excreted through the kidneys while the larger compounds had an increased liver excretion pathway. Uptake in the thyroid, stomach, lungs, and spleen indicated that release of astatine also increased with the size of the polymer.[95] In a second study, both L- and D-isomers of the polylysine were compared for their biodistribution properties. Interestingly, the poly-D-lysine, probably more resistant to metabolism, exhibited a significantly lower release of astatine as indicated by a decreased uptake in the lungs, spleen, stomach, and thyroid. However, because of an elevated uptake in kidneys for this isomer, the poly-L-lysine was preferred.[96] Recently, this astatinated biotinylated poly-L-lysine was investigated for use with mAb MX35 conjugated to avidin and administered intraperitonealy to tumor-free mice. High uptake of astatine was observed in the lungs, spleen, stomach, and throat, which could be reduced in a second experiment by preadministration of sodium perchlorate as a blocking agent.[97] However, while more studies are necessary to assess the efficiency of this poly-L-lysine derivative for the treatment of tumors, it remains equally clear that improvement of the astatine stability is required.

Other small molecules. Several other small astatinated molecules have been investigated for their propensity to be incorporated quickly to some tumor cells. However, because of their small size, many of these compounds have a natural tendency to be rapidly metabolized, resulting in marked deastatination being observed *in vivo*. This is the case of the majority of such investigated compounds, for example, 6-[^{211}At]-astatomethyl-19-norcholest-5(10)-en-3β-ol, which targets the adrenal gland,[45] 4-[^{211}At]-astato-*N*-piperidinoethyl benzamide considered for the treatment of melanoma and glioma,[57] or 5-[^{211}At]-astato-2′-deoxyuridine for DNA-targeting strategy[58] (structures in Fig. 15).

Other examples, however, show that small molecules can be very stable with minimal release of ^{211}At. This is the case of two ^{211}At-arylbisphosphonates studied for applications in bone metastasis pain palliation[98] and 1-(3-[^{211}At]-astatobenzyl)guanidine ([^{211}At]MABG) with potential applications in the treatment of glioma[99] (see structures in Fig. 16). These compounds could be interesting to consider as

prosthetic groups for radiolabeling substrates that have demonstrated instabilities cited above, although it is not clear if the stability comes from the molecular structures themselves or from biodistribution pathways circumventing deastatination mechanisms.

Nanoparticles and microspheres. Although devoid of active targeting properties, nanoparticles and larger particles have been investigated with potential applications for locoregional administration. Larsen et al.[100] prepared ^{211}At-microspheres by conjugation of aminated polymer particles to SAB. The resulting particles with a size of 1.8 μm were stable in various media *in vitro*.[100] They were compared to free $^{211}At^-$ and astatinated antibodies by i.p. administration to mice inoculated with the K13 hybridoma cell line.[101] Biodistribution studies indicated that free $^{211}At^-$ spread rapidly in the whole body, whereas the microsphere and the antibodies were mostly retained in the peritoneal cavity, highlighting a good stability. However, the authors concluded that the efficiency of the astatinated antibodies was superior to the microspheres due to a better diffusion in the peritoneal area.

Another approach developed by Kucka et al.[102] is the preparation of astatinated silver nanoparticles coated with poly(ethylene oxide) (PEO). The authors suggested that the high affinity of silver for astatine could result in a stable radiolabeling. They incubated ^{211}At with nanoparticles made of a silver proteinate core coated with PEO (size of 2000 and 5000 g/mol) in the presence of a reducing agent ($NaBH_4$). Quantitative yields were obtained, and *in vitro* measurements indicated a good stability, even in the presence of high concentration of chloride ions as a competitive agent. However, no data on *in vivo* behavior are available.

More recently, use of carbon nanotubes was proposed by Hartman et al.[103] The free carbon nanotubes, with a length in the 20–50 nm range, were incubated with [^{211}At]-astatide. The astatine trapped inside the nanotubes was then oxidized into the AtCl form in the presence of chloramine-T or *N*-chlorosuccinimide. The stability of the labeling was assessed by successive washing with water or with human serum. Even though moderate, a loss of activity was observed in both cases. This phenomenon was attributed to either a release of the AtCl portion close to the ends of the nanotubes, or by leakage through damage in the walls of the nanotubes caused by the high-energy α-particles from ^{211}At decay.

Alpha-Therapy of Cancers with ^{211}At-Labeled Targeting Agents

In vitro studies

A number of *in vitro* studies on astatinated bioconjugates have focused on the determination of the cytotoxicity and microdosimetric data with various carriers (mostly antibodies) and cell lines. Cell conditions have varied from suspended isolated cells to monolayers to spheroid cell clusters, thereby modeling different possible configurations occurring *in vivo*, but then also making difficult any actual direct comparison between the studies. While it is not intended to make an exhaustive description of all *in vitro* studies, a selection of reports covering different aspects of ^{211}At effects on *in vitro* cells is described below.

Larsen et al. investigated the cytotoxicity of astatinated mAb 81C6 (targeting tenascin in the extracellular matrix of the cell), mAb Me1-14 (targeting proteoglycan chondroitin sulfate on the cell membrane), and TPS3.2 (nonspecific) on microcolonies of D-247 MG glioma cells and SK-MEL-28 melanoma cells.[104] After 1-hour incubation with 18 kBq/mL activity concentration, results indicated two-to-five times more activity bound to the cells of the specific antibodies compared to the nonspecific mAb. A survival fraction of 0.37 (D_0) was obtained with one to two α-decays hitting the cell nucleus with only little differences between both specific mAbs and both cell lines. In another study, the cytotoxicity of ^{211}At-trastuzumab was investigated against three breast carcinoma cell lines expressing the HER2 receptor (SKBr-3, BT-474, and MCF7/HER2-18).[105] Cell survival studies indicated a relative biological effectiveness (RBE) of ^{211}At-trastuzumab 10-fold higher than external irradiation. At the low amount of antibody used, the toxicity was attributed exclusively to the α-decay of ^{211}At, with no contribution from trastuzumab. To estimate absorbed dose and toxicity *in vivo* on nonspecific tissues, the anti-CD20 mAb, rituximab, labeled with ^{211}At was investigated on cultured RAEL lymphoma cells and bone marrow cells.[106] The absorbed dose when using a 10 kBq/mL activity concentration was 0.645 and 0.021 Gy for lymphoma cells and bone marrow cells, respectively, after 1-hour exposure. However, a higher radiosensitivity to α-particles was observed for bone marrow (D_0=0.34 Gy) compared to lymphoma cells (D_0=0.55 Gy), whereas reversed sensitivity was observed from exposure to ^{60}Co γ-irradiation (D_0=1.21 and 0.72 Gy for bone marrow and lymphoma, respectively). Despite these observations, the high specificity of RAEL cell binding of ^{211}At-rituximab over bone marrow cells made these results interesting in the perspective of the treatment of non-Hodgkin's lymphoma. Recently, Petrich et al. investigated ^{211}At-anti-CD33 antibodies to overcome the cellular resistance observed in a number of patients to gemtuzumab ozogamicin (GO), the recently withdrawn toxin–mAb conjugate Mylotarg, used in the treatment of acute myeloid lymphoma.[107] The better results observed for ^{211}At-anti-CD33 over GO were promising in the perspective of treatment of GO-resistant cases of acute myeloid lymphoma.

Within the realm of preclinical studies, cetuximab was investigated in combination with astatinated cMab U36 on cultured squamous cell carcinomas. The results indicated a higher growth inhibition for the combination therapy compared to RIT alone or cetuximab alone. However, a radioprotective effect was observed in the presence of cetuximab, as well as a decrease of the internalization of cMab U36.[108] Although these phenomena have not been explained yet, the results suggest that RIT after treatment with cetuximab would be more efficient than combination of both treatments at the same time to avoid this radioprotective effect.

Alternatively, a limited number of nonantibody carriers have also been studied *in vitro*, including ^{211}At-EGF, a small protein (MW ≈ 6 kDa) targeting the EGF receptor, which is overexpressed in a number of cancerous tumors. Internalization of ^{211}At-EGF in A-431 carcinoma cells was compared to the [^{125}I]iodinated counterpart. Interestingly, a longer retention for the astatinated compound was observed, resulting in an increased biological half-life from 1.5 hours for ^{125}I-EGF to 3.5 hours for ^{211}At-EGF.[109] These results suggested that ^{211}At conjugated to EGF would be a radionuclide of choice due to its favorable biological and physical characteristics. In another study, 5-[^{211}At]-astato-2′-deoxyuridine (^{211}AtdU) was

investigated for its DNA incorporation properties in Chinese hamster V79 lung fibroblasts. It was shown that < 1% of free $^{211}At^{-}$ was incorporated compared to ^{211}AtdU. The survival study indicated a D_0 of 1.3 decays/cell, and that unlabeled cells were killed by neighboring labeled cells. Furthermore, DNA double-strand break (DSB) levels were 10-fold higher with ^{211}AtdU compared to the [^{125}I]iodinated counterpart.[58]

A limited number of studies have specifically focused on the radiobiology of ^{211}At and the biological consequences of the α-decay to the cell material. The most recent reports were published by Claesson et al.,[110] who investigated the RBE for induction of DSB for ^{211}At on human fibroblasts compared to ^{60}Co γ-irradiation and X-rays. In a first article, it was observed that two to three times more DSB occurred with ^{211}At compared to ^{60}Co γ-rays and X-rays. Furthermore, the study of the size of the DNA fragments induced by ^{211}At revealed a nonrandom distribution compared to γ-rays and X-rays, which resulted in a random distribution.[110] In a second study, the RBE of DSB for ^{211}At and X-rays was investigated at different cell cycle phases (V79-379A fibroblasts synchronized with mimosine in G1, early, mid-, and late S phase). As expected, ^{211}At exhibited a higher efficiency in generating DSB, with DSB varying in the cell cycle phases according to the following sequence: G1 < S early < S late < S mid < mitosis. It was however observed that X-rays were more efficient in inducing clustered damage than ^{211}At.[111]

Preclinical therapy studies

A number of preclinical therapy animal studies have been performed to assess the targeting properties of the astatinated biomolecules and their efficacy and toxicity, sometimes in comparison with other radionuclides of interest. Therapy studies were conducted mostly with antibodies or their fragments as delivery vectors as described below. Interestingly, models involving locoregional administration of the radiopharmaceutical have been more frequently investigated over systemic injection. Indeed, the biological and physical half-lives of the astatinated proteins seem particularly appropriate to localized compartmental tumors such as in i.p. implanted ovarian tumor models. Furthermore, concerns on the deastatination of the proteins as a result of accelerated metabolism when administered intravenously may have been a limiting factor with some carriers.

Nonetheless, the feasibility of therapy using i.v. injected astatinated antibodies has been demonstrated in several studies, and promising results have been obtained for the treatment of disseminated cancers. The astatinated anti-CD25 antibody 7G7/B6 was evaluated in a murine model of leukemia. Therapy with i.v. injection of 0.55 MBq (15 μCi) ^{211}At-7G7/B6 in karpas299 leukemia-bearing mice resulted in 70% survival at 46 days and 33% survival after 5 months, whereas untreated mice and mice treated with nonspecific antibody (^{211}At-11F11) all died after 46 days.[112] These promising results led the authors to investigate ^{211}At-7G7/B6 in combination with mAb daclizumab for therapy in mice inoculated with MET-1 human T-cell leukemia. Excellent results were obtained with improved survival for combination therapy (91% survival at 94 days) compared to RIT with 0.44 MBq (12 μCi) ^{211}At-7G7/B6 (32% survival at 94 days) or daclizumab treatment alone (47% at 94 days) while all mice died after 70 days when treated with nonspecific ^{211}At-11F11.[113] The same authors also investigated the anti-CD30 antibody ^{211}At-HeFi-1 in a model of karpas299 leukemia-bearing mice. Again, the combination of RIT with cold HeFi-1 significantly prolonged the survival of the animals (33% and 84% survival at 120 days for RIT alone and combination therapy, respectively).[114] In another study, Cheng et al.[115] evaluated the astatinated mAb U36 for the treatment of head and neck squamous cell carcinoma (HNSCC). Intravenous injection of 200 kBq radiolabeled antibody in mice inoculated with HNSCC resulted in the reduction or the stabilization of the tumor volume, while control group (treated with non-labeled U36) had its tumor volume steadily increasing after treatment.[115] Alternatively to full antibodies, Robinson et al.[116] investigated the smaller C6.5 diabody (targeting HER2 receptors) that exhibits faster targeting properties compared to antibodies. Mice bearing HER2/neu-positive MDA-MB-361/DYT2 tumors were treated by i.v. injection of 0.74 MBq (20 μCi) to 1.67 MBq (45 μCi) ^{211}At-C6.5. Compared to the control group, the tumor volume doubling time was delayed by 30 days for the 20 μCi group and by 57 days with 60% of the mice being tumor free after 1 year for the 45 μCi group.[116] Unfortunately, no biodistribution data were reported for the ^{211}At-C6.5 diabody. The *in vivo* stability of the ^{211}At-diabody bond of this engineered antibody fragment, which can be expected to be rapidly metabolized, would be interesting to study.

In the case of locoregional injections, the most documented astatinated compound is probably MX35 in its F(ab')$_2$ form. MX35 targets an antigen (Le^y) expressed in 90% of human epithelial ovarian cancers. It has been extensively studied for α-RIT in a murine model of ovarian NIH:OVCAR-3 cancer cells inoculated intraperitoneally at the Sahlgrenska academy at Göteborg University. Early investigations on ^{211}At-MX35 F(ab')$_2$ allowed for the determination of the minimum required dose by i.p. administration of doses ranging from 25 to 200 kBq 4 weeks after inoculation of NIH:OVCAR-3 cells in mice. With an increase from 22% to 50% of animals presenting no sign of tumor with doses of 50 and 100 kBq, respectively, it was concluded that 100 kBq of ^{211}At-MX35 F(ab')$_2$ was the minimal required dose to give clear evidence of the therapeutic efficacy of this treatment.[117] The authors also investigated the efficacy of the treatment against different tumor sizes. In this study, groups of mice were treated with 400 kBq ^{211}At-MX35 F(ab')$_2$ at different times (1, 3, 4, 5, or 7 weeks) after inoculation of the NIH:OVCAR-3 cells. Eight weeks after treatment, the mice were sacrificed, and the proportions of tumor- free mice were found to be 95%, 68%, 58%, 47%, and 26% for 1–7 weeks post-treatment, respectively, thus confirming the suitability of α-radiation for the treatment of smaller tumors.[118] Fractionated administration of the treatment was also compared to single injection. Four weeks after inoculation of the NIH:OVCAR-3 cells, groups of mice received a total of 800, 400, or 50 kBq ^{211}At-MX35 F(ab')$_2$ in a single injection or in three equal injections separated by 4 days. However, no advantages were found in fractionated treatment with the best results being obtained for the 800 kBq single-injection group (56% tumor-free animals 8 weeks post-treatment compared to 41% for the corresponding fractionated-injection group).[119] However, a subsequent investigation showed that weekly repeated injections of a 400 kBq dose of ^{211}At-MX35 F(ab')$_2$ (from one to six injections) led to a significantly

higher therapeutic efficacy after three or more injection with 17% free tumor animals after one injection, 39% after three injection, and up to 67% after six injections. Furthermore, no ascites were detected in the group receiving five or six injections, while 15 out of 18 animals exhibited ascites when receiving one injection.[120] Recently, the ^{211}At-MX35 F(ab')$_2$ efficacy was compared to its ^{213}Bi counterpart. Groups of mice were treated with either 2.7 MBq of ^{213}Bi-MX35 F(ab')$_2$ or 440 kBq of ^{211}At-MX35 F(ab')$_2$ 2 or 4 weeks after inoculation of NIH:OVCAR-3 cells. No significant superiority of either radionuclide was observed.[121] Finally, with the promising results obtained for ^{211}At-MX35 F(ab')$_2$ in preclinical studies and the absence of significant toxicity of these treatments at the doses employed, one of the first clinical trial with a ^{211}At radiopharmaceutical was recently initiated with this antibody (see next section).

Another antibody that deserves attention is ch81C6, as it was used in the first phase I ^{211}At-mAb clinical trial (see next section). It was initially used in the murine form for the treatment of neoplastic meningitis in preclinical studies. In a rat model, animals were inoculated with TE-671 human rhabdomyosarcoma cells by intrathecal injection into the subarachnoid space. In a series of experiments, dose escalation was first performed by intrathecal administration of 0.15–0.48 MBq (4–13 μCi) of ^{211}At-81C6 mAb to determine the dose inducing a therapeutic effect. Increases in median survival of 30%, 29%, and 51% were observed with 4, 7, and 13 μCi, respectively, compared to control (saline) with 20% of the animals still alive after 190 days in the 13 μCi group. In a second experiment, animals were treated with 0.44 MBq (12 μCi) or 0.67 MBq (18 μCi) of ^{211}At-81C6 and compared with nonspecific ^{211}At-45.6 mAb and saline. No significant increase in the median survival was observed for the nonspecific mAb compared to saline while 113% and 357% survival prolongation was observed for the 12 μCi and the 18 μCi ^{211}At-81C6 groups, respectively.[122] To reduce the potential immunogenicity of the treatment from the perspective of the clinical use of the 81C6 mAb, the human/mouse chimeric version of the antibody (ch81C6) was assessed. Biodistribution, dosimetry, and toxicity studies were performed and confirmed the superior characteristics of the ch81C6 mAb over its murine form.[123]

Trastuzumab, an anti-HER2, labeled with ^{211}At is another antibody that has shown promising results in recent studies. In a radioresistant SKOV-3 ovarian tumor model implanted in mice intraperitoneally, ^{211}At-trastuzumab was investigated in a series of experiments. First, a dose–escalation study from 0 to 800 kBq of the radiolabeled antibody injected i.p. was performed. A dose-dependent reduction of the tumor size was observed from 0 to 400 kBq without better results at 800 kBq compared to the 400 kBq dose. In a second experiment, the mice were treated with 400 kBq ^{211}At-trastuzumab in combination with increasing doses of cold trastuzumab (5–500 μg). Increased efficacy was observed while increasing the dose of cold trastuzumab with the best result obtained at 500 μg cold trastuzumab with a total eradication of the tumors. Finally, fractionated administration at various doses of ^{211}At-trastuzumab combined with various doses of cold trastuzumab did not exhibit any advantages.[124] In another study, ^{211}At-trastuzumab was also investigated for the treatment of breast carcinomatous meningitis by intrathecal injection with significantly improved survival compared to the control groups (saline or nonspecific astatinated mAb).[125]

Clinical studies

To date, only two phase-I clinical trials have been reported. The first one was published in 2008 by the Zalutsky group at the Duke University. Astatinated ch81C6 was used for the treatment of residual disease after surgical removal of the glioma tumor in the brain. The classical treatment for this pathology is surgery followed by external radiotherapy and chemotherapy. In this study, 18 patients with glioblastoma multiforme or anaplastic oligodendroglioma were enrolled and received an injection of ^{211}At-ch81C6 (71–347 MBq) in the cavity resulting from the surgery. The biodistribution was monitored directly by a γ-camera and demonstrated that 96.7% ± 3.6% of the ^{211}At decays occurred within the cavity. Blood counts indicated minimal leakage from the cavity with < 0.05% of injected dose measured. These data highlighted the low catabolism of the antibody when injected into the cavity. Final results were promising with a median survival time that increased from 31 weeks with the classical treatment of GMB to 54 weeks with additional ^{211}At-RIT without dose-limiting toxicity being observed.[76]

The second clinical trial was reported in 2009 for the treatment of ovarian cancer with ^{211}At-MX35 F(ab')$_2$. The classical treatment for ovarian carcinoma is surgery in combination with chemotherapy, but in many cases, relapse occurs with a low chance of survival. The purpose of this study was to demonstrate the potential of α-RIT after a clinical trial has failed as a phase-III study with a β^--emitter (HMFG1 mAb radiolabeled with ^{90}Y). The disappointing results obtained with ^{90}Y-HMFG1 were attributed to the nature of the radionuclide and its associated β^--particles being unsuitable for the treatment of microscopic tumors. Nine female patients in total remission after chemotherapy were enrolled in the study. After laparoscopy to check the absence of macroscopic tumor, the patients received 20–100 MBq ^{211}At-MX35 via a catheter. The biodistribution was monitored with a γ-camera and indicated that most of the radioactivity was retained in the abdomen. A noticeable uptake in the thyroid was observed for the patients who did not receive a blocking agent before the treatment. No significant uptake was observed in the other organs. Analyses of the dosimetric data indicated that this treatment allowed for the deposition of the necessary dose for the destruction of micrometastases without noticeable toxicity to the bone marrow and to the other healthy organs.[126] No conclusions on the therapeutic efficacy of this treatment are available as yet, but further investigations and reports can be expected in the near future.

Conclusions

Shortly after the discovery of ^{211}At in 1940, the therapeutic potential of this radionuclide was investigated, with applications considered for the treatment of thyroid disorders.[127] However, because of the high toxicity of α-radiation to healthy tissue, it appeared obvious that ^{211}At could not be used alone, and needed to be conjugated to an appropriate targeting carrier, especially for potential applications in the treatment of cancers.

With the exploration of the chemical properties of astatine, methodologies for the radiolabeling of various molecules of interest have been proposed. However, it is still difficult today to work with this radionuclide because of the unpredictable aspects of its reactivity and its halogen/metalloid duality. Fortunately, simple, fast, and reproducible radiolabeling methods applicable to a number of molecules of interest have been developed. Particularly, antibodies and their engineered fragments promising for RIT of cancers can now be astatinated efficiently using astatobenzoyl-based prosthetic groups. The high potential of ^{211}At for the treatment of residual disease has been recently highlighted by the first clinical trials realized with a chimeric antibody (ch81C6) and a F(ab')$_2$ fragment (MX35) using such radiolabeling methods. Promising results were obtained with a real therapeutic gain and/or limited toxicity observed.

However, many compounds of interest labeled with ^{211}At have been eliminated from the process of development of new radiopharmaceuticals because of the lack of stability on radiolabeling with astatine. From the review of the recent literature, it is clear that an effort in the understanding of the chemistry of astatine for the development of new radiolabeling approaches is required to provide new astatinated radiopharmaceuticals. Recent reports show that several research groups are working on alternative chemistries to reach that goal.[40,128,129] Furthermore, implementation of new high-energy cyclotrons capable of producing ^{211}At should improve the availability of this radionuclide in the near future and accelerate the development of new astatinated radiopharmaceuticals.[11,130]

Acknowledgment

This work was supported by the Intramural Research Program of the NIH, National Cancer Institute, Center for Cancer Research.

Disclosure Statement

No competing financial interests exist.

References

1. Kim Y-S, Brechbiel MW. An overview of targeted alpha therapy. Tumor Biol 2012;33:573.
2. Yong K, Brechbiel MW. Towards translation of 212Pb as a clinical therapeutic; getting the lead in! Dalton Trans 2011;40:6068.
3. Corson DR, MacKenzie KR, Segrè E. Possible production of radioactive isotopes of element 85. Phys Rev 1940; 57:1087.
4. Hyde EK. The present status of elements 85 and 87. J Phys Chem 1954;58:21.
5. Gmelin L, Berei K, Kugler HK, et al. Gmelin Handbook of Inorganic Chemistry: At, Astatine. Berlin, New York: Springer-Verlagt, 1985.
6. Palm S, Humm JL, Rundqvist R, et al. Microdosimetry of astatine-211 single-cell irradiation: Role of daughter polonium-211 diffusion. Med Phys 2004;31:218.
7. Turkington TG, Zalutsky MR, Jaszczak RJ, et al. Measuring astatine-211 distributions with SPECT. Phys Med Biol 1993;38:1121.
8. Meyer GJ, Lambrecht RM. Excitation function for the 209-Bi(7-Li,5n)211-Rn nuclear reaction as a route to the 211-Rn-211-At generator. J Label Compd Radiopharm 1981; 28:233.
9. Vinodkumar AM, Loveland W, Sprunger PH, et al. Fusion of ^{9}Li with ^{208}Pb. Phys Rev C 2009;80:054609.
10. Harrison J, Leggett R, Lloyd D, et al. Polonium-210 as a poison. J Radiol Prot 2007;27:17.
11. Zalutsky MR, Pruszynski M. Astatine-211: Production and availability. Current Radiopharm 2011;4:177.
12. Hermanne A, Tárkányi F, Takács S, et al. Experimental study of the cross-sections of [alpha]-particle induced reactions on ^{209}Bi. Appl Radiat Isot 2005;63:1.
13. Lindegren S, Bäck T, Jensen HJ. Dry-distillation of astatine-211 from irradiated bismuth targets: A time-saving procedure with high recovery yields. Appl Radiat Isot 2001; 55:157.
14. Yordanov A, Pozzi O, Carlin S, et al. Wet harvesting of no-carrier-added ^{211}At from an irradiated ^{209}Bi target for radiopharmaceutical applications. J Radioanal Nucl Chem 2005;262:593.
15. Alliot C, Cherel M, Barbet J, et al. Extraction of astatine-211 in diisopropylether (DIPE). Radiochim Acta 2009;97:161.
16. Bourgeois M, Guerard F, Alliot C, et al. Feasibility of the radioastatination of a monoclonal antibody with astatine-211 purified by wet extraction. J Label Compd Radiopharm 2008;51:379.
17. Zalutsky MR, Zhao XG, Alston KL, et al. High-level production of alpha-particle-emitting (211)At and preparation of (211)At-labeled antibodies for clinical use. J Nucl Med 2001;42:1508.
18. Appelman EH, Sloth EN, Studier MH. Observation of astatine compounds by time-of-flight mass spectrometry. Inorg Chem 1966;5:766.
19. Johnson GL, Leininger RF, Segrè E. Chemical properties of astatine. I. J Chem Phys 1949;17:1.
20. Appelman EH. The oxidation states of astatine in aqueous solution. J Am Chem Soc 1961;83:805.
21. Visser GWM, Diemer EL. Inorganic astatine chemistry: Formation of complexes of astatine. Radiochim Acta 1983; 33:145.
22. Visser GWM. Inorganic astatine chemistry part II: The chameleon behaviour and electrophilicity of At-species. Radiochim Acta 1989;47:97.
23. Dreyer I, Dreyer R, Chalkin VA. Investigation of the movement of astatine in an electric field. Radiochem Radioanal Lett 1978;35:257.
24. Dreyer I, Dreyer R, Chalkin VA. Cations of astatine in water: illustration and properties. Radiochem Radioanal Lett 1978;36:389.
25. Dreyer R, Dreyer I, Rosch F, et al. Studies of polyhalogenide ions of astatine. Radiochem Radioanal Lett 1982;54:165.
26. Ruth TJ, D'Auria JM, Dombsky M, et al. The Radiochemistry of Astatine. DOE sponsored Nuclear Science Series monogram (NAS-NS-3064; DE88015386) 1988. Available at www.ntis.gov/search/product.aspx?ABBR=DE88015386 Accessed on July 16, 2012.
27. Pruszyński M, Bilewicz A, Wąs B, et al. Formation and stability of astatide-mercury complexes. J Radioanal Nucl Chem 2006;268:91.
28. Pruszyński M, Bilewicz A, Zalutsky MR. Preparation of Rh[16aneS4-diol]^{211}At and Ir[16aneS4-diol]^{211}At complexes as potential precursors for astatine radiopharmaceuticals. Part I: Synthesis. Bioconjug Chem 2008;19:958.

29. Appelman EH. Solvent extraction studies of interhalogen compounds of astatine. J Phys Chem 1961;65:325.
30. Fischer S, Dreyer R, Albrecht S. Pseudohalogen compounds of astatine: Synthesis and characterization of At/I/-tricyanomethanide-and At/I/-azide-compounds. J Radioanal Nucl Chem 1987;117:275.
31. Dreyer R, Dreyer I, Fischer S, et al. Synthesis and characterization of cationic astatine compounds with sulphur-containing ligands stable in aqueous solutions. J Radioanal Nucl Chem 1985;96:333.
32. Fischer S, Dreyer R, Hussein H, et al. Synthesis and first characterization of cationic At/I/-compounds with selenium-containing neutral ligands. J Radioanal Nucl Chem 1987;119:181.
33. Ludwig R, Dreyer R, Fisher S. First investigation of complex formation of At(I) with phosphorous organic compounds. Radiochim Acta 1989;47:129.
34. Milesz S, Jovchev M, Schumann D, et al. The EDTA complexes of astatine. J Radioanal Nucl Chem 1988; 127:193.
35. Milesz S, Norseev YV, Szücs Z, et al. Characterization of DTPA complexes and conjugated antibodies of astatine. J Radioanal Nucl Chem 1989;137:365.
36. Schumann D, Milesz S, Jovchev M, et al. Nitrilotriacetate complex of univalent astatine. Radiochim Acta 1992; 56:173.
37. Ning L, Jiannan J, Shangwu M, et al. Preparation and preliminary evaluation of astatine-211 labeled IgG via DTPA anhydride. J Radioanal Nucl Chem 1998;227:187.
38. Ludwig R, Fischer S, Dreyer R, et al. Complex formation equilibria between astatine(I) and sulphur-containing chelating ligands. Polyhedron 1991;10:11.
39. Yordanov AT, Deal K, Garmestani K, et al. Synthesis and biodistribution study of a new 211-At-calix[4]arene complex. J Label Compd Radiopharm 2000;43:1219.
40. Champion J, Alliot C, Huclier S, et al. Determination of stability constants between complexing agents and At(I) and At(III) species present at ultra-trace concentrations. Inorg Chim Acta 2009;362:2654.
41. Greenwood N, Earnshaw A. Chapter 17: The halogens: Fluorine, Chlorine, Bromine, Iodine and Astatine. In: Chemistry of the Elements. 2nd edition, Elsevier, Oxford, UK: Butterworth-Heinemann, 1997;789.
42. Pozzi OR, Zalutsky MR. Radiopharmaceutical chemistry of targeted radiotherapeutics, part 3: Alpha-particle-induced radiolytic effects on the chemical behavior of (211)At. J Nucl Med 2007;48:1190.
43. Berei K, Vasáros L. Recent Advances in the Organic Chemistry of Astatine. In: PATAI'S Chemistry of Functional Groups. John Wiley and Sons, Ltd; 2009. Available at http://onlinelibrary.wiley.com/doi/10.1002/9780470682531.pat0014/abstract Accessed on July 16, 2012.
44. Coenen HH, Moerlein SM, Stöcklin G. No-carrier added radiohalogenation methods with heavy halogens. Radiochim Acta 1983;34:47.
45. Liu BL, Jin YT, Liu ZH, et al. Halogen exchanges using crown ethers: Synthesis and preliminary biodistribution of 6-[^{211}At]astatomethyl-19-norcholest-5(10)-en-3 beta-ol. Int J Appl Radiat Isot 1985;36:561.
46. Brown I, Carpenter RN, Link E, et al. Potential diagnostic and therapeutic agents for malignant melanoma: Synthesis of heavy radiohalogenated derivatives of methylene blue by electrophilic and nucleophilic methods. J Radioanal Nucl Chem Lett 1986;107:337.
47. Meyer GJ, Walte A, Sriyapureddy SR, et al. Synthesis and analysis of 2-[^{211}At]-l-phenylalanine and 4-[^{211}At]-l-phenylalanine and their uptake in human glioma cell cultures *in-vitro*. Appl Radiat Isot 2010;68:1060.
48. Visser GWM, Diemer EL. The reaction of astatine with aromatic diazonium compounds. Radiochem Radioanal Lett 1982;51:135.
49. Meyer GJ, Rössler K, Stöcklin G. Reaction of aromatic diazonium salts with carrier-free radioiodine and astatine. Evidence for complex formation. J Am Chem Soc 1979;101:3121.
50. Wunderlich G, Fischer S, Dreyer R, et al. A simple method for labelling proteins with ^{211}At via diazotized aromatic diamine. J Radioanal Nucl Chem Lett 1987;117:197.
51. Norseyev YV, Nhan DD, Khalkin VA, et al. The preparation of astatine labelled tyrosine using an electrophilic reaction. J Radioanal Nucl Chem 1985;94:185.
52. Norseev YV. Synthesis of astatine-tagged methylene blue, a compound for fighting micrometastases and individual cells of melanoma. J Radioanal Nucl Chem 1998;237:155.
53. Visser GWM, Diemer EL, Kaspersen FM. The preparation and stability of astatotyrosine and astato-iodotyrosine. Int J Appl Radiat Isot 1979;30:749.
54. Visser GWM, Diemer E, Kaspersen FM. The preparation of aromatic astatine compounds through aromatic mercury compounds part II: Astatination of pyrimidines and steroids. J Label Compd Radiopharm 1981;18:799.
55. Vaidyanathan G, Affleck DJ, Alston KL, et al. A kit method for the high level synthesis of [^{211}At]MABG. Bioorg Med Chem 2007;15:3430.
56. Vaidyanathan G, Affleck DJ, Zalutsky MR. Monoclonal antibody F(ab')$_2$ fragment labeled with *N*-succinimidyl 2,4-dimethoxy-3-halobenzoates: *In vivo* comparison of iodinated and astatinated fragments. Nucl Med Biol 1994; 21:105.
57. Garg PK, John CS, Zalutsky MR. Preparation and preliminary evaluation of 4-[^{211}At]astato-*N*-piperidinoethyl benzamide. Nucl Med Biol 1995;22:467.
58. Vaidyanathan G, Larsen RH, Zalutsky MR. 5-[^{211}At]Astato-2′-deoxyuridine, an {alpha}-particle-emitting endoradiotherapeutic agent undergoing DNA incorporation. Cancer Res 1996;56:1204.
59. Narula AS, Zalutsky MR. No-carrier added astatination of *N*-succinimidyl-3-(tri-*n*-butylstannyl) benzoate (ATE) via electrophilic destannylation. Radiochim Acta 1989;47:131.
60. Valliant JF, Guenther KJ, King AS, et al. The medicinal chemistry of carboranes. Coord Chem Rev 2002;232:173.
61. Wilbur DS, Zalutsky MR, Wedge TJ, et al. Reagents for astatination of biomolecules: Comparison of the *in vivo* distribution and stability of some radioiodinated/astatinated benzamidyl and nido-carboranyl compounds. Bioconjug Chem 2004;15:203.
62. Wilbur DS. [^{211}At]Astatine-labeled compound stability: Issues with released [^{211}At]astatide and development of labeling reagents to increase stability. Current Radiopharm 2008;1:144.
63. Larsen RH, Slade S, Zalutsky MR. Blocking [^{211}At]astatide accumulation in normal tissues: Preliminary evaluation of seven potential compounds. Nucl Med Biol 1998;25:351.
64. Hamilton JG, Asling CW, Garrison WM, et al. Destructive action of astatine 211 (element 85) on the thyroid gland of the rat. Proc Soc Exp Biol Med 1950;73:51.
65. Durbin PW, Asling CW, Johnston ME, et al. The induction of tumors in the rat by astatine-211. Radiat Res 1958; 9:378.

66. McLendon RE, Archer GE, Garg PK, et al. Radiotoxicity of systematically administered [^{211}At]astatide in B6C3F1 and BALB/c (nu/nu) mice: A long-term survival study with histologic analysis. Int J Radiat Oncol Biol Phys 1996; 35:69.
67. Zalutsky MR, Reardon DA, Pozzi OR, et al. Targeted alpha-particle radiotherapy with ^{211}At-labeled monoclonal antibodies. Nucl Med Biol 2007;34:779.
68. Aaij C, Tschroots WRJM, Lindner L, et al. The preparation of astatine labelled proteins. Int J Appl Radiat Isot 1975;26:25.
69. Vaughan AT, Fremlin JH. The preparation of astatine labelled proteins using an electrophilic reaction. Int J Nucl Med Biol 1978;5:229.
70. Vaughan AT, Fremlin JH. The preparation of astatotyrosine. Int J Appl Radiat Isot 1977;28:595.
71. Visser GWM, Diemer EL, Kaspersen FM. The preparation and stability of ^{211}At-astato-imidazoles. Int J Appl Radiat Isot 1980;31:275.
72. Visser GWM, Diemer EL, Kaspersen FM. The nature of the astatine-protein bond. Int J Appl Radiat Isot 1981;32:905.
73. Friedman AM, Zalutsky MR, Fitch FW, et al. Preparation of a biologically stable and immunogenically competent astatinated protein. Int J Nucl Med Biol 1977;4:219.
74. Zalutsky MR, Narula AS. Astatination of proteins using an *N*-succinimidyl tri-*n*-butylstannyl benzoate intermediate. Int J Rad Appl Instrum A 1988;39:227.
75. Pozzi OR, Zalutsky MR. Radiopharmaceutical chemistry of targeted radiotherapeutics, part 1: Effects of solvent on the degradation of radiohalogenation precursors by ^{211}At alpha-particles. J Nucl Med 2005;46:700.
76. Zalutsky MR, Reardon DA, Akabani G, et al. Clinical experience with alpha-particle emitting ^{211}At: Treatment of recurrent brain tumor patients with ^{211}At-labeled chimeric antitenascin monoclonal antibody 81C6. J Nucl Med 2008;49:30.
77. Reist CJ, Foulon CF, Alston K, et al. Astatine-211 labeling of internalizing anti-EGFRvIII monoclonal antibody using N-succinimidyl 5-[^{211}At]astato-3-pyridinecarboxylate. Nucl Med Biol 1999;26:405.
78. Vaidyanathan G, Affleck DJ, Bigner DD, et al. N-succinimidyl 3-[^{211}At]astato-4-guanidinomethylbenzoate: An acylation agent for labeling internalizing antibodies with alpha-particle emitting ^{211}At. Nucl Med Biol 2003;30:351.
79. Hadley SW, Wilbur DS, Gray MA, et al. Astatine-211 labeling of an antimelanoma antibody and its Fab fragment using *N*-succinimidyl *p*-astatobenzoate: Comparisons *in vivo* with the *p*-[^{125}I]iodobenzoyl conjugate. Bioconjug Chem 1991;2:171.
80. Garg PK, Harrison CL, Zalutsky MR. Comparative tissue distribution in mice of the alpha-emitter ^{211}At and ^{131}I as labels of a monoclonal antibody and F(ab')$_2$ fragment. Cancer Res 1990;50:3514.
81. Talanov VS, Yordanov AT, Garmestani K, et al. Preparation and *in vivo* evaluation of novel linkers for ^{211}At labeling of proteins. Nucl Med Biol 2004;31:1061.
82. Talanov VS, Garmestani K, Regino CAS, et al. Preparation and *in vivo* evaluation of a novel stabilized linker for ^{211}At labeling of protein. Nucl Med Biol 2006;33:469.
83. Yordanov AT, Garmestani K, Zhang M, et al. Preparation and *in vivo* evaluation of linkers for ^{211}At labeling of humanized anti-Tac. Nucl Med Biol 2001;28:845.
84. Wilbur DS, Chyan M-K, Hamlin DK, et al. Reagents for astatination of biomolecules. 2. Conjugation of anionic boron cage pendant groups to a protein provides a method for direct labeling that is stable to *in vivo* deastatination. Bioconjug Chem 2007;18:1226.
85. Wilbur DS, Chyan M-K, Hamlin DK, et al. Preparation and *in vivo* evaluation of radioiodinated *closo*-decaborate(2-) derivatives to identify structural components that provide low retention in tissues. Nucl Med Biol 2010;37:167.
86. Wilbur DS, Chyan M-K, Hamlin DK, et al. Reagents for astatination of biomolecules. 5. Evaluation of hydrazone linkers in ^{211}At- and ^{125}I-labeled *closo*-decaborate(2-) conjugates of fab' as a means of decreasing kidney retention. Bioconjug Chem 2011;22:1089.
87. Vaidyanathan G, Affleck D, Welsh P, et al. Radioiodination and astatination of octreotide by conjugation labeling. Nucl Med Biol 2000;27:329.
88. Vaidyanathan G, Boskovitz A, Shankar S, et al. Radioiodine and ^{211}At-labeled guanidinomethyl halobenzoyl octreotate conjugates: Potential peptide radiotherapeutics for somatostatin receptor-positive cancers. Peptides 2004; 25:2087.
89. Vaidyanathan G, Affleck DJ, Schottelius M, et al. Synthesis and evaluation of glycosylated octreotate analogues labeled with radioiodine and ^{211}At via a tin precursor. Bioconjug Chem 2006;17:195.
90. Lesch HP, Kaikkonen MU, Pikkarainen JT, et al. Avidin-biotin technology in targeted therapy. Expert Opin Drug Deliv 2010;7:551.
91. Foulon CF, Schoultz BW, Zalutsky MR. Preparation and biological evaluation of an astatine-211 labeled biotin conjugate: Biotinyl-3-[^{211}At]astatoanilide. Nucl Med Biol 1997;24:135.
92. Foulon CF, Alston KL, Zalutsky MR. Astatine-211-labeled biotin conjugates resistant to biotinidase for use in pretargeted radioimmunotherapy. Nucl Med Biol 1998;25:81.
93. Wilbur DS, Hamlin DK, Chyan M-K, et al. Biotin reagents in antibody pretargeting. 6. Synthesis and *in vivo* evaluation of astatinated and radioiodinated aryl- and *nido*-carboranyl-biotin derivatives. Bioconjug Chem 2004; 15:601.
94. Wilbur DS, Chyan M-K, Hamlin DK, et al. Reagents for astatination of biomolecules. 3. Comparison of *closo*-decaborate(2-) and closo-dodecaborate(2-) moieties as reactive groups for labeling with astatine-211. Bioconjug Chem 2009;20:591.
95. Lindegren S, Andersson H, Jacobsson L, et al. Synthesis and biodistribution of ^{211}At-labeled, biotinylated, and charge-modified poly-L-lysine: Evaluation for use as an effector molecule in pretargeted intraperitoneal tumor therapy. Bioconjug Chem 2002;13:502.
96. Lindegren S, Karlsson B, Jacobsson L, et al. (211)At-labeled and biotinylated effector molecules for pretargeted radioimmunotherapy using poly-L- and poly-D-lysine as multicarriers. Clin Cancer Res 2003;9:3873S.
97. Frost SHL, Bäck T, Chouin N, et al. In vivo distribution of avidin-conjugated MX35 and ^{211}At-labeled, biotinylated poly-L-lysine for pretargeted intraperitoneal α-radioimmunotherapy. Cancer Biother Radiopharm 2011;26:727.
98. Larsen RH, Murud KM, Akabani G, et al. ^{211}At- and ^{131}I-labeled bisphosphonates with high *in vivo* stability and bone accumulation. J Nucl Med 1999;40:1197.
99. Vaidyanathan G, Zalutsky MR. 1-(*m*-[^{211}At]astatobenzyl)guanidine: Synthesis via astato demetalation and preliminary *in vitro* and *in vivo* evaluation. Bioconjug Chem 1992;3:499.

100. Larsen RH, Hassfjell SP, Hoff P, et al. 211-At-labelling of polymer particles for radiotherapy: Synthesis, purification and stability. J Label Compd Radiopharm 1993;33:977.
101. Larsen RH, Hoff P, Vergote IB, et al. Alpha-particle radiotherapy with ^{211}At-labeled monodisperse polymer particles, ^{211}At-labeled IgG proteins, and free ^{211}At in a murine intraperitoneal tumor model. Gynecol Oncol 1995;57:9.
102. Kucka J, Hrubý M, Konák C, et al. Astatination of nanoparticles containing silver as possible carriers of ^{211}At. Appl Radiat Isot 2006;64:201.
103. Hartman KB, Hamlin DK, Wilbur DS, et al. ^{211}AtCl@US-tube nanocapsules: A new concept in radiotherapeutic-agent design. Small 2007;3:1496.
104. Larsen RH, Akabani G, Welsh P, et al. The cytotoxicity and microdosimetry of astatine-211-labeled chimeric monoclonal antibodies in human glioma and melanoma cells *in vitro*. Radiat Res 1998;149:155.
105. Akabani G, Carlin S, Welsh P, et al. *In vitro* cytotoxicity of ^{211}At-labeled trastuzumab in human breast cancer cell lines: Effect of specific activity and HER2 receptor heterogeneity on survival fraction. Nucl Med Biol 2006;33:333.
106. Aurlien E, Kvinnsland Y, Larsen RH, et al. Radiation doses to non-Hodgkin's lymphoma cells and normal bone marrow exposed *in vitro*. Comparison of an alpha-emitting radioimmunoconjugate and external gamma-irradiation. Int J Radiat Biol 2002;78:133.
107. Petrich T, Korkmaz Z, Krull D, et al. *In vitro* experimental ^{211}At-anti-CD33 antibody therapy of leukaemia cells overcomes cellular resistance seen *in vivo* against gemtuzumab ozogamicin. Eur J Nucl Med Mol Imaging 2010;37:851.
108. Nestor M, Sundström M, Anniko M, et al. Effect of cetuximab in combination with alpha-radioimmunotherapy in cultured squamous cell carcinomas. Nucl Med Biol 2011;38:103.
109. Orlova A, Sjöstrom A, Lebeda O, et al. Targeting against epidermal growth factor receptors. Cellular processing of astatinated EGF after binding to cultured carcinoma cells. Anticancer Res 2004;24:4035.
110. Claesson AK, Stenerlöw B, Jacobsson L, et al. Relative biological effectiveness of the alpha-particle emitter (211)At for double-strand break induction in human fibroblasts. Radiat Res 2007;167:312.
111. Claesson K, Magnander K, Kahu H, et al. RBE of α-particles from ^{211}At for complex DNA damage and cell survival in relation to cell cycle position. Int J Rad Biol 2011;87:372.
112. Zhang M, Yao Z, Zhang Z, et al. The anti-CD25 monoclonal antibody 7G7/B6, armed with the α-emitter ^{211}At, provides effective radioimmunotherapy for a murine model of leukemia. Cancer Res 2006;66:8227.
113. Zhang Z, Zhang M, Garmestani K, et al. Effective treatment of a murine model of adult T-cell leukemia using ^{211}At-7G7/B6 and its combination with unmodified anti-Tac (daclizumab) directed toward CD25. Blood 2006;108:1007.
114. Zhang M, Yao Z, Patel H, et al. Effective therapy of murine models of human leukemia and lymphoma with radiolabeled anti-CD30 antibody, HeFi-1. Proc Natl Acad Sci U S A 2007;104:8444.
115. Cheng J, Ekberg T, Engström M, et al. Radioimmunotherapy with astatine-211 using chimeric monoclonal antibody U36 in head and neck squamous cell carcinoma. Laryngoscope 2007;117:1013.
116. Robinson MK, Shaller C, Garmestani K, et al. Effective treatment of established human breast tumor xenografts in immunodeficient mice with a single dose of the α-emitting radioisotope astatine-211 conjugated to anti-HER2/neu diabodies. Clin Cancer Res 2008;14:875.
117. Elgqvist J, Andersson H, Bernhardt P, et al. Administered activity and metastatic cure probability during radioimmunotherapy of ovarian cancer in nude mice with ^{211}At-MX35 F(ab')$_2$. Int J Radiat Oncol Biol Phys 2006;66:1228.
118. Elgqvist J, Andersson H, Back T, et al. {alpha}-radioimmunotherapy of intraperitoneally growing OVCAR-3 tumors of variable dimensions: Outcome related to measured tumor size and mean absorbed dose. J Nucl Med 2006;47:1342.
119. Elgqvist J, Andersson H, Bäck T, et al. Fractionated radioimmunotherapy of intraperitoneally growing ovarian cancer in nude mice with 211At-MX35 F(ab')$_2$: Therapeutic efficacy and myelotoxicity. Nucl Med Biol 2006;33:1065.
120. Elgqvist J, Andersson H, Jensen H, et al. Repeated intraperitoneal α-radioimmunotherapy of ovarian cancer in mice. J Oncol 2010;2010:1.
121. Gustafsson AME, Bäck T, Elgqvist J, et al. Comparison of therapeutic efficacy and biodistribution of ^{213}Bi- and ^{211}At-labeled monoclonal antibody MX35 in an ovarian cancer model. Nucl Med Biol 2012;39:15.
122. Zalutsky MR, McLendon RE, Garg PK, et al. Radioimmunotherapy of neoplastic meningitis in rats using an alpha-particle-emitting immunoconjugate. Cancer Res 1994;54:4719.
123. Zalutsky MR, Stabin MG, Larsen RH, et al. Tissue distribution and radiation dosimetry of astatine-211-labeled chimeric 81C6, an α-particle-emitting immunoconjugate. Nucl Med Biol 1997;24:255.
124. Palm S, Back T, Claesson I, et al. Therapeutic efficacy of astatine-211–labeled trastuzumab on radioresistant SKOV-3 tumors in nude mice. Int J Radiat Oncol Biol Phys 2007;69:572.
125. Boskovitz A, McLendon RE, Okamura T, et al. Treatment of HER2-positive breast carcinomatous meningitis with intrathecal administration of [alpha]-particle-emitting ^{211}At-labeled trastuzumab. Nucl Med Biol 2009;36:659.
126. Andersson H, Cederkrantz E, Bäck T, et al. Intraperitoneal {alpha}-particle radioimmunotherapy of ovarian cancer patients: Pharmacokinetics and dosimetry of ^{211}At-MX35 F(ab')$_2$-a phase I study. J Nucl Med 2009;50:1153.
127. Hamilton JG, Soley MH. A comparison of the metabolism of iodine and of element 85 (eka-iodine). Proc Natl Acad Sci U S A 1940;26:483.
128. Wilbur DS, Thakar MS, Hamlin DK, et al. Reagents for astatination of biomolecules. 4. Comparison of maleimido-*closo*-decaborate(2-) and meta-[^{211}At]astatobenzoate conjugates for labeling anti-CD45 antibodies with [^{211}At]astatine. Bioconjug Chem 2009;20:1983.
129. Guerard F, Rajerison H, Faivre-Chauvet A, et al. Radiolabelling of proteins with stabilised hypervalent astatine-211: Feasability and stability. J Nucl Med 2011;52:1486.
130. Haddad F, Barbet J, Chatal JF. The ARRONAX project. Current Radiopharm 2011;4:186.

1 Radioactive waste

Radioactive waste is the term used to describe radioactive substances for which no further use is planned or considered.

A radioactive substance is one that contains naturally occurring or man-made radionuclides, the radioactive level or concentration of which calls for radiation protection control.

According to the French Environmental Code (Art. L 542.1-1), final radioactive waste means radioactive waste for which no further treatment is possible under existing technical and economic conditions. Treatment particularly entails extracting any part of the waste that can be recycled or reducing any pollutants or hazardous substances it contains.

The radionuclides contained in radioactive waste may be man-made, such as caesium-137, or found in nature, such as radium-226.

The radioactive properties of this waste are:

- the type of radionuclides contained and the radiation emitted (alpha, beta, gamma), the activity (number of atomic nuclei which spontaneously disintegrate per unit time - expressed in becquerels);
- the radioactive half-life (the time it takes for a radioactive sample to loose half of its activity).

Containers for vitrified waste (left) and compacted waste (right).

Most radioactive waste comes from the nuclear industry. The remainder comes from the use of radioactive elements in hospitals, universities, and some non-nuclear industries and defence-related activities.

Definitions and classification

Radioactive waste is classified according to its activity level and the radioactive half-life of the radionuclides it contains. The activity level determines the degree of protection to be provided. Waste is therefore divided into categories, namely very low-, low-, intermediate- and high-level waste. Radioactive waste is said to be "short-lived" if it merely only contains radionuclides with a half-life of less than 31 years.

It is said to be "long-lived "if it contains a significant quantity of radionuclides with a half-life of over 31 years.

Radionuclide	Half-life
Cobalt-60	5.2 years
Tritium	12.2 years
Strontium-90	28.1 years
Caesium-137	30 years
Americium-241	432 years
Radium-226	1,600 years
Carbon-14	5,730 years
Plutonium-239	24,110 years
Neptunium-237	2,140,000 years
Iodine-129	15,700,000 years
Uranium-238	4,470,000,000 years

Waste categories are as follows:

- **very short-lived waste (VSLW)** much of which comes from medical applications of radioactivity (diagnoses and therapy), containing radioactive elements with a half-life of less than 100 days;
- **very low-level waste (VLLW)** which comes from the nuclear industry, in particular from facility decommissioning operations. It consists of very slightly contaminated dismantled equipment parts and rubble;
- **low- and intermediate-level short-lived waste (LILW-SL)** which mainly comes from the nuclear industry, as well as a few research laboratories;
- **low-level long-lived waste (LLW-LL)** which for the major part consists either of waste contaminated by radium (known as radium-bearing waste), resulting mainly from naturally radioactive raw materials used in industry, the retrieval of radium-bearing objects and the cleanup of polluted sites, or graphite waste, which comes from the decommissioning of old French gas-cooled reactors (GCRs);
- **intermediate-level long-lived waste (ILW-LL)** most of which is the result of spent fuel reprocessing (spent fuel claddings, reprocessing sludge, etc.) and nuclear facility maintenance work;
- **high-level and long-lived waste (HLW-LL)** consisting of products resulting from spent fuel reprocessing that cannot be recycled.

Decommissioning operations (VLLW).

Graphite sleeve.

Solid waste in cemented drums before being embedded in cement.

Embedding in cement.

Management solutions

Radioactive waste is extremely varied in terms of physical and chemical form, radioactivity and the half-life of the radioactive elements it contains, as well as volume. In France, a specific process is adopted for each category of waste, including a series of operations such as sorting, treatment, conditioning, storage and disposal.

Sorting: this consists in separating waste according to its different properties, in particular the half-lives of the radionuclides it contains. It also involves separating waste that can be compacted, incinerated or melted down to reduce the volume.

Treatment and conditioning: different types of waste undergo different types of treatment (incineration, calcination, melting, compacting, cementation, vitrification, etc.). It is then sealed in a container. The result is a radioactive waste package.

Storage and disposal: storage facilities are designed to accommodate waste packages for a limited period of time. Disposal is the final stage of the waste management process and implies that the packages have reached their final destination or, at least, that there is no intention of retrieving them. That means, of course,

VLLW comprises rubble, scrap metal and piping, primarily from decommissioned nuclear facilities.

that the steps taken must protect people and the environment both in the short and very long term.

Very short-lived waste (VSLW), the radioactivity level of which disappears almost entirely in a few weeks to a few hundred days, is stored long enough to decay before disposal, in particular via hospital waste systems.

Very low-level waste (VLLW) is sent to a disposal facility in Morvilliers (Aube) operated by Andra, the French National Radioactive Waste Management Agency. Once all nuclear power plants have been decommissioned, this waste should represent an estimated volume of one to two million m^3.

Low- and intermediate-level short-lived waste (LILW-SL, also called LLW-ILW or "A" waste) is incinerated, melted, embedded or compacted. Most of it is cemented in metal or concrete containers. It is disposed of at two surface facilities: the CSM disposal facility (Manche), which was closed in 1994, having reached its design capacity of 527,000 m^3, and the CSA disposal facility (Aube), opened in 1992 and operated by Andra since.

Low-level long-lived waste (LLW-LL) is stored by the organisations that generated it pending a disposal solution.

Intermediate-level long-lived waste (ILW-LL, also called "B" waste) is compacted or cemented to make packages that are stored where the waste was generated.

High-level and long-lived waste (HLW-LL, also called "C" waste) is vitrified. This involves incorporating highly radioactive waste in molten glass.

The waste, which is in a liquid form, is mixed with molten glass and poured into stainless steel containers, then hermetically sealed by a welded lid. Once the glass has cooled down, the radioactivity is trapped inside the matrix.These waste

VLLW comprises rubble, scrap metal and piping, primarily from decommissioned nuclear facilities.

packages are currently stored by the organisations that generated the waste (CEA, Areva, their past (Marcoule, Gard) or present (La Hague, Manche) production sites.

Uranium mill tailings are also considered as waste. Areva is responsible for the tailings, which are disposed of on twenty or so mining sites. They represent about 52 million tonnes of material. All uranium mines in France are now closed.

Spent fuel, which contains uranium and plutonium and is stored in spent fuel pools at Areva's La Hague plant, is not considered as waste as the French Government implements a recycling policy.

Different types of waste package.

Management solutions developed as part of the PNGMDR* for various waste categories

<table>
<tr><th>Half-life</th><th>Very short-lived
(less than 100 days)</th><th>Short-lived
(less than 31 years)</th><th>Long-lived
(more than 31 years)</th></tr>
<tr><td>Very low-level waste</td><td rowspan="4">Managed by radioactive decay</td><td colspan="2">Dedicated surface disposal
Recycling solutions (activity < 100 Bq/g)</td></tr>
<tr><td>Low-level waste</td><td rowspan="2">Surface disposal (CSA disposal facility - Aube)</td><td>Dedicated subsurface disposal (under consideration)</td></tr>
<tr><td>Intermediate-level waste</td><td rowspan="2">Solutions under consideration under Article 3 of the Programme Act of 28 June 2006 on the sustainable management of radioactive materials and waste</td></tr>
<tr><td>High-level waste</td></tr>
</table>

* French national radioactive materials and waste management programme.

Every three years, Andra, the French National Radioactive Waste Management Agency, prepares and publishes an inventory of radioactive materials and waste in France

(Equivalent conditioned m³)	Waste existing at the end of 2010	Forecasts for the end of 2020	Forecasts for the end of 2030
HLW	2,700	4,000	5,300
ILW-LL	40,000	45,000	49,000
LLW-LL	87,000	89,000	133,000
LILW-SL	830,000	1,000,000	1,200,000
VLLW	360,000	762,000	1,300,000
Management solution to be defined	3,600		
Total	approx. 1,320,000	approx. 1,900,000	approx. 2,700,000

Volumes at the end of 2010 and forecasts for the end of 2020 and 2030 for each radioactive waste category (National Inventory 2012 - source Andra).

At Andra's CSA disposal facility (Aube), waste packages are placed in concrete cells or "disposal structures". When they are full, the cells are covered with a concrete slab and polyurethane membrane.